DETERMINATION OF IONIZED MAGNESIUM WITH ION-SELECTIVE ELECTRODES

Ekram Yousif Danish

Thesis submitted to the University of Newcastle-upon-Tyne
for the degree of Doctor of Philosophy

July 1996.

ACKNOWLEDGMENTS.

I would like to express my utmost appreciation and gratitude to Prof. A. K. Covington for his invaluable supervision, advice and guidance throughout the course of this work. I am also grateful to Dr. Patricia Kelly for her assistance, constructive discussions and friendship.

I would like to extend my thanks to the workshop and technical staff of the Chemistry Department, especially Peter and Doug, for their support.

My special gratitude goes to my husband for his encouragement and support, and for providing the means for taking care of our lovely daughter Rawan.

Finally, I would like to dedicate this work to my parents for their love and guidance throughout my life.

ABSTRACT

The role of magnesium is acknowledged in human physiology even though it is incompletely understood, and measurement of ionized magnesium by ion-selective electrode analysers is becoming commoner as recent research has alerted clinicians to its importance.

Standardisation of ionized magnesium in blood samples in the form of a reference method is required. A prototype reference cell, which was developed for the reference method for ionized calcium, has been tested and found to perform well for magnesium. Selectivity coefficients, and the effects of pH and of proteins on various magnesium selective membranes have been determined. None of these membranes showed sufficient selectivity for magnesium over calcium and sodium for use with serum samples without simultaneous measurement of calcium.

Knowledge of magnesium speciation is required for a full understanding of its role in physiology. Stability constants for magnesium and calcium with various ligands have been determined by using a new method in which a pH electrode and a Mg (or Ca) electrode have been employed simultaneously in alkalimetric titrations. The results were analysed using the program SUPERQUAD. In general, agreement was very good between values obtained from titrations with Mg (or Ca) electrodes and from pH. The protonation constants of the ligands were also determined and agree well with literature values. Results for Mg-citrate, lactate, glycinate, aspartate and glutamate complexation constants compare well with recently published data.

New systems investigated were Mg-pyroglutamate (Mg-5-oxo-2-pyrrolidinecarboxylic acid) and Mg-pyridoxine (Mg-3-hydroxy-4,5-bis(hydroxymethyl)-2-methylpyridine). Also HEPES (N-(2-hydroxyl) piperazine-N-ethanesulfonic acid), used in calibration standards as a pH buffer, was found not to complex magnesium at physiological pH.

CONTENTS

CHAPTER 1

INTRODUCTION

The concentration and speciation of magnesium is important in both clinical chemistry and industry. From the physiological aspect, magnesium is one of the most fundamental components in the human body. The total body magnesium in healthy individuals is about 25 g which is mainly contained in bone and muscular mass [1]. In most biological systems, magnesium exists in three different states: bound to protein, complexed to anions, and ionized [2]. About 1% of the total body magnesium content is present in blood. The total concentration of magnesium in blood serum varies from 0.7 to 1.1 mol/L [1, 3], of this, approximately 30% is bound to protein, mainly albumin, and several percent to other ligands, mainly hydrogen carbonate, lactate, oxalate and phosphate [4-6].

The magnesium ion is involved in a variety of physiological and metabolic processes, e.g. by acting as a cofactor for more than 300 enzymes and playing an essential role in the metabolism of carbohydrates, fats and proteins, it is also an important factor in regulating membrane permeability and pivotal in transferring, storing and utilizing energy [7, 8]. At present, total magnesium is measured routinely but measurement of ionized magnesium is limited due to the absence of a method to measure its concentration accurately. Recent research has shown that measurement of ionized magnesium can be more instructive than measuring total magnesium (see section 4.1) [9, 10].

Knowledge of the speciation of magnesium is important for a fuller understanding of the processes in which magnesium is involved in the body. One of the most significant applications of magnesium speciation

studies is to develop magnesium therapy. For example, a ligand which can associate with magnesium to form a neutral complex in the gastrointestinal fluid is more effective for clinical management of magnesium malabsorption than one forming a charged complex [11]. Neutral magnesium complexes are more lipid soluble and so can dissolve into the outer layer of the gastrointestinal membrane (phospholipid membrane), thereby leading to magnesium ion absorption [11].

This work has focused on two aspects: the measurement of ionized magnesium in blood and speciation of magnesium with biologically active ligands: citrate, lactate, glycinate, aspartate, glutamate, pyroglutamate (pidolate) and pyridoxine (vitamin B6). Complexation constants of these ligands with magnesium are low and for their evaluation an accurate and precise method is required, therefore, a new method has been used in this work for their determination. The metal ion-selective electrode is used in conjunction with a glass electrode in an alkalimetric titration for simultaneous pH and pM titrimetric determination of complex stability constants. This method can give greater confidence in the accuracy of the values of the complex stability constants obtained as the results from the two electrodes can be compared with each other. The response of the magnesium ion-selective electrode (Mg ISE) to pH changes in the metal-ligand solutions can also be compared with the percentage magnesium distribution diagram which is constructed by using the complex stability constants values obtained by the two electrodes.

The aim of this work was:

-to test a reference cell design and develop a set of calibration solutions in order to improve the reliability of the determination of ionized magnesium

measurements in blood.

-to test a new method for establishing reliable values for the complex stability constants of magnesium with previously determined physiologically important ligands, such as citrate, lactate, glycinate, aspartate and glutamate, and also to determine the stability constants for the magnesium-ligand systems of Mg-pyroglutamate, Mg-pyridoxine and Mg-HEPES.

This thesis has been divided into two parts: The first part is concerned with a reference cell method for the measurement of ionized magnesium in blood. Assessment of magnesium selective ionophores developed to determine ionized magnesium in blood serum was carried out. The performance of the reference cell proposed for calcium measurements in blood was tested to determine its suitability for measuring magnesium ion concentration. The second part focused on the determination of acidity and stability constants of various magnesium complexes. The acid protonation constants of citric, lactic, glycinic, aspartic, glutamic, pyroglutamic acids and pyridoxine, and the stability constants of their magnesium complexes were determined using simultaneous pH and pMg titrations. The secondary calibration solutions used for standardisation of magnesium measurement contain HEPES as a buffer. Magnesium binding to this buffer has also been evaluated. Due to possible calcium competition with magnesium in forming complexes with the above ligands in biological applications, the formation constants of the calcium complexes were also determined. A non-linear least squares data fitting program, SUPERQUAD, has been used to calculate the constants from the titration data.

References.

1. C. Sachs, In: P. D'Orazio, M. F. Burritt and S. F. Sena, *Electrolyte, Blood Gases and Other Critical Analysis: the Patient, the Measurement and the Government*, 14, 144 (1992).

2. R. J. Elin, In: B. M. Ultura, J. Durlach and M. S. Seelig, *Magnesium in Cellular Processes and Medicine*, p. 67 (1987).

3. C. Ritter, M. Ghahramani and H. Marsoner, In: R. W. Burnett, N. Gochman, G. A. Graham, A. H. J. Maas, R. F. Moran and A. L. Vankessel, *Proc. Int. Symp on Methodology and Clinical Applications of Blood Gases, pH, Electrolytes and Sensor Technology*, IFCC, 12, 201 (1990).

4. M. Speich, B. Bousquet and G. Nicolas, *Clin. Chem.*, 27, 246 (1981).

5. M. H. Kroll and R. J. Elin, *Clin. Chem.*, 31, 244 (1985).

6. B. T. Altura, B. M. Altura, *Scand. J. Clin. Lab. Invest.*, 54, 83 (1994).

7. W. E. C. Wacker, *Magnesium and Man*, Cambridge: Harvard Univ. Press, p. 11 (1980).

8. M. F. Ryan, *Ann. Clin. Biochem.*, 28, 19 (1991).

9. R. J. Elin, *Magnesium Metabolism in Health and Disease*, 34, 165 (1988).

10. B. T. Altura, T. L. Shirey, C. C. Young, K. Dell'Orfano and B. M. Altura, In: P. D'Orazio, M. F. Burritt and S. F. Sena, *Electrolyte, Blood Gases and Other Critical Analysis: the Patient, the Measurement and the Government*, 14, 152 (1992).

11. C. Blaquiere and G. Berthon, *Inorg. Chim. Acta*, 135, 179 (1987).

PART I MAGNESIUM-SELECTIVE ELECTRODES.

CHAPTER 2

ION-SELECTIVE ELECTRODES, GENERAL PRINCIPLES

2.1 The Principles of Ion Selective Electrodes.

Ion-Selective Electrodes are devices that permit the activity, and therefore the concentration under specific conditions, of a given ion in an aqueous medium to be determined potentiometrically despite the presence of other ions. The principle of the ion selective electrode is shown in figure 2.1. The sample solution is separated from an internal solution of known constant composition by an ion-selective membrane and an internal reference electrode is placed within the internal solution. An external reference electrode, such as a mercury-calomel electrode, is also immersed in the sample solution. By selective transfer of the ion to be measured (primary ion *i*) from the sample solution to the membrane phase on either side of the membrane, a potential difference is generated between the two solutions contacting the membrane which is dependent on the activity of the primary ion in the sample solution.

2.2 The Nernst and the Nicolsky-Eisenman Equations.

In an electrochemical cell (figure 2.1), if the membrane is behaving ideally, so that it responds to only one type of ion (primary ion *i*) in the presence of any other ion, the potential difference across the membrane, E_M, is described by the Nernst equation:

$$E_M = E^{\circ'} \pm \frac{RT}{z_i F} \ln a_i \qquad (2.1)$$

where E_M is the membrane potential, the potential difference between the internal filling solution and sample solution

$E^{\circ'}$ is the constant potential difference corresponding to the

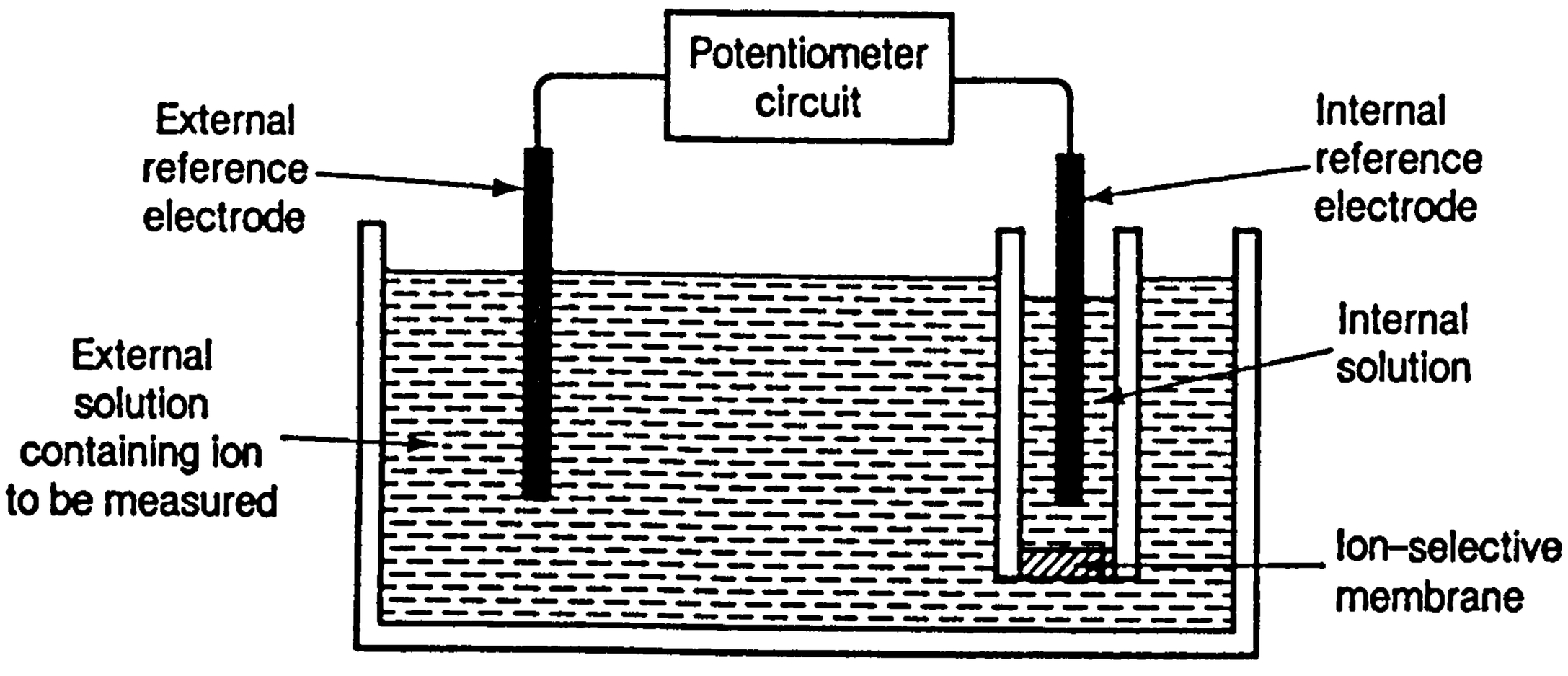

Fig. 2.1. Schematic Diagram of An Ion-Selective Electrode

contribution from the internal reference side of the membrane

R is the gas constant

T is the temperature in Kelvin

z_i is the charge on ion i

F is the Faraday constant

a_i is the activity of ion i

The sign in the equation is positive when *i* is a cation and negative when it is an anion.

In practice, however, the ideal behaviour described by equation 2.1 is rarely if ever achieved. The membrane is normally not only sensitive to the primary ion, but also to several others present in solution. For cation-selective electrodes other cations will interfere as will anions at higher concentrations. The electrode potential will consequently have contributions from both the primary ion *i* and the interfering ion *j* which of the same sign of charge type as ion *i*. For an electrode response to the ion *i*, in a solution containing an interfering ion *j*, the emf of the measuring cell is described by use of the Nicolsky-Eisenman equation (equation 2.2). This equation was first developed to describe the interference of sodium ions on the pH sensitive glass electrode [1], since when it has been adopted, in general, to describe the response of any ion-selective electrode [2].

$$EMF = E^{\circ} \pm \frac{RT}{Z_i F} \ln\left\{a_i + k_{i,j} a_j^{z_i/z_j}\right\} \qquad (2.2)$$

$$E^{\circ} = E^{\circ'} + E_{REF} + E_{LJ}$$

EMF is the electromotive force of the cell assembly

E_{REF} is the reference electrode potential

E_{LJ} is the liquid junction potential generated between the sample and bridge solution.

a_i and a_j are the activities of the primary and interferent ions respectively

z_i and z_j are the charges of the primary and interferent ions respectively

$k_{i,j}$ is the selectivity coefficient.

The $E^{\circ'}$ and E_{REF} do not depend on the sample composition, therefore if the sample solution is the only solution which is changed between measurements, the values of $E^{\circ'}$ and E_{REF} remain constant. E_{LJ} is recognized to be variable and sample dependent (see section 2.4).

2.3 Activity, Concentration and Activity Coefficient.

Since ion-selective electrodes respond to the activity rather than the concentration of the single ionic species [3], it is essential to elaborate on the relationship between the activity and concentration.

The term activity is used to denote the active or effective concentration of the ion in the solution. Activity correction in very dilute solutions is not necessary but at concentrations above 10^{-2} mol/L it does become significant. The relationship between the activity and the concentration of an ion is given by equation 2.3

$$a_i = \gamma_i \, c_i \tag{2.3}$$

where a_i , c_i ,and γ_i are the activity, concentration and activity coefficient of species i respectively. It is not possible to measure the single ion activity coefficient, only the mean activity coefficient for a cation-anion pair is measurable and it is defined for single charged ions by:

$$\gamma_{\pm}^2 = \gamma_+ \cdot \gamma_-$$

$$\text{or} \qquad \gamma_{\pm}^3 = \gamma_+ \cdot \gamma_-^2 \quad \text{for } MgCl_2 \tag{2.4}$$

The basis of theoretical calculations of activity coefficients for electrolytes is the model of Debye and Hückel [4]. In this, the mean activity coefficient is related to the ionic strength of the solution by the following equation

$$\log \gamma_{\pm} = -A \left| z_+ \, z_- \right| I^{1/2} \tag{2.5}$$

which is the Debye-Hückel limiting law and it is suitable for solutions of ionic strength up to 10^{-3} mol/L. z_+, z_- are the charges of the ions, I is the ionic strength of the solution, and A is the Debye-Hückel slope constant :

$$A = \frac{1}{\ln 10}\left[\frac{e}{\sqrt{DkT}}\right]^3 \sqrt{2\pi\, d_o\, N_A}$$

d_o = solvent density, T = temperature /K, N_A = Avogadro number, e = electronic charge, k = Boltzmann constant, D = solvent dielectric constant

A = 0.509 $(mol/L)^{-1/2}$ at 25 °C for water.

The ionic strength is given by:

$$I = \tfrac{1}{2} \sum_i^n c_i\, z_i^2 \qquad (2.6)$$

In this equation, c_i and z_i are the concentration and valency of the ions in solution. Equation 2.5 is fairly accurate at low concentrations, but at higher ionic strength of up to 10^{-1} mol/L, the full Debye-Hückel equation is required:

$$\log \gamma_{\pm} = \frac{-A\,|z_+ z_i|\, I^{1/2}}{1 + \beta a I^{1/2}} \qquad (2.7)$$

where $$\beta = \sqrt{\frac{8\pi e^2 d_o N_A}{D k T}}$$

a is the ion-size parameter

At higher concentrations (I > 0.1 mol/L), equation 2.7 has to be extended further to:

$$\log \gamma_{\pm} = \frac{-A|z_{+}z_{i}|I^{1/2}}{1 + \beta a I^{1/2}} + C I \qquad (2.8)$$

where a and C are fitting parameters which depend on the ion type and are obtained from experimental data.

It is possible to calculate the activity coefficient at ionic strength greater than 10^{-1} mol/L using the Robinson and Stokes's hydration theory [5], and the Pitzer equations [6, 7].

2.4 Liquid Junction Potentials.

At the interface between two ionic solutions, the ions from each solution interdiffuse. Diffusion with different rates, due to the different ionic mobilities, causes an electric potential gradient to develop within the junction, which is called a diffusion or liquid junction potential.

The liquid junction potentials affect the results of analysis using ion-selective electrodes. In order to minimize this effect, the liquid junction potential should be small and vary as little as possible between samples. The usual method to achieve these objectives is to use a concentrated solution of an equitransferent salt, such as KCl, as the bridge solution [8]. The mobilities of the potassium and chloride ions are close in value [9], so they diffuse at approximately the same rate; the solution is then described as equitransferent [8, 10]. If the solution is concentrated, the majority of the diffusion occurring is from the bridge solution into the sample solution and the liquid junction potential remains almost constant as it is dominated by the bridge solution composition.

The junction potential is also affected by the geometry of the junction. This is influenced by the leakage rate of outward flowing filling solution into the sample. The criterion for choosing a particular geometry should be

the establishment of a well defined reproducible liquid junction, ensuring emf stability. An in-depth review of factors affecting liquid junction is found in reference 10.

The liquid junction potential may be calculated, making certain assumptions, from mobilities of the ions involved. Methods for calculating liquid junction potentials are discussed elsewhere [11].

2.5 Classification of Ion-Selective Membrane Electrodes.

The composition of the membrane, particularly the electroactive material, is responsible for the selectivity behaviour of the electrode. According to the nature of the basic membrane material, ion-selective electrodes can be classified into the following categories [12, 13] (in parentheses are examples of ions/compounds which they are used to sense):

a- Glass membrane electrodes (e.g. H^+, Na^+, K^+).

b- Solid-state membrane electrodes based on various crystalline materials (e.g. S^{2-}, F^-).

c- Liquid membrane electrodes based on charged sites (e.g. Ca^{2+}, NO_3^-). The membrane consists of an ion exchanger salt dissolved in a suitable lipophilic solvent and usually incorporated in a PVC matrix.

d- Neutral carrier liquid membrane electrodes (e.g. K^+, Mg^{2+}, Ca^{2+}). The membrane is formed from an organic solution of electrically neutral, ion-specific complexing agents (ion carriers, ionophores), usually held in a PVC matrix.

e- Special arrangements, such as gas-sensitive electrodes (e.g. CO_2, NO_2, NH_3) and enzyme electrodes (e.g. urea, some amino-acids).

2.6 Magnesium-Selective Ionophores and Magnesium-Selective Electrodes.

2.6.1 Introduction.

In designing a magnesium-selective electrode it is required that the electrode should be selective for magnesium in the presence of alkali metal and other alkaline earth metal ions in order to work effectively in different natural media and biological fluids. The magnesium ion has a small ionic radius, small coordination sphere and high free energy of hydration in comparison with the alkali and other alkaline earth metal ions (table 2.1) [14]. It was therefore understood from the outset of attempts that the molecular design of a carrier exhibiting magnesium ion selectivity is particularly difficult [15].

Table 2.1. Data on some ionic parameters of cations [14]

Property	Li^+	Na^+	K^+	Mg^{2+}	Ca^{2+}	Sr^{2+}	Ba^{2+}
Ionic radius (Å)	0.66	0.95	1.33	0.65	0.99	1.13	1.35
ΔH_{hyd} (kcal/mol)	124	95	76	459	371	353	325
Coordination number	4,6	4,6	8,10	6	6,8	6,8	8,10

Research for magnesium-selective carriers has a history of about 20 years. Different efforts have been made to develop magnesium-selective electrodes and to design Mg^{2+}-selective neutral carriers which can be used for intracellular and/or extracellular magnesium ion measurements. In these efforts, several neutral carrier-based electrodes exhibiting good selectivity for ionized magnesium have been published, but the interference effects from physiological concentrations of Ca^{2+}, Na^+, K^+ or H^+ have not, as yet, been completely overcome.

In the following, the various attempts to design Mg^{2+}-selective carriers and develop Mg^{2+}-selective electrodes are reviewed. The importance of the other membrane components is also discussed.

2.6.2 Magnesium and Calcium-Selective Ionophores.

Magnesium ionophores may be divided into two classes: naturally occurring ionophores and synthetic ionophores. The latter type forms by far the largest proportion. Most of these synthetic ionophores were synthesised by Wilhelm Simon's research group at ETH Zürich. All these ligands have been characterized for their selectivities against the physiologically relevant mono- and divalent cations. Table 2.2 summarises some of the published selectivity data for magnesium selective membranes.

A number of naturally occurring ionophores have been reported to show Mg^{2+} selectivity in extraction studies. In 1979, Otake and Mitani [16] reported the monocarboxylic polyether antibiotic-6016 (fig. 2.2(a)) to be magnesium ion selective. The ionophore was observed to display preferential extraction of Mg^{2+} over Ca^{2+} and Ba^{2+} from an aqueous into an organic phase. However, potentiometrically, no such selectivities were detected when the antibiotic was incorporated in solvent polymeric membranes, the larger alkaline-earth cations were preferred over Mg^{2+} [17]. Another natural carboxylic polyether antibiotic A23187 (fig. 2.2(b)) is generally used for Mg^{2+}- transport studies in electrophysiology [18, 19]. This ionophore was shown to have excellent selectivity for Mg^{2+} over all monovalent ions when used in a fibre optical probe [20]. The logarithmic selectivity coefficient over calcium, however, was -0.4. These results were in contrast to Covington and Kumar who reported selectivity sequences of $Ba^{2+} > Ca^{2+} > Mg^{2+}$ [21].

Table 2.2. Published selectivity data for magnesium selective membranes.

Ionophore	Matrix [a]	Interferent j	Interferent conc. (mol/L)	log $k_{Mg,j}$	Method [b]	Comments	Ref.	Year
antibiotic-A23187	4% ionophore 71% DBS 25% PVC	Na^+ K^+ Ca^{2+} Li^+	0.01 0.01 0.01 0.01	<-5 <-5 -0.4 <-5	Fluorescence intensity		20	1989
cyclopeptide: cyclo(-L-Pro-L-Leu-)$_5$	1% ionophore 66% o-NPOE 33% PVC +58 mol % KTpClPB to ionophore	Na^+ K^+ Ca^{2+} Li^+ H^+	0.1 0.1 0.1 0.1 pH 7.5 or 8.8	-2.3 -1.0 -0.1 -2.6 +0.4	SSM	pH = 7.5 or 8.8 Corrected for activities and liquid junction potential 3 M KCl bridge	22	1985
cyclopeptide: cyclo(-L-Pro-D-Leu-)$_5$	1% ionophore 66% o-NPOE 33% PVC +82 mol % KTpClPB to ionophore	Na^+ K^+ Ca^{2+} Li^+ H^+	0.1 0.1 0.1 0.1 pH 7.5 or 8.8	-1.2 +1.2 -2.1 -1.6 +0.7	SSM	pH = 7.5 or 8.8 Corrected for activities and liquid junction potential 3 M KCl bridge	22	1985
Dibenzoyl-methane (DBM)	1.7% ionophore 34.7% PVC 31.8% tris(2-ethyl hexyl)phosphate 31.8% 5-phenyl-1-pentanol	Na^+ K^+ Ca^{2+} Li^+ H^+	0.1 0.1 0.1 0.1 0.1	-1.1 -1.3 +1.5 +0.2 +3.8	SSM	pH=8.4 of internal filling solution Corrected for activities and liquid junction potential 3 M KCl bridge	28	1987

Table 2.2 (cont.)

Ionophore	Matrix [a]	Interferent j	Interferent conc. (mol/L)	log $k_{Mg,j}$	Method [b]	Comments	Ref.	Year
ETH 1224	1.7% ionophore 34.7% PVC 31.8% tris(2-ethyl hexyl)phosphate 31.8% 5-phenyl-1-pentanol	Na^+ K^+ Ca^{2+} Li^+ H^+	0.1 0.1 0.1 0.1 0.1	+0.2 -0.5 +1.9 +1.9 +5	SSM	pH=8.8 of internal filling solution Corrected for activities and liquid junction potential 3 M KCl bridge	28	1987
2-acetyl-1-tetralone	12% ionophore 27% PVC 60% DBE	Na^+ K^+ Ca^{2+}	0.1 0.1 0.1	-2.7 -1.9 -2.2	SSM	pH=10 0.3 M NH_4NO_3 bridge	26	1990
ETH 1117	1-2% ionophore 33% PVC 65-66% o-NPOE +50 mol % KTpClPB to ionophore	Na^+ K^+ Ca^{2+} Li^+ H^+	0.1 0.1 0.1 0.1 0.1	-2.3 -1.2 +1.5 -0.9 +6.5	SSM		17	1980
ETH 1117	20% ionophore +1% NaTPB in PC	Na^+ K^+ Ca^{2+} Li^+ H^+	0.1 0.1 0.1 0.1 0.1	-1.1 -1.4 +1.1 +0.1 +2.8	SSM	Microelectrode Corrected for activities and liquid junction potential	57	1980
ETH 2220	1% ionophore 33% PVC 64-66% o-NPOE 73% KTpClPB	Na^+ K^+ Ca^{2+} Li^+ H^+	0.1 0.1 0.1 0.1 pH 8.8	-2.6 -2.3 -2.5 -2.6 +10.8	SSM	pH = 8.8 Corrected for activities and liquid junction potential	33	1988

Table 2.2 (cont.)

Ionophore	Matrix [a]	Interferent j	Interferent conc. (mol/L)	log $k_{Mg,j}$	Method [b]	Comments	Ref.	Year
ETH 4030	1% ionophore 33% PVC 66% ClP +70 mol % KTpClPB to ionophore	Na^+ K^+ Ca^{2+} Li^+ H^+	0.1 0.1 0.1 0.1 0.1	-3.8 -3.7 0 -3.1 +1.7	SSM	3 M KCl bridge Activities used in calculations	34	1988
ETH 4030	1% ionophore 33% PVC 66% o-NPPE +70 mol % KTpClPB to ionophore	Na^+ K^+ Ca^{2+}	0.1 0.1 0.1	-3.5 -2.3 -0.2	SSM	3 M KCl bridge Activities used in calculations	34	1988
ETH 5214	10% ionophore 87% o-NPOE 3% KTpClPB	Na^+ K^+ Ca^{2+} Li^+ H^+	0.1 0.1 0.1 0.1 0.1	-2.2 -2.3 +0.6 -1.2 +1.5	SSM	Microelectrode 3 M KCl bridge Corrected for activities and liquid junction potential	35	1989
ETH 5220	1% ionophore 33% PVC 32.5% o-NPOE 32.5% ClP +70 mol% KTpClPB	Na^+ K^+ Ca^{2+} Li^+ H^+	0.1 0.1 0.1 0.1 0.1	-3.0 -2.2 -0.2 -1.9 +1.5	SSM	Corrected for activities and liquid junction potential	36	1990

Table 2.2 (cont.)

Ionophore	Matrix [a]	Interferent j	Interferent conc. (mol/L)	log $k_{Mg,j}$	Method [b]	Comments	Ref.	Year
ETH 5282	1% ionophore 33% PVC 66% o-NPOE +150 mol% KTpClPB to ionophore	Na^+ K^+ Ca^{2+} H^+	0.1 0.1 0.1 0.1	-3.9 -2.4 -0.8 +1.2	SSM	3 M KCl bridge	38	1990
ETH 7025	1% ionophore 33% PVC 66% o-NPOE +155 mol% KTpClPB to ionophore	Na^+ K^+ Ca^{2+} Li^+ H^+	0.1 0.1 0.1 0.1 0.1	-4.3 -2.8 -1 -4.3 +1.3	SSM		40	1991
ETH 7025	1% ionophore 33% PVC 66% o-nitrophenyl-dihydrophytol ether +155mol% KTpClPB to ionophore	Na^+ K^+ Ca^{2+} Li^+ H^+	0.1 0.1 0.1 0.1 0.1	-5 -3.4 -1.5 -5.5 +0.7	SSM		40	1991
ETH 7025	1% ionophore 33% PVC 63% o-NPOE 3% ETH 500 +155mol% KTpClPB to ionophore	Na^+ K^+ Ca^{2+} Li^+ H^+	0.1 0.1 0.1 0.1 0.1	-4.7 -2.9 -1.2 -4.8 +0.9	SSM		40	1991
ETH 7025	10% ionophore 81.6% o-NPOE 5% ETH 500 3.4% (60 mol% to ionophore) KTpClPB	Na^+ K^+ Ca^{2+} Li^+ H^+	0.1 0.1 0.1 0.1 0.1	-3.1 -3.1 +0.7 -2.6 +1.6	SSM	Microelectrode 3M KCl bridge Corrected for activities and liquid junction potential	42	1993

Table 2.2 (cont.)

Ionophore	Matrix [a]	Interferent j	Interferent conc. (mol/L)	log $k_{Mg,j}$	Method [b]	Comments	Ref.	Year
ETH 7025	10% ionophore 80.4% o-NPOE 1% ETH 500 8.6% (150mol% to ionophore) KTpClPB	Na^+ K^+ Ca^{2+} Li^+ H^+	0.1 0.1 0.1 0.1 0.1	-3.2 -2.7 -0.7 -3.4 +2.3	SSM	Microelectrode 3M KCl bridge Corrected for activities and liquid junction potential	42	1993
ETH 7025	6μg/g ionophore 360μg/g PVC 600μg/g o-NPOE 35μg/g ETH 500 1.55 mol/(mol of ligand) KTpClPB	Ca^{2+} Ca^{2+}		-1.05 -0.80	SSM specific application method	Corrected for activities and liquid junction potential	58	1993
ETH 7025	1% ionophore 33% PVC 66% o-NPOE +155 mol% KTpClPB to ionophore	Na^+ K^+ Ca^{2+} Li^+ H^+	0.1 0.1 0.1 0.1 0.1	-4.2 -2.7 -1 -4.6 +0.9	SSM	3M KCl bridge Corrected for activities and liquid junction potential	44	1993
ETH 7025	1% ionophore 33% PVC 66% ETH 5373 +155 mol% KTpClPB to ionophore	Na^+ K^+ Ca^{2+} Li^+ H^+	0.1 0.1 0.1 0.1 0.1	-4.5 -3.3 -1.3 -4.9 +1.5	SSM	3M KCl bridge Corrected for activities and liquid junction potential	44	1993

Table 2.2 (cont.)

Ionophore	Matrix [a]	Interferent j	Interferent conc. (mol/L)	log $k_{Mg,j}$	Method [b]	Comments	Ref.	Year
ETH 7160	1% ionophore 33% PVC 66% o-NPOE +155 mol% KTpClPB to ionophore	Na^+ K^+ Ca^{2+} Li^+ H^+	0.1 0.1 0.1 0.1 0.1	-4.2 -2.0 -1.2 -4.3 +1.9	SSM	3M KCl bridge Corrected for activities and liquid junction potential	44	1993
ETH 7160	1% ionophore 33% PVC 66% ETH 5373 +155 mol% KTpClPB to ionophore	Na^+ K^+ Ca^{2+} Li^+ H^+	0.1 0.1 0.1 0.1 0.1	-4.0 -3.1 -1.6 -4.4 +2.3	SSM	3M KCl bridge Corrected for activities and liquid junction potential	44	1993
ETH 3832	1% ionophore 33% PVC 66% o-NPOE +155 mol% KTpClPB to ionophore	Na^+ K^+ Ca^{2+} Li^+ H^+	0.1 0.1 0.1 0.1 0.1	-4.1 -3.0 -1.4 -4.6 -1.0	SSM	3M KCl bridge Corrected for activities and liquid junction potential	44	1993
ETH 3832	1% ionophore 33% PVC 66% ETH 5373 +155 mol% KTpClPB to ionophore	Na^+ K^+ Ca^{2+} Li^+ H^+	0.1 0.1 0.1 0.1 0.1	-5.0 -3.8 -1.7 -5.4 -0.3	SSM	3M KCl bridge Corrected for activities and liquid junction potential	44	1993

Table 2.2 (cont.)

Ionophore	Matrix [a]	Interferent j	Interferent conc. (mol/L)	log $k_{Mg,j}$	Method [b]	Comments	Ref.	Year
ETH 5506	1% ionophore 33% PVC 66% o-NPOE +155 mol% KTpClPB to ionophore	Na^+ K^+ Ca^{2+} Li^+ H^+	0.1 0.1 0.1 0.1 0.1	-4.4 -2.7 -1.7 -4.7 +0.1	SSM	3M KCl bridge Corrected for activities and liquid junction potential	44	1993
ETH 5506	1% ionophore 33% PVC 66% ETH 5373 +155 mol% KTpClPB to ionophore	Na^+ K^+ Ca^{2+} Li^+ H^+	0.1 0.1 0.1 0.1 0.1	-4.7 -3.7 -1.9 -4.8 +0.9	SSM	3M KCl bridge Corrected for activities and liquid junction potential	44	1993
1,2-bis(ditolyl phosphine oxide) benzene	2.66% ionophore 32% PVC 64% o-NPOE +50 mol% KTpClPB to ionophore	Na^+ K^+ Ca^{2+} Li^+		-3.1 -3.3 -2.8 -3.8	MSM		51	1994
NOVA	not published	Ca^{2+}	0.01	-1.1	SSM		56	1994

(a) DBS = dibutyl sebacate
PVC = poly(vinyl chloride)
o-NPOE = o-nitrophenyl octyl ether
KTpClPB = potassium tetrakis(p-chlorophenyl)borate
DBE = dibenzyl ether
NaTPB = Sodium tetraphenylborate
PC = Propylene carbonate
ClP = Chloroparaffin
o-NPPE = o-nitrophenyl phenyl ether
ETH 500 = tetradodecyl ammonium-tetrakis(p-chlorophenyl)-borate.

(b) SSM = Separate solutions method
MSM = Mixed solutions method

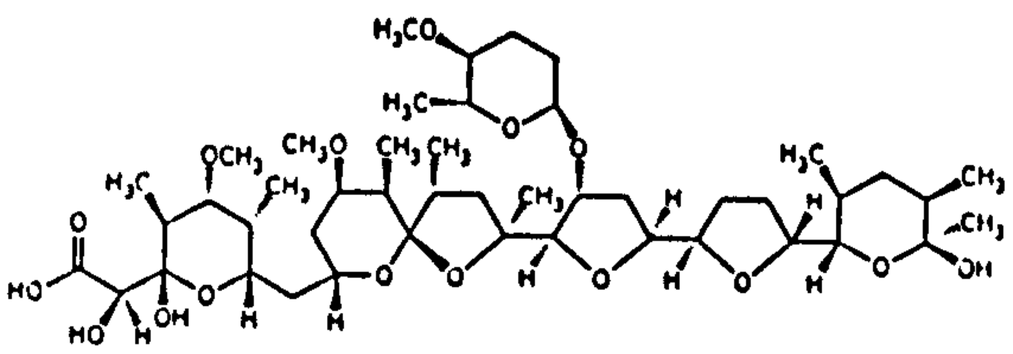

(a) Antibiotic-6016

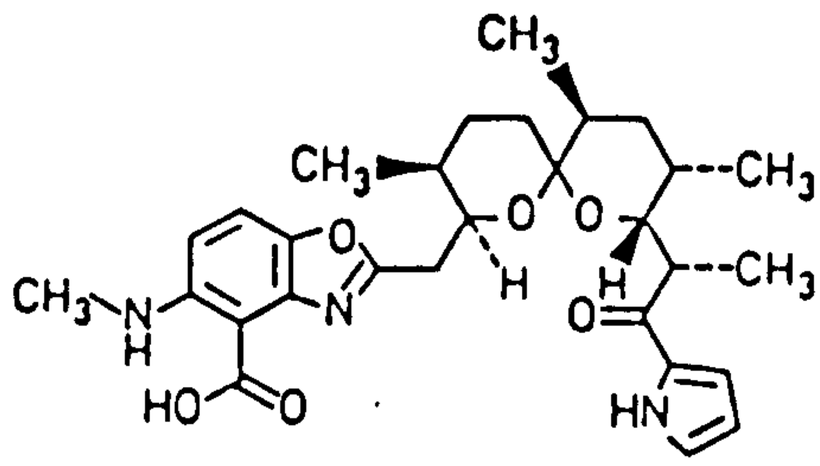

(b) Antibiotic A23187

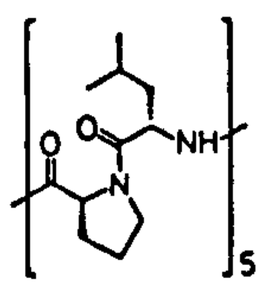

(c) cyclo(-L-Pro-L-Leu-)$_5$

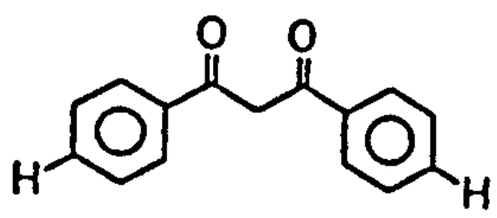

(d) dibenzoylmethane

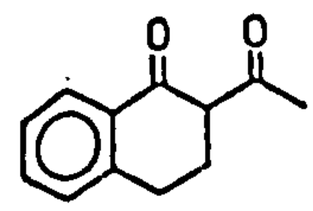

(e) 2-acetyl-1-tetralone

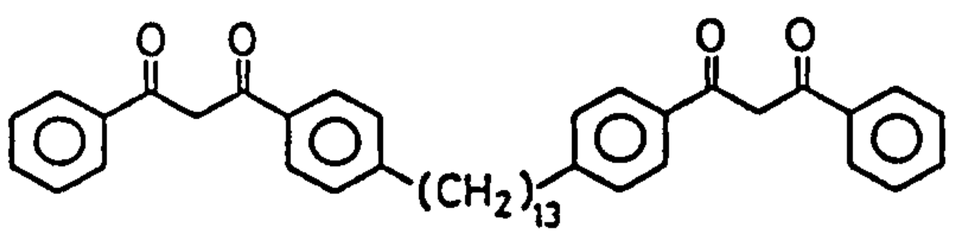

(f) Bis-β-diketones (ETH 1224)

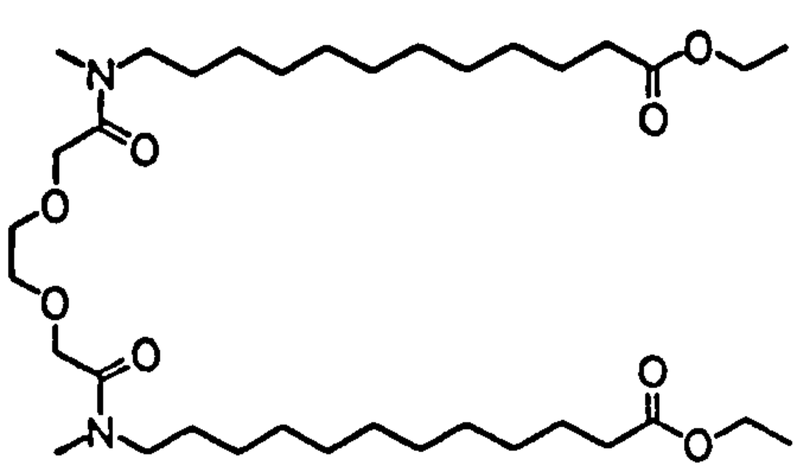

(g) Neutral ionophore for calcium (ETH 1001)

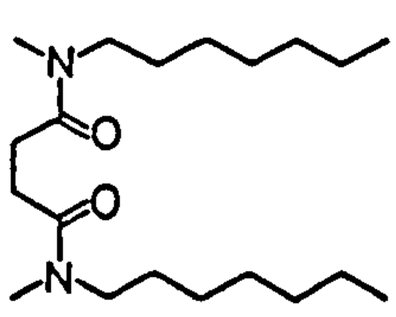

(h) ETH 1117

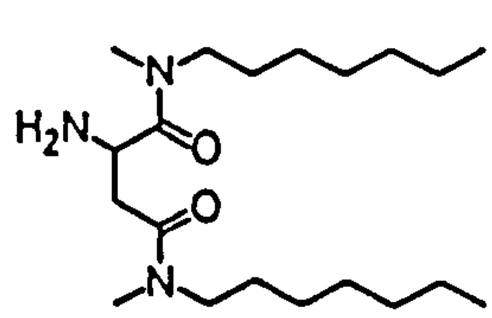

(i) ETH 2220

Fig. 2.2 Magnesium and Calcium-Selective Ionophores

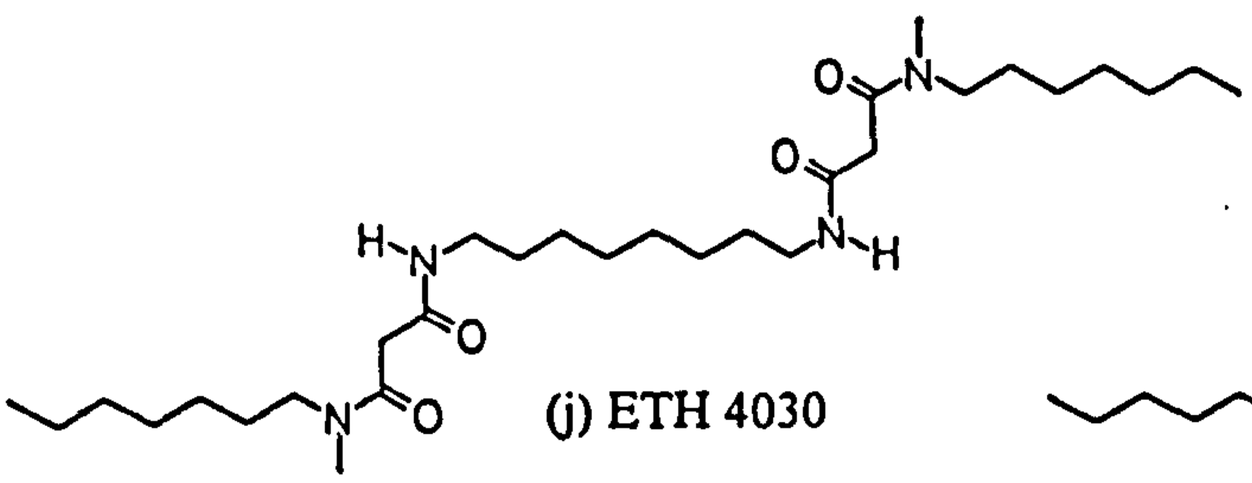

(j) ETH 4030

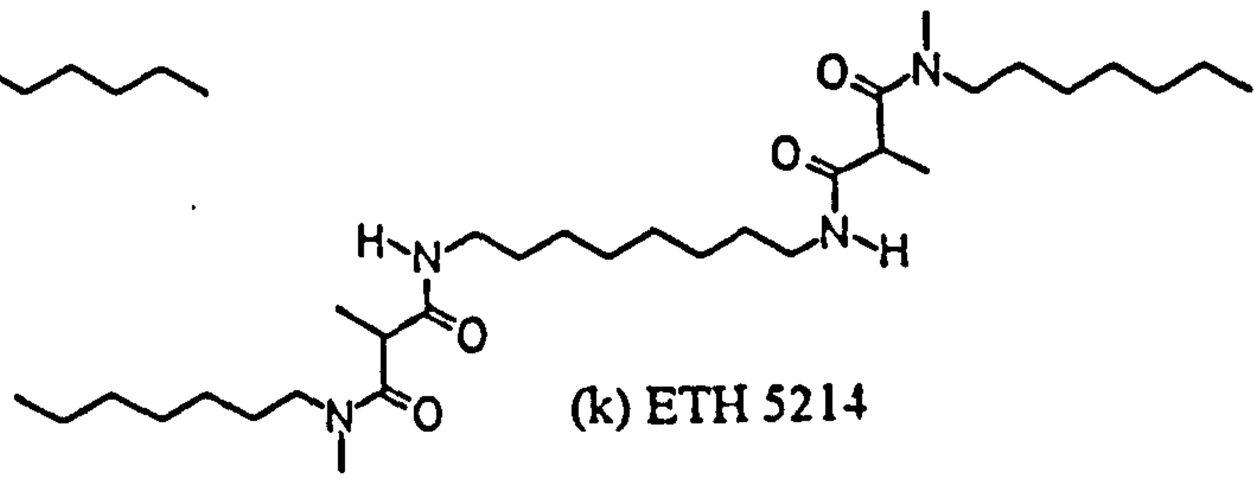

(k) ETH 5214

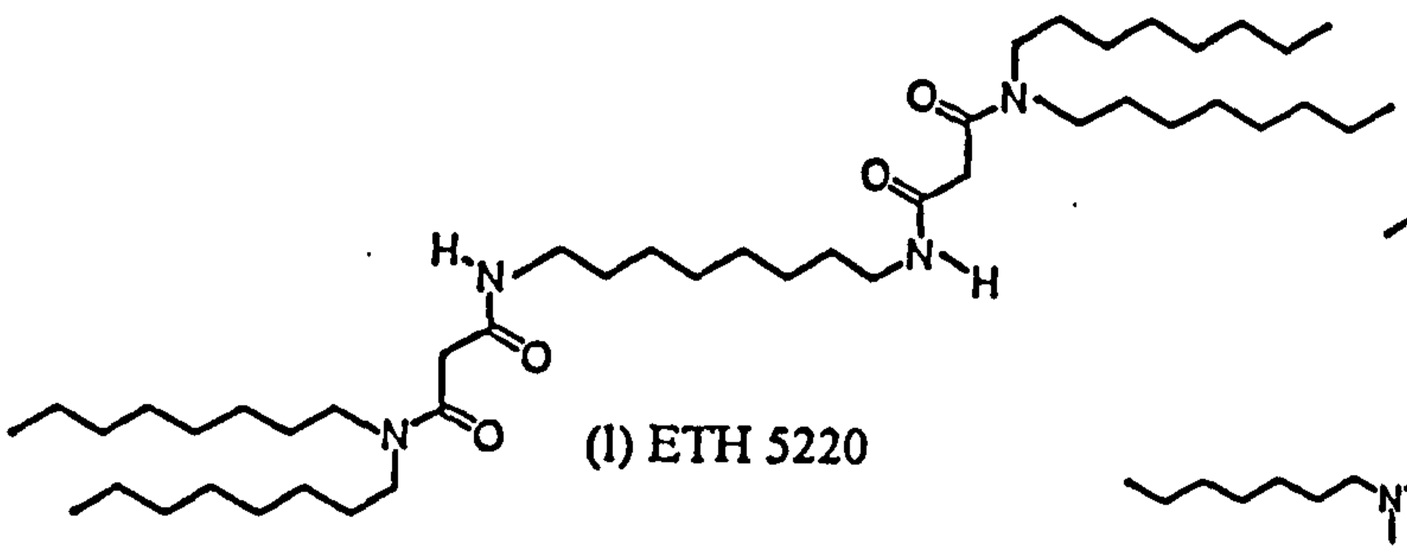

(l) ETH 5220

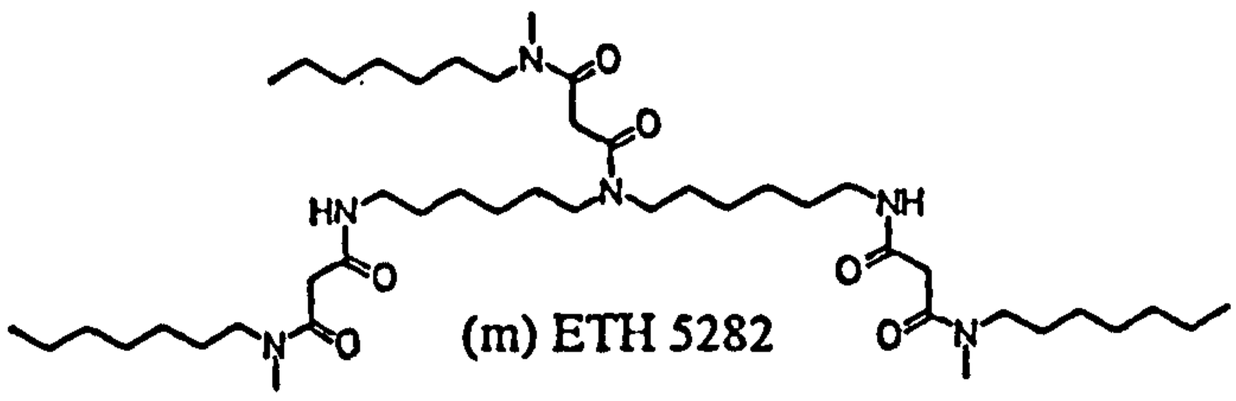

(m) ETH 5282

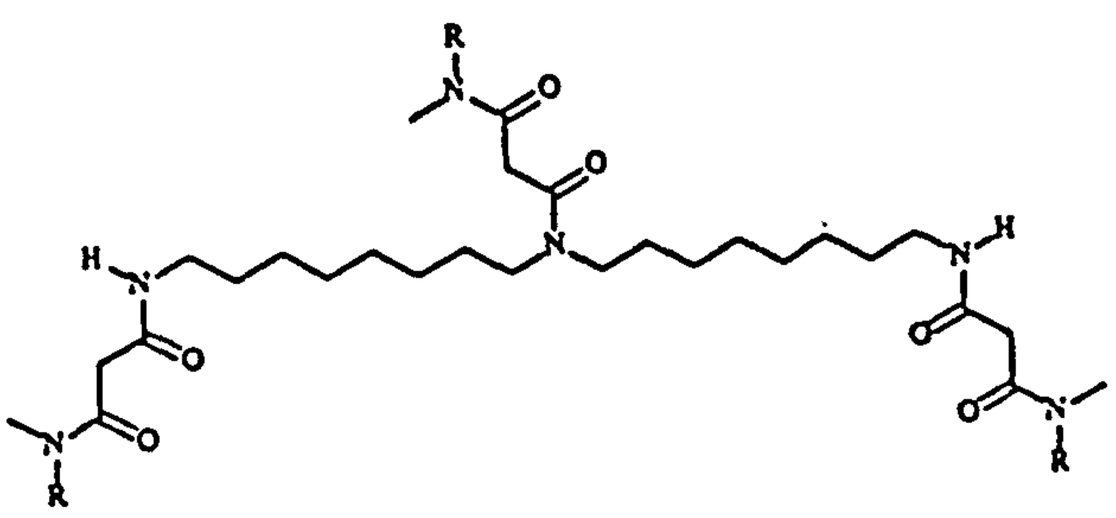

(n) ETH 7025 R = $CH_2(CH_2)_5CH_3$ (heptyl group)

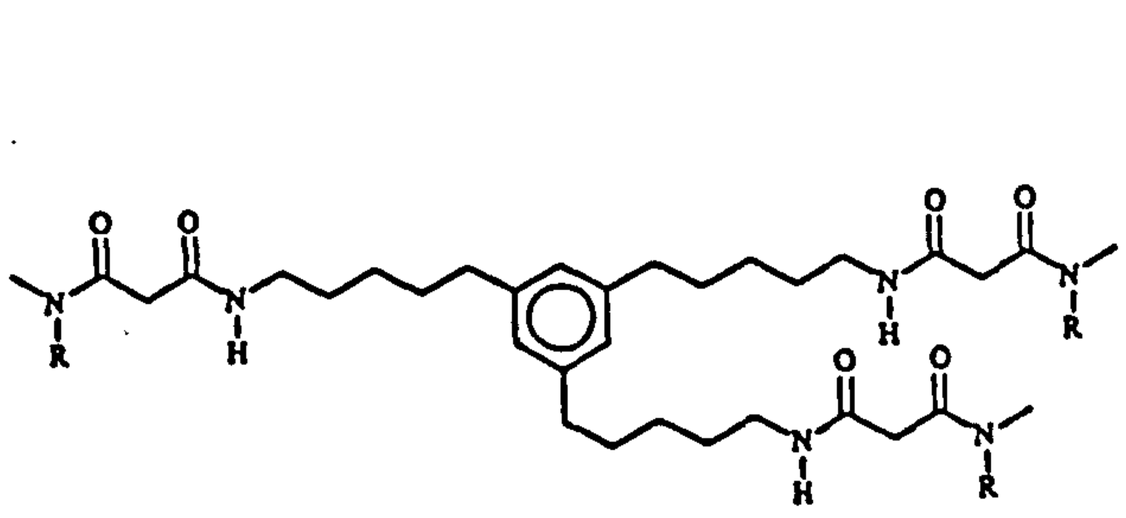

(o) ETH 3832 R = $CH_2(CH_2)_5CH_3$ (heptyl group)

(p) ETH 7160 R = 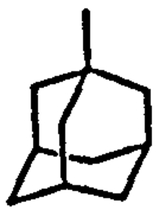 (adamantyl group)

(q) ETH 5506 R =  (adamantyl group)

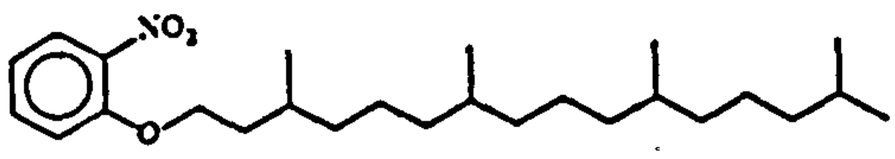

(r) ETH 5373

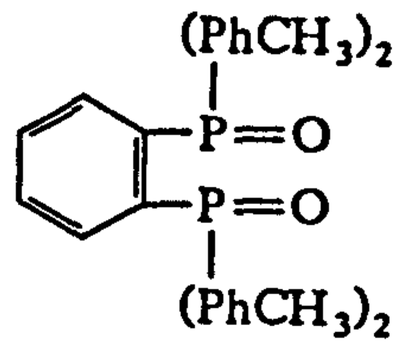

(s) 1,2-bis(ditolylphosphine oxide)benzene

Fig. 2.2 (cont.)

In the class of synthetic carriers, cyclic octa- and decapeptides were synthesized as potential magnesium selective carriers by Simon et al. [22]. When their ion selectivity in solvent PVC membranes was tested, of the eight compounds synthesized, three were found to have useful properties. One (fig. 2.2(c)) having selectivity toward the Mg^{2+} ions in the presence of Li^+, Na^+, and K^+, but poorly selective in the presence of Ca^{2+} ions, and the other two selective toward Mg^{2+} in the presence of Ca^{2+}, but sensitive toward alkali metal ions [22].

β-diketones such as dibenzoylmethane (DBM, fig. 2.2(d)) were demonstrated to have chelating tendencies toward metal ions especially of group II divalent metals [23, 24]. Various lipophilic β-diketones have been prepared and investigated in PVC liquid membrane selective electrodes for magnesium [25, 26]. The ionophore 4,4'-dichlorodibenzoylmethane was shown to induce relatively high preference for Mg^{2+} and Ca^{2+} over Na^+ and K^+ [25]. It has been suggested for the preparation of sensors to assay water hardness [27]. Nagashima et al. [26] reported that an electrode based on 2-acetyl-1-tetralone (fig. 2.2(e)), which is a β-diketone, has good Mg^{2+} selectivity and strongly discriminates against calcium ions but only under high pH conditions (pH 10). The keto-enol equilibrium of the β-diketone compound varies with the sample solution pH. The proton of the α-carbon between the carbonyl carbons of the β-diketone is released in high pH solution, so that the compound converts from a keto form to an enol form. Consequently, an electrode based on the β-diketones apparently responds preferentially to magnesium ions in alkaline solution (pH > 8) [26].

Bis-β-diketones were bridged by covalently linking two β-diketone subunits (fig. 2.2(f)) and substituted by electron donor groups, hopefully to

improve the Mg^{2+} selectivity induced by membranes containing β-diketones as complexing agents [28]. Potentiometric studies showed no improvement of the ion selectivities induced by the bridged systems when compared to unbridged compounds. No magnesium selectivity over calcium was obtained [28].

Di- and tri-oxaalkane diamides have been investigated by Simon and coworkers for some years as possible synthetic neutral ligands for alkaline earth cations. This led to the development of the first neutral carrier for calcium [29]. A slightly improved structure, made in 1975 [30], is shown in figure 2.2(g). The successful development of this compound gave rise to model calculations of interactions between compounds of similar structure with calcium as well as magnesium [31].

According to model calculations, a preference for Mg^{2+} was suggested to be achieved by an octahedral coordination of the cation with the O-atoms present in the high-dipole-moment ligand group [31]. A number of electrically neutral lipophilic di- and triamides were synthesized and their ion selectivity in solvent polymeric membranes was studied [17]. These ligands were considered likely ionophores for Mg^{2+} due to the possibility that they might form magnesium ligand complexes having an octahedral coordination of Mg^{2+} with the ligand O-atoms. A noncyclic diamide was shown to exhibit magnesium ion selectivity. The neutral carrier ETH 1117 (fig. 2.2(h)) rejected Na^+ and K^+ in respect to Mg^{2+}. However, it was unselective for Mg^{2+} over Ca^{2+}. The ionophore was suggested [17] to have sufficient selectivity for intracellular Mg^{2+} measurements.

Following this, a large series of neutral carriers including derivatized mono-, bis-, and tris- malondiamides, as well as some glutaramides and aspartamides were synthesized and tested [32]. Among the large number

of compounds investigated, the following proved to be particularly suited for analytical applications because of their selectivity for magnesium.

The aspartamide derivative ETH 2220 (fig. 2.2(i)) was shown to have high selectivity for Mg^{2+} over Ca^{2+} while rejecting all alkali and all other alkaline earth metal cations. Unfortunately, there existed a strong interference by hydrogen ions which limited the application to hydrogen ion buffered solutions at pH values 8 to 9 [33].

In the class of bis-malondiamides, the neutral carrier ETH 4030 (fig. 2.2(j)) exhibited a high rejection of Na^+ and K^+ at about equal selectivity for Mg^{2+} and Ca^{2+} [34]. The membrane plasticizer has a marked effect on the selectivity of the membrane. With chloroparaffin as a plasticizer, the membrane containing this ligand was optimized, in respect to equal selectivity for Mg^{2+} and Ca^{2+} and high discrimination of Na^+ and K^+, for a water hardness assay. The high selectivity against Na^+ allows the measurements also to be carried out successfully in the presence of high sodium chloride concentrations (e.g. in sea water). Although ETH 4030 and other bis-malondiamides exhibit good selectivities for Mg^{2+}, their solubilities in plasticizers such as o-NPOE are limited, showing a strong tendency to crystallize in the membrane. However, in chloroparaffin ($\approx$ 60 %) they are sufficiently soluble for use in ISEs. The compound ETH 5214 (fig. 2.2(k)), which is a bis-malondiamide, did not show the above adverse effect of crystallization in the membrane [35]. However, its selectivity properties were only sufficient for intracellular magnesium measurements. The ligand ETH 5220 (fig. 2.2(l)) [36], which has similar selectivity properties to ETH 4030, also has the advantage of high lipophilicity, P (log P = 11.4, P is the partition coefficient between octan-

1-ol and water [37]). Thus it is leached out of membranes very slowly, giving rise to longer lifetime membranes.

The neutral ionophore ETH 5282 (fig. 2.2(m)), a tris-malondiamide, has been used for the determination of free ionized magnesium in blood serum [38]. The ligand still does not induce the required discrimination against calcium but this was corrected by calibrating the electrode with standard solutions containing physiological concentrations of calcium.

A major step forward was obtained with compound ETH 7025 (fig. 2.2(n)) which has lipophilicity (log P ≈ 7) of about 2 units higher than the aforementioned ionophore ETH 5282 and showed a lower calcium interference [39, 40]. Its selectivities and behaviour in certain membrane matrices was sufficient to allow the measurement of ionized magnesium in extracellular as well as in intracellular fluids [40-42, 84].

A further Mg selective ligand synthesized by Simon's group was ETH 3832 (fig. 2.2(o)) that showed better magnesium selectivities than ETH 7025 [43, 44]. On substitution of the heptyl groups of the ETH 7025 and 3832 by adamantyl groups, to give ETH 7160 (fig. 2.2(p)) and 5506 (fig. 2.2(q)) respectively , the selectivities of magnesium over calcium were improved [44]. With the use of ETH 5373 (fig. 2.2(r)) as a plasticizer, instead of o-nitrophenyl octyl ether (o-NPOE), all of the four aforementioned ionophores showed an improvement in magnesium selectivities especially against calcium and potassium. Among these four ionophores, ETH 5506, with its log $K_{Mg,Ca}$ = -1.9 and log $K_{Mg,K}$ = -3.7, showed the highest magnesium selectivities [44].

Other attempts to improve the ion selectivities of magnesium ionophores, especially over calcium, were carried out by synthesizing a series of ETH 7025 isologues by changing the number and position of the

secondary amide groups of ETH 7025 [45]. However, none of these ionophores induced higher magnesium selectivities than ETH 7025.

There are also many publications presenting other magnesium-selective compounds [46-50], but none of the selectivity patterns of these carriers competes with the ETH carriers mentioned above.

Recently, organo-phosphorus compounds such as that shown in figure 2.2(s) have been tested in magnesium selective electrodes [51]. Among several compounds investigated, it was found that a magnesium-selective PVC membrane electrode based on the neutral bidentate organo-phosphorus compound, shown in figure 2.2(s), has excellent magnesium selectivity over Ca^{2+}. The electrode also exhibited good selectivity for magnesium in comparison with alkali and other alkaline earth cations.

Properties of a further synthetic magnesium ionophore have been reported by NOVA Biomedical, however the structure has not been revealed. The NOVA ionophore was shown to be suitable for extracellular Mg^{2+} determination having little interference from calcium [52-56].

2.6.3 Magnesium-Selective Membranes based on Neutral Carriers.

The membranes incorporating neutral carriers are generally composed of:

- a neutral carrier, or ionophore
- a solvent/plasticizer
- a polymer
- a lipophilic anion salt

The polymer PVC is that most commonly used as a membrane support in neutral carrier membranes. For cation selective membranes, the polymer plays a role in the exclusion of anions from the membrane phase [59, 60].

(a) Plasticizers.

The role of the plasticizers in neutral carrier membranes, apart from softening the PVC polymer, is the contribution to the function and selectivity of the membrane. This characteristic makes the choice of the plasticizer critical.

Müller et al. [34] found that with *p*-nonyl-phenol (*p*-NP) as a plasticizer, the magnesium carrier ETH 4030, in a membrane with 70 mol % lipophilic borate, KTpClPB, relative to the ligand, did not induce any selectivity toward the magnesium ion while through the use of other plasticizers such as chloroparaffin (ClP) or o-nitrophenyl phenyl ether (o-NPPE), ETH 4030 membranes exhibited good selectivity (see table 2.2). The most common plasticizer for use with magnesium selective neutral ionophores is o-nitrophenyloctyl ether (o-NPOE). It is relatively polar compared with the plasticizers used with alkali metal selective membranes, such as di(ethylhexyl)sebacate (abbreviated to DOS). A high dielectric constant (ε) of the plasticizer improves the selectivity toward Mg^{2+} over the monovalent and other divalent ions. Magnesium ion with its a smaller radius is less rejected by a more polar liquid membrane medium. Generally an increased/enhanced discrimination of divalent over monovalent ions is achieved by increasing the polarity (dielectric constant) of the membrane solvent. Such a trend has been observed in potentiometric studies with neutral carrier-based liquid membranes [61, 62].

Chloroparaffin was found to have a higher lipophilicity than o-NPOE, however, the polarity (dielectric constant) is lower (table 2.3). A solvent with high lipophilicity would increase the life time of the membrane [63] and possibly minimize the effect of protein adsorption on the membrane surface [64].

Table 2.3. Lipophilicity and dielectric constant of o-nitrophenyloctylether (o-NPOE), chloroparaffin (ClP) and di(ethylhexyl)sebacate (DOS) taken from [65].

plasticiser	log P	ε
o-NPOE	5.9	23.9
ClP	6.4-9.3	7.9
DOS	10.95	3.9

(The lipophilicity, P, is the partition coefficient between octan-1-ol and water [37])

(b) Effect of the lipophilic anion.

The addition of the salt of a lipophilic anion such as potassium tetrakis(p-chlorophenyl)borate (KTpClPB) to the neutral carrier membrane has proved to have several beneficial effects such as:- reduction of interferences by anions in the sample [66], reduction of the electrical resistance of the membrane [67], and improvement of the selectivity and response behaviour of the membrane [68, 69].

The optimum amount of lipophilic anion to be incorporated into the membrane phase has been investigated theoretically and experimentally [68, 70]. The Mg^{2+}-selective neutral carriers ETH 1117 [70], ETH 5282 and ETH 2220 [68] were applied as test compounds for evaluating the changing selectivities of selective carriers related to varying concentrations of KTpClPB added to the membrane bulk. The selectivity factors were determined using separate solutions of the primary and interferent ions. The experimental results, as well as a theoretical treatment of such systems, show that the selectivity characteristics of certain electrodes can be improved to a large extent by the optimization of the KTpClPB/ionophore ratio. The theoretical predictions for the optimum mole ratio of anionic additive to neutral ligand are summarised in table 2.4. The optimum ratio is dependent on the ion charges and stoichiometries of

the ion-ligand complexes but virtually independent of the ionic distribution coefficients and complex stability constants.

Table 2.4. Optimum amounts of charged sites trapped in neutral carrier based ion-selective membranes [68]

$\|z_i\|$	$\|z_j\|$	n_i	n_j	molar ratio anionic site/ionophore
2	2	1	2	1.41
2	2	2	3	0.77
2	2	3	4	0.54
2	1	1	1	1.62
2	1	2	2	0.73
2	1	3	3	0.46
1	1	1	2	0.71

z = the ion charge ; n = stoichiometry of the ion-ligand complex ;
i = the primary ion ; j = the interferent ion

The selectivity characteristics of the neutral carrier membranes studied were strongly dependent on the concentration of anionic membrane components. Not only the selectivity factors for monovalent ions, but also those for calcium and barium ions (relative to magnesium ion), were sensitive to changes in the additive/carrier ratio.

Several neutral carriers, such as the magnesium carriers ETH 5282 [68] and ETH 4030 [34], did not induce any selectivity in membranes in the absence of anionic sites. This phenomenon was considered to have occurred due to kinetic limitations in the transfer of ions from the sample solution to the membrane phase [71]. Lipophilic anionic components could catalyze this cation transfer [71]. The amount of added salt, however, must be strictly limited because excessive concentrations would cause the membrane to behave as a pure ion-exchange membrane and the ionophore would no longer affect the response.

The optimum selectivity for ETH 5282 based membranes was obtained with approximately 150 mol % of anionic sites relative to the ligand content. This indicates that Mg^{2+} forms 1:1 complexes with ETH 5282 [68]. The Mg^{2+}-selective ionophore ETH 2220 was assumed to form 1:2 complex with magnesium [33]. If a singly charged interferent ion also complexes with 2 ionophore molecules, the predicted optimum salt addition, which confers the optimum selectivity scale, would be 73 mol % compared to the molar concentration of the ligand. The molecular design model of the complex Mg^{2+}-ETH 7025 indicates a 1:1 stoichiometry for the magnesium-ligand-complex and a 1:2 stoichiometry for the calcium-ligand-complex [72]. The ionophore ETH 1117 was expected to form a 1 : 3 Mg^{2+}/ligand complex [17]. However, a ^{13}C NMR study of $Mg(SCN)_2$ with ETH 1117 pointed to a formation of 2 : 3 Mg^{2+}/ligand complex [17].

Highly substituted borates, e.g. sodium tetrakis[3,5-bis(tri-fluoromethyl)phenyl]borate (NaTFPB), and sulphonic acid compounds, e.g. dinonylnaphthalenesulphonic acid (DNNS) have also been suggested for use as anionic additives for extending the life time of membranes [69].

2.6.4 Applications of Magnesium-Selective Electrodes.

In 1980, Simon et al. reported the first Mg^{2+}-selective liquid membrane microelectrode containing the neutral carrier ETH 1117 [57]. The liquid membrane was prepared with a solution of sodium tetraphenylborate (NaTPB) in propylene carbonate (PC). The microelectrode has been successfully used in intracellular Mg^{2+} studies [73-78], however, it suffered from K^+ interference. Later, an improved microelectrode with ETH 5214 as ionophore was described [35]. This

ionophore is particularly useful for microelectrodes because of its good solubility in the membrane phase. In spite of slight interference from K^+, the electrode is sufficiently selective for intracellular Mg^{2+} assays. A water hardness ion-selective electrode based on this neutral carrier with an optimized membrane composition was also described [79]. In 1989, the first report of the successful determination of magnesium in natural water using an ISE based on ionophore ETH 4030 was published [80]. Rouilly et al. [38] were successful in measuring blood serum ionized magnesium with an ISE based on magnesium ionophore ETH 5282. The calcium activity at the physiological level still interferes but this was corrected by calibrating the electrode with standard solutions containing calcium at the same concentration as in the serum to be measured. In 1990, a magnesium ion-selective electrode incorporating the ionophore ETH 5220 was used for the first automated method of measurement of ionized magnesium in blood serum [36]. Other electrodes which have been used for automated measurement of ionized magnesium are those containing the ionophore ETH 7025 [81-83] and that of NOVA [56] (see section 4.2, commercial analyzers). In 1993, microelectrodes based on the ionophore ETH 7025 were described [42]. They were used for intracellular as well as, under certain conditions, extracellular Mg^{2+} activity measurements.

References.

1. J. O. Isard, In: G Eisenman (editor), *Glass electrodes for hydrogen and other cations, Principles and Practice*, Marcel Dekker, Inc., New York, (1967), p.51.

2. Analytical Chemistry Division, Commision on Analytical Nomenclature, *Pure and Appl. Chem.*, 48, 129 (1975).

3. R. G. Bates and M. Alfenaar, *Ion-Selective Electrodes*, R. A. Durst (ED.), NBS, Spec. Publ., No.314, Washington, (1969).

4. P. Debye and E. Hückel, *Physikalische Zeitschrift*, 24, 185 (1923).

5. R. A. Robinson and R. H. Stokes, *Electrolyte Solutions*. 2nd edition. Butterworths, London, (1959), p. 238.

6. K. S. Pitzer, *Acc. Chem. Research*, 10, 371 (1977).

7. J. F. Zemaitis Jr., D. M. Clark, M. Rafal and N. C. Scrivner, *Handbook of aqueous electrolyte thermodynamics*, AICHE, New York, (1986).

8. T. Mussini, *J. Chem. Education*, 65, 242 (1988).

9. R. A. Robinson and R. H. Stokes, *Electrolyte Solutions*, 2nd edition. Butterworths, London, (1959), p. 463.

10. A. K. Covington and M. J. F. Rebelo, *Ion-Selective Electrode Reviews*, Volume 5, Pergamon Press, Oxford, (1983), p. 93.

11. K. Smith, *Liquid Junction Effects in Potentiometry*, PhD Thesis, University of Newcastle-upon-Tyne, (1988), chapter 2.

12. P. L. Bailey, *Analysis with Ion-Selective Electrodes*, Heyden, London, (1976).

13. W. E. Morf, *The Principles of Ion-Selective Electrodes and of Membrane Transport*, Elsevier, Amsterdam, (1981).

14. W. Wierenga, In: *The total synthesis of Natural Products*, J. ApSimon (Ed.), Wiley-Interscience, New York, NY, Vol. 4, p. 265 (1981).

15. W. E. Morf and W. Simon, *Helv. Chim. Acta.*, 54, 2683 (1971).

16. N. Otake and M. Mitani, *Agric. Biol. Chem.*, 43, 1543 (1979).

17. D. Erne, N. Stojanac, D. Ammann, P. Hofstetter, E. Pretsch and W. Simon, *Helv. Chim. Acta*, 63, 2271 (1980).

18. P. W. Reed and H. A. Lardy, *J. Biol. Chem.*, 247, 6970 (1972).

19. P. W. Flatman and L. M. Smith, *Magnesium a Relevant Ion*, B. Lasserre and I. Durlach, Eds., John Libbey and Comp. Ltd., London, p. 191 (1991).

20. K. Suzuki, K. Tohda, Y. Tanda, H. Ohzora, S. Nishihama, H. Inoue and T. Shirai, *Anal. Chem.*, 61, 382 (1989).

21. A. K. Covington, and N. Kumar, *Anal. Chim. Acta*, 85, 175 (1976).

22. F. Behm, D. Ammann, W. Simon, K. Brunfeldt and J. Halstrøm, *Helv. Chim. Acta*, 68, 100 (1985).

23. L. G. Van Uitert, W. C. Fernelius and B. E. Douglas, *J. Am. Chem. Soc.*, 75, 2736 (1953).

24. R. C. Mehrotra, R. Bohra and D. P. Gaur, *Metal β-Diketones and Allied Derivatives*, Academic Press, London, 1978.

25. D. Erne, W. E. Morf, S. Arvanitidis, Z. Cimerman, D. Ammann and W. Simon, *Helv. Chim. Acta*, 62, 994 (1979).

26. S. Nagashima, K. Tohda, Y. Matsunari, Y. Tsunekawa, K. Watanabe, H. Inoue, and K. Suzuki, *Anal. Lett.*, 11, 1993 (1990).

27. P. C. Meier, D. Erne, Z. Cimerman, D. Ammann and W. Simon, *Mikrochim. Acta*, I, 317 (1980).

28. M. Maj-Zurawska, W. Buchser, D. Ammann, D. Welti, E. Pretsch, W. Keller-Schierlein and W. Simon, *Mikrochim. Acta*, II, 1 (1987).

29. D. Ammann, E. Pretsch and W. Simon, *Anal. Lett.*, 5, 843 (1972).

30. D. Ammann, M. Güggi, E. Pretsch and W. Simon, *Anal. Lett.*, 8, 709 (1975).

31. W. Simon, W. E. Morf and D. Ammann, *in Proceedings of the International Symposium on Calcium-Binding Proteins and Calcium Function in Health and Disease*, Cornell University, Ithaca, NY, June 5-7, 1977.

32. M. Rouilly, Ph.D Thesis, ETH Nr. 9081 (1990).

33. M. V. Rouilly, M. Badertscher, E. Pretsch, G. Suter and W. Simon, *Anal. chem.*, 60, 2013 (1988).

34. M. Müller, M. Rouilly, B. Rusterholz, M. Maj-Zurawska, Z. Hu and W. Simon, *Mikrochim. Acta*, III, 283 (1988).

35. Z. Hu, T. Bührer, M. Müller, B. Rusterholz, M. Rouilly and W. Simon, *Anal. Chem.*, 61, 574 (1989).

36. M. Maj-Zurawska and A. Lewenstam, *Anal. Chim. Acta*, 236, 331 (1990).

37. O. Dinten, U. E. Spichiger, N. Chaniotakis, P. Gehrig, B. Rusterholz, W. E. Morf and W. Simon, *Anal. Chem.*, 63, 596 (1991).

38. M. Rouilly, B. Rusterholz, U. E. Spichiger and W. Simon, *Clin. Chem.*, 36, 466 (1990).

39. U. E. Spichiger, R. Eugster, A. Schmid, P. Gehrig, B. Rusterholz and W. Simon, In: R. W. Burnett, N. Gochman, G. A. Graham, A. H. J. Maas, R. F. Moran and A. L. Vankessel, *on Methodology and Clinical Applications of Blood Gases, pH, Electrolytes and Sensor Technology*, IFCC, 12, 279 (1990).

40. U. E. Spichiger, R. Eugster, E. Hasse, G. Rumpf, P. Gehrig, A. Schmid, B. Rusterholz and W. Simon, *Fresenius J. Anal. Chem.*, 341, 727 (1991).

41. U. E. Spichiger, R. Eugster, U. Schaller, E. Hasse and W. Simon, *Magnesium Bulletin*, 13, 4, 140 (1991).

42. U. Schaller, U. E. Spichiger and W. Simon, *Pflügers Arch.*, 423, 338 (1993).

43. U. E. Spichiger, R. Eugster, D. Citterio, H. Li, A. Schmid and W. Simon, *Proc. IVth European Cong. on Magnesium*, September 21-23, Giessen, BRD/FRG, (1992).

44. J. O'Donnell, H. Li, B. Rusterholz, U. Pedrazza and W. Simon, *Anal. Chim. Acta*, 281, 129 (1993).

45. J. O'Donnell, B. Rusterholz, B. Aebersold, D. Rüegg, W. Simon and E. Pretsch, *Mikrochim. Acta*, 113, 45 (1994).

46. K. Hiratani, K. Taguchi and H. Sugihara, *J. Membrane Science*, 56, 153 (1991).

47. E. Kimura, Y. Kimura, T. Yatsunami, M. Shionoya and T. Koike, *J. Am. Chem. Soc.*, 109, 6212 (1987).

48. M. Otto, P. M. May, K. Murray and J. D. R. Thomas, *Anal. Chem.*, 57, 1511 (1985).

49. R. Delgado, L. C. Siegfried and T. A. Kaden, *Helv. Chim. Acta*, 73, 140 (1990).

50. A. L. Grekovich and S. E. Didina, *Soviet Electrochemistry*, 26, 426 (1990).

51. M. B. Saleh, *J. Electroanal. Chem.*, 273, 89 (1994).

52. B. T. Altura and B. M. Altura, *Magnesium Trace Elem*, 9, 311 (1990).

53. B. T. Altura, T. Shirey, C. C. Young, J. Hiti, K. Dell'Orfano, S. M. Handwerker and B. M. Altura, *Methods Find. Exp. Clin. Pharmacol.*, 14, 297 (1992).

54. B. T. Altura, T. Shirey, C. C. Young, K. Dell'Orfano and B. M. Altura, In: P. D'Orazio, M. F. Burritt and S. F. Sena, *Electrolytes, Blood Gases, and Other Critical Analytes:The Patient, the Measurement, and the Government*, IFCC, 14, 152 (1992).

55. B. T. Altura and B. M. Altura, *Magnesium Trace Elem*, 10, 90 (1992).

56. B. T. Altura, T. L. Shirey, C. C. Young, K. Dell'Orfano, J. Hiti, R. Welsh, Q. Yeh, R. L. Barbour and B. M. Altura, *Scand. J. Clin. Lab. Invest.*, 54, Suppl. 217, 21 (1994).

57. F. Lantner, D. Erne, D. Ammann and W. Simon, *Anal. Chem.*, 52, 2400 (1980).

58. R. Eugster, B. Rusterholz, A. Schmid, U. E. Spichiger and W. Simon, *Clin. Chem*, 39, No.5, 855 (1993).

59. W. E. Morf and W. Simon, *Anal. Lett.*, 22, 1171 (1989).

60. R. D. Armstrong and G. Horvai, *Electrochimica Acta*, 35, 1 (1990).

61. U. Fiedler, *Anal. Chim. Acta*, 89, 111 (1977).

62. D. Ammann, E. Pretsch and W. Simon, *Anal. Lett.*,5 ,843 (1972)

63. U. Oesch, A. Xu, Z. Brzózka, G. Suter and W. Simon, *Chimia*, 40, 351 (1986).

64. U. Oesch, D. Ammann and W. Simon, In: A. H. J. Maas, A. B. T. J. Boink, N. E. L. Saris, R. Sprokholt and P. D. Wimberley (editors), *Methodology and clinical applications of ion-selective electrodes*, IFCC, 7, 273 (1986).

65. O. Dinten, Ph.D Thesis, ETH Nr. 8591 (1988).

66. W. E. Morf, G. Kahr and W. Simon, *Anal. Lett.*, 7, 9 (1974).

67. D. M. Band and J. Kratochvil, *J. Physiol.*, 239, 10P (1974).

68. R. Eugster, P. M. Gehring, W. E. Morf, U. E. Spichiger and W. Simon, *Anal. Chem.*, 63, 2285 (1991).

69. T. Rosatzin, E. Bakker, K. Suzuki and Wilhelm Simon, *Anal. Chim. Acta*, 280, 197 (1993).

70. P. C. Meier, W. E. Morf, M. Läubli and W. Simon, *Anal. Chim. Acta*, 156, 1 (1984).

71. P. M. Gehring, W. E. Morf, M. Welti, E. Pretsch and W. Simon, *Helv. Chim. Acta*, 73, 203 (1990).

72. U. E. Spichiger, R. Eugster, U. Schaller, E. Hasse and W. Simon, *Magnesium Bulletin*, 13, 4, 140 (1991).

73. Ref. 57.

74. P. Hess and R. Weingart, *J. Physiol.*, 318, 14 P (1981).

75. P. Hess, P. Metzger and R. Weingart, *J. Physiol*, 333, 173 (1982).

76. J. R. López, L. Alamo, C. Caputo, J. Vergara and R. Dipolo, *Biochimica et Biophysica Acta*, 804, 1 (1984).

77. F. J. Alvarez-Leefmans, S. M. Gamiño, F. Giraldez and H. González-Serratos, *J. Physiol*, 378, 461 (1986).

78. M. MacDermott, *Experimental Physiology*, 75, 763 (1990).

79. Z. Hu and D. Qi, *Anal. Chim. Acta*, 248, 177 (1991).

80. M. Maj-Zurawska, M. Rouilly, W. E. Morf and W. Simon, *Anal. Chim. Acta*, 218, 47 (1989).

81. H. J. Marsoner, U. E. Spichiger, Ch. Ritter, Ch. Sachs, M. Ghahramani, H. Offenbacher, H. Kroneis, C. Kindermans and M. Dechaux, *Scand. J. Clin. Lab. Invest.*, 54, Suppl. 217, 45 (1994).

82. C. Sachs, Ch. Ritter, A. C. Puaud, M. Gahramani, C. Kindermans, U. E. Spichiger and H. J. Marsoner, In: M. Aizawa, T. Goto, M. Hattori, K. Kuwa, A. H. J. Maas, E. Niki, T. Ogata, K. Sugahara, Y. Ujihira, M. Umemoto and K. Yasuda, *Methodology and Clinical Applications of Blood Gases, pH, Electrolytes and Sensor Technology*, IFCC, 13, 177 (1992).

83. A. C. Truttmann, D. M. Gerber, D. Lüthi and J. A. S. McGuigon, *J. Physiol.*, 477, 3P (1994).

84. W. Zhang, A. C. Truttmann, D. Lüthi and J. A. S. McGuigan, *Magnesium Bull.*, 17, 4, 125 (1995).

CHAPTER 3

CALIBRATION AND SELECTIVITY MEASUREMENTS ON ISEs

Before considering the application of any ion-selective electrode to a particular situation, it is necessary to know how it will perform. There are many methods used to assess the performance of an ion-selective electrode and judge its potential usefulness, such as [1, 2]:

1. Calibration slope
2. Detection limit
3. Selectivity
4. Stability and reproducibility.

In this chapter, the first three methods will be dealt with. The stability and reproducibility are discussed in chapter 4. The electrodes tested were magnesium ion-selective electrodes based on the ionophores ETH 1117, 4030 and 7025, and calcium ion-selective electrode based on ETH 1001. These electrodes have been used either as dip-type sensors or were incorporated in a flow-through system.

In the following, experimental details will be given on the preparation of solvent polymeric membranes, their incorporation into the ion-selective electrodes, the electrochemical cells, the instrumentation used for potential difference measurements and then the methods used to assess the performance of the ion-selective electrodes.

3.1 Preparation of Membranes.

The membranes of the magnesium and calcium ion-selective electrodes were prepared using the following steps.

The membrane components were weighed on a Sartorius 2474 five figure balance. Table 3.1 gives the membrane composition of the magnesium and

calcium ionophores used in this work together with the weights of the components used (in parenthesis). The total weight of the membrane components used was ≈ 500 mg. The chemicals used were obtained from Fluka.

Table 3.1

Ionophore	Membrane composition [a]
ETH 1117	1 % ionophore (5 mg) 30 % PVC (150 mg) 69 % o-NPOE (345 mg) + KTpClPB (5.1 mg), in a mole ratio of 0.7 mole KTpClPB : 1 mole ETH 1117
ETH 4030	1 % ionophore (5 mg) 33 % PVC (165 mg) 66 % ClP (330) + KTpClPB (3.22 mg), in a mole ratio of 0.7 mole KTpClPB : 1 mole ETH 4030
ETH 7025	1 % ionophore (5 mg) 33 % PVC (165 mg) 63 % o-NPOE (315 mg) 3 % ETH 500 (15 mg) + KTpClPB (4.45 mg), in a mole ratio of 1.55 mole KTpClPB : 1 mole ETH 7025
ETH 1001	1 % ionophore (5 mg) 33 % PVC (165 mg) 66 % o-NPOE (330 mg) + KTpClPB (2.54 mg), in a mole ratio of 0.7 mole KTpClPB : 1 mole ETH 1001

(a) PVC = poly(vinyl chloride)
o-NPOE = 2-nitro phenyl octyl ether
KTpClPB = potassium tetra (4-chlorophenyl) borate
ETH 500 = tetradodecyl ammonium-tetrakis(p-chlorophenyl)-borate.

The membrane components were dissolved in 4-5 ml of tetrahyhydrofuran (THF), obtained from BDH. THF is unstable in air where it forms explosive peroxides, therefore it is supplied with a stabiliser added. The THF was thus dried over CaH_2 and freshly distilled prior to use. Complete

dissolution of the membrane components was achieved by agitation for several hours on a mechanical shaker. The solution was left to stand for about 30 minutes to allow bubbles caused by the shaking to dissipate. The solution was then transferred to a PTFE circular mould (size = 5 cm diameter, area = 19.6 mm^2). The mould was covered with a wad of filter papers and allowed to stand overnight to evaporate the THF. The resulting membrane was then removed from the mould and stored in a dry dark place.

3.2 Electrode Construction.

In this work, two types of electrode have been used: dip-type where the electrode is dipped into the samples, and flow-type where the samples are injected past the electrode. The electrode construction of the dip-type are described below. Those of the flow-type will be described in the next chapter.

The electrode of the dip-type used in this work is shown in figure 3.1. It has the basic design of Moody and Thomas [3, 4]. The electrode body consists of a glass stem with a B7 ground glass joint at the top to accommodate the Ag/AgCl electrodes which are generally used in the laboratory. A section of PVC tubing approximately 2 cm long was fixed on to the glass tube using a glue of PVC in THF. A disc of ion-selective membrane was cut from the master membrane using a suitable cork-borer and glued to the bottom of the PVC tubing. The glue was allowed to dry for an hour. The resultant seal was checked by suspending the electrode in distilled water and gently blowing nitrogen down the electrode body. If bubbles were observed, which indicate improper sealing, the gluing process was repeated and the electrode re-checked. The electrode was

filled with an internal reference solution of 10^{-2} mol/L chloride salt of the ion of interest. The Ag/AgCl internal reference electrode was inserted in the B7 joint. The filled electrode was conditioned by overnight immersion in 10^{-3} mol/L chloride of the primary ion.

3.3 Reference Electrodes.

Throughout this study, the silver-silver chloride has been used as an internal reference electrode and was prepared in the laboratory. The calomel electrode was used as external electrode. The general requirements of reference electrodes are chemical stability, low temperature sensitivity and thermodynamic reversibility to allow recovery from any current flow [5].

3.3.1 Preparation of the Silver-Silver Chloride Electrode.

The silver-silver chloride electrode used in this work was of the thermal-electrolytic type prepared according to the basic method of Bates [6]. The basic form of the Ag-AgCl electrode used in order to fit inside a dip-type electrode is shown in fig.3.2. Those used in the reference cell are described in chapter 4.

The electrode was formed by welding a copper wire to a piece of platinum wire approximately 3 cm long. The platinum was then sealed into a glass stem with a B7 Quickfit joint. The end of the platinum wire was formed into a loop and then cleaned by dipping in concentrated nitric acid and rinsed with water several times. A layer of silver oxide paste was applied to the loop, this was air dried for 10 minutes and then suspended in a furnace at 500 °C for around 30 minutes until it had turned white. This application of silver oxide paste was repeated until a smooth 3 mm

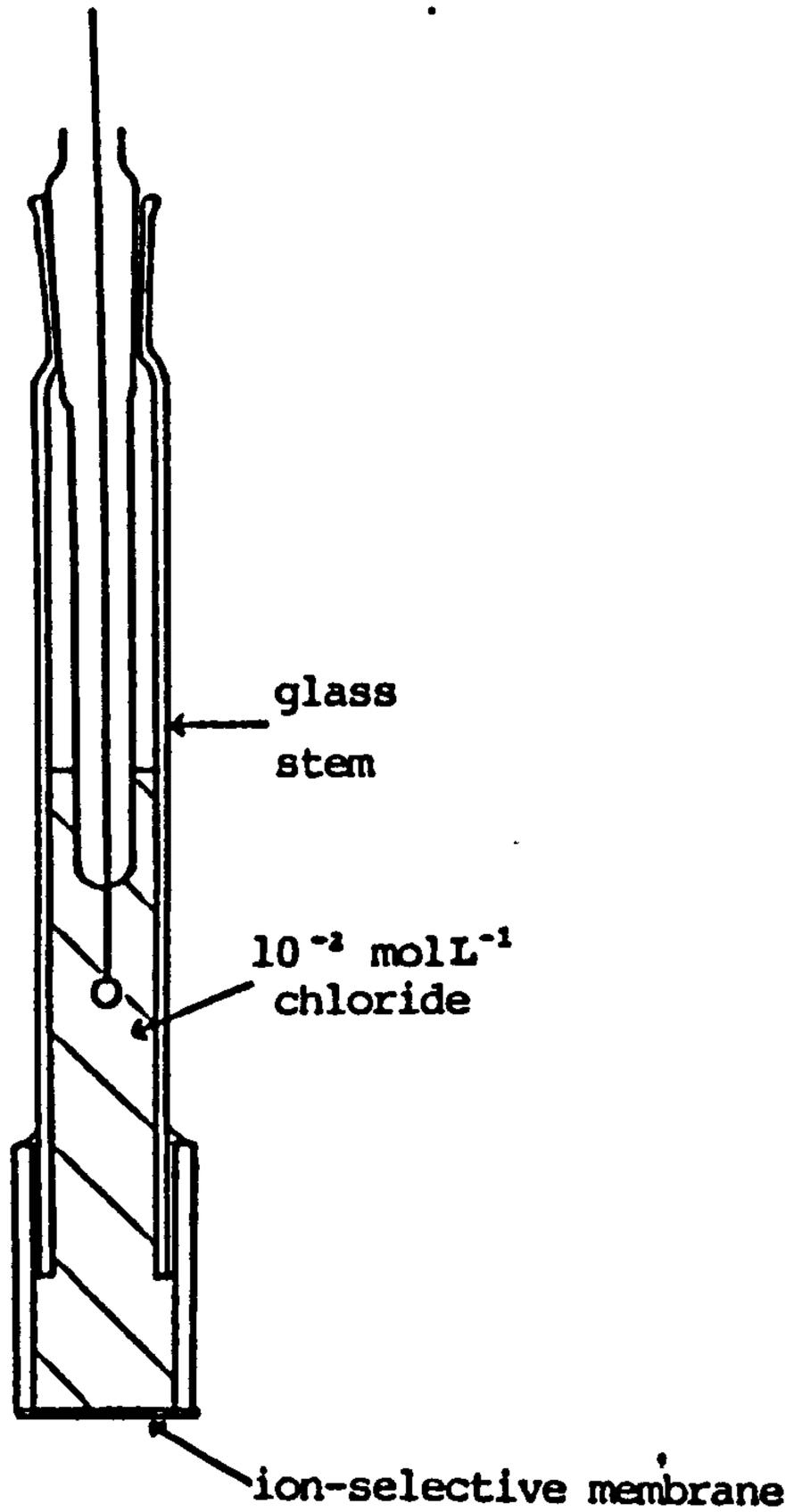

Fig. 3.1. Dip-type ion-selective electrode

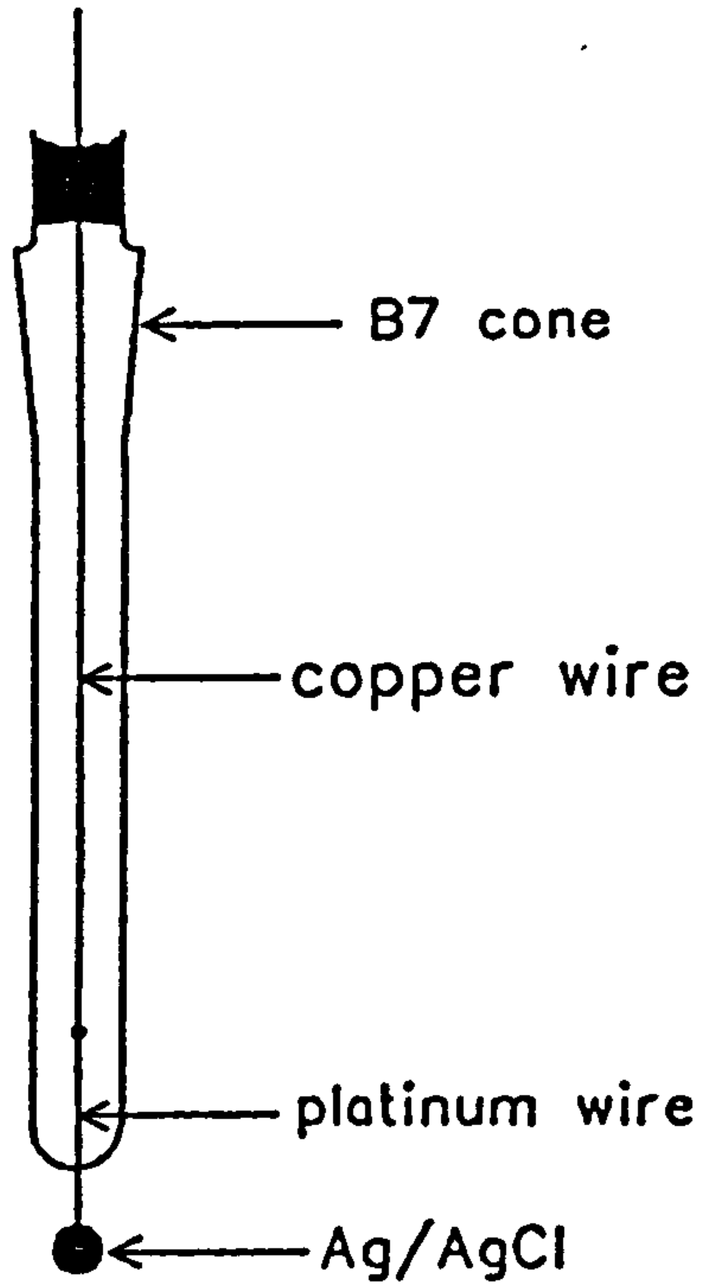

Fig. 3.2. Internal Ag/AgCl electrode

diameter sphere of silver was obtained. The electrode was then allowed to cool and the chloridation process followed. The cell consisted of the silver electrode as the anode, a platinum electrode as the cathode, and 0.5 mol/L Analar HCl. The passage of 10 mA of current for 7-8 minutes converted a small proportion of Ag to AgCl. The prepared electrodes were left in 0.05 mol/L HCl overnight.

The silver oxide paste was obtained by adding drops of sodium hydroxide solution to a silver nitrate solution while stirring vigorously. The solution was decanted off and the precipitate was washed thoroughly with distilled water again with vigorous stirring. This washing procedure was repeated more than forty times as recommended [6], for the removal of all water soluble impurities.

3.3.2 The Calomel Electrode.

In all cases the calomel electrode was employed as an external electrode combined with a salt bridge of a concentrated solution of potassium chloride (3.5 mol/L or saturated).

The calomel electrode was either suspended directly into the sample, in which case the liquid junction is formed between the sample and the internal filling solution of the electrode, or into a separate bridge solution (see section 4.4). In the first case, the type of liquid junction was a slow flow (constrained diffusion) of the internal filling solution through a ceramic frit sealed into a glass tube. The ceramic frit was regularly washed to remove any solid electrolyte material that may have accumulated. The internal reference solution was regularly replaced to ensure that solid electrolyte material did not interfere with the liquid junction.

3.4 Measuring Instrument.

The membrane resistance of ISEs is very high, as much as 10^8 Ω or more (e.g. Ca^{2+} /ISE membrane = 1 MΩ [7]). In order to measure the potentials of such high-resistance circuits accurately, it is necessary that the voltmeter have an electrical resistance that is several orders of magnitude greater than the resistance of the cell being measured. If the meter resistance is too low, current is drawn from the cell, which has the effect of lowering its output potential, thus creating a negative error. In order to achieve an accuracy of > 0.1% in a cell potential measurement, the input resistance of the measuring devices must be 10^3 times greater than the cell impedance [8]. The other necessity of using high input impedance devices is to avoid the flow of measurable current through the cell which may disturb the chemical equilibrium and cause polarization of electrodes [9].

In the initial measurements, a high impedance meter was not available in this work. so the potentiometric measurements were performed by using a low impedance digital voltmeter (Thandar TM451) with a buffer amplifier inserted between the voltmeter and electrochemical cell. A buffer amplifier, in simple terms, is an intermediary that allows measurements of potential without perturbing the electrochemical cell significantly, i.e. it is of high input impedance and draws very little current. The basic circuit diagram is shown in figure 3.3. The buffer amplifier used has one high impedance input. It has unity voltage gain but increases the current which can be drawn by the voltmeter without affecting the measured voltage. The earth is connected to the reference electrode input to reduce electrostatic noise to an acceptable level. Later, and for the most experimental measurements during this work, a computer linked electronic high

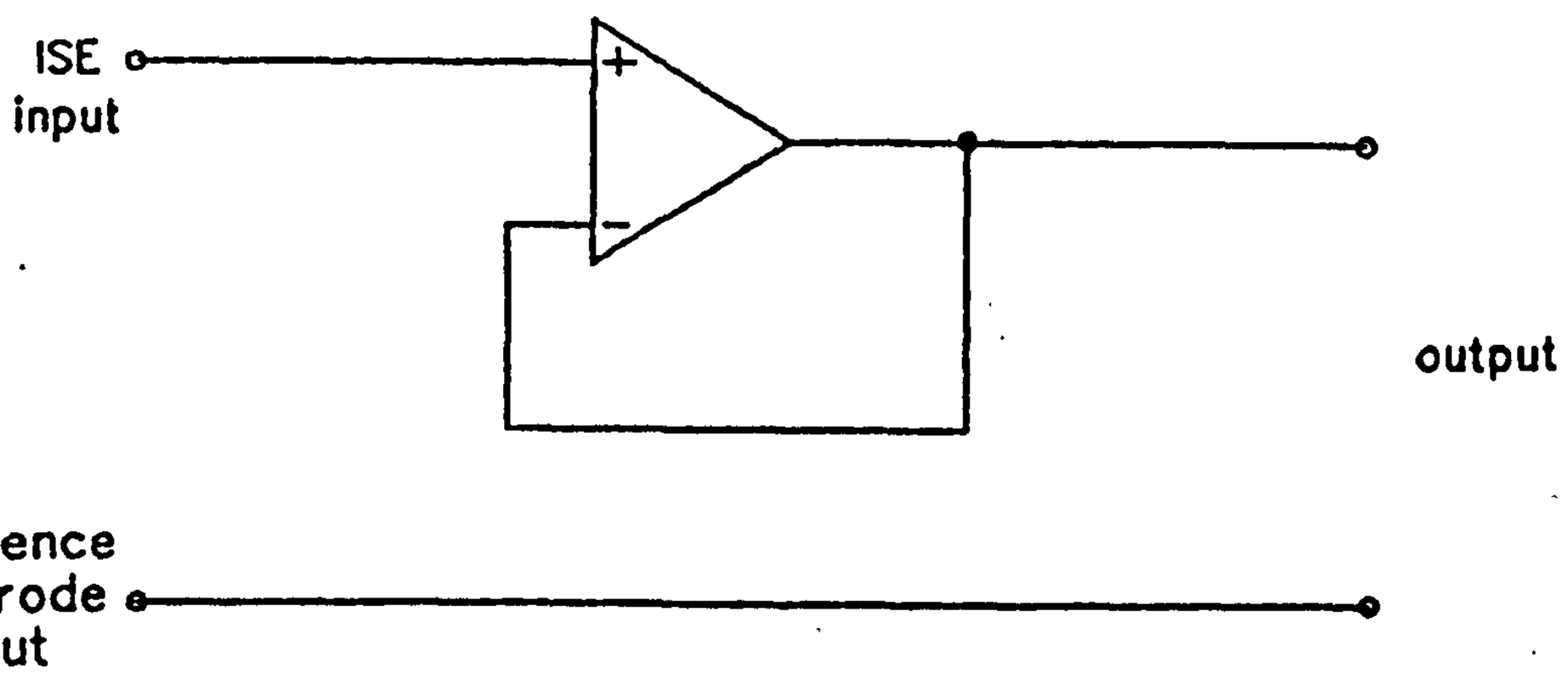

Fig. 3.3. Basic circuit diagram of a single high impedance input buffer amplifier

impedance measuring device was used. The system was floating with respect to ground, with resistance between the inputs and earth > 10^8 Ω. Further descriptions of this system are given in section 4.9.

3.5 Calibration.

Slope:

An ideal ion-selective electrode for ion *i* (primary ion) produces a potential E in solutions of this ion described by the Nernst equation:

$$E = E^o + s \log a_i$$

where E^o is the standard potential of the electrode, s is the Nernst slope which equals 2.303 RT/z_iF and a_i is the activity of the primary ion in the sample solution. Therefore, by taking potential difference measurements at a number of primary ion activities, a calibration curve can be constructed by plotting the electrode potential against log a_i. The plot will be linear with a slope of 59.2 mV and 29.6 mV (at 25 °C) for a monovalent and a divalent ion respectively. If the electrode responds non-ideally, deviation from Nernstian slope will occur.

Detection Limit:

The detection limit determines the measuring range of an ISE. According to the IUPAC [1], the limit of detection is taken as the activity of the primary ion at the point of intersection of the two linear part of the calibration curve as illustrated in figure 3.4.

Linear Limit:

The linear limit of potential response is taken as the activity of the primary ion at the point of deviation from the linear part of the plot, the part where the electrode is responding to changing activity, as shown in figure 3.4.

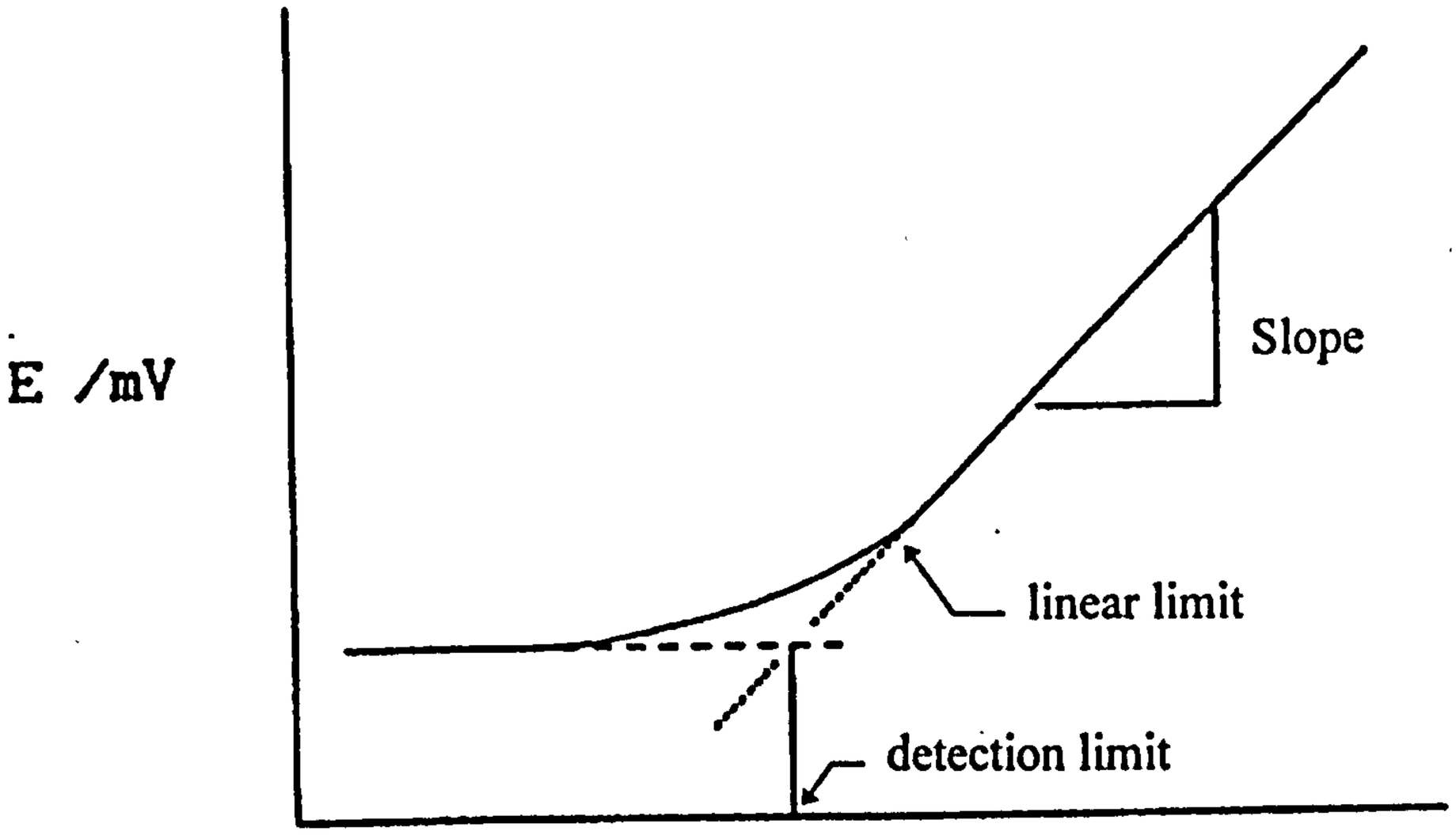

Fig. 3.4. Response of an ion-selective electrode

3.5.1 Experimental Procedure.

A cell assembly of the following type was used for the measurements:

$$Hg, Hg_2Cl_2 \left| \begin{matrix} 3.5\ mol L^{-1} \\ \text{or satd. } KCl \end{matrix} \right| \text{test solution} \left| \begin{matrix} \text{magnesium or} \\ \text{calcium electrode} \end{matrix} \right.$$

the magnesium and calcium electrodes were of a dip-type construction as described in section 3.2.

Different concentrations of $MgCl_2$ or $CaCl_2$ solutions (10^{-1}, 10^{-2}, 10^{-3}, 10^{-4}, 10^{-5} and 10^{-6} mol/L) were prepared from stock solutions of 10^{-1} mol/L $MgCl_2$ and $CaCl_2$ respectively. The series of measurements was taken starting with the lowest concentration first (10^{-6} mol/L) and increasing thereafter. The test solution was stirred to ensure the ion-selective membrane surface rapidly reached equilibrium with it. Before taking a measurement, the stirrer was switched off to avoid a noisy emf response, then the potential value was taken when the reading became stable. In between measurements, the excess solution was removed from both electrodes (the ISE and calomel electrode) using tissue to prevent carry-over.

The calibration graph was constructed by plotting the electrode potential against the logarithm of the primary ion activity. The primary ion activities were calculated using the Debye-Hückel theory; the equations and parameters were given earlier (see section 2.3).

3.5.2 Results and Discussion.

Figures 3.5 - 3.7 show the calibration curves of the ETH 1117, ETH 4030 and ETH 7025 based magnesium electrodes respectively. Figure 3.8 shows the calibration curve of the ETH 1001 based calcium electrode. The slopes and linear limits are shown in table 3.2.

Fig. 3.5 Calibration of ETH 1117 membrane

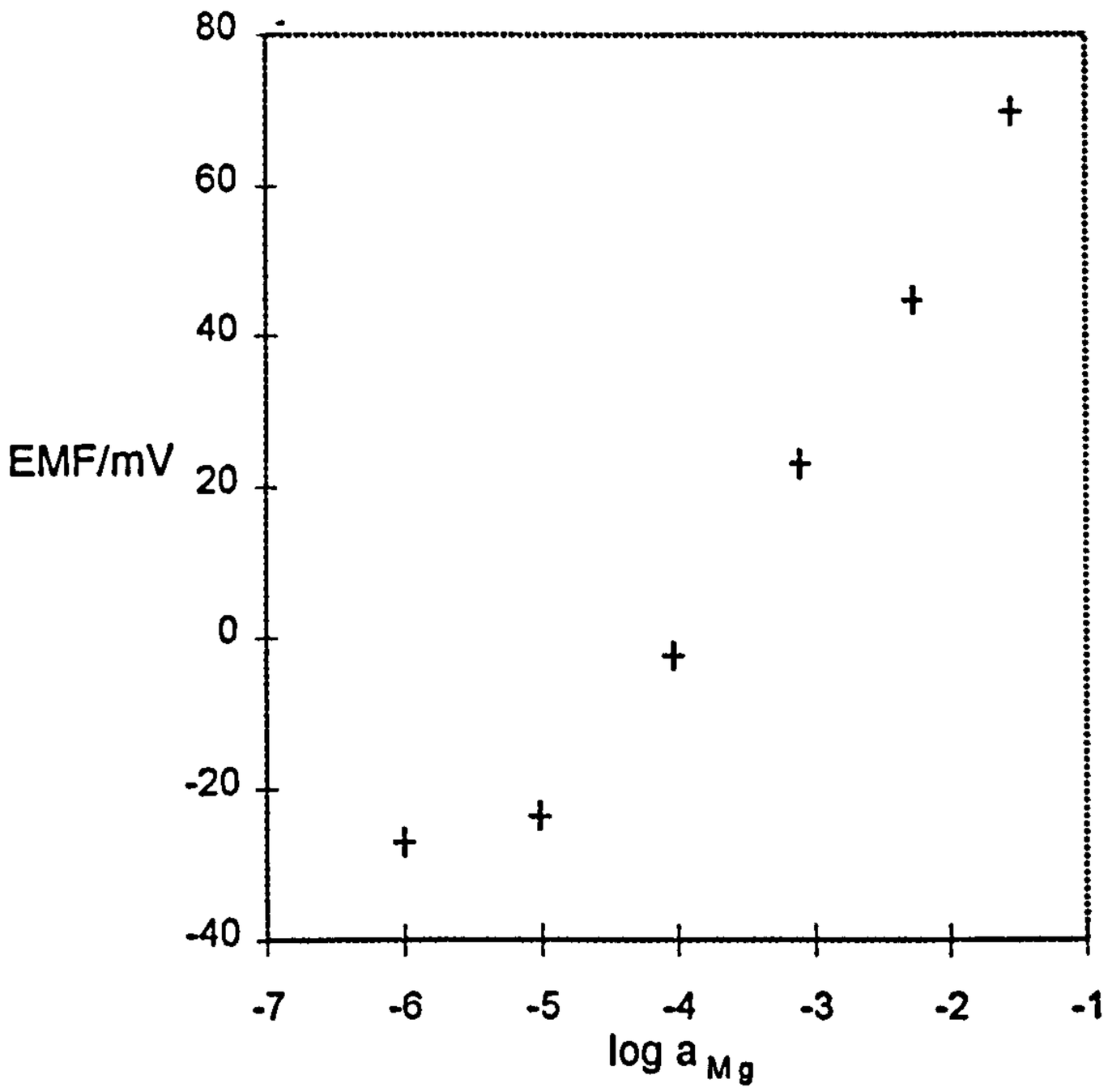

Fig. 3.6 Calibration of ETH 4030 membrane

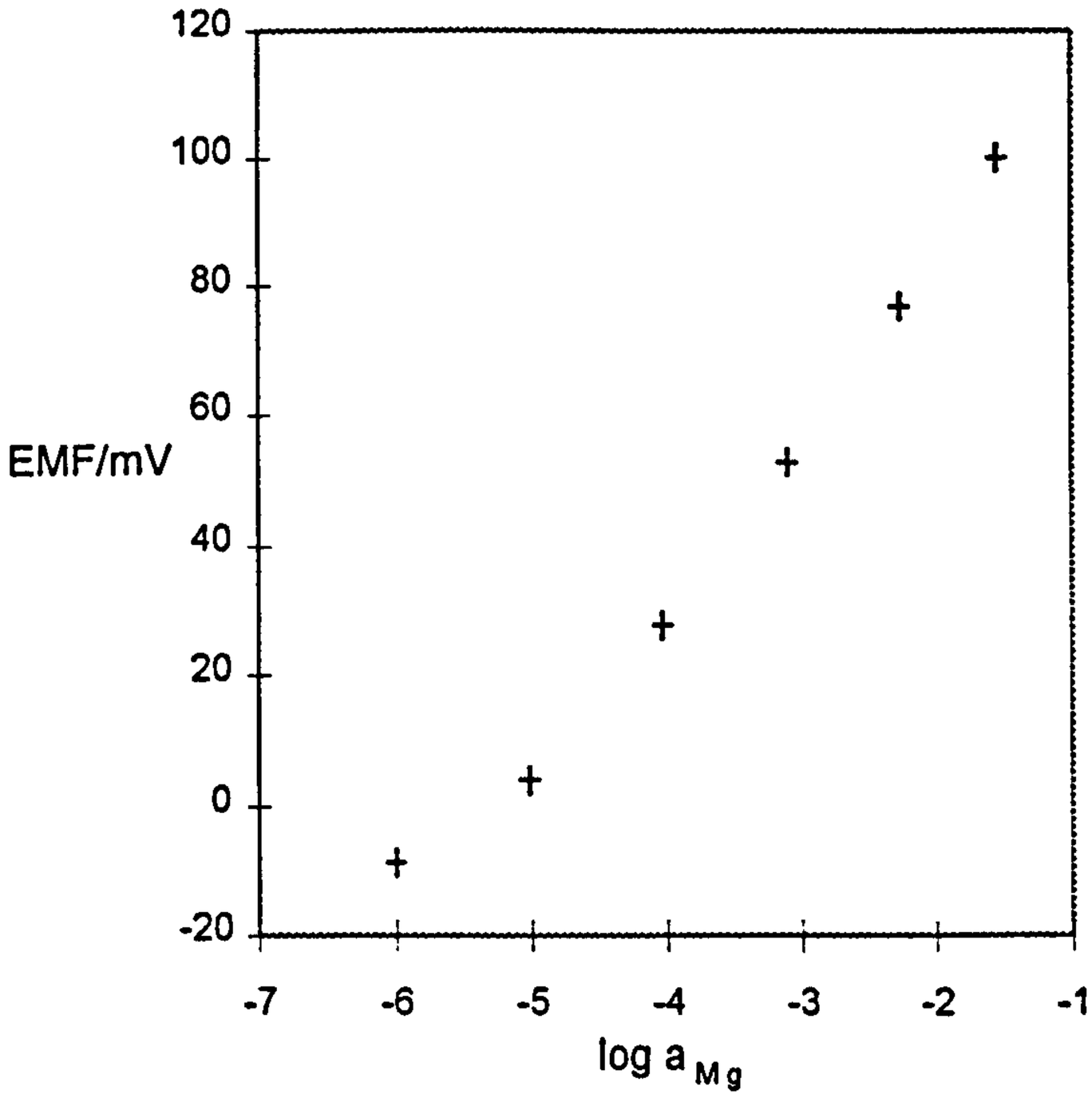

Fig. 3.7 Calibration of ETH 7025 membrane

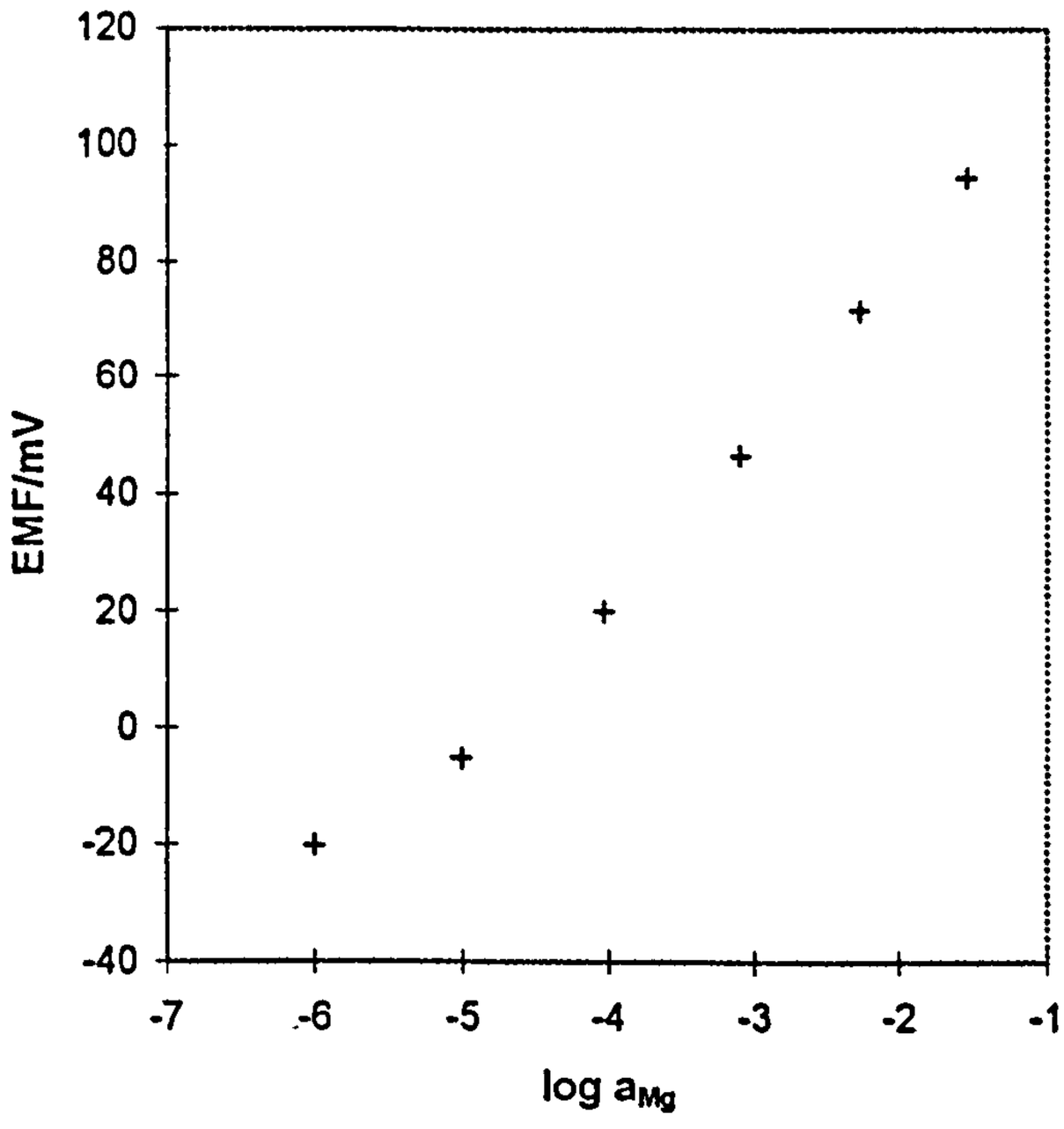

Fig 3.8 Calibration of ETH 1001 membrane

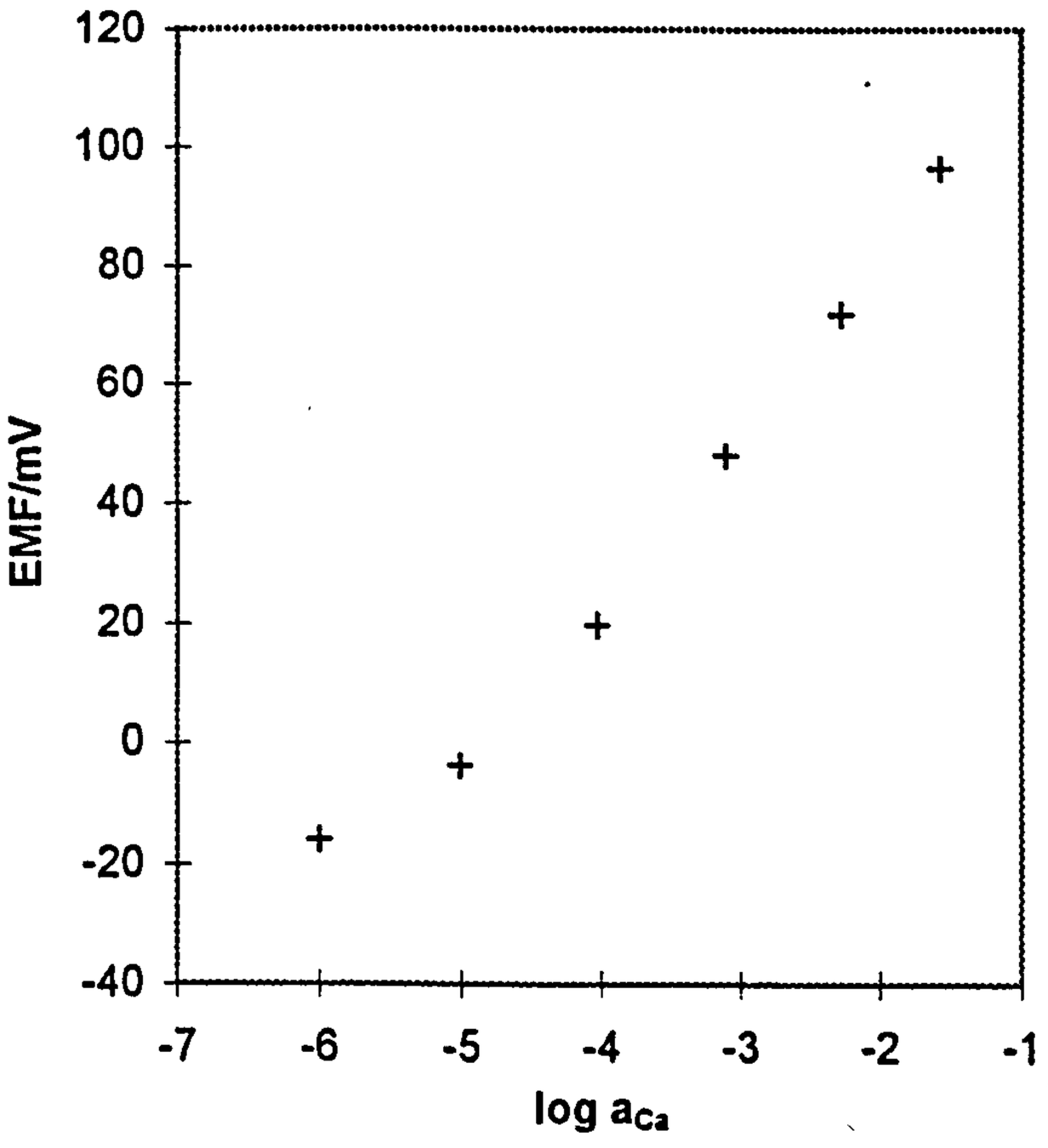

The results show that the slope values for the electrodes based on the ETH 1117 and ETH 4030 are close to the theoretical Nernstian value for a divalent cation while the ETH 7025 and ETH 1001 show excellent Nernstian slope. For each electrode, the response is linear to concentrations of at least 10^{-4} mol/L.

Table 3.2 Calibration Results.

Ionophore	slope[a] /mV	linear limit (log a_i)
ETH 1117	28.2 ± 0.5	-4.5
ETH 4030	28.4 ± 0.6	-4.6
ETH 7025	29.5 ± 0.3	-4.9
ETH 1001	29.4 ± 0.5	-4.6

a. The standard deviation of a slope is calculated for 3 repeated experiments.

3.6 Selectivity and Selectivity Coefficient.

In solutions containing other ions in addition to the primary ion *i*, the ion-selective electrode, as stated earlier, is normally not only responsive to the ion *i*, but also to the interferents. The selectivity of an ion-selective electrode to the primary ion *i*, over an interferent ion *j* present in solution, is usually described by the Nicolsky-Eisenman equation which is a modified form of the Nernst equation [1] (see section 2.2)

$$E = E^{\circ} \pm \frac{RT}{z_i F} \ln\left\{a_i + k_{i,j} a_j^{z_i/z_j}\right\} \qquad (3.1)$$

where z_i and z_j are the charges of the primary and interferent ions, a_i and a_j are the corresponding activities, E, E^o, R, T and F have their normal significance. k_{ij} is the selectivity coefficient, which is a measure of the preference of the electrode for the primary ion *i* over ion *j* at a stated concentration of *j*. The smaller the value of k_{ij}, the greater the electrode's performance for the principal ion.

There are two fundamental methods for determining the selectivity coefficient of an ion-selective electrode: using separate solutions of the primary and interferent ions, or mixed solutions. The use of mixed solutions is recommended as it usually corresponds more closely to the practical situation.

3.6.1 Separate Solution Method.

In this method the potential of the ion-selective electrode is measured for two separate solutions, one containing only the primary ion *i* and the other containing only the interferent ion *j*; both of the same activity or concentration. Alternatively, two calibration curves are plotted; one for the primary ion and the other for the interferent, or one calibration plot for the primary ion and a single point measurement of the interferent. The potential of the electrode in the solution containing only *i* is

$$E_i = E^\circ + s\log a_i$$

and in solution containing only *j* is

$$E_j = E^\circ + s\log k_{ij} a_j^{z_i/z_j}$$

then for $a_i = a_j$ the selectivity coefficient ($\log k_{ij}$) is given by

$$\log k_{ij} = \frac{E_j - E_i}{s} + \left(1 - \frac{z_i}{z_j}\right)\log a_i$$

Alternatively, when $E_j = E_i$

$$\log k_{ij} = \frac{a_i}{a_j^{z_i/z_j}}$$

3.6.2 Mixed Solution Method.

The potential of the electrode is measured for solutions containing both the primary and interferent ions.

a- Fixed primary ion concentration: The concentration of the primary ion is kept constant while the interferent concentration is varied. This method is generally used to study the effect of pH on the electrode response (see section 3.7.2).

b- Fixed interferent concentration: The concentration of the interferent ion is kept constant while the primary ion concentration is varied. A plot of E versus log a_i is then constructed from which the value of k_{ij} is deduced.

A typical selectivity curve is illustrated in figure 3.9a. At high activities of the primary ion (region A to B) the electrode is responding solely to the primary ion i in a Nernstian manner. As the activity of the primary ion decreases the electrode shows a mixed response to both primary and interferent ions in the region B to C. At very low activity of the primary ion (region C to D) the electrode is responding entirely to interferent ion j.

The usual methods for calculating k_{ij} from such plot are as follows:

(i) By extrapolation of the linear parts of the selectivity curve, AB and CD, to give the point F where the electrode is responding equally to both i and j ions, thus log k_{ij} can be calculated from

$$\log k_{ij} = \frac{a_i'}{a_j^{z_i/z_j}}$$

here, a_i' is the activity of the primary ion at point F and a_j is the constant activity of the interferent ion. This method is only applicable when CD is a straight line.

(ii) If the region CD of the curve is not straight, or the plot does not level out at lower activities of primary ion, the activity of the primary ion a_i',

where both ions equally contribute to the electrode response can be determined by the following method.

For the pure primary ion solution

$$E_1 = E^\circ + s\log a_i'$$

For the mixed solution

$$E_2 = E^\circ + s\log\left(a_i' + k_{ij}\, a_j^{z_1/z_j}\right)$$

when $a_i' = k_{ij}\, a_j^{z_1/z_j}$

$$E_2 = E^\circ + s\log\left(2a_i'\right)$$

giving $\Delta E = E_2 - E_1 = s\log 2$

so a_i' can be found by extrapolating AB and locating the point at which this deviates from the selectivity plot by (s log 2) mV, as shown in figure 3.9b.

Another mixed solution method suggested for measurement of the selectivity coefficient is the 'specific application method' put forward by Simon et al. [10], which involves a special evaluation procedure of a "realistic" selectivity, and slope, of the emf response function within the relevant dynamic range. They considered that the membrane response does not follow the Nikolsky equation and their theoretical treatment resulted in equation 3.2 which includes a term for the activity of ligand at the membrane surface.

$$E = E^\circ + \frac{RT}{2F}\ln\left\{a_s(0)\left[a_{Mg}(') + k_{MgCa}\, a_s(0)\, a_{Ca}(')\right]\right\} \qquad (3.2)$$

where $a_{Mg}(')$ is the magnesium activity in the sample solution
$a_{Ca}(')$ is the calcium activity in the sample solution
$a_s(0)$ is the activity of the ligand at the membrane surface
k_{MgCa} is the selectivity coefficient

(a)

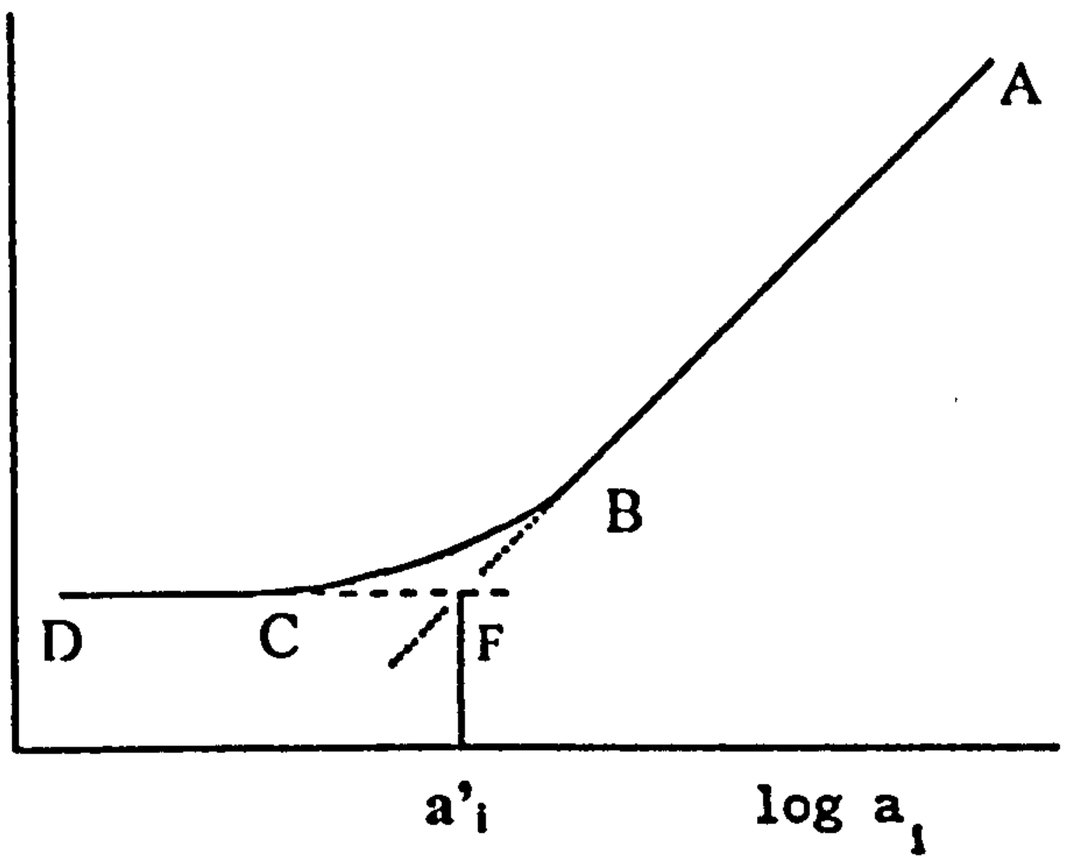

(b)

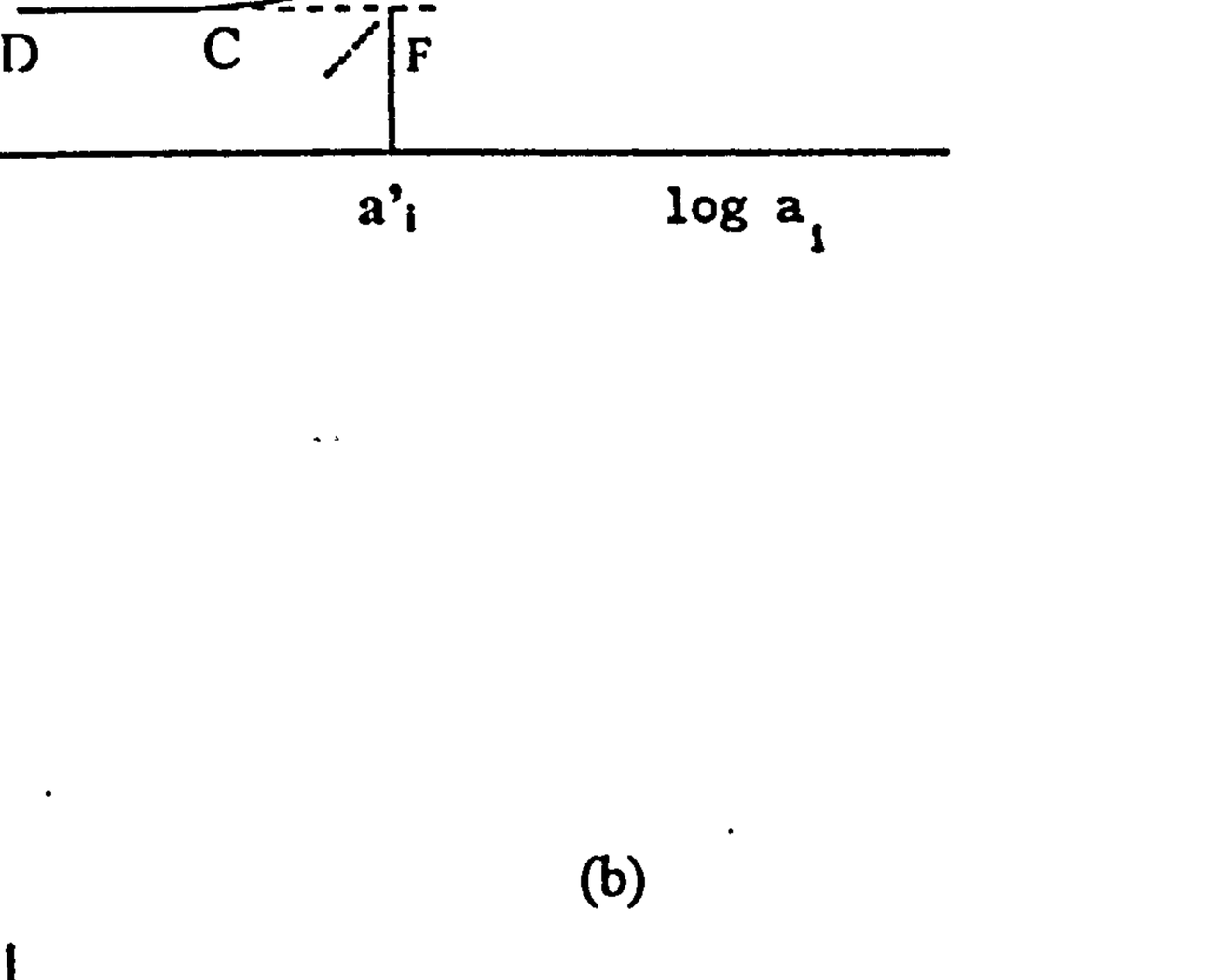

Fig. 3.9. Mixed solution method plot

The activity of the ligand at the membrane surface was considered to be dependent on the ratio of primary ion / interferent ion in the solution, i.e. dependent on sample composition. From this, they concluded that the selectivity coefficient should be determined using solutions close in composition to those which are to be measured. In an experiment using Mg-selective electrode based on ionophore ETH 7025, they used ten solutions of various Mg / Ca ratios and quantities and from the emf results for these, and using the Nikolsky-Eisenman equation (equation 3.1), they determined the selectivity coefficient applicable to that sample composition by iterative data fitting (hence the term 'specific application method'). They illustrated that this method resulted in an optimum membrane composition and gave different values to those obtained using the separate solution method.

This concept has been used previously- the secondary (and even the primary) IFCC calibration solutions have carefully worked out compositions to give different interferent ion backgrounds (from which in principle k_{ij} could be worked out), however, they do not provide as many different compositions as used in the Simon paper. The same idea is also used in the composition of clinical analyser calibration solutions (see section 4.2).

The selectivity coefficient is of much greater importance in measurements of magnesium and lithium than in other ion measurements. This is because the ionophores for these two ions are still not selective enough over the other ions in blood and corrections for other ions present have to be made [11].

Selectivity coefficients are in general measured under the same conditions (usually 0.1 mol/L primary and interferent ion concentrations)

as they have traditionally been used to compare the properties of new ionophores with those already published or to make comparisons between a set of new ionophores. The 'specific application method' is then a method for a different end use to the traditional one - either to optimise membrane composition for a particular application or to use as a correction factor for the presence of a significantly interfering ion.

3.7 Selectivity - Experimental Procedure.

3.7.1 Fixed Interferent Concentration.

The performance of electrodes was tested by comparing the response of the electrode to pure solutions of the ion of interest with response to solutions containing the primary ion and other electrolyte(s). In the case of the magnesium electrodes, the test solutions contained Ca^{2+}, Na^{+} and/or K^{+} as interferents. For the calcium electrodes the interferents were Na^{+} or K^{+}.

Both dip-type and flow-through electrodes were used. The cell and the electrode construction of the dip-type were as described in sections 3.5.1 and 3.2, respectively. Those of the flow-through systems are described in chapter 4. Of the flow-through systems, a prototype calcium reference cell was used here for testing the ETH 1117 based membrane, and the final design of reference cell for the ETH 4030 and 7025. The ETH 1117 membrane was used in the prototype cell as the reference cell had not yet been developed and only ETH 1117 was available in the laboratory when starting this work in 1990/1991.

The internal filling solution and the solution used for conditioning the electrodes of the flow-through type were 0.57 mmol/L $MgCl_2$.

I- Procedure.

The following aqueous solutions have been tested:

using a dip-system

-solution with magnesium or calcium chloride only (0.01, 0.1, 1, 10, and 100 mmol/L)

-magnesium or calcium chloride with a background of sodium chloride (150 mmol/L)

-magnesium or calcium chloride with potassium chloride at 150 mmol/L.

-magnesium chloride with a background of calcium chloride (1.25 mmol/L) and also with other concentrations (1, 0.1 and 10 mmol/L)

using a flow-through system

-solution with magnesium chloride only at concentrations in the physiological free range (0.1, 0.3, 0.57, 0.84 and 1 mmol/L)

-magnesium chloride with a background of sodium chloride

-magnesium chloride with background of sodium chloride (150 mmol/L) and potassium chloride (4.5 mmol/L)

-magnesium chloride with background of sodium chloride, potassium chloride and calcium chloride.

The measurements were performed at room temperature (22 ± 0.5 °C). The magnesium and calcium ion activities were calculated using the Debye-Hückel theory; the equations and parameters were given in section 2.3. The selectivity coefficients log k_{ij} were obtained by the mixed solution method (see section 3.6.2).

II- Results and Discussion.

Figures 3.10-3.17 show the selectivity plots for the ion-selective electrodes used in this work. The slopes, linear limits and selectivity coefficients are shown in table 3.3. The slopes in the magnesium physiological range are shown in table 3.4.

ETH 1117

Figure 3.10 show the response of the ETH 1117 based magnesium electrode to different magnesium activities in the presence of various calcium concentrations. The presence of 0.1 mmol/L $CaCl_2$ as interferent has no effect on magnesium response at high concentrations of $MgCl_2$. However, the curves flatten progressively with lower Mg^{2+} activities giving a lower detection limit of $\log a_{Mg} \approx -3.3$. At high concentrations of calcium chloride (1-10 mmol/L), the electrode gave no response to magnesium.

Figure 3.11 shows the emf response of the electrode to different magnesium activities in the presence of 150 mmol/L NaCl. The response was linear for changing Mg^{2+} activities at high magnesium levels. However, at lower magnesium concentrations, the electrode deviates from linearity giving a detection limit of $\log a_{Mg} = -3.5$.

Figure 3.12 shows the electrode response in the magnesium physiological range (10^{-3} to 10^{-4} mol/L $MgCl_2$) with 150 mmol/L NaCl as interferent. The slope of the electrode was 26.4 mV/decade with aqueous $MgCl_2$ solutions. Addition of sodium background lowered the slope to 18.2 (in the range of 10^{-3} - 10^{-4} mol/L $MgCl_2$).

Fig. 3.10 EMF response of ETH 1117 membrane

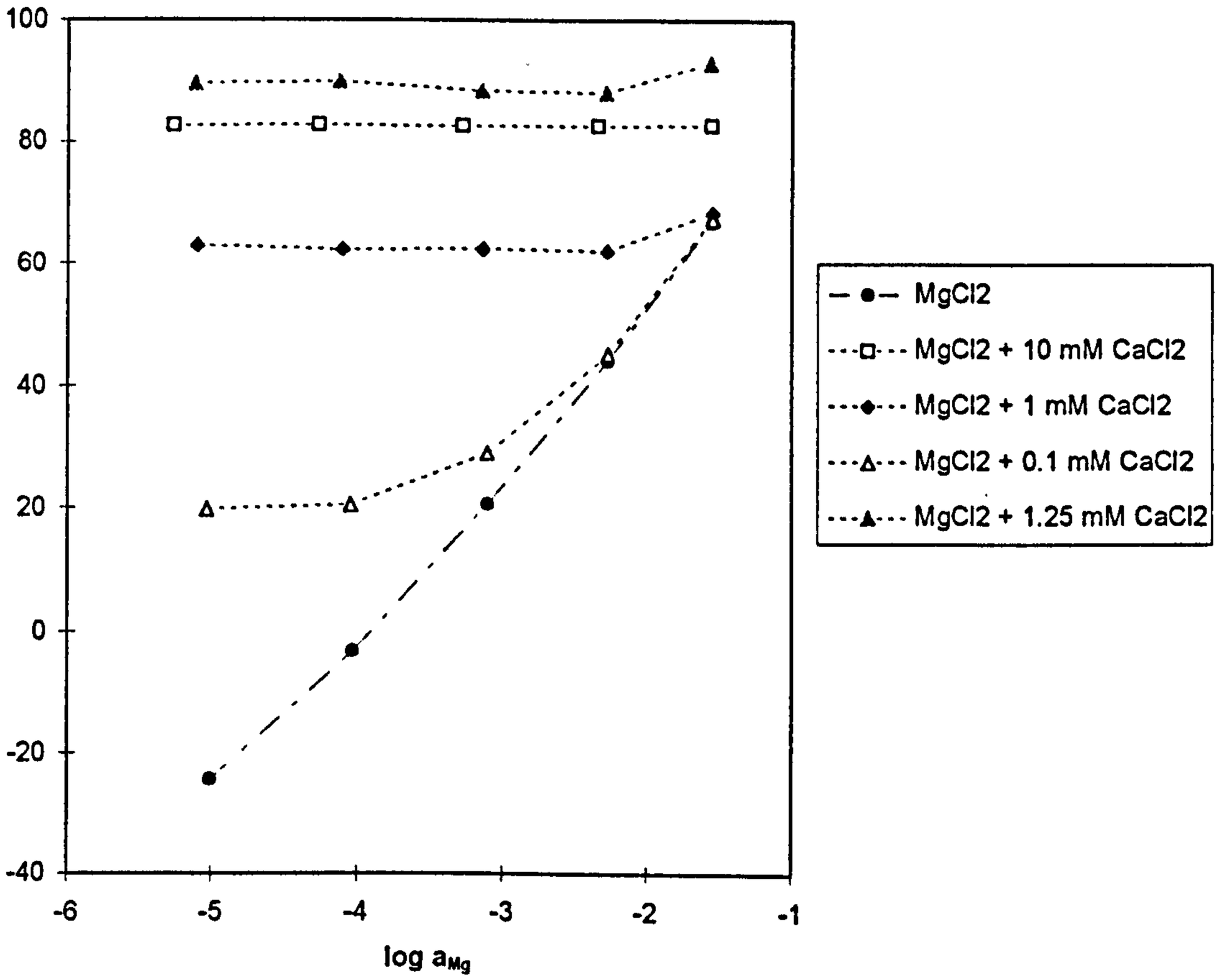

Fig. 3.11 EMF response of ETH 1117 membrane

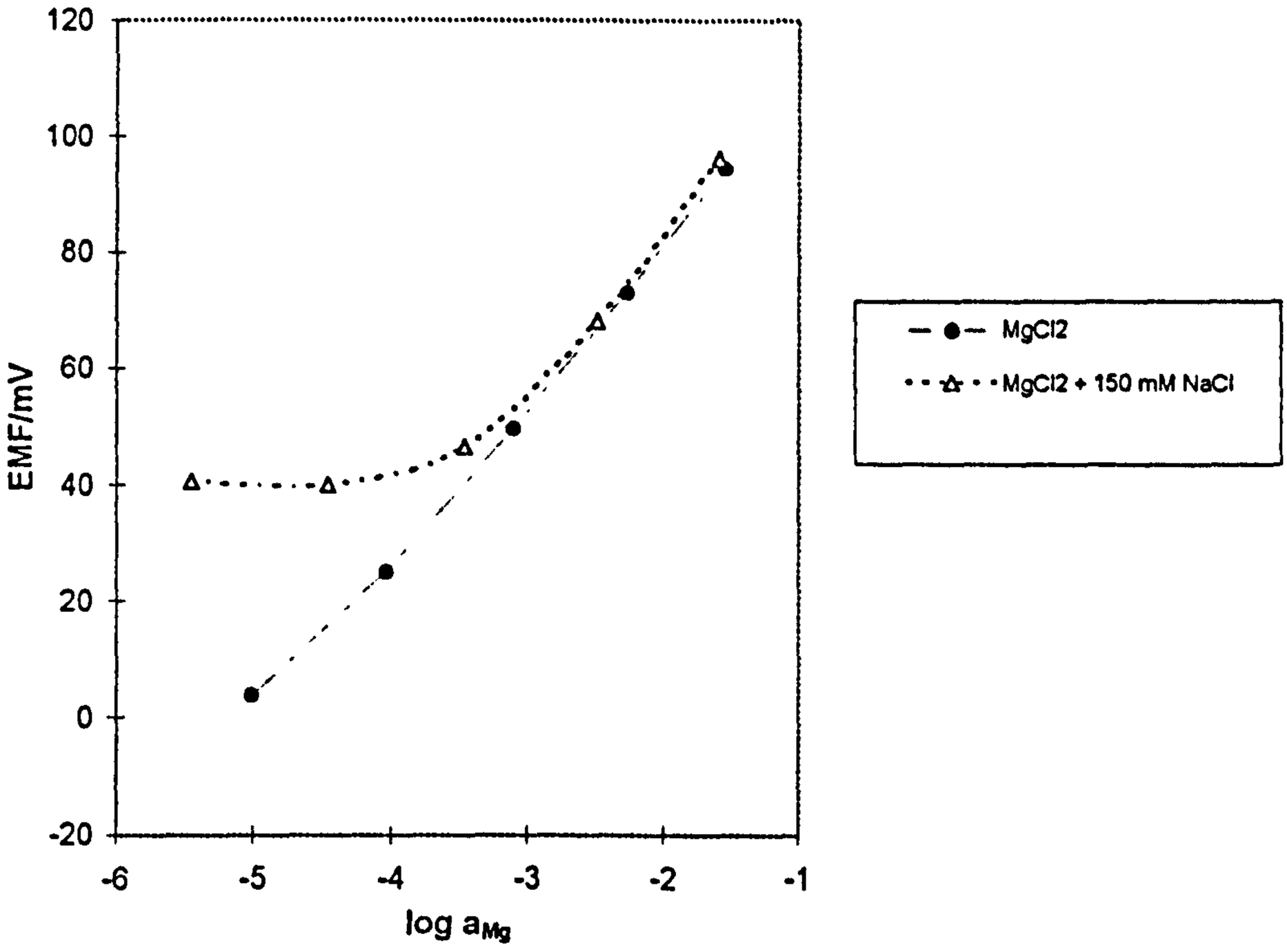

Fig. 3.12 EMF response of ETH 1117 membrane

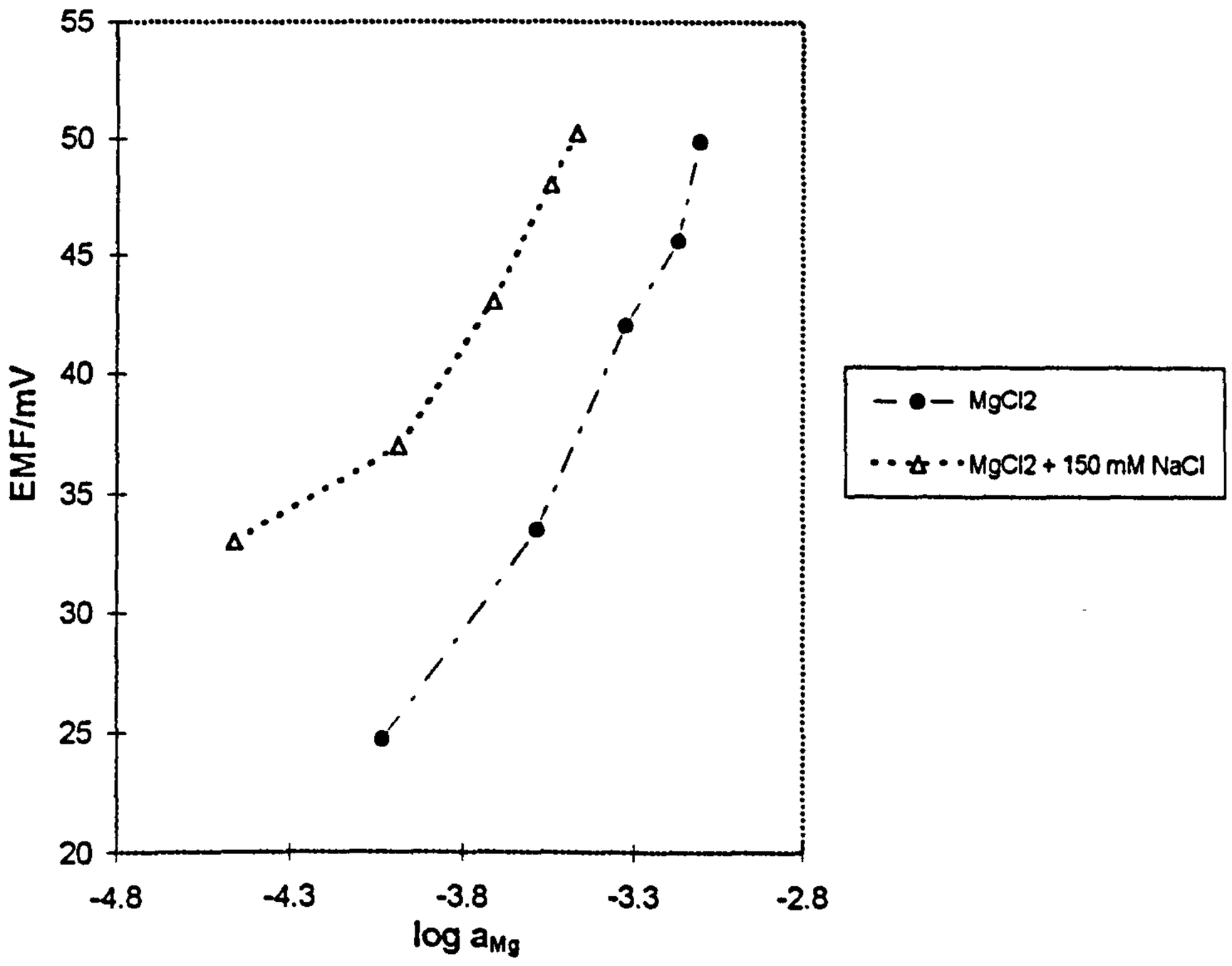

Fig. 3.13 EMF response of ETH 4030 membrane

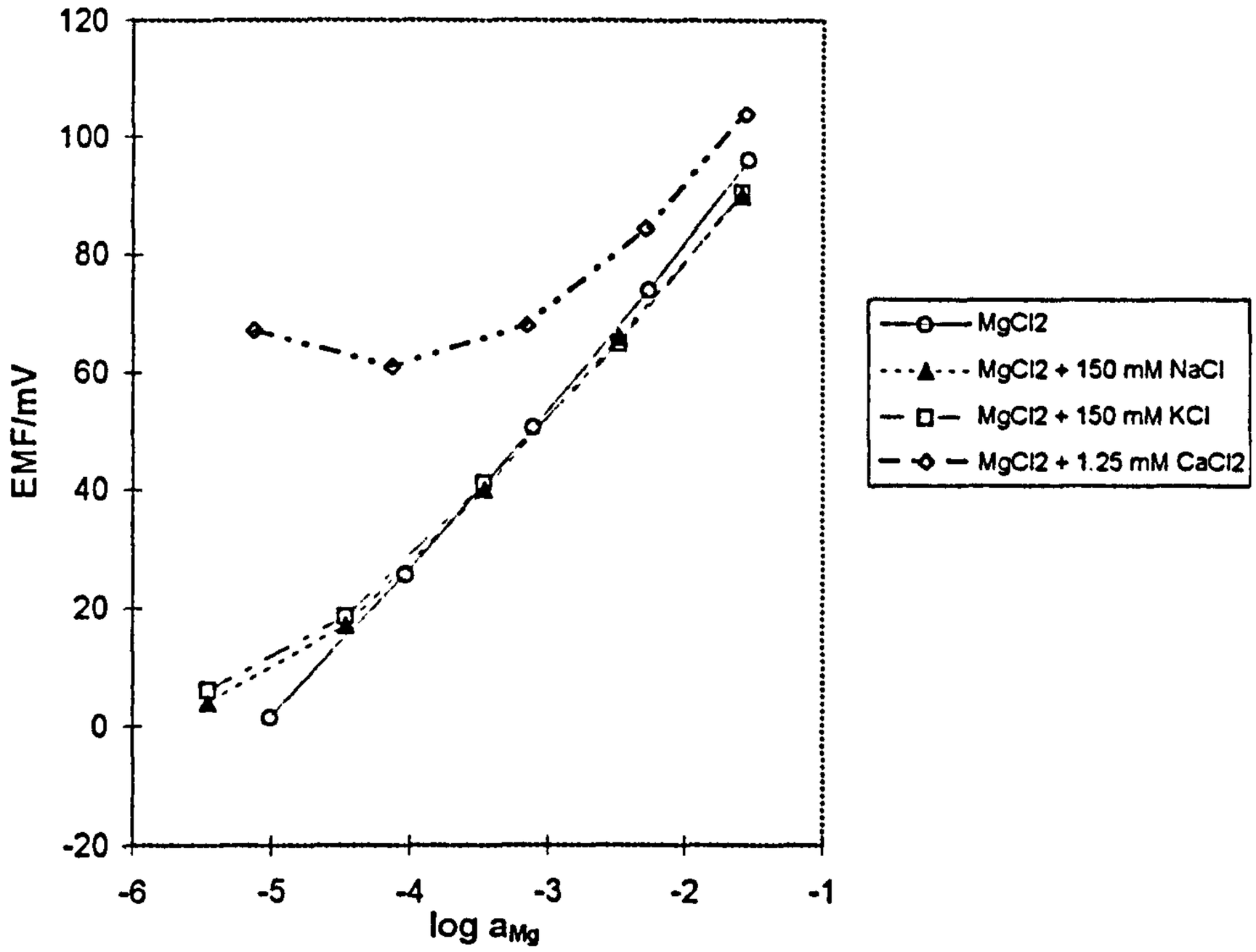

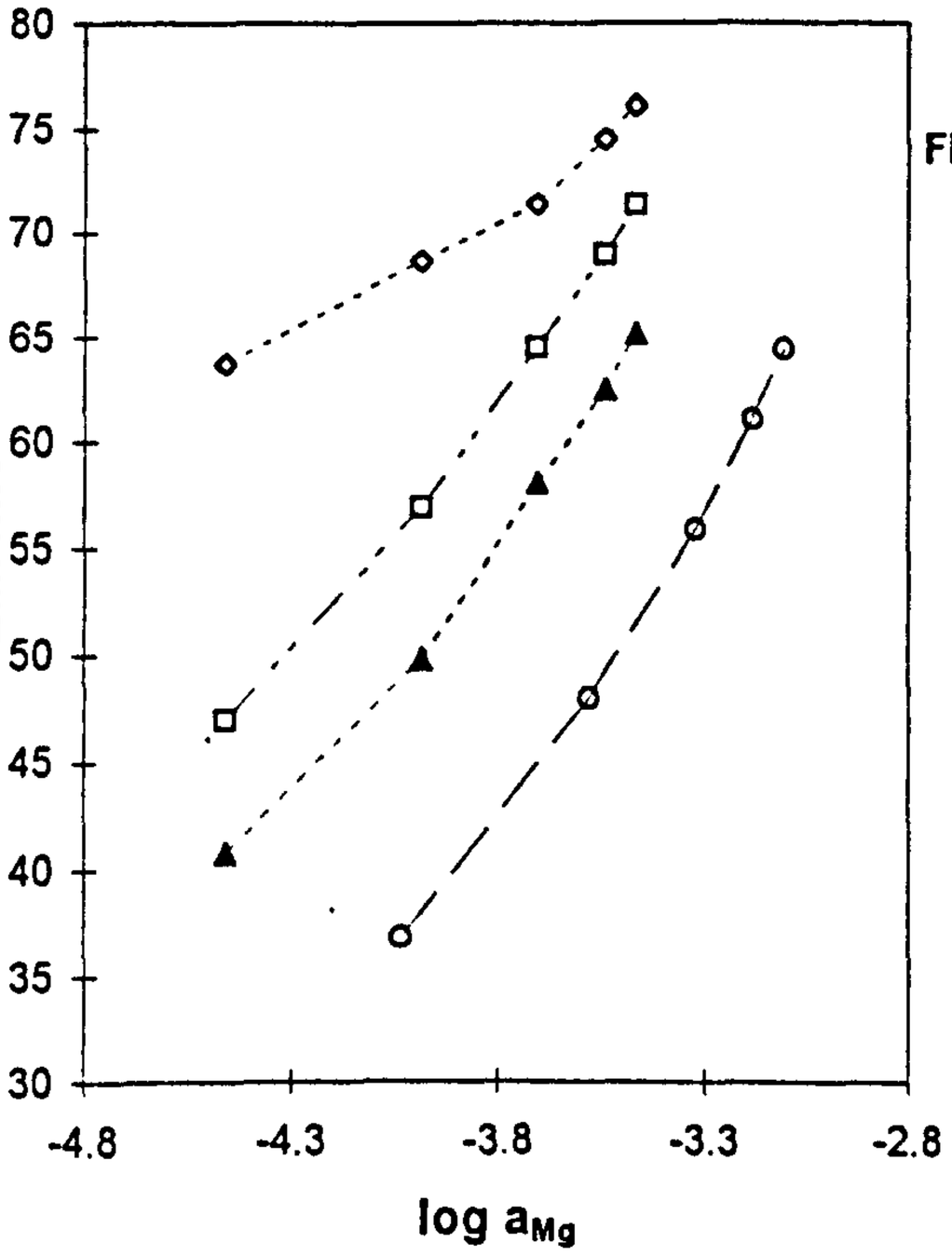

Fig. 3.14 EMF response of ETH 4030 membrane to different magnesium chloride activities in the physiological range with varying background

Fig. 3.15 EMF response of ETH 7025 membrane

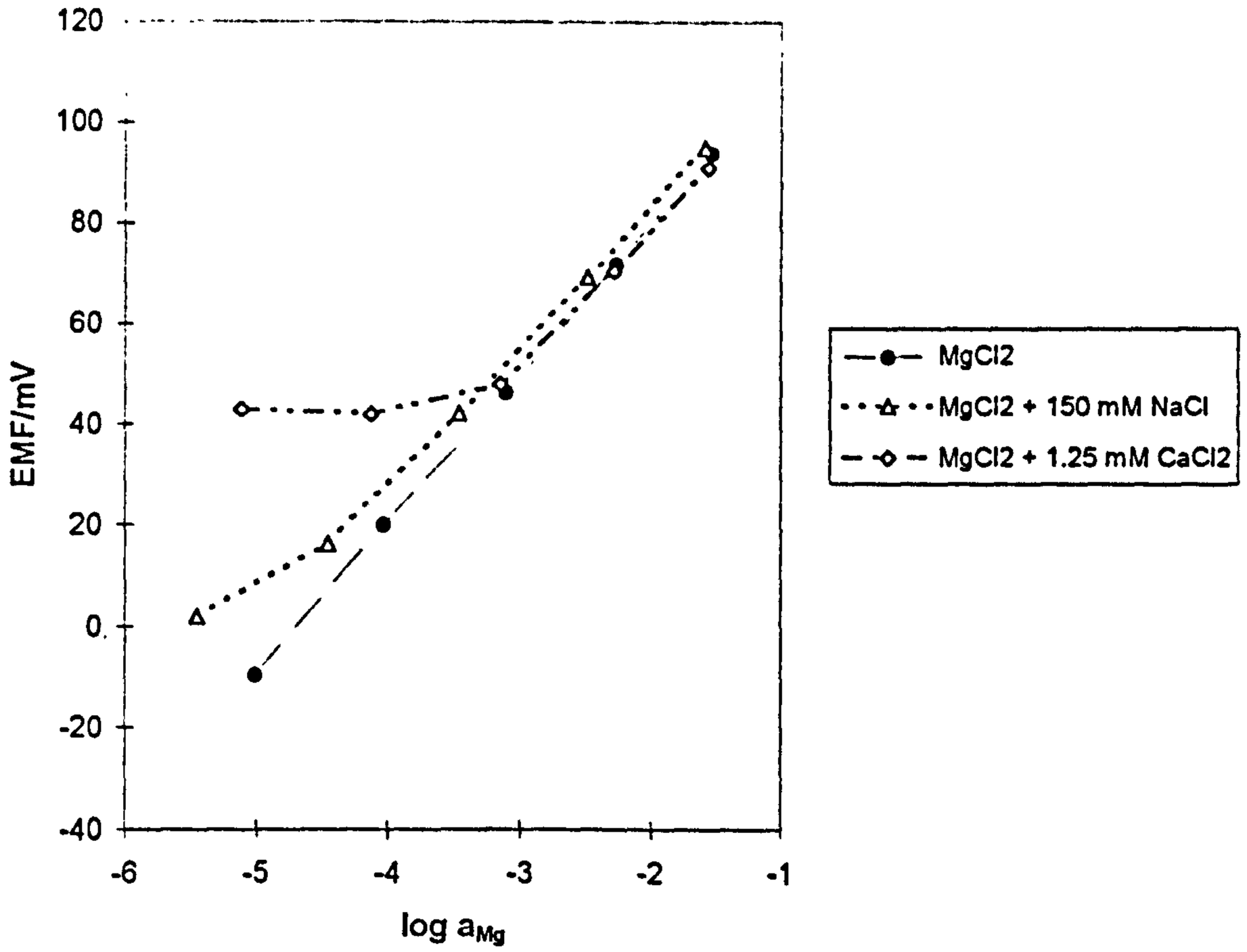

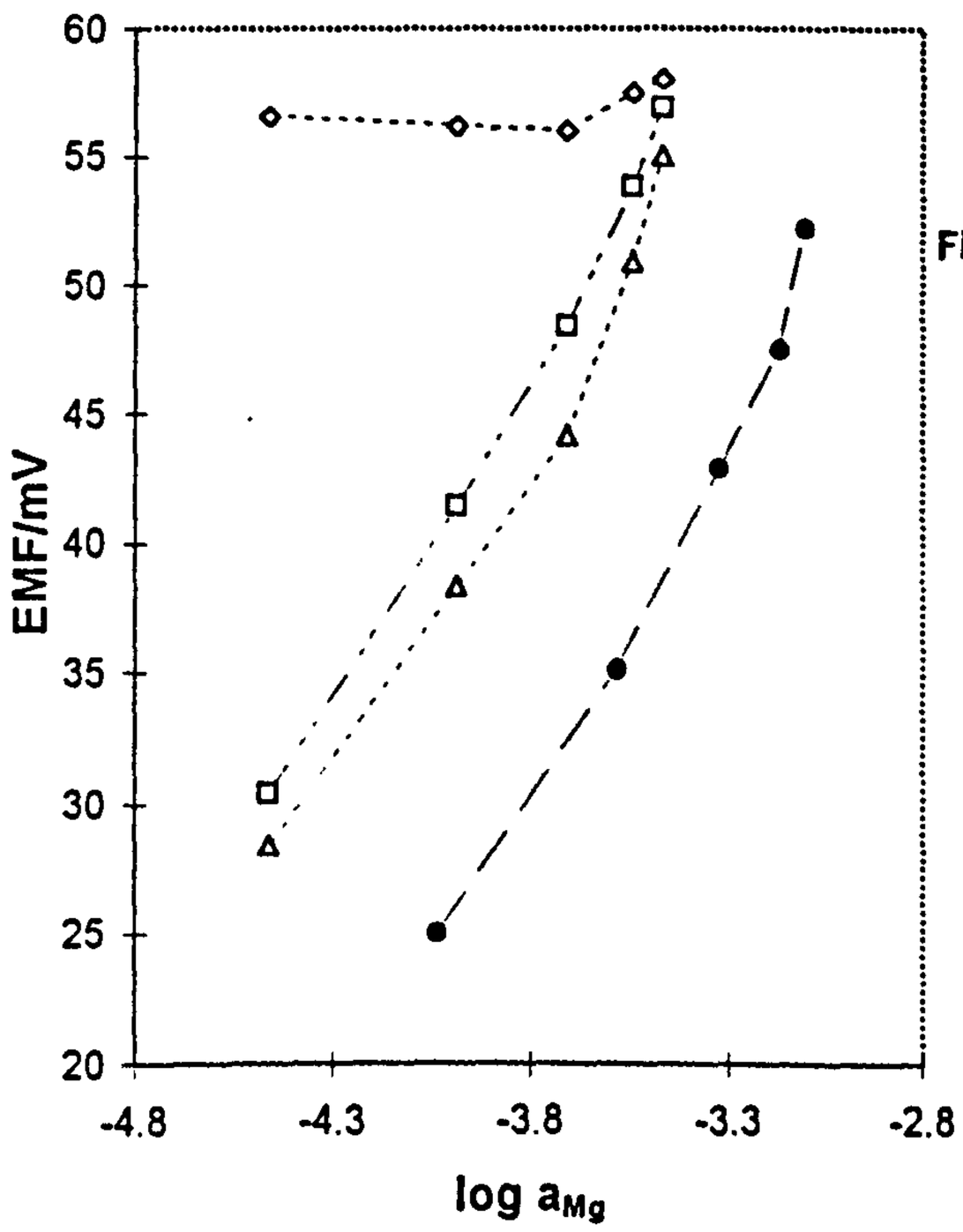

Fig. 3.16 EMF response of ETH 7025 membrane to different magnesium chloride activities in the physiological range with varying background

Fig 3.17 EMF response of ETH 1001 membrane

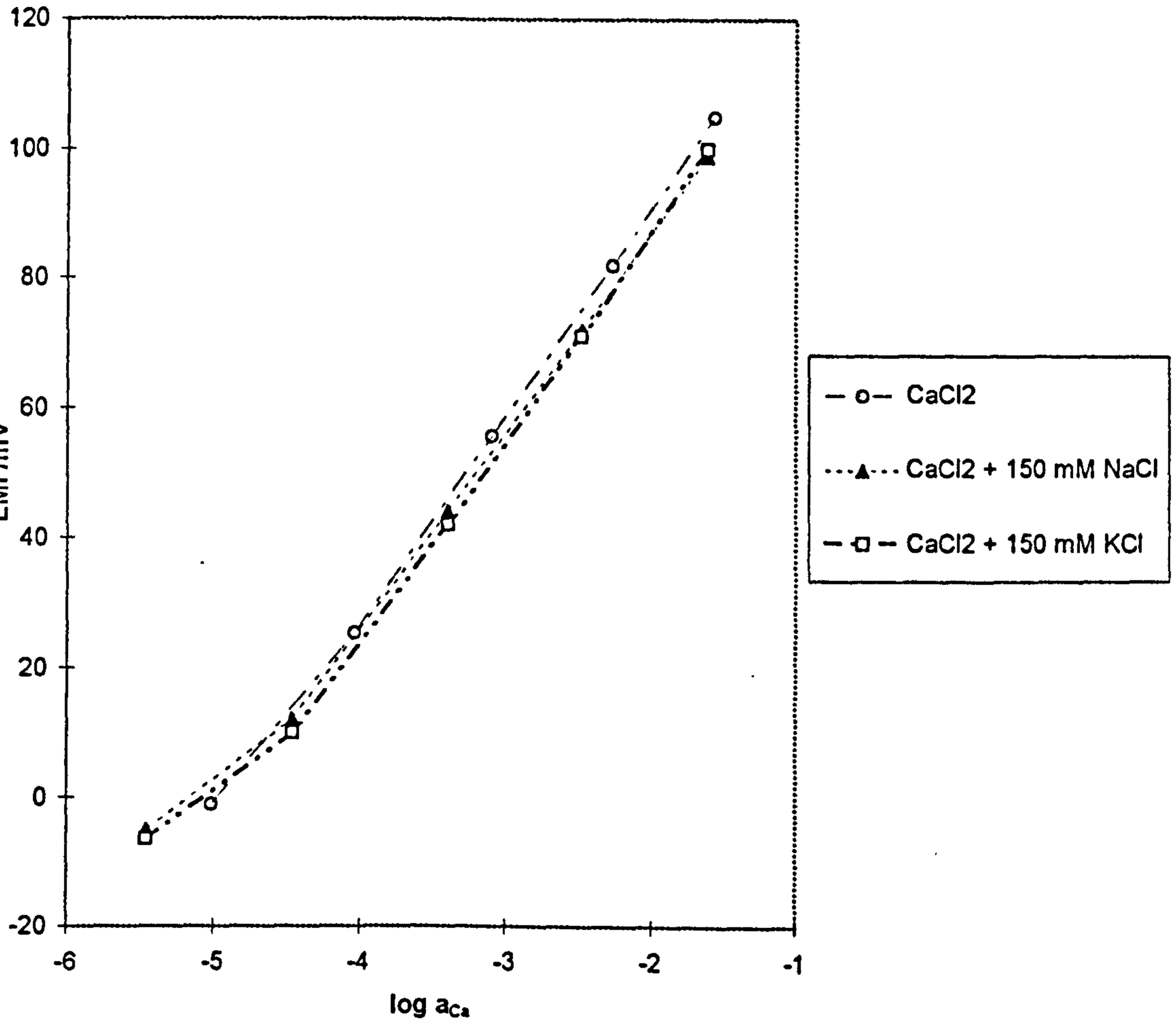

Table 3.3 Selectivity results of Mg and Ca ISEs.

Magnesium ionophore	Calibration ($MgCl_2$) slope /mV	linear limit (log a_i)	$MgCl_2$ + 150 mmol/L NaCl slope /mV	linear limit (log a_i)	log $k_{Mg,Na}$	$MgCl_2$ + 150 mmol/L KCl slope /mV	linear limit (log a_i)	log $k_{Mg,K}$	$MgCl_2$ + 1.25 mmol/L $CaCl_2$ slope /mV	linear limit (log a_i)	log $k_{Mg,Ca}$
ETH 1117	28.0	-4.4	26.9	-2.9	-2.1	*	*	*	-	-	-
ETH 4030	27.9	-4.6	26.5	-4.3	-3.3	26.1	-4.2	-3.1	24.5	-2.8	+0.6
ETH 7025	29.3	-5.0	27.6	-4.2	-3.1	*	*	*	27.4	-3.2	-0.7
Calcium ionophore	Calibration ($CaCl_2$) slope /mV	linear limit (log a_i)	$CaCl_2$ + 150 mmol/L NaCl slope /mV	linear limit (log a_i)	log $k_{Ca,Na}$	$CaCl_2$ + 150 mmol/L KCl slope /mV	linear limit (log a_i)	log $k_{Ca,K}$			
ETH 1001	29.3	-4.5	27.5	-4.3	-3.8	27.8	-4.2	-3.9			

* 'not determinable'

Table 3.4 Selectivity results of Mg ISEs in the physiological range (10^{-4} - 10^{-3} mol/L $MgCl_2$).

Ionophore	$MgCl_2$ slope/mV	$MgCl_2$ + 150 mmol/L NaCl slope/mV	MgCl2 + 150 mmol/L NaCl + 4.5 mmol/L KCl slope/mV	$MgCl_2$ + 150 mmol/L NaCl + 4.5 mmol/L KCl + 1.25 mmol/L $CaCl_2$ slope/mV
ETH 1117	26.4	18.2	-	-
ETH 4030	27.5	27.0	26.3	12
ETH 7025	28.5	26.3	26.7	<8

ETH 4030

Figure 3.13 shows the response of the ETH 4030 based magnesium electrode to different magnesium activities in the presence of 150 mmol/L NaCl, 150 mmol/L KCl or 1.25 mmol/L $CaCl_2$ as interferent. The response of the electrode was linear over a wide range of magnesium concentrations in the presence of sodium and potassium. Addition of 1.25 millimolar calcium chloride induced a positive shift as compared to magnesium chloride solutions; the linear limit of potential response was at log a_{Mg} = -2.8.

Figure 3.14 shows the emf response of the electrode to different magnesium chloride activities in the physiological range with varying background. In the absence of interfering ions, the slope of the electrode response was 27.5 mV. The slope decreased slightly when 150 mmol/L NaCl was added, as shown in table 3.4. For aqueous $MgCl_2$, with added background of NaCl and KCl solutions the slope of the electrode reached 26 - 26.5 mV/decade; it decreased to about 12 ± 1 mV/decade in presence of 1.25 mmol/L calcium background.

ETH 7025

Figure 3.15 shows the response of the ETH 7025 based magnesium electrode to different magnesium activities in the presence of 150 mmol/L NaCl or 1.25 mmol/L $CaCl_2$ as interferent. In the presence of sodium, the electrode shows almost Nernstian response to the primary ion over a wide concentration range. In the presence of calcium, the electrode deviates from the linearity at log a_{Mg} = -3.1, giving a detection limit of log a_{Mg} = -3.3.

Figure 3.16 shows the emf response of the electrode to different magnesium chloride activities in the physiological free range with varying background. The slope of the electrode was 26.7 mV with aqueous $MgCl_2$-NaCl and KCl solutions; it dropped to < 8 with a physiological calcium ion concentration of 1.25 mmol/L.

The above results show that the ETH 7025 gives the best selectivity to magnesium over calcium and ETH 4030 over sodium, however the selectivity is still not good enough for the measurement of magnesium in blood serum. Thus, for the reference method it would be necessary to measure calcium, and maybe sodium, alongside magnesium for serum samples.

ETH 1001

Figure 3.17 shows the response of the ETH 1001 based calcium electrode to different calcium activities in the presence of 150 mmol/L NaCl or KCl. The response shows a large linear response range for calcium in the presence of sodium or potassium.

3.7.2 pH Effect on magnesium and calcium ISEs.

The effect of pH on the electrode response was measured using the fixed primary ion method, in which the primary ion activity is kept as constant as possible while the pH of the solution is changed. The pH can be altered by adding increments of acid or alkali to a solution of the primary ion or by making up separate pH buffered solutions containing the primary ion [12]. The former method has been used in this work.

I- Procedure.

The test solutions were composed of 0.01 mol/L $MgCl_2$ or $CaCl_2$, both containing HCl (initial pH of the test solutions was ≈ 2) and 0.15 mol/L KCl. KCl was added in order to maintain the activity coefficients of the components constant. The pH values of the test solutions were altered by adding small increments of 0.1 or 1 mol/L KOH.

Measurements were carried out at room temperature (22 ± 0.5 °C), with a Russell SW2 glass electrode and Mg ISE or Ca ISE in conjunction with a Russell CRR2 Calomel reference electrode. The types of Mg and Ca electrodes used were as described in section 3.2. The responses of the glass (in pH) and magnesium or calcium (in mV) electrodes were recorded simultaneously using a Molspin computer-linked pH meter. The description of this pH meter will be given in chapter 7.

The pH glass electrode was calibrated using NBS phthalate and phosphate buffers [13]:

0.05 mol/L potassium hydrogen phthalate: pH = 4.01

0.03043 mol/L disodium hydrogen orthophosphate + 0.08695 mol/L potassium dihydrogen orthophosphate : pH = 7.41.

All reagents were obtained from BDH.

II- Results.

Figures 3.18-3.20 show the effect of pH on the response of the electrodes.

The results show that the magnesium-selective electrode based on the ETH 1117 suffers from strong hydrogen interference at low pH (figure 3.18). However, in the pH range 5.5 - 10 the electrode potential remains approximately constant (±0.7 mV).

ETH 7025 shows a rather larger pH dependence. The electrode response was influenced by pH changes mostly in the pH range 5-8 (figure 3.19).

ETH 4030 and ETH 1001 were less pH sensitive. The potentials for these electrodes were almost constant (±0.3 mV for the ETH 4030 and ±0.2 mV for the ETH 1001) over a wide pH range (pH 3 ~ 10) (figures 3.19 and 3.20, respectively).

Fig. 3.18 pH Effect on Magnesium Membrane

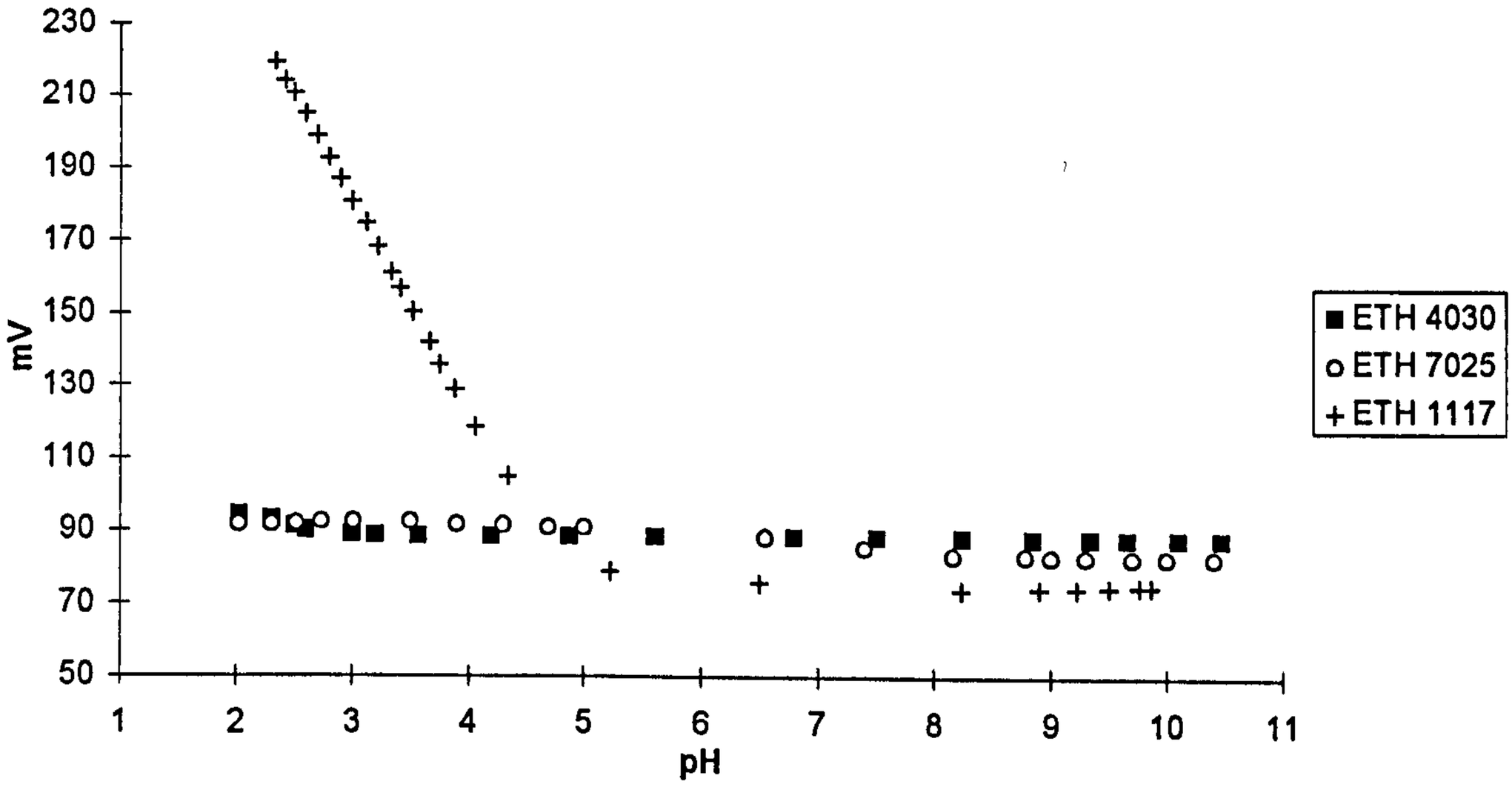

Fig. 3.19 pH Effect on Magnesium Membrane

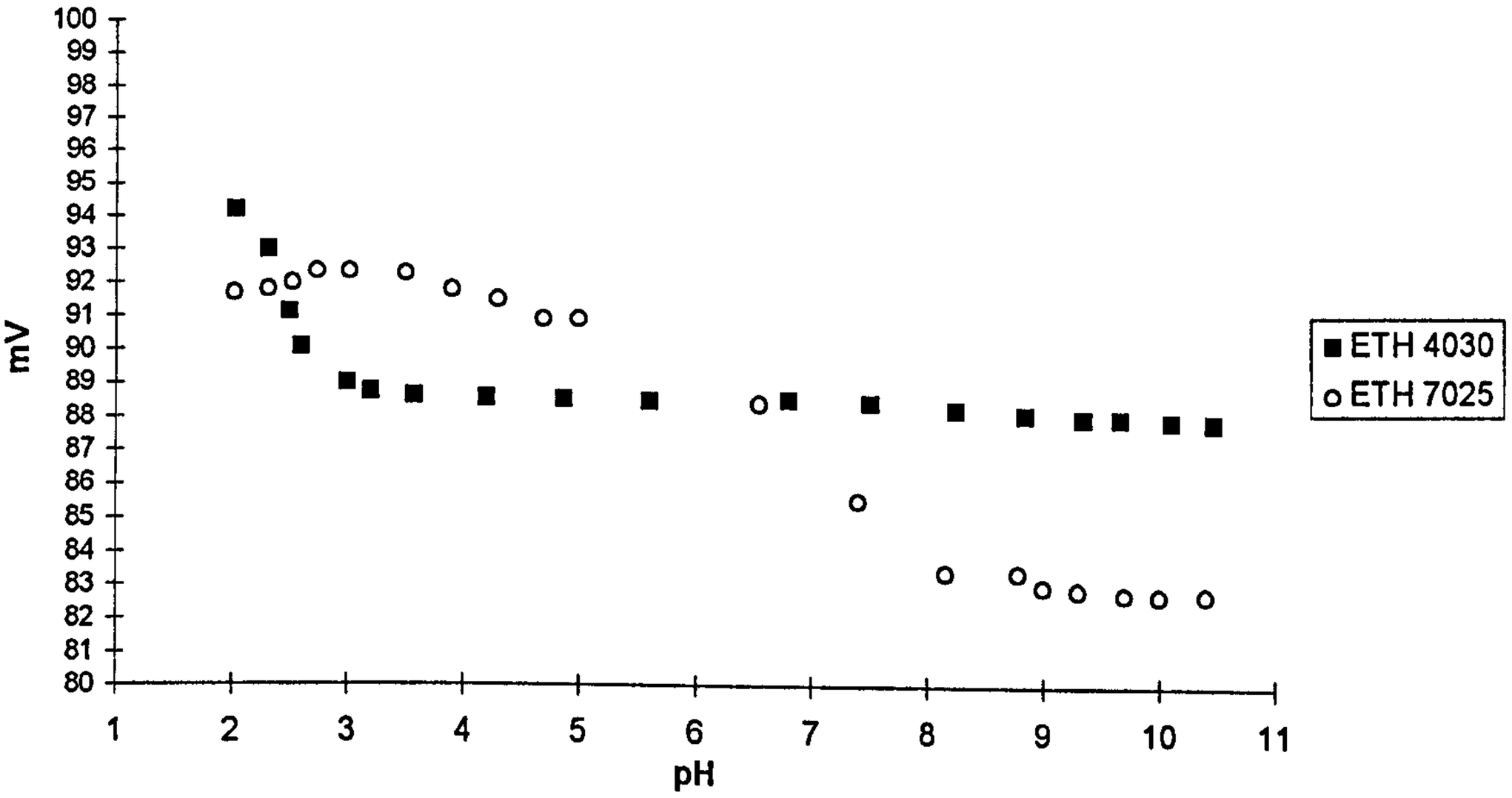

Fig. 3.20 pH Effect on Calcium Membrane

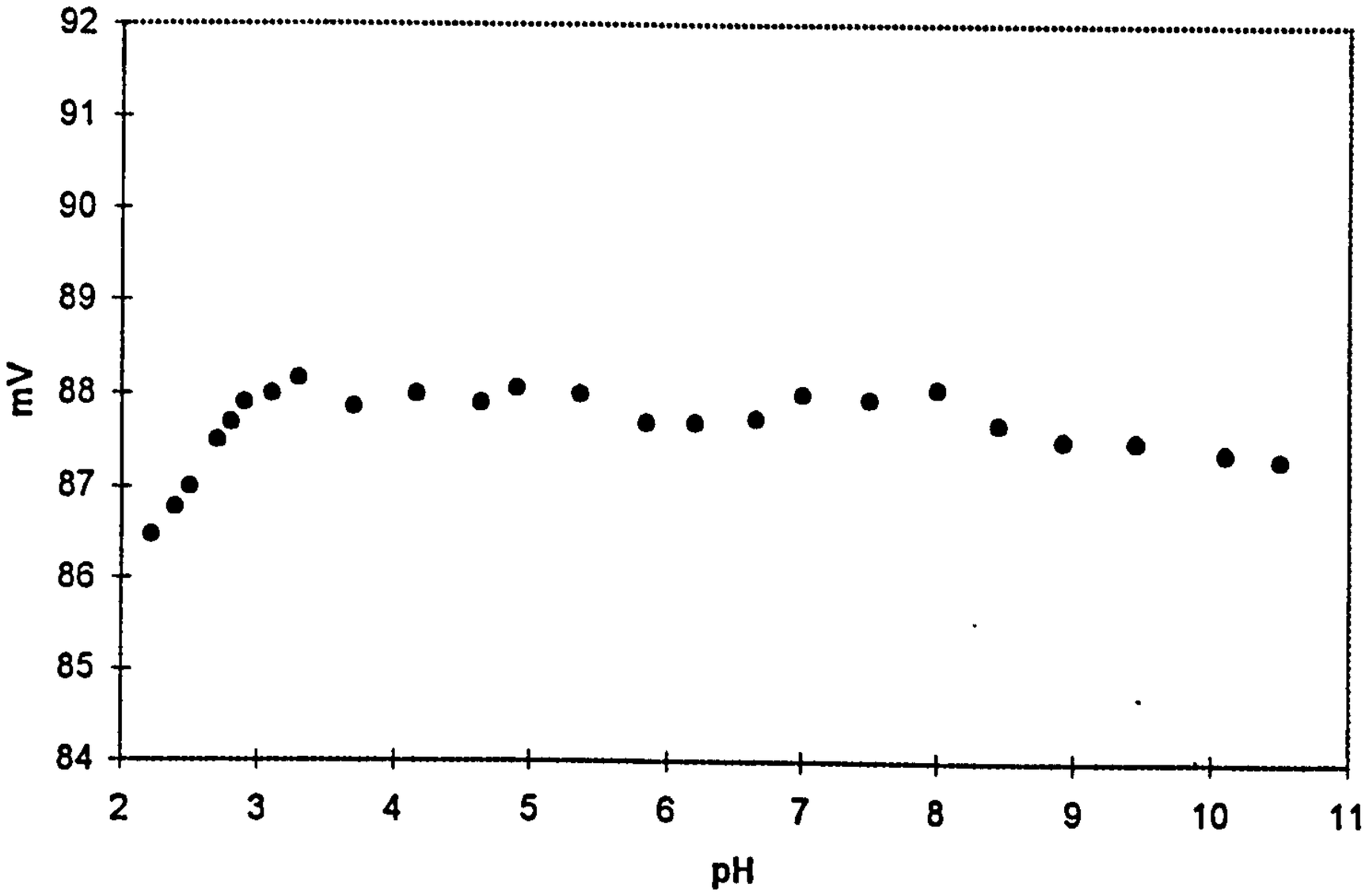

References.

1. Analytical Chemistry Division, Commission on Analytical Nomenclature, *Pure and Appl. Chem.*, 48, 129 (1975).

2. P. L. Bailey, *Analysis with Ion Selective Electrodes*, Heyden, London, (1976), p. 52.

3. G. J. Moody, R. B. Oke and J. D. R. Thomas, *Analyst*, 95, 910 (1970).

4. Craggs, G. J. Moody and J. D. R. Thomas, *J. Chem. Education*, 51, 541 (1974).

5. G. J. Janz and D. J. G. Ives, *Ann. N. Y. Acad. Sci.*, 148, 210 (1968).

6. R. G. Bates, *Determination of pH*, 2nd edition, John Wiley & Sons, New York, London, (1973), p. 331.

7. A. K. Covington and D. M. Zhou, *Electrochimica Acta*, 37, 2691 (1992).

8. D. A. Skoog, D. M. West and F. J. Holler, Harcourt Brace Jovanovich, *Fundamential of Analytical Chemistry*, (1992), p. 422.

9. D. A. Skoog, D. M. West and F. J. Holler, Saunders College Publishing, *Fundamentials of Analytical chemistry*, (1988) p. 375.

10. R. Eugster, B. Rusterholz, A. Schmid, U. E. Spichiger and W. Simon, *Clin. Chem.*, 39, 855 (1993).

11. C. Ritter, H. Kontschieder and H. J. Marsoner, In: A. H. J. Maas, B. Buckley, H. Marsoner, N. E. L. Saris and R. Sprokholt, *Methodology and Clinical Applications of Ion-Selective Electrodes*, 8, 281 (1987).

12. M. V. Rouilly, M. Badertscher, E. Pretsch, G. Suter and W. Simon, *Anal. Chem.*, 60, 2013 (1988).

13. British Standards Institution, BS 1647: *pH measurement*, part 2, 1984.

CHAPTER 4

REFERENCE CELL METHOD FOR IONIZED MAGNESIUM

4.1 Need for a Standardisation Method for Determination of Mg^{2+}.

Knowledge of ionised magnesium fractions and also its concentration in blood is essential because of its physiological and biological role. Abnormalities in magnesium homeostasis are related to disease. Hypomagnesemia (magnesium deficiency) is commonly observed in hospitalized patients [1]. It may result from insufficient dietary intake or pathological conditions affecting the absorption of this element, such as intestinal mucosal disease, increased secretion, fat malabsorption, renal wastage, etc. [1-4]. Mg deficiency has also been connected with a number of chronic diseases, such as diabetes mellitus, cancer, psychological disorders, etc. [5-8]. Hypermagnesemia has been observed in many cases, such as acute and chronic renal failure and adrenal insufficiency [4, 7].

At present, total magnesium is routinely determined by spectrophotometry in clinical laboratories [9]. In contrast, measurement of ionized magnesium is limited due to the lack of sensitive techniques to assess precisely its fraction. However, the measurement of ionized magnesium is thought by some clinicians to be more instructive than total magnesium [7, 10-12]. Recent studies on diseased human subjects such as cardiac cases, abnormal pregnancy, diabetics have shown significant alterations of blood ionized magnesium levels from normality, but no change in total magnesium [10, 11]. Previous estimates of ionized magnesium levels have relied upon total Mg measurements of protein-free ultrafiltrates [13]. Such techniques as ultrafiltration do not provide sufficient precision and rapidity, as they do not lend themselves to

automation, for measuring the ionized magnesium content. Thus the solution was sought in potentiometry using ion-selective electrodes (see section 2.6), and nowadays commercial ISE analysers for blood ionized magnesium determinations are available (see section 4.2). As in the case of calcium, the basic problem will be that different analysers can legitimately give different results for the same sample, resulting in hospitals having different reference ranges for a 'normal' blood sample. This is due to the lack of a reference method to standardise measurements of ionized magnesium concentration. If a reference method can be put in place before analysers come into wide spread use, then such a problem could be avoided.

The total concentration of magnesium in blood is routinely determined by complexiметric/spectrophotometric methods [14, 15]. To standardise these measurements, results can be compared with those obtained on the same samples using as reference method atomic absorption spectrophotometry. Atomic absorption spectrophotometry was chosen as a reference method for the determination of serum total magnesium concentration owing to its sensitivity, specificity and accuracy [16]. Total magnesium determined by the reference method can be checked by comparison with results from a definitive method: Neutron activation isotope dilution method [17]. The definitive method must have very high accuracy and precision (higher than reference methods) and can be used to assign 'true' values for normal blood samples [18].

As no definitive method exists for ionized magnesium, a reference method needs to be developed and firmly defined to be able to give a reproducible 'normal' value. This would then be used to standardise commercial magnesium analysers so that they can give the same results for

the same sample [19]. Such standardisation would improve the reliability of the determination of ionized magnesium measurements in blood serum thereby leading to better clinical diagnosis of patients, particularly the critically ill. The present study was aimed at contributing towards achieving this goal.

4.2 Commercial ISE Analysers for Mg^{2+} in Blood.

Analysers for the measurement of ionised magnesium in blood have been developed by some manufacturers providing analysis within minutes usually with automatic calibration sequences. All of them are multifunctional allowing the measurement of two or more analytes simultaneously. Table 4.1 summarises information on analysers for Mg^{2+}, giving values of published ionized magnesium concentration or reference ranges for blood samples.

The required selectivity coefficients for a magnesium sensor to be used for measurements in blood serum are given in table 4.2. The achieved selectivity factors are shown in table 4.1. Due to the insufficient selectivities of all the ion selective magnesium sensors over Ca^{2+}, and some of them against Na^{+}, magnesium ions in serum samples are determined by applying the chemometric procedure which was developed earlier for the measurement of lithium by ISE [29]. This involves simultaneous measurement of ionized calcium, and possibly sodium, in each sample and then correction for Ca^{2+} (and Na^{+}) interference. The calibration solutions are worked out to give different interferent ion backgrounds, from which, in principle, the actual selectivity coefficient of the electrode can be determined. This value of the selectivity coefficient is then used to correct for the presence of calcium (and sodium) interfering ions.

Table 4.1. Commercial ISE Analysers for Mg^{2+} in Blood.

Analyser	Manufacturer	Membrane neutral carrier	Other parameters	Calibration solution (mmol/L) Ion Cal.1 Cal.2 Cal.3 Cal.4	Bridge solution	T °C	log $K_{Mg,j}$ j	Concentration / Reference range (mmol/L)	Sample Volume (µL)	Response time (sec)	Life time (days)	reference
Microlyte 6	Kone Finland	ETH 5220	Na , K , Ca , pH	Na^+ 140 120 150 K^+ 4.5 6.0 3.0 Ca^{2+} 1.25 0.75 1.75 Mg^{2+} 0.6 0.3 1.2 Cl^- 101.5 82.0 108.0 pH 7.4 7.0 7.8			Ca -0.2 Na -3	0.54 - 0.74 serum (corrected to pH 7.4)	150			20, 21
AVL 987	AVL Austria	ETH 7025	Na , Ca , pH	Na^+ 150 100 150 K^+ 5 1.8 5 Ca^{2+} 0.9 1.25 0.9 Mg^{2+} 0.3 0.3 0.9 pH 7.38 6.84 7.38			Ca -0.14 Na -0.3 K -3.0 H -8.8	0.583 ± 0.106 serum 0.554 ± 0.082 plasma		> 60	21 ± 7	22
commercial flow-through electrolyte analyser based on methacrylate		ETH 7025	Ca	$MgCl_2$ 0.60 $CaCl_2$ 1.35 NaCl 140 KCl 4.0 one calibration solution, pH 7.40 (HEPES/NaOH 6 mmol/L)	1.2 M KCl	37	Ca -1.2 Na -4.6 K -2.8 Li -4.8	0.57 serum (pool)				23
AVL 988-4	AVL Austria	ETH 7025	Na , Ca , pH	Na 150.0 100.0 150.0 100.0 K 5.0 1.80 5.0 5.0 Ca 0.9 1.25 0.9 0.9 Mg 0.3 0.3 0.9 0.3 pH 7.38 7.00 7.38 7.38 $I^{(a)}$ 159.2 106.5 161.0 109.2	1.2 M KCl	37	Ca -1.2 Na -4.7 K -2.9 Li -4.9	0.584 ± 0.004 plasma 0.587 ± 0.005 whole blood		30	14-120	24, 25
NOVA	NOVA Biomedical, Waltham, MA	NOVA	Na , K , Ca , pH , hematocrit	2 aqueous solutions containing different concentrations of MgCl2 in the presence of known pH and concentrations of Na+, K+, and Ca2+.			Ca -1.1	0.57 - 0.60 mean levels (whole blood, plasma, serum) 0.53 - 0.67 plasma	250	90 - 120	7	26

(a) I = Ionic strength.

Table 4.2. Required Logarithmic Selectivity Coefficients for a Magnesium Selective Assay in Human Blood and Serum Samples*.
Taken from ref [27]

Interfering Ions	Concentration (mmol/L)	activity (mmol/L)	Required Log Selectivity Coefficient log kij	
			Without	With Background Calibration
Calcium	1.2	0.43	-2.63	-1.94
Potassium	4.0	3.0	-1.02	-0.51
Sodium	140	105	-3.98	-2.89

* Mg^{2+} activity = 0.12 mmol/L, Mg^{2+} concentration = 0.34 mmol/L, I = 0.149 mol/L.
The selectivity coefficient was calculated for the lowest possible magnesium activity (a_i) and the highest possible activity of the interfering ion (a_j) within the physiological range, accepting less than 1% systematic error for the measured magnesium activity, according to the following equation [23, 28]:

$$\log k_{ij} \leq \log \left(0.01 \,.\, \left(a_i / a_j^{z_i/z_j}\right)\right)$$

where z_i, z_j are the charges of the measured and the interfering ion, respectively.

For the system calibrated at a physiological activity of the interfering ions, the following equation was used

$$\log k_{ij} \leq \log \left[0.01 \,.\, \left(a_i / \left[a_{j1}^{z_i/z_j} - a_{j2}^{z_i/z_j}\right]\right)\right]$$

where a_{j1} and a_{j2} are the activity of the calibrator and the unknown solution of the interfering ion.

4.3 Reference Cell Method.

Magnesium, like calcium, has no definitive method for its ion determination in blood. The International Federation of Clinical Chemistry (IFCC) has proposed a reference method for the measurement of ionized calcium in whole blood, plasma and serum [30]; the method of choice was potentiometry with ion-selective electrodes (ISEs). Specifications were given which include the reference solutions to be used and a protocol for measurements. The design of the reference cell was then developed in Newcastle and Utrecht to comply with the IFCC draft specifications of the calcium reference method. Several designs of glass cell were constructed and evaluated but none of them was found to be suitable for the reference method [31]. The final design was a demountable, water jacketted perspex cell with a separate glass external reference electrode vessel (see section 4.4) [32]. The performance of this cell was tested in an inter-laboratory study, funded by the Bureau Communitaire de Reference (BCR) of the European Community, using the ETH 1001 calcium ionophore. The cell was found to perform well enough for the reference method and play an important role in the standardization of ionized calcium measurement in plasma [33, 34].

The present study was carried out to test the performance of the reference cell proposed for calcium measurements in blood, when applied to the determination of magnesium ion concentration, which has a lower concentration than calcium in blood. The appraisal tests detailed in the draft ionized calcium document [30] have been carried out. The magnesium membrane used was based on the ionophore ETH 7025, which is currently used in some commercial Mg ISE analysers. Due to the insufficient selectivity of the ETH 7025 membrane electrode toward

magnesium over calcium (see section 3.7), the samples analysed in this work were aqueous solutions which did not contain calcium ions.

4.4 The Reference Cell-Design.

The design of the reference cell proposed for the determination of ionized calcium in blood is shown in figure 4.1.

The reference cell is a flow-through system, with the sample introduced using a syringe allowing a small volume of sample solution to flow across the membrane in a closed flow system isolated from air. The cell consists of a measurement electrode holder connected to an external reference electrode system via a liquid junction. The cell was made of machined perspex (poly(methyl methacrylate), PMMA), thermostatted by water jacketting [32]. The external reference electrode system was a glass vessel, containing a reference electrode (SCE) and bridge solution (saturated KCl). The cell was arranged to obtain a stable and reproducible liquid junction by having the higher density salt bridge solution below the test solution. In the initial design used, the reference electrode was connected to the sample via bridge solution housed in a J-shaped capillary (fig. 4.2) [35]. In the final design of the reference cell (figure 4.1), the external reference electrode and the bridge solution are contained in a water thermostatted glass vessel. There is a capillary between the ion-selective electrode section and the bulk of the bridge solution. The liquid junction capillary, of about 0.5 mm inner diameter, is dipped into the bridge solution.

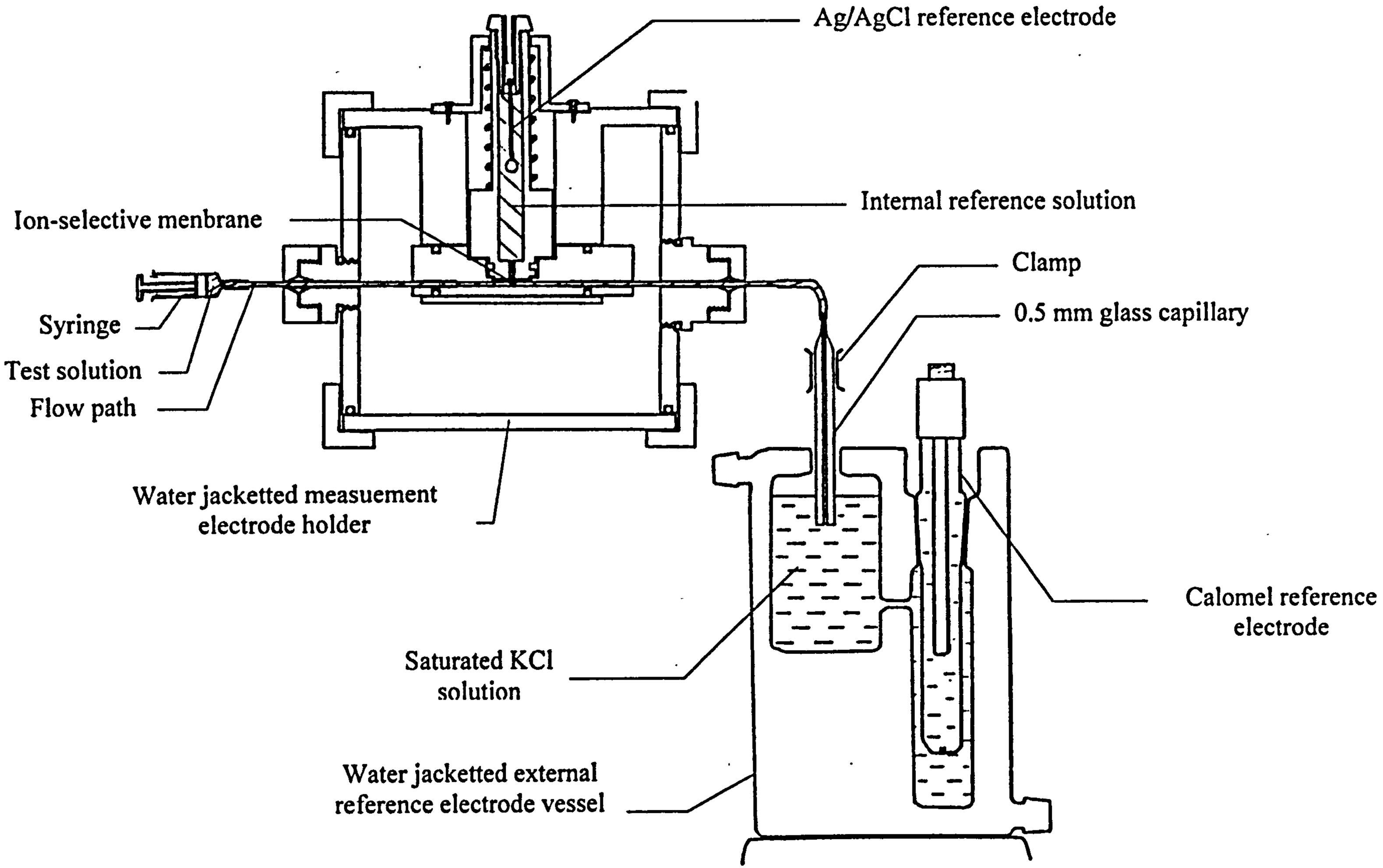

Fig. 4.1. Reference cell design

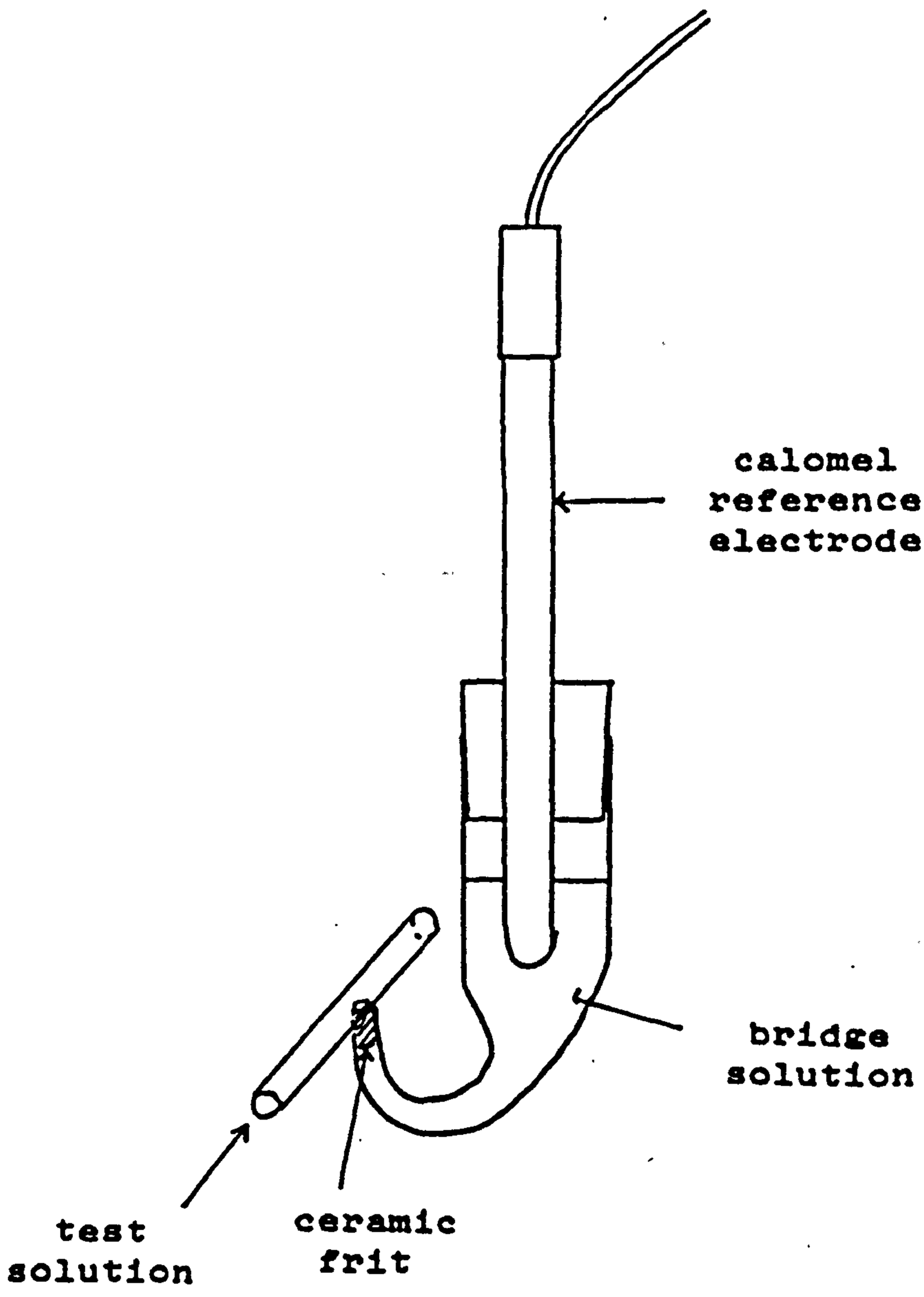

Fig. 4.2. J-shaped reference electrode holder

4.5 Calibration Solutions.

Calibration solutions for ISE instruments are usually prepared on concentration basis, although ion-selective electrodes respond to changes in the activity of ion in solution. The activity is equal to the concentration multiplied by the activity coefficient. so the calibration solutions for magnesium measurement in blood need to have approximately the same ionic strength, and therefore magnesium ion activity coefficient, as that present in normal blood samples.

Ideally, calibration solutions for ISE measurements in blood should be similar in composition to the sample in order to compensate for liquid junction and ionic strength effects. However, the Reference Method requires simple solutions of salts which can be obtained in a reliably high purity state in order to allow for the calculation of activity coefficients.

Several sets of calibration solutions have been proposed for ionized magnesium measurements in blood and they have been used in commercial ISE analysers (see section 4.2). All of them are pH buffered, mimic blood composition to some extent and cover the range in blood of magnesium and several other electrolytes.

Calibration solutions for standardisation of magnesium measurement in blood have not been fixed. The IFCC calibration solutions proposed for ionized calcium measurement in blood have been used in this work, with some modifications to be suitable for magnesium. A brief description of the IFCC calcium calibration solutions is given below.

4.5.1 The IFCC Calibration Solutions.

The IFCC Working Group have proposed two sets of calibration solutions for standardisation of calcium measurements in blood: primary

calibration solutions and secondary (multi-ion) calibration solutions [30]. Tables 4.3 and 4.4 show the composition of the calibration solutions for the two sets. The primary calibration solutions are calcium chloride solutions with a background concentration of sodium chloride, bringing the ionic strength up to approximately that of blood. The concentrations of ionized calcium at 37 °C were chosen to cover the range encountered physiologically in blood. The primary calibration solutions have been chosen for use with the reference method.

The secondary calibration solutions developed are pH buffered solutions. They were designed to cover the physiological range of Na^+, K^+, Ca^{2+} and pH. The buffer solution used to control the pH values was one of the Good buffers [36], either HEPES or MOPS, at a total concentration of about 10 mmol/L. A low concentration of buffer is preferred in order to minimise binding of the buffer to metal ions.

Table 4.3. Composition of the primary calibration solutions
(C = molarity/mmol L^{-1} at 37 °C, m = molality /mmol kg^{-1},
I = ionic strength 160.0 ± 0.5 mmol kg^{-1})
taken from reference [30]

Solution No.	C_{Ca2+}	m_{Ca2+}	m_{Na+}	m_{Cl-}
1	1.25	1.266[(a)]	156.25	158.75
2	0.25[(b)]	0.253	159.25	159.75
3	2.50	2.526	152.50	157.50

(a) corrected to 1.263 mmol/L [37]
(b) changed to 0.4 mmol/L [37].

Table 4.4. Proposed Secondary Calibration Solutions
(I = 0.160 mol L^{-1}, concentration in mmol L^{-1})
taken from reference [30]

Solution No.	C_{Na+}	C_{K+}	C_{Ca2+}	C_{Cl-}	C_{HEPES}	C_{HEPES-}	C_{MOPS}	C_{MOPS-}	pH 37 °C
Secondary Calibration solutions (HEPES)									
1H	159.6	0.1	0.1	154.9	4.06	5	---	---	7.40
2H	130	9	7	148	4.06	5	---	---	7.40
3H	145	9	2	153	4.06	5	---	---	7.40
4H	154.75	3	0.75	154.25	4.06	5	---	---	7.40
5H	151.75	4.5	1.25	153.75	4.06	5	---	---	7.40
Secondary Calibration solutions (MOPS)									
1M	159.6	0.1	0.1	154.9	---	---	6.73	5	6.86
2M	130	9	7	148	---	---	6.73	5	6.86
3M	145	9	2	153	---	---	6.73	5	6.86
4M	154.75	3	0.75	154.25	---	---	6.73	5	6.86
5M	151.75	4.5	1.25	153.75	---	---	6.73	5	6.86

4.5.2 Calibration Solutions for Ionized Magnesium Measurements.

In this work, two sets of calibration solutions have been used for standardisation of magnesium measurements:

1- $MgCl_2$ + NaCl (primary calibration solutions)

2- pH buffered $MgCl_2$ + NaCl + KCl solutions (secondary calibration solutions)

Tables 4.5 and 4.6 show the composition of the three calibration solutions used for the two sets. Three concentrations of ionized magnesium concentration at 37 °C were chosen to cover the physiological range encountered in blood. For the primary calibration solutions, the contribution of ionized magnesium concentrations was deducted from the

total molal ionic strength of 160 mmol/kg to give an approximate sodium ion molality, i.e. $m_{Na} \approx 160 - 3C_{Mg}$. In the case of the secondary calibration solutions, the contribution of ionized magnesium and potassium concentrations were deducted, i.e. $m_{Na} \approx 160 - (3C_{Mg} + C_K)$. Assuming that the density of all solutions was equal to 0.9989 g/ml (the density of ≈ 160 mmol/L NaCl = 0.9989 at 37 °C [30]), the molality of the magnesium in the solutions, and the molality of the potassium in the secondary calibrants, was calculated; the equation to convert between molarity and molality is given in Appendix A.

Table 4.5. The primary calibration solutions.

Solution No.	C_{Mg2+}	m_{Mg2+}	C_{Na+}	m_{Na+}	I
1	0.57	0.576	156.66	158.29	160.02
2	0.30	0.303	157.46	159.10	160.01
3	0.84	0.849	155.86	157.48	160.03

Table 4.6. The secondary calibration solutions (pH = 7.40 at 37 °C).

Solution No.	C_{Mg2+}	m_{Mg2+}	C_{Na+}	m_{Na+}	C_{K+}	m_{K+}	C_{HEPES}	$C_{NaHEPES}$	I
1	0.57	0.576	152.19	153.79	4.5	4.548	4.06	5	160.07
2	0.30	0.303	152.99	154.6	4.5	4.548	4.06	5	160.06
3	0.84	0.849	151.40	152.98	4.5	4.548	4.06	5	160.08

C = molarity /mmol L^{-1} at 37 °C, m = molality /mmol kg^{-1} , I = ionic strength /mmol kg^{-1}.

4.5.3 Preparation of Magnesium Calibration Solutions.

The compositions of the calibration solutions are given above. The chemicals used for preparation were BDH (Analar Grade) $MgCl_2.6H_2O$, previously dried in an oven at 80 °C, NaCl and KCl, HEPES and NaHEPES (obtained from Sigma Chemical Co.) and deionized water. The solutions were made up in 500 ml polythene bottles; magnesium chloride solution was measured by volume, other reagents solutions and water by weight. The quantities used for the two sets are shown in table 4.7 and 4.8.

Table 4.7 Quantities required for preparation of the primary calibration solutions for magnesium measurements.

Solution Number :	1	2	3
Volume of 10^{-2} mol/L $MgCl_2$ (ml)	20	10	40
Weight of NaCl (g)	3.212	3.069	4.336
Total weight of water (g)	347.22	330.03	471.14
Total solution weight (g)	350.45	333.11	475.52

Table 4.8. Quantities required for preparation of the secondary (multi-ion) calibration solutions for magnesium measurements.

Solution Number :	1	2	3
Volume of 10^{-2} mol/L $MgCl_2$ (ml)	20	10	40
Weight of NaCl (g)	3.121	2.982	4.212
Weight of KCl (g)	0.118	0.112	0.160
Weight of HEPES (g)	0.336	0.319	0.456
Weight of NaHEPES (g)	0.452	0.430	0.613
Total weight of water (g)	347.22	330.03	471.14
Total solution weight (g)	351.27	333.89	476.62

4.6 Samples Analysed.

The samples analysed in this work were aqueous solutions in the absence of calcium ions due to the insufficient selectivity of the ETH 7025 magnesium membrane against calcium.

In the BCR study [33] for testing the performance of the reference cell proposed for calcium measurement, the IFCC proposed primary calibration solutions (table 4.3) were used to calibrate the cell. Different sample types were analysed including aqueous solutions. The aqueous solutions which were tested were the IFCC secondary standard solutions of the HEPES set (table 4.4).

In this work, both primary and secondary magnesium standard solutions have been used as calibrants and also as samples. Due to the ETH 7025 membrane response being pH dependent (see section 3.7), the samples used with each calibration set were aqueous solutions of the same set.

The reason for using the secondary standard solutions, in addition to the primary, in this work was to test the performance of the reference cell with pH buffer solutions as calibrants, which is necessary for the use of the ETH 7025 membrane with serum samples.

4.7 Reference Electrodes.

The internal reference electrode recommended by the IFCC for use with the reference cell is the silver-silver chloride electrode. The form of the Ag-AgCl electrode used with the perspex reference cell is described below. The recommended external electrode is the calomel electrode with a filling solution of KCl saturated at 37°C. A special calomel electrode (figure 4.3), commissioned from Russell pH Ltd., was used. It differs from the normal Russell calomel electrode in having the calomel/mercury

element below the ground glass joint, thus it is within the thermostatted region of the vessel. The length of electrode below the ground glass joint was specified at 5 cm.

4.7.1 Preparation of Ag-AgCl Electrodes for the Perspex Reference Cell.

Figure 4.4 show the form of the Ag-AgCl electrode used with the perspex cell. It was of the thermal-electrolytic type prepared as follows [37].

A piece of platinum wire approximately 6 cm long and 0.5 mm diameter (Johnson Matthey) was bent into a V shape. The ends were twisted to form loops and then cleaned thoroughly with concentrated nitric acid and rinsed with deionized water. A sphere of porous silver was formed on each loop of the wire by applying layers of silver oxide paste, allowing them to dry in air for 10 minutes, and then suspending them in a furnace at 450 - 500 C for 30 minutes or until the layer had become white. The wire was then bisected, forming 2 electrodes.

In order to seal the platinum wire into the socket (standard 2 mm) which screws into the top of the electrode body, the socket was first adapted by shortening the metal pin and drilling a hole in it. The wire was then soldered into the hole ensuring no solder touched the bottom section of the wire near the silver. The centre of the polyamide part of the socket was drilled out and the metal pin was then placed inside and sealed in with Epotek H54 epoxy resin. Several layers of Kodak KPR4 photoresist were then applied over the epoxy resin, the polyamide part of the socket and a small portion of the platinum wire.

The electrodes were each chloridised by anodising against a platinum foil cathode at 10 mA for 4 minutes.

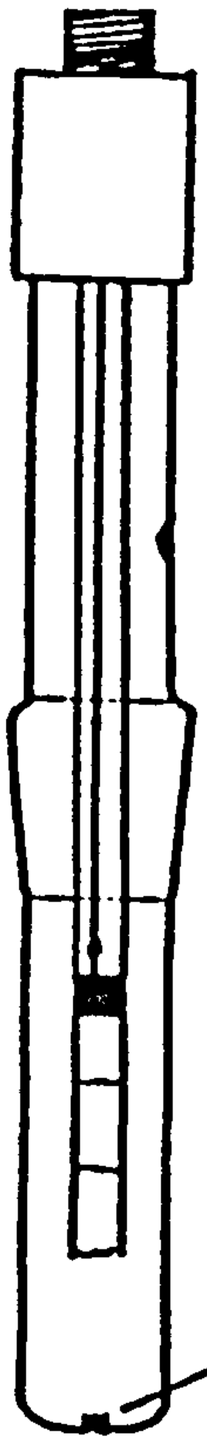

Fig. 4.3. Calomel electrode for use with the reference cell

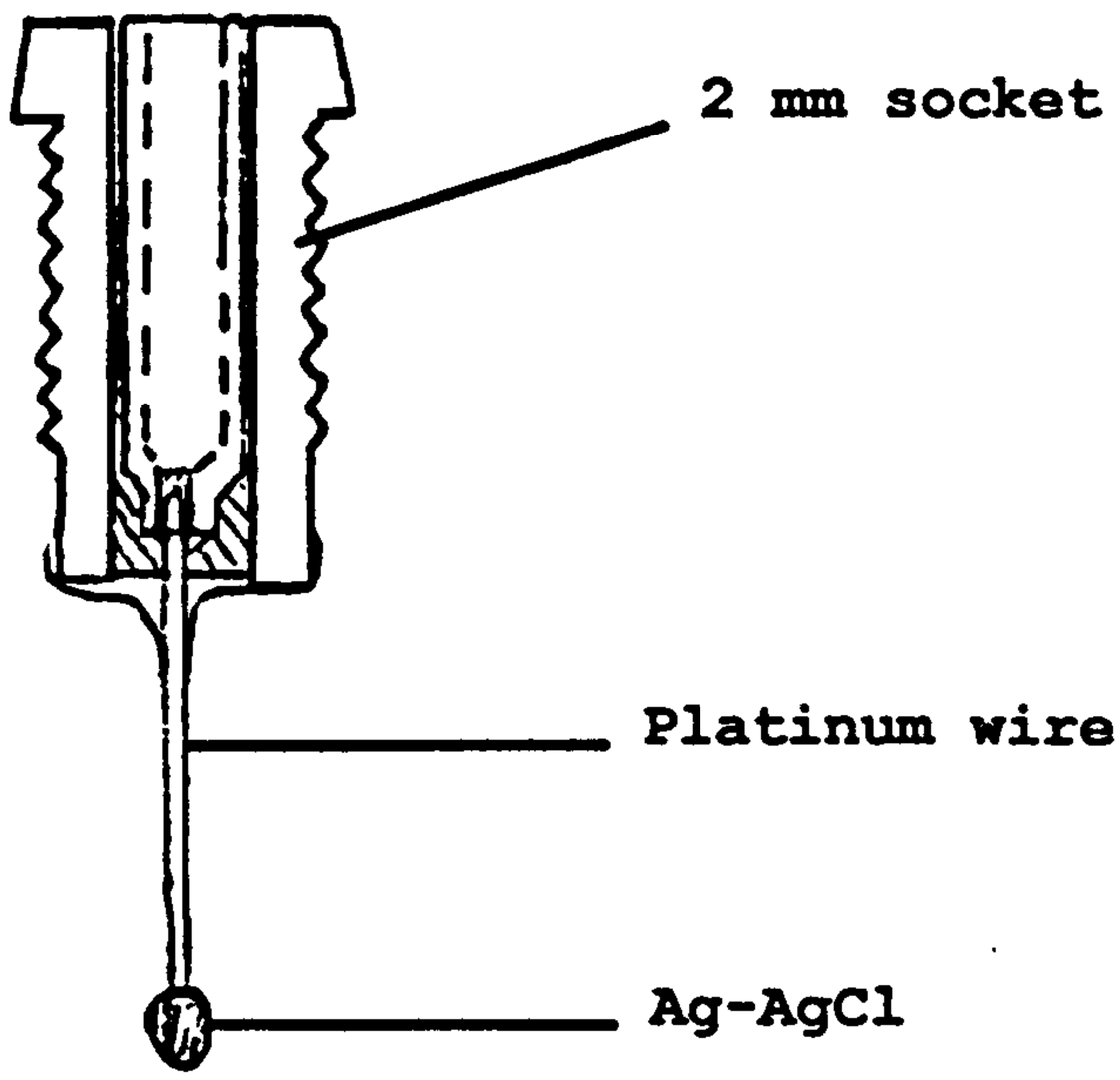

Fig. 4.4. Ag-AgCl electrode form used with the prespex reference cell

After making the Ag-AgCl electrodes, the seal of the platinum wire into the socket was tested. The potential of the electrode was measured against a stable calomel electrode. First the Ag-AgCl electrode was dipped into a test solution until a stable potential reading was obtained; the electrode was then lowered further into the solution so that the joint was immersed. Improper sealing (leakage) was suspected if any disturbance in the reading was observed.

4.8 Construction of the Cell.

The apparatus and assembly of the reference cell are detailed elsewhere [34, 37]. The cell set up for measurements is illustrated in figure 4.1. The cell and reference electrode vessel were themostatted at 37 °C by circulation of water from a thermostat bath into their surrounding jackets, using Techne Tecam water pump unit. The water bath was heated by a Techne Tempette Junior TE-8J temperature/circulation unit. In order to make sure that both the ISE's internal reference solution and the saturated KCl bridge solution were maintained at the same temperature i.e. 37 °C, a glass thermometer was positioned between the cell and the reference electrode vessel in a Y shaped tubing adaptor inserted into the tubing carrying the thermostatting water, to measure the temperature.

To form the Mg-electrode, a disc of 5 mm diameter was cut from the master membrane and put in position in the cell, over the sample flow area, using a pair of tweezers. The electrode body was filled with the internal reference solution (solution (1)), pre-warmed to 37 °C. A small drop of the internal filling solution was put either in the centre of the membrane, or on the end of the frit at the base of the electrode body. The electrode body was then fixed inside the cell. The Ag/AgCl internal electrode was

screwed into the electrode body and sealed in with Nescofilm, supplied by Nippon Shoji Kaisha Ltd., to prevent evaporation from the internal solution. The membrane was conditioned by flushing solution (1) repeatedly through the cell and leaving this solution in the sample path for several hours.

A capillary tube of 0.5 mm diameter was used to form the junction between the bridge and sample solution. The calomel electrode was inserted into the bridge solution. Calomel electrodes suffer from temperature hysteresis and the potential of the electrode may take a long time to recover from a temperature change [38], therefore the calomel electrode was kept continuously thermostatted.

Due to crystallization of KCl occurring which is hard to redissolve without shaking or stirring, the bridge solution was regularly renewed (approximately every day).

4.9 Instrumentation.

A computer controlled high input impedance system for voltage measurement was used. It was developed by Molspin Ltd. for calcium measurements and complies with the IFCC reference method specification [30]. The specifications of the measuring device are given in the Molspin manual [47].

The measuring equipment was linked to an IBM-PC compatible computer and controlled by software provided by Molspin Ltd. The program allowed the measurement to be taken as a single emf reading, or a trace of emf versus time could be displayed on the computer screen. The latter was produced by setting the total measurement time, the time interval between measurements, the voltage range and the voltage offset

before commencing measurement. The data were saved to computer disc if required. Further details regarding the Molspin system are given in the Molspin manual [47].

4.10 Method of Sample Analysis.

4.10.1 Measurement Protocol and Calculation.

In accordance with the draft IFCC proposal [30], the sequence of calibration and measurement used was as follows.

Number	Type of Solution	Potential
1	Solution 1	$E_{1,1}$
2	Solution 2	$E_{2,1}$
3	Solution 1	$E_{1,2}$
4	Solution 3	$E_{3,1}$
5	Solution 1	$E_{1,3}$
6	Solution 2	$E_{2,2}$
7	Solution 1	$E_{1,4}$
8	Solution 3	$E_{3,2}$
9	Solution 1	$E_{1,5}$
10	Sample X	$E_{X,1}$
11	Solution 1	$E_{1,6}$
12	Sample X	$E_{X,2}$
13	Solution 1	$E_{1,7}$

The concentration of ionized magnesium present in the sample was then calculated by mathematical interpolation:

$$C_X = C_1 \; 10^Y \qquad (4.1)$$

where $$Y = \frac{\Delta E_X}{\Delta E_S} \log \frac{C_S}{C_1}$$

C_X = the concentration of ionized magnesium in the sample, in mmol/L.

C_1 = concentration of the mid-point calibration solution of ionized

magnesium: Solution (1) = 0.57 mmol/L.

C_S = concentration of high or low concentration calibration solution of ionized magnesium, depending on whether the sample concentration is greater, or lower, than the concentration of the mid-point solution respectively. i.e. 0.30 mmol/L when $C_X < 0.57$ mmol/L and 0.84 mmol/L when $C_X > 0.57$ mmol/L.

ΔE_X = the average potential difference between the mid-point calibration solution and the sample.

ΔE_S = the average potential difference between the mid-point calibration solution and the second calibration solution.

$$\Delta E_X = \frac{1}{4}\left[(E_{1,5} - E_{X,1}) + (E_{1,6} - E_{X,1}) + (E_{1,6} - E_{X,2}) + (E_{1,7} - E_{X,2})\right] \quad -(4.2)$$

For a negative value of ΔE_X, i.e. $C_X > 0.57$ mmol/L:

$$\Delta E_S = \frac{1}{4}\left[(E_{1,5} - E_{2,1}) + (E_{1,2} - E_{2,1}) + (E_{1,3} - E_{2,2}) + (E_{1,4} - E_{2,2})\right] \quad -(4.3)$$

For a positive value of ΔE_X , i.e. $C_X < 0.57$ mmol/L:

$$\Delta E_S = \frac{1}{4}\left[(E_{1,2} - E_{3,1}) + (E_{1,3} - E_{3,1}) + (E_{1,4} - E_{3,2}) + (E_{1,5} - E_{3,2})\right] \quad -(4.4)$$

The above method of calculating the result from the calibration and measurement sequence has the advantage of carry-over reduction and drift correction [39].

A simple program, written in Turbo Pascal by P. M. Kelly for calculation of results, has been used.

4.10.2 Measurement Procedure.

An emf measurement was obtained for each solution as follows. The aqueous solutions were pre-warmed by immersing their bottles in the water bath at 37 °C. The solution bottle was removed from the water bath and the solution was drawn into a 5 ml plastic syringe. The syringe was inverted and any air pushed out. The solution was pushed through the cell and capillary (0.5 mm) without the reference vessel in place until the flow path was full. The syringe was removed and the solution allowed to flow

from the capillary under gravity for about 2-3 seconds. These processes of filling and draining were repeated twice more to reduce the possibility of carryover. The flow path was then filled, the syringe was left in place to hold the solution in the cell and excess solution was wiped from the end of the capillary using a tissue, taking care not to draw any out. The vessel containing the bridge solution was brought up under the capillary and was supported with the capillary dipping at least 5 mm into it.

With the computer-linked measuring system, a measurement was initiated and trace of emf versus time was produced on the screen. The potential value was taken when the reading became stable. For the solutions used in this work, it was found that the potential came to equilibrium within 2-3 minutes. Therefore, a signal at three minutes following sample introduction has been used for all measurements in this work.

Unstable (noisy) readings were occasionally observed during the course of these experiments, due to air bubble formation. Air bubbles were observed in the sample solution at the membrane, in the connecting tubing between the cell and liquid junction and at the liquid junction itself. To remove the bubbles, more sample solution was pushed through and the measurement was taken again. Bubbles were also found to be formed in the internal reference solution between the internal electrode and the frit. In such case, the solution was topped up or replaced. If the reading was still noisy, the electrode body was removed and a drop of solution was placed on the base of the frit. The electrode body was then replaced and the response checked again [37].

4.11 Results.

The results of ionized magnesium analysis obtained in this work are summarised in table 4.9. The detailed results are given in Appendix B.

Table 4.9 Results of ionized magnesium analysis (values in mmol/L).

Calibrants: the primary standard solutions	
Sample x	$\overline{C}_x$ (n = 5)
Solution (2)	0.299 ± 0.003
Solution (1)	0.571 ± 0.002
Solution (3)	0.840 ± 0.003
Calibrants: the secondary standard solutions	
Sample x	$\overline{C}_x$ (n = 5)
Solution (2)	0.299 ± 0.001
Solution (1)	0.570 ± 0.002
Solution (3)	0.836 ± 0.002

Table 4.10 summarises the precision achieved in measurements in terms of agreement between repeat measurements of solution (1) in each calibration. The stability requirements of electrochemical response, specified by the IFCC, are: in each calibration sequence, all the readings of solution (1) should agree to within 0.2 mV and the three last readings of solution (1) should not vary more than 0.1 mV. Table 4.10 shows that, for the primary calibration solutions, 20% of calibrations all the emf values for solution (1) agree to within 0.2 mV, and 40% of the last 3 emf values for solution (1) agree to within 0.1 mV. In the case of the secondary calibration solutions, 33% of all measurements of solution (1) agree to within 0.2 mV, and for the last three measurements of solution (1), 60% are within 0.1 mV of each other.

Table 4.10 Precision in measurements.

(using the primary calibration solutions)

sample (x)	n	all sol (1) ≤ 0.2 mV	last 3 sol (1) ≤ 0.1 mV
sol (2)	1	-	-
	2	-	-
	3	-	-
	4	-	✓
	5	-	-
sol (1)	1	-	✓
	2	-	-
	3	-	✓
	4	-	✓
	5	✓	-
sol (3)	1	-	-
	2	✓	✓
	3	-	-
	4	✓	✓
	5	-	-

(using the secondary calibration solutions)

sample (x)	n	all sol (1) ≤ 0.2 mV	last 3 sol (1) ≤ 0.1 mV
sol (2)	1	-	-
	2	✓	✓
	3	✓	✓
	4	-	-
	5	✓	-
sol (1)	1	-	✓
	2	-	✓
	3	-	✓
	4	-	-
	5	✓	✓
sol (3)	1	-	✓
	2	-	-
	3	-	-
	4	✓	✓
	5	-	✓

The cause of the deviation from the IFCC specifications in some calibrations was a drift in emf for the cell. The reasons for this drift might be:

(i)-drift in the Ag/AgCl half cell potential due to changes in the concentration of the internal filling solution (e.g. by evaporation) and temperature.

(ii)-change in the junction potential due to

-leakage of air into the system owing to poor tubing connections between the cell and the liquid junction capillary or syringe.

-altering of the sample solution composition.

-altering of the bridge solution composition by evaporation, loss of KCl by creepage or by contamination from samples.

(iii)-change in the calomel electrode potential due to changes in its filling solution composition and temperature.

The drift of emf for the solution (1) during each calibration, was assessed by linear regression of all the potential difference measurements. The drift for each calibration of the primary and secondary calibration solutions is shown in figure 4.5. The mean drift for all calibrations for the two sets were:

primary calibration solutions: (0.131 ± 0.453) mV

secondary calibration solutions: (-0.223 ± 0.172) mV.

The drift was also assessed by taking linear regression through the first 5 readings for solution (1). The mean drift for the primary and secondary calibration solutions were (0.156 ± 0.409) and (-0.204 ± 0.157) mV respectively.

The results of ionized magnesium concentration and drift obtained in this work were compared (table 4.11) with those of calcium obtained by

Fig. 4.5 Drift during each calibration.
(drift assessed by taking linear regression through the all 7 readings for solution (1))

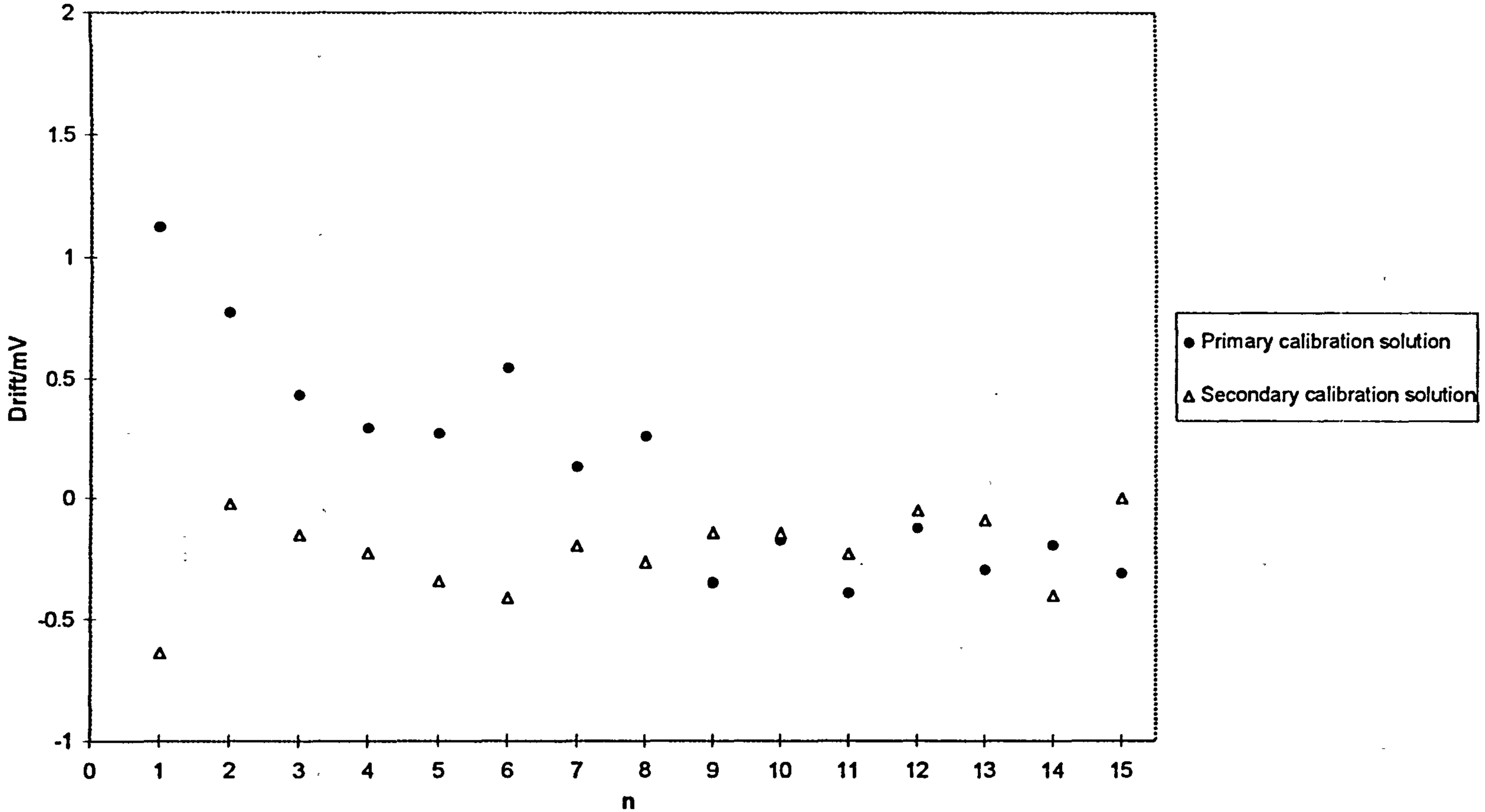

Kelly [37]. The results in table 4.11b show that the performance of the reference cell for the ETH 7025 magnesium membrane was better than for ETH 1001 calcium ionophore in the corresponding solutions.

Table 4.11 A comparison between magnesium and calcium reference cell results.

(a) Mean drift for 15 calibrations for the primary calibration solutions.
(drift assessed by taking linear regression through the first 5 readings for solution (1)).

	Magnesium	Calcium
Mean Drift /mV	0.156 ± 0.409 (n=15)	0.174 ± 0.195 (n=15)*

* (n=15) calibrations for the H1-H3 solutions.

(b) Results of sample analysis.

	Sample concentration (mmol/L)	Measured concentration (mmol/L)
Calcium	0.1	0.101 ± 0.001
	7	6.799 ± 0.058
	2	1.933 ± 0.005
	0.75	0.718 ± 0.003
	1.25	1.201 ± 0.003
Magnesium	0.30	0.299 ± 0.001
	0.57	0.570 ± 0.002
	0.84	0.836 ± 0.002

Percentage theoretical slope:

The 'slopes' S2 and S3 (relative sensitivity) for the lower concentration section (solution (1) → solution (2)) and for the higher concentration section (solution (1) → solution (3)), respectively, were calculated by the method given in the IFCC Reference Method [30]

$$S = \frac{dE / (RT / 2F) \ln 10}{d \log a_{Mg^{2+}}}$$

where E is the cell potential

$a_{Mg^{2+}}$ is the molal activity of the magnesium ion

$RT/2F$ ln 10 is the theoretical Nernstian slope (= 30.77 mV at 37 °C).

The mean fraction of the theoretical slope obtained for the primary and secondary calibration solutions is shown in table 4.12. The results show that:

(a) the relative sensitivity values of S2 and S3 are lower than unity hence the slopes are lower than the theoretical Nernstian slope.

(b) the high concentration range has a higher slope than the low range.

These mainly occurred due to the insufficient selectivity of the electrode, particularly at the low concentration of calibrant (solution (2)), toward magnesium over the other interferent ions (see section 3.7).

Table 4.12. Relative sensitivity.

	S2	S3
Primary calibration solutions	0.864 ± 0.037	0.877 ± 0.047
Secondary calibration solutions	0.855 ± 0.007	0.902 ± 0.008

4.12 Effect of Protein on the Magnesium Selective Membrane.

Solvent-polymeric membranes often show a shift of the standard potential (E°) when they are contacted by sample solutions containing proteins after conditioning in aqueous standards [40]. Simon et al. [41] have described this shift as a result of the contamination of the PVC membrane surface by proteins. The shift was termed the "asymmetry potential" since it affects only one side of supposedly symmetric PVC membranes.

Rouilly et al. [42] found that the standard potential E° of magnesium electrodes based on the neutral carrier ETH 5282 shifted by about 0.4 mV after the first contact with serum. This shift was sometimes constant during

further serum contacts, but occasionally it increased or decreased irregularly. A solution to this problem is normally attempted by aqueous recalibration after contact with the sample [40, 42].

Another approach to dealing with the problem involves attempts at eliminating or reducing the protein adsorption of ion-selective membranes by modifications to membrane chemistry. This includes use of different membrane compositions [43-45, 48] such as, for example, replacement of PVC in the membrane with polyurethane [43, 46, 49].

D'Orazio et al. [43] have studied the effect of protein on the PVC-calcium selective membrane. The membrane was based on the neutral carrier ETH 1001. They found that the first exposure of the calcium membrane to blood serum produced a shift of about 0.7 mV in emf for the 1.25 mmol/L $CaCl_2$ IFCC aqueous standard. The signal in the standard returned to its original value with subsequent introductions and measurements of the aqueous standard only (after 8 measurements). When the PVC in the calcium membrane was replaced with a polyurethane, "Tecoflex" SG-80A, the protein induced calibration shift was reduced to be close to zero.

The above benefit of polyurethane in reducing the protein-induced potential shift has also been observed by Park et al. [49] for ETH 129-based calcium-selective membranes. The potential shift was 3.6 mV for the ETH 129-based PVC membrane electrodes, while the corresponding polyurethane membranes showed less than 0.5 mV shift.

Protein contamination is a source of error in the measurement of ionized magnesium in whole blood, serum and plasma by ion selective electrode. The development of a reference method for Mg^{2+} based on

direct potentiometry will require this effect to be well understood and dealt with through a detailed calibration protocol or, ideally, eliminated.

The present study was carried out to determine the effect of protein on the ETH 7025 based magnesium membrane. The effect of protein containing aqueous solutions on the calibration stability of the magnesium selective electrode has been determined.

4.12.1 Experimental.

Electrode system:

The cell used was the calcium reference cell, thermostatted at 37 °C. The electrode was based on the neutral carrier ETH 7025. The composition of the membrane and its preparation were as described in section 3.1. The internal reference solution was solution (1) of the secondary calibration solutions.

Standards and Samples:

The aqueous standard was solution (1) of the secondary calibration solutions (see table 4.6). The solution used contained bovine serum albumin (BSA), and was supplied by Eurotrol B. V., The Netherlands; the concentrations of its components are shown in table 4.13.

Table 4.13.

Composition	Concentrations
pH	7.41
Na^+	139.5 mmol/L
K^+	4.43 mmol/L
Ca^{2+}	1.22 mmol/L
Ca^{Total}	2.18 mmol/L
Li^+	0.82 mmol/L
Cl^-	100 mmol/L
Total Protein	72.4 g/L

Due to the insufficient selectivity of the ETH 7025 based membrane toward magnesium over calcium, an aqueous solution containing calcium has also been used to test if there is any effect from the calcium ion interference on the precision of the measurement system. Table 4.14 shows the composition of the calcium-containing solution prepared.

Table 4.14.

C_{Mg}	C_{Na}	C_K	C_{ca}	C_{HEPES}	C_{HEPES^-}	pH
0.57	148.5	4.5	1.25	4.06	5	7.4

4.12.2 Results.

Figure 4.7 shows the effect on the cell response to solution (1) after exposure of the Mg^{2+} membrane to BSA protein solutions. The response towards solution (1) before and after the first protein exposure is shown in figure 4.6. In order to check the precision of the measurement system, solution (1) was measured many times prior to introducing the protein sample. Solution (1) was also measured before and after introducing an aqueous solution containing calcium (the solution differs from solution 1 in containing 1.25 mmol/L $CaCl_2$) .

The first four points in figure 4.7 show good reproducibility of the cell when exposed to the aqueous solutions, and the fifth point shows no effect from calcium interference. The first exposure of the magnesium membrane to protein containing solution for three minutes (data not shown) produced a shift of about 0.75 mV in emf for solution (1). However, this shift decreased with subsequent protein exposures and the potential of solution (1) gradually returned to its original value after several changes of solution (1), as shown in figure 4.7.

Fig. 4.6 Mg^{2+} Cell response to sol(1) before / after first protein exposure

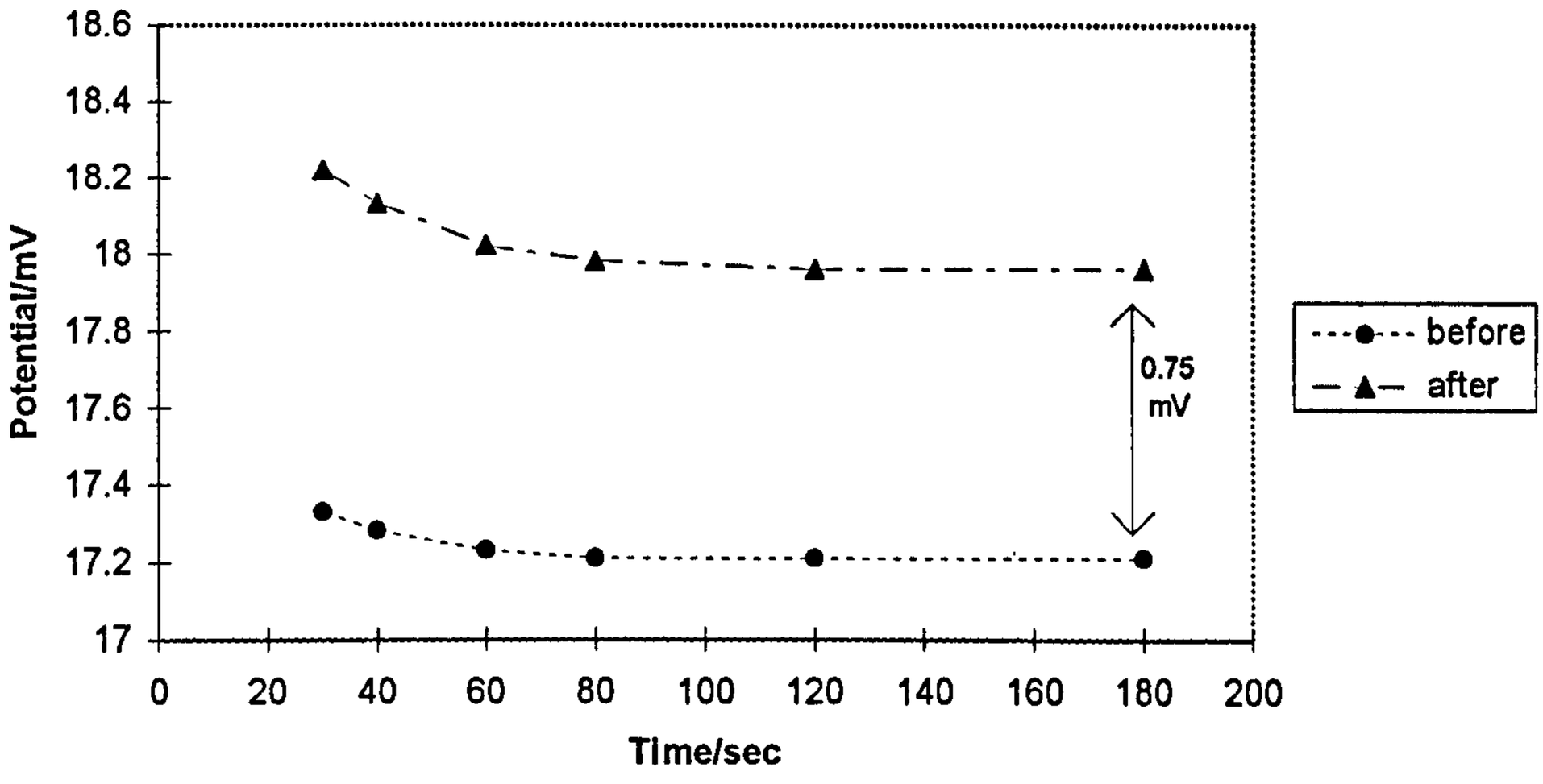

Fig. 4.7 Effect of protein solutions on ETH 7025 membrane

▲ Indicates a 3 minutes calcium solution exposure

↑ Indicates a 3 minutes protein solution exposure

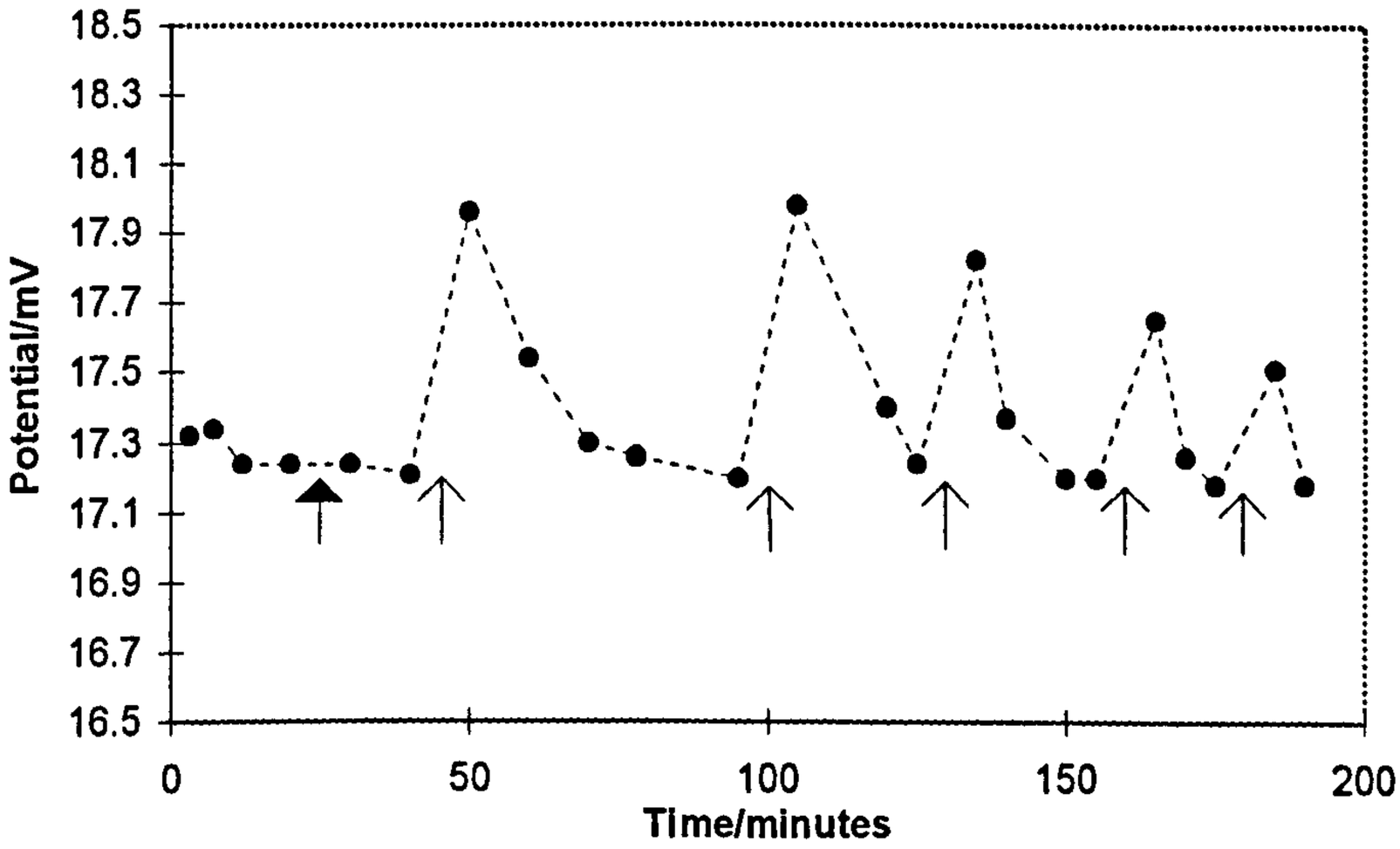

From the above results, it can be seen that the effect of protein on the PVC-magnesium membrane is similar in magnitude to that for the PVC-calcium membrane obtained by D'Orazio et al. [43]. The magnitude of the shift in emf for the aqueous standard after the first contact of both membranes with protein is approximately the same (≈ 0.7 mV). This might indicate that the protein adsorption on the magnesium membrane, which induced the above calibration shift, is due to the PVC in the magnesium membrane and not to the ETH 7025 ionophore.

References.

1. E. B. Flink, in: A. S. Prasad and D. Oberleas (editors), *Trace Elements in Human Health and Disease*, Vol. 2, Academic Press, London, (1976), p. 1.

2. J. Bengoa and R. Wood, *Absorption and Malabsorption of Mineral Nutrients*, Alan R. Liss, New York, (1984), p. 69.

3. M. E. Shils, in A. S. Prasad and D. Oberleas (editors), *Trace Elements in Human Health and Disease*, Vol. 2, Academic Press, London, (1976), p. 1.

4. N. Brautbar, A. T. Roy and P. Hom, in: H. Sigel and A. Sigel (editors), *Metal Ions in Biological Systems*, vol. 26, (1990), p. 285.

5. R. J. Elin, In: B. M. Altura, J. Durlach and M. S. Seelig, *Magnesium in Cellular Processes and Medicine*, (1987), p. 67.

6. A. M. Fiabane and D. R. Williams, *The principles of Bioinorganic Chemistry*, The Chemical Society, London, (1977).

7. C. Sachs, In: P. D'Orazio, M. F. Burritt and S. F. Sena, *Electrolyte, Blood Gases and Other Critical Analysis: the Patient, the Measurement and the Government*, 14, 144 (1992).

8. R. J. Elin, *Clin. Chem.*, 33, 1965 (1987).

9. J. M. Fernandez-Romero, M. D. Luque de Castro and M. Valcárcel, *Anal. Chim. Acta*, 283, 447 (1993).

10. B. A. Altura, J. L. Burack, R. Q. Cracco, L. Galland, S. M. Handwerker, M. S. Markell, A. Auskop, Z. S. Memon, L. M. Resnick, Z. Zisbrod and B. M. Altura, *Scand. J. Clin. Lab. Invest.*, 54, 53 (1994).

11. B. T. Altura, T. L. Shirey, C. C. Young, K. Dell'Orfano and B. M. Altura, Electrolyte, In: P. D'Orazio, M. F. Burritt and S. F. Sena, *Blood Gases and Other Critical Analysis: the Patient, the Measurement and the Government*, 14, 152 (1992).

12. B. T. Altura, F. Bertschat, A. Jeremias, H. Ising and B. M. Altura, *Scand. J. Clin. Lab. Invest.*, 54, 77 (1994).

13. M. D'Costa and P. T. Cheng, *Clin. Chem.*, 29, 519 (1983).

14. E. M. Gindler and D. A. Heth, *Clin. Chem.*, 17, 663 (1971).

15. E. S. Baginski and S. S. Maril, *Sel. Methods Clin. Chem.*, 9, 227 (1982).

16. M. R. Wills, F. W. Sunderman and J. Savory, *Magnesium*, 5, 317 (1986).

17. R. Kataky, *Ion-Selective Sensors Applied to the Analysis of Blood Electrolytes*, PhD thesis, University of Newcastle-upon-Tyne, (1988), p. 9.

18. AACC position paper. In: J. H. Boutwell (editor), Proceedings of a conference. *American Association for Clinical Chemistry*, Washington DC. (1978), p. 73.

19. C. Sachs and A. K. Covington. In: M. Aizawa and K. Kuwa, *Methodology and Clinical Applications of Blood gases, pH, Electrolytes and Sensor Technology*, IFCC, 13, 107 (1992).

20. M. Maj-Zurawska, A. Hulanicki, D. Drygieniec, M. Pertkiewicz, M. Krokowski, A. Zebrowski and A. Lewenstam, *Electroanalysis*, 5, 713 (1993).

21. M. Maj-Zurawska, *Scand. J. Clin. Lab. Invest.*, 54, 69 (1994).

22. C. Sachs, Ch. Ritter, A. C. Puaud, M. Gahramani, C. Kindermans, U. E. Spichiger and H. J. Marsoner, In: M. Aizawa and K. Kuwa, *Methodology and Clinical Applications of Blood Gases, pH, Electrolytes and Sensor Technology*, IFCC, 13, 177 (1992).

23. U. E. Spichiger, R. Eugster, E. Haase, G. Rumpf, P. Gehrig, A. Schmid, B. Rusterholz and W. Simon, *Fresenius J. Anal. Chem.*, 341, 727 (1991).

24. H. J. Marsoner, U. E. Spichiger, CH. Ritter, CH. Sachs, M. Ghahramani, H. Offenbacher, H. Kroneis, C. Kindermans and M. Dechaux, In: P. D'Orazio, M. F. Burritt and S. F. Sena,*Electrolytes, Blood Gases and Other Critical Analytes: the Patient, the Measurement and the Government*, 14, 174 (1992).

25. H. J. Marsoner, U. E. Spichiger, CH. Ritter, CH. Sachs, M. Ghahramani, H. Offenbacher, H. Kroneis, C. Kindermans and M. Dechaux, *Scand. J. Clin. Lab. Invest.*, 54, 45 (1994).

26. T. Altura, T. L. Shirey, C. C. Young, K. Dell'Orfano, J. Hiti, R. Welsh, Q. Yeh, R. L. Barbour and B. M. Altura, *Scand. J. Clin. Lab. Invest.*, 54, 21 (1994).

27. U. E. Spichiger, *Electroanalysis*, 5, 739 (1993).

28. U. E. Spichiger, R. Eugster, A. Schmid, P. Gehrig, B. Rusterholz and W. Simon, *IFCC, Proc. Int. Symp. on Methodology and Clinical Applications of Blood Gases, pH, Electrolytes and Sensor Technology*, MVI Publishing, IFCC Secretariat, Copenhagen, Denmark, 12, 279 (1990).

29. C. Ritter, H. Kontschieder, H. J. Marsoner, In: A. H. J. Mass, B Buckley, H. Marsoner, N. E. L. Saris and R. Sprokholt (editors), *Methodology and Clinical Applications of Ion-Selective Electrodes*, 8, 281 (1987).

30. A. B. T. J. Boink, B. M. Buckley, T. F. Christiansen, A. K. Covington, A. H. J. Mass, O. Mueller-Plathe, C. Sachs and O. Siggaard-Andersen, In: A. H. J. Mass, B Buckley, H. Marsoner, N. E. L. Saris and R. Sprokholt (editors), *Methodology and Clinical Applications of Ion-selective Electrodes*, IFCC, 8, 39 (1987).

31. A. K. Covington, P. M. Kelly and A. H. J. Mass, In: A H J Mass, B. Buckley, A. Manzoni, R. F. Moran, O. Siggaard-Andersen and R. Sprokholt (editors), *Methodology and clinical applications of Ion-Selective Electrodes*, IFCC, 10, 119 (1989).

32. A. K. Covington and P. M. Kelly, In: M. F. Burritt and R. F. Moran (editors), *Methodology and clinical applications of electrochemical and fiber optic sensors*, IFCC, 11, 163 (1989).

33. A. K. Covington and P. M. Kelly, In: P. D'Orazio, M. F. Burritt and S. F. Sena, *Electrolyte, Blood Gases and other Critical Analytes: the Patient, the Measurement and the Government*, IFCC, 14, 10 (1992).

34. Commission of the European Communities, Community Bureau of Reference, Contract No. 5373/1/6/380/90/06-BCR-UK (10). 31st January (1992).

35. C. Sachs, M. Chaneac, Ph. Rabouine, C. Kindermans, M. Dechaux and A. Covington, In: A H J Mass, B. Buckley, A. Manzoni, R. F. Moran, O. Siggaard-Andersen and R. Sprokholt (editors), *Methodology and clinical applications of Ion-Selective Electrodes*, IFCC, 10, 177 (1989).

36. N. E. Good, G. D. Winget, W. Winter, T. N. Connolly, S. Izawa and R. M. M. Singh, *Biochemistry*, 5, 467 (1966).

37. P. M. Kelly, *Proposed Reference Method For the Measurement Of Ionized Calcium In Blood*, PhD Thesis, University of Newcastle-upon-Tyne, (1993).

38. G. Mattock, *pH measurement and titration*. Heywood and Co.Ltd., London, p. 150 (1961).

39. Reference 37, p. 98.

40. N. Fogh-Andersen, T. F. Christiansen, L. Komarmy and O. Siggaard-Andersen, *Clin. Chem.*, 24, 1545 (1978).

41. L. F. J. Durselen, D. Wegmann, K. May, U. Oesch and W. Simon, *Anal. Chem.*, 60, 1455 (1988).

42. M. Rouilly, B. Rusterholz, U. E. Spichiger and W. Simon, *Clin. Chem.*, 36, 466 (1990).

43. P. D'Orazio, I. Laios and G. N. Bowers, In: P. D'Orazio, M. F. Burritt and S. F. Sena, *Electrolyte, Blood Gases and other Critical Analytes: the Patient, the Measurement and the Government*, IFCC, 14, 21 (1992).

44. Reference 37, p. 173.

45. U. Oesch, D. Ammann and W. Simon, In: A. H. J. Maas, A. B. T. J. Boink, N. E. L. Saris, R. Sprokholt and P. D. Wimberley (editors), *Methodology and Clinical Applications of Ion-selective Electrodes*, IFCC, 7, 273 (1986).

46. G. S. Cha, D. Liu, M. E. Meyerhoff, H. C. Cantor, A. R. Midgley, H. D. Goldberg and R. B. Brown, *Anal. Chem.*, 63, 1666 (1991).

47. pH, Auto-titration, Calcium, Manual, Molspin Ltd., U.K.

48. M. Umemoto, W. Tani, K. Kuwa and Y. Ujihira, *Anal. Chem.*, 66, 6, 352A (1994).

49. S. B. Park, S. Chung, G. S. Cha and H. D. Kim, *Bull. Korean Chem. Soc.*, 16, 1033 (1995).

PART II DETERMINATION OF MAGNESIUM STABILITY CONSTANTS.

CHAPTER 5

DETERMINATION OF STABILITY CONSTANTS, DEFINITIONS AND CONCEPTS.

5.1 Classification of Complexes.

Complex formation reactions are usually treated in terms of the Lewis acid-base theory. According to this theory, the ligands, which are the substances which combine with the metal ion, are electron donors (Lewis base) and the metal ions are electron acceptors (Lewis acid). The number of bases (ligands) to be bound depends on the coordination number and the space available. Ligands which are bound to the central ion by one pair of electrons are called unidentate ligands. If a ligand contains more than one electron-donating group, it is said to be multidentate. Such multidentate ligands can form cyclic complexes, which often have very high stability. These are known as chelates. Complexes containing only a single central atom or ion (e.g. ML, ML_2) are called mononuclear complexes. Polynuclear complexes contain more than one central atom (e.g. M_2L, M_3L_2). Complexation with multidentate ligands may lead to complexes which contain protons in addition to the metal ion and ligand. These are called protonated complexes (e.g. MLH, ML_2H_2). Complexes containing more than one kind of ligand are called mixed-ligand complexes. Mixed-ligand complexes include those which contain hydroxide ions as ligands besides other ligands. The complex formation in water is, in reality, formation of mixed water-ligand complexes, but since water is usually not considered as a foreign ligand, this is formally treated as formation of complexes with only one type of ligand. It is understood

that water completes the coordination sphere of the metal-ligand complexes.

5.2 Definitions of Acidity and Complex Stability Constants.

The Brønsted concept of an acid is of a compound which is capable of releasing a proton. This concept has been adopted in this work. In aqueous solutions, the equilibrium protolytic reaction of the Brønsted acid, HL, can be represented by

$$HL + H_2O \rightleftharpoons H_3O^+ + L^- \qquad (5.1)$$

The thermodynamic equilibrium constant, K_T for this reaction is

$$K_T = \frac{a_{H_3O^+} \cdot a_{L^-}}{a_{HL} \cdot a_{H_2O}} \qquad (5.2)$$

where a is the activity of the indicated species.

In dilute solutions the activity of H_2O is not appreciably different from that in pure water, so it can be taken as a constant and combined with K_T on the left side. That is

$$K_T \cdot a_{H_2O} = K_a = \frac{a_{H_3O^+} \cdot a_{L^-}}{a_{HL}} \qquad (5.3)$$

K_a is the thermodynamic acidity constant or acid dissociation constant.

The dissociation reaction (5.1) is generally simplified by omitting the solvent. Thus the acid dissociation constant K_a will be defined by the reaction

$$HL \rightleftharpoons H^+ + L^- \qquad (5.4)$$

$$K_a = \frac{a_{H^+} \cdot a_{L^-}}{a_{HL}} = \frac{[H^+]\,[L^-]\,f_{H^+}\,f_{L^-}}{[HL]\,f_{HL}} \qquad (5.5)$$

The brackets and f denote concentrations and activity coefficients respectively.

The smaller the value of K_a, the smaller the extent of dissociation and the weaker the acid. Owing to the large differences in K_a that occur, a logarithmic scale is often used. The pK_a, defined as follows, as a convenient measure of acidity:

$$pK_a = -\log K_a$$

The equilibrium constants (K) for the acid can be expressed in term of protonation constants. These refer to the association reaction, which is the reverse of equation (5.1), i.e.

$$H_3O^+ + L^- \rightleftharpoons HL + H_2O \qquad (5.6)$$

and $\log K = pK_a$

Two other acidity constants are commonly used in cases where it is difficult to determine accurate values of the thermodynamic constants. These are the stoichiometric or concentration acidity constant defined by

$$K_C = \frac{[H^+]\,[L^-]}{[HL]} \qquad (5.7)$$

and the mixed, practical or Brønsted acidity constant defined by

$$K_B = \frac{a_{H^+}\,[L^-]}{[HL]} \qquad (5.8)$$

Concentration and Brønsted constants are only true constants under conditions of constant ionic strength. One way to achieve this is to use a large concentration of inert background electrolyte which does not interfere with the reaction of interest.

Weak acids, according to the Brønsted concept, yield, on protolysis/dissociation, strong bases, most of which form complexes with metal ions, particularly polyvalent metal ions.

For the formation of a metal-ligand complex ML (ionic charges are omitted for clarity and generality),

$$M + L \rightleftharpoons ML \tag{5.9}$$

the strength of the complex is expressed by its formation or stability constant

$$K_T = \frac{a_{ML}}{a_M\ a_L} = \frac{[ML]\ f_{ML}}{[M]\ [L]\ f_M\ f_L} \tag{5.10}$$

K_T is the thermodynamic stability constant. The larger the value of K_T, the more stable is the complex.

Under conditions of constant ionic strength, the activity coefficients are constant and the equilibrium constant of the reaction (5.9) is defined by the concentration stability constant K_C

$$K_C = \frac{[ML]}{[M]\ [L]} \tag{5.11}$$

5.2.1 The Overall Stability (Formation) Constant β.

For the formation of a metal-ligand complex ML_n

$$M + nL \rightleftharpoons ML_n \tag{5.12}$$

the complex ML_n is formed in a stepwise manner, according to the following reaction equations

$$\begin{aligned} M + L &\rightleftharpoons ML \\ ML + L &\rightleftharpoons ML_2 \\ &\vdots \quad\quad \vdots \\ ML_{n-1} + L &\rightleftharpoons ML_n \end{aligned}$$

The stepwise formation constants (K), are as follows

$$K_1 = \frac{[ML]}{[M]\,[L]}\ ; \qquad K_2 = \frac{[ML_2]}{[ML]\,[L]}\ ; \qquad K_n = \frac{[ML_n]}{[ML_{n-1}]\,[L]} \tag{5.13}$$

By successive substitution, the following equations are obtained

$$\begin{aligned} [ML] &= K_1\,[M]\,[L] \\ [ML_2] &= K_1\,K_2\,[M]\,[L]^2 \\ &\vdots \\ [ML_n] &= K_1 \ldots . K_n\,[M]\,[L]^n \end{aligned} \tag{5.14}$$

The products of the stepwise stability constants have been designated β and the corresponding subscript, to obtain

$$\beta_1 = \frac{[ML]}{[M]\,[L]} = K_1$$

$$\beta_2 = \frac{[ML_2]}{[M]\,[L]^2} = K_1\,K_2$$

$$\beta_n = \frac{[ML_n]}{[M]\,[L]^n} = K_1 \ldots . K_n = \prod_1^n K_i \tag{5.15}$$

β_n is called the overall complex stability constant of the nth complex.

$$\log \beta_n = \log K_1 + \log K_2 + \ldots . + \log K_n = \sum_{i=1}^{n} \log K_i \tag{5.16}$$

For a polybasic acid H_nL, the stepwise protonation constant K_{Hn} is defined by the reaction

$$LH_{n-1} + H \rightleftharpoons LH_n \tag{5.17}$$

$$K_{Hn} = \frac{[LH_n]}{[LH_{n-1}]\,[H]} \tag{5.18}$$

and the <u>overall stability (protonation) constant</u> is

$$\beta_{Hn} = \frac{[LH_n]}{[L]\,[H]^n} \tag{5.19}$$

For a protonated complex MLH_n,

$$K_n = \frac{[MLH_n]}{[M]\,[LH_n]} \tag{5.20}$$

and

$$\beta_n = \frac{[MLH_n]}{[M]\,[L]\,[H]^n} = K_n\,\beta_{Hn} \tag{5.21}$$

5.3 Methods Available for Determining Stability Constants.

There are several methods available for the determination of metal-complex stability constants of complexes of metal ions with weak acids. These methods are described in detail in references [1-4]. A partial list of these is presented in table 5.1.

The most widely used method is potentiometric pH titration using a glass electrode. This is possibly partly due to convenience, since the measurements using this method are not time-consuming and the instruments necessary are not expensive. The same experimental set up can be used to determine acidity constants and complex stability constants and the methods can be readily applied to polybasic acids and binding systems of multiple equilibria. The chief difficulties are caused by uncertainty over the values of liquid junction potentials and single ion activities.

The use of metal-ion-selective electrodes for the study of metal-ligand complex equilibria offers an attractive alternative to other methods. For example, calcium-ion-selective electrodes have been employed by

Table 5.1 Methods for Determining Stability Constants.

Electrochemical Methods

Potentiometry:- Direct methods: - measurement of free metal ion concentrations (electrode reversible to free metal ions)

- measurement of free ligand concentrations (electrode reversible to free ligand)

Indirect methods: - measurement of free ligand concentrations indirectly through measuring of pH (electrode reversible to free hydrogen ions)

Polarography

Conductimetry

Coulometry

Optical and Spectroscopic Methods

Ultraviolet and Visible spectrophotometry

Infrared spectroscopy

Nuclear magnetic resonance

Electron spin resonance

Fluorimetry

Distribution Methods

Solubility

Liquid-liquid partition (extraction)

Ion-exchange

Thermal Methods

Calorimetry

Reaction Kinetics Methods

different workers to determine the complexation between Ca^{2+} and citrate [5-8]. The method depends on monitoring the change in free calcium ion level caused by the addition of the citrate ligand.

Magnesium-ion-selective electrodes have also been employed before for the study of ionic equilibria [9, 10]. Recently, Zhang et al. [11] have used Mg^{2+} macroelectrodes based on the neutral carrier ETH 7025 to measure the Mg-ATP dissociation constant. The solution of Na_2ATP was titrated with $MgCl_2$ and the changes in $[Mg^{2+}]$ monitored with the macroelectrode. The pH was maintained constant during the titration.

In this work, however, the metal-ion-selective electrodes (Mg or Ca ISEs) have been used in a new and different manner in which the metal-ion- selective electrode is used in conjunction with a glass electrode in an alkalimetric titration for simultaneous pH and pM titrimetric determination of complex stability constants. The principles behind this method and the experimental technique used are explained in chapters 6 and 7 of this work.

According to the stability constants-database [12], only a few workers have used both metal-ion selective and glass electrodes in potentiometric pH titrations. Recently, Maeda et al. [13] used the Ca ISE and glass electrode, jointly, to study the complex formation of Ca^{2+} with amino acids including glycine and aspartic acid. However, a Mg ISE has not been used before in conjunction with glass electrode to study magnesium complexes.

5.4 Previous Work on Magnesium Complexes.

The magnesium ion, as with the other alkaline earth metal ions, forms complexes with various ligands of different kinds [14, 15]. Many of these ligands are of biological interest and are present both in biofluids and in natural waters. Since magnesium is generally present in significant amounts in all natural fluids, knowledge of the stability constants of its complexes is quite important to understand the mechanism of biological and other reactions [8, 16, 17]. Another important application of stability data is to design metal ion buffers for use in biological systems and for standardizing ion-selective electrodes [18, 19].

There are many publications [1, 14, 15, 20] containing cumulative tables of stability constants of metal complexes and these include values for complexation of magnesium with various/a variety of ligands. Recently, a software stability constants database (SC-database) was prepared by L. Pettit and H. Powell. It is a collection of literature values of stability constants, directing the user to the literature references. This program has been the source used (most often) in this work to collect the required literature data for comparison. Examples of using SC-database are given in Appendix C.

In this work, the stability constants of magnesium with important organic ligands shown in table 5.2 was determined.

Table 5.2

Ligand	Name	Structure (acid form)	Effective no. of dissociable H of acid form
Citric acid	2-Hydroxypropane-1,2,3-tricarboxylic acid	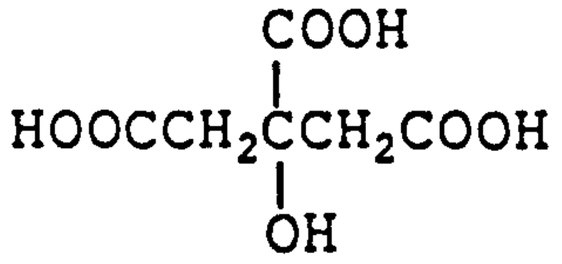	3 or 4 [21]
Lactic acid	α-Hydroxypropionic acid	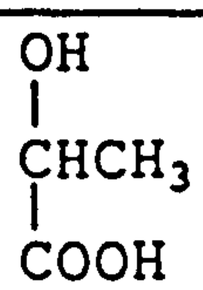	1
Glycine	Aminoacetic acid	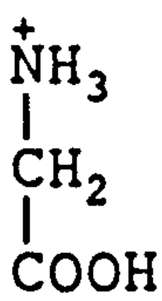	2
Aspartic acid	2-Aminosuccinic acid	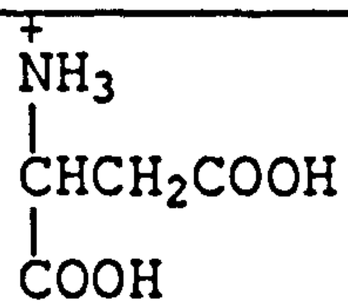	3
Glutamic acid	2-Aminoglutaric acid	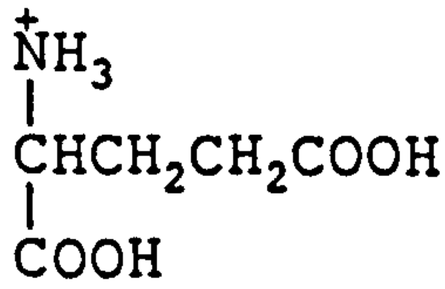	3
Pyroglutamic (Pidolic) acid	5-Oxo-2-pyrrolidinecarboxylic acid, or 5-Oxo-L-proline	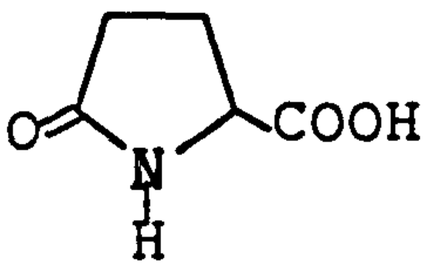	1
Pyridoxine (Vitamin B_6)	3-Hydroxy-4,5-bis (hydroxymethyl)-2-methylpyridine	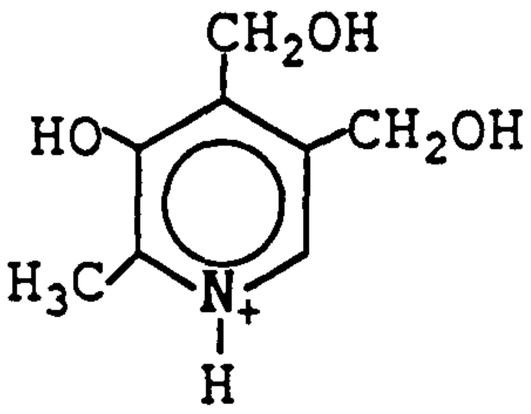	2
HEPES	[N-(2-hydroxyl)piperazine-N-ethanesulfonic acid]		2

In the literature there exists a remarkable lack of agreement amongst values for the stability constants of magnesium, as well as of calcium, with

the above ligands. The published compositions of the complex species present in the solutions of these ligands in the presence of magnesium or calcium ions are also different. Furthermore, very few studies have been made on the interaction of magnesium with HEPES, pyroglutamic acid and vitamin B_6. Thus it was of interest to make a more complete investigation of the equilibria existing in the solutions of the above ligands in the presence of magnesium or calcium.

References.

1. F. J. C. Rossotti and H. Rossotti, *The Determination of Stability Constants*, McGraw-Hill, New York, 1961.

2. M. T. Beck, *Chemistry of Complex Equilibria*, Van Nostrand-Reinhold, London, 1970.

3. F. R. Hartley, C. Burgess and R. M. Alcock, *Solution Equilibria*, Ellis Horwood, Chichester, 1980.

4. K. A. Connors, *Binding Constants: The Measurement of Molecular Complex Stability*, John Wiley and Sons, New York, 1987.

5. G. A. Rechnitz and T. M. Hseu, *Anal. Chem.*, 41, 111 (1969).

6. A. Craggs, G. J. Moody and J. D. R. Thomas, *Analyst*, London, 104, 961 (1979).

7. R. P. Singh, Y. D. Yeboah, E. R. Pambid and P. Debayle, *J. Chem. Eng. Data*, 36, 52 (1991).

8. P. G. Daniele and M. Marangella, *Ann. Chem.*, 72, 25 (1982).

9. T. Nakamura, H. Higuchi and K. Izutsu, *Bull. Chem. Soc. Jpn.*, 61, 1020 (1988).

10. M. Bonnery, V. LoGatto, M. Persin and G. Durand, *Bull. Soc. Chim. Fr.*, I, 49 (1988).

11. W. Zhang, A. Truttmann, D. Lüthi and J. A. S. McGuigan, *J. Physiol.*, 473, 6P (1993).

12. L. D. Pettit and H. K. J. Powell, *IUPAC Stability Constants Database* Academic Software, 1995.

13. M. Maeda, K. Okada, Y. Tsukamoto, K. Wakabayashi and K. Ito, *J. Chem. Soc. Dalton Trans.*, 2337 (1990).

14. J. Bjerrum, G. Schwarzenbach and L. G. Sillen, *Stability Constants*, The Chemical Society, London, Special Publication No. 6, 1957.

15. A. E. Martell, R. M. Smith, *Critical Stability Constants*, Plenum Press, London-New york, 1977.

16. C. Blaquiere and G. Berthon, *Inorg. Chim. Acta*, 135, 179 (1987).

17. M. L. S. Simões Gonçalves and P. Valenta, *J. Electroanal. Chem.*, 132, 357 (1982).

18. D. D. Perrin and B. Dempsey, *Buffers for pH and Metal-Ion control*, Chapman and Hall, London, 1974.

19. A. K. Covington and R. Kataky, In: A. H. J. Maas, B. Buckley, H. Marsoner, N. E. L. Saris and R. Sprokholt, *Methodology and Clinical Applications of Ion-Selective Electrodes*, IFCC, 8, 35 (1986).

20. G. Anderegg, *Critical Survey of Stability Constants of EDTA Complexes*, IUPAC Chemical Data Series No. 14, Pergamon Press, Oxford, 1977.

21. M. J. Blais and G. Berthon, *Inorg. Chim. Acta*, 67, 109 (1982).

CHAPTER 6

THEORETICAL AND PRACTICAL CONSIDERATIONS OF pH MEASUREMENTS.

6.1 The Definition of pH.

6.1.1 Notional Definition.

The pH of a solution was originally defined by Sørensen [1] as

$$pH = -\log c_H \qquad (6.1)$$

where C_H is the hydrogen ion concentration (in mol/L). This definition, after the subsequent realisation that electrodes respond to activity rather than concentration, was modified [2] to

$$pH = -\log a_H \qquad (6.2)$$

equation 6.2 is often written as

$$pH = -\log m_H \gamma_H \quad \text{or} \quad pH = -\log c_H y_H \qquad (6.3)$$

Since pH is a dimensionless quantity, the full forms of equation (6.3) will be either

$$pH = -\log \frac{m_H \gamma_H}{m_o} \quad \text{or} \quad pH = -\log \frac{c_H f_H}{c_o} \qquad (6.4)$$

where m_o and c_o are standard state constants equal to 1 mol/kg and 1 mol/L respectively. m_H is the molality and c_H is the molarity of the hydrogen ion. γ_H and f_H are single ion activity coefficients of the hydrogen ion on the molality and molarity scales respectively.

However, the quantity pH, defined as $-\log a_H$, is not an explicitly measurable quantity, because it is not possible to determine the activity of a single ion. Therefore, it is accepted of greater use to define pH in operational terms, that is, by the method used in its determination.

6.1.2 Operational Definition.

The operational cells for pH measurements consist of

$$Hg \mid Hg_2Cl_2 \mid KCl\,(\geq 3.5\,mol/L) \parallel Standard, S \mid H_2 \mid Pt \qquad (I)$$

$$Hg \mid Hg_2Cl_2 \mid KCl\,(\geq 3.5\,mol/L) \parallel Unknown, X \mid H_2 \mid Pt \qquad (II)$$

The hydrogen electrode is often replaced by a glass electrode. The pH of the unknown solution is then related to that of the standard by the definition:

$$pH_{(x)} = pH_{(s)} + \frac{E_s - E_x}{(RT/F)\ln 10} \qquad (6.5)$$

This equation is known as the operational definition of pH. E_S and E_X refer to the potentials of cell (I) and (II) respectively. Equation (6.5) is only applicable if the liquid junction potentials in cells (I) and (II) are equal (see section 10.4).

6.2 pH Scales.

Measurements using the operational definition of pH are based upon the direct calibration of the meter with prescribed standard buffers followed by potentiometric determination of the pH of unknown solutions. In potentiometric titrations using a glass electrode, standardisation may be carried out with either a solution of known hydrogen ion concentration (concentration scale) or, more commonly, of assigned hydrogen ion activity (activity scale).

6.2.1 Activity Scale.

There are essentially two pH scales in current use. These are the US National Bureau of Standards (NBS) multistandard scale and the British standard (BS) single standard scale.

6.2.1(a) The National Bureau of Standards (NBS) Scale.

On the NBS scale, the pH of the standard solutions are assigned by making measurements in cells without liquid junction:

$$\mathrm{Pt(Pd)\,|\,H_2\,|\,Buffer,\ Cl^-\,|\,AgCl\,|\,Ag} \qquad \text{(III)}$$

Emf measurements are made with this cell on solutions of the standard solutions with varied amounts of added Cl^-.

The emf of the cell is given by:

$$E = E^\circ - k \log \frac{m_H \gamma_H m_{Cl} \gamma_{Cl}}{m_\circ^2} \qquad (6.6)$$

where m signifies molality and γ the activity coefficient of the indicated species, k is the theoretical slope (RTln10/F), $m_\circ$ is the molal standard state concentration of 1 mol kg^{-1} and E° is the standard potential, derived from measurements on the cell:

$$\mathrm{Pt\,|\,H_2\,|\,HCl\,(0.01\ mol\ kg^{-1})\,|\,AgCl\,|\,Ag} \qquad \text{(IV)}$$

and calculated from equation (6.6) for which the mean ionic activity coefficient $\gamma_\pm$ of HCl is known.

Equation 6.6 can be rearranged to

$$-\log \frac{m_H \gamma_H \gamma_{Cl}}{m_\circ} = \frac{E - E^\circ}{k} + \log \frac{m_{Cl}}{m_\circ} \qquad (6.7)$$

By obtaining values of - log ($m_H \gamma_H \gamma_{Cl} / m_\circ$) at various chloride concentrations m_{Cl}, the value of - log ($m_H \gamma_H \gamma_{Cl} / m_\circ$) of the standard solution at zero chloride concentration can be obtained by extrapolation. Then, the $p(a_H)$ of the standard solution can be obtained from

$$P(a_H) = \left[-\log \frac{m_H \gamma_H \gamma_{Cl}}{m_\circ}\right]_{m_{Cl} \to 0} + \log \gamma_{Cl} \qquad (6.8)$$

where γ_{Cl} is given by the Bates-Guggenheim convention [4] in which the following form of the Debye-Hückel equation is used:

$$-\log \gamma_{Cl} = \frac{A\, I^{1/2}}{1 + 1.5\, I^{1/2}} \qquad (6.9)$$

This method has been applied to seven primary standards used in defining the NBS pH scale. Requirements for an NBS primary standard are that they are available in a highly pure state and exhibit only a small residual liquid junction potential. Secondary standards, failing these requirements, are also used, but the pH values of these solutions are assigned in a similar manner. pH values of the standard solutions for the pH range of 1.7 to 13 at temperatures from 0 to 95 °C on the NBS scale are given by Bates [5].

6.2.1(b) The British Standard (BS) Scale.

The BS scale is based on a single solution, 0.05 mol/kg potassium hydrogen phthalate (one of the NBS primary standards), together with the theoretical slope, RT ln10/F. The pH of the potassium hydrogen phthalate solution is assigned using a cell without a liquid junction as described above and the convention of equation 6.9 [6]. All other standards are refered to as secondary (or operational) and their pH values are assigned using the operational definition of pH (equation 6.5), which can be represented by the cell:

$$\mathrm{Pt} \,|\, \mathrm{H_2} \,|\, \mathrm{X\ or\ S} \,\Big\|\, \begin{array}{c} \geq 3.5\ \mathrm{mol\ L^{-1}} \\ \text{or} \\ \geq 1\ \mathrm{mol\ L^{-1}\ KNO_3} \end{array} \Big|\, \text{Reference electrode} \qquad (V)$$

where S is the standard phthalate buffer and X is an operational standard. The liquid junction in the cell is formed in a 1 mm capillary tube. The residual liquid junction potential incorporated into the pH value of the

operational standard is considered to be negligible in the pH range 3-9, being less than ± 0.02 in pH. Values for the pH of the standard solutions for the pH range of 1.7 to 13 at temperatures from 0 to 95 °C according to the BS scale are given by the British Standards Institution (BSI) [7].

The reference standard potassium hydrogen phthalate, due to its high quality (purity) compared with the other pH reference materials, is designated as the reference value pH standard (RVS) [3].

The virtues of the NBS and BS pH scales have been critically reviewed by Covington [8] and Bates [9].

6.2.2 Concentration Scale.

In the case of the concentration scale, the pH-meter is calibrated in terms of hydrogen ion concentration so as to allow the determination of p[H] and hence the concentration of the hydrogen ion in the test solution (see below). This has found use in the investigation of protonation and complex formation equilibria. For equilibrium constant measurements, the pH of the solution is often determined to give a measure of the hydrogen ion concentration [H^+] which is then used for substitution in mass balance equations (see section 8.2) and directly in the expression for the concentration constants (see section 5.2 for the definition of the concentration constants). To make direct use of pH meter readings in these calculations, it is necessary to assume that the liquid junction potential for the cell containing the standard buffer solution is the same as for the cell containing the test solution and that some simple equation (e.g. Debye-Huckel equation) accurately defines the single ion activity coefficient for H^+ for a mixed electrolyte solution, and allows precise conversion of measured pH to p[H]. However, neither of these assumptions is fully

maintainable and together they introduce uncertainties in p[H] and errors in the derived concentration constants. In order to avoid these assumptions and minimize the errors, several workers in this field [10-12] calibrate the glass-reference electrode pairs against solutions of known p[H] and with the same ionic strength and ionic background as the test solutions. The calibration solutions are normally solutions of weak acids with known pK values (e.g. acetate, phosphate) or strong acids (e.g. HCl, $HClO_4$). Measurements are made under conditions of constant ionic strength, maintained by an inert supporting electrolyte. The concentrations of the components investigated and of the standard are presented in negligible concentrations with respect to that of the background electrolyte.

Although, the above method of standardisation of the glass electrode seems to have many positive points, its application is limited. The determination of metal complex stability constants requires a range of solution compositions in which a varying proportion of the supporting electrolyte is replaced by a salt of the complexing metal. This range of solution compositions can not easily be matched by suitable p[H] standards. Furthermore, the method requires low concentrations of the components investigated (relative to the background electrolyte), and there are some cases in which the stability constants for complex species can only be determined at high concentrations. Another important difficulty concerning p[H] standards is that, as a result of using low buffer concentrations, their buffer capacity is small.

6.3 pH Glass Electrode.

6.3.1 Introduction.

The glass electrode is the most widely used electrode for pH measurement. The pH-sensitive part of the electrode is a thin glass membrane constructed at the bottom of the electrode stem. The glass is made from a silicate lattice. The silicate consists of an infinite three-dimensional network of SiO_4^{4-} groups [13] in which each silicon is bonded to four oxygens and each oxygen is shared by two silicons. The holes in the three-dimensional pattern are occupied by cations, such as Na^+, Li^+, Ca^{2+} and Ba^{2+}, to balance the negative charge of the silicate groups. The metal ions in the lattice disrupt the silicon-oxygen network structure and create the ion-exchange sites which lead to the pH response of the membrane.

6.3.2 Transfer Processes Occurring in the Glass Electrode.

When a thin piece of glass is immersed in an aqueous solution, a hydrated gel layer is formed on its surface. In this layer, alkali metal ions (such as sodium) from the glass are replaced by hydrogen ions from the solution. The process involves the monovalent cations almost entirely because di- and trivalent cations are too strongly held within the silicate structure to exchange with ions in the solution.

The ion-exchange reaction can be written as

$$H^+_{solution} + Na^+A^-_{glass} = Na^+_{solution} + H^+A^-_{glass} \qquad (6.10)$$

where A^- represents one of many negatively charged sites in the glass surface.

The hydrogen ions in the glass surface (gel layer) cannot migrate across the dry bulk glass [14]. The H^+ equilibrium across the solution/gel interfaces can be represented by

$$H^+_{solution(1)} + A^-_{glass(1)} = H^+A^-_{glass(1)} \quad (6.11)$$

$$H^+A^-_{glass(2)} = H^+_{solution(2)} + A^-_{glass(2)} \quad (6.12)$$

where subscript (1) refers to the interface between the glass and the analyte solution and subscript (2) refers to the interface between the internal solution and the glass. Na+ ions in the silicate lattice transport charge and are responsible for the conductivity within the bulk of the glass membrane. The mechanism of the glass electrode is therefore different from other ISEs as the species diffusing across the membrane is not the same as the species selectively adsorbed at each membrane surface.

6.4 The Magnesium ISEs (Choice of Ionophores).

The applicability of Mg ISEs in potentiometric (alkalimetric) titrations to determine the stability constants of magnesium complexes requires high selectivity of the membrane electrode for magnesium over the hydrogen ion. The experimental results of the effect of pH on different magnesium membranes (see section 3.7.2) indicates that the Mg ISE based on ionophore ETH 4030 is suitable to be used in such systems. This electrode, in contrast to ETH 1117 and ETH 7025 Mg ISEs, is highly selective to magnesium over pH. Furthermore, the high selectivity of the ETH 4030 membrane against Na^+ and K^+ ions (see section 3.7.1) allows the measurements to be carried out in the presence of high concentrations of sodium or potassium chloride as a background electrolyte. The Ca ISE based on ETH 1001 was also shown to have the above requirements for using ISEs in acid-base titrations, and was used to determine the stability constants of calcium complexes. There was, however, a little interference from hydrogen ions in a strong acidic medium of pH $\leq$ 3. Therefore, use of both the Mg and Ca ISEs was restricted in this work to pH more than 3.

References.

1. S. P. L. Sørensen, *Biochem*. Z., 21, 131 (1909).

2. S. P. L. Sørensen and K. Linderstrom-lang, *Compt. Rend. Trav. Lab. Carlsberg*, 15, No. 6 (1924).

3. A. K. Covington, R. G. Bates and R. A. Durst, *Pure Appl. Chem*., 57, No. 3, 531 (1985).

4. R. G. Bates and E. A. Guggenheim, *Pure Appl. Chem*., 1, 163 (1960).

5. R. G. Bates, *Determination of pH. Theory and practice*, 2nd edn., Wiley, New York (1973).

6. British Standard Institution, BS 1647, *pH measurement*, Part 1 (1984).

7. British Standard Institution, BS 1647, *pH measurement*, Part 2 (1984).

8. A. K. Covington, *Anal. Chim. Acta*, 127, 1 (1981).

9. R. G. Bates, *Crit. Rev. Anal. Chem*., 10, 247 (1981).

10. H. M. Irving, M. G. Miles and L. D. Pettit, *Anal. Chim. Acta*, 38, 475 (1967).

11. A. E. Martell and R. J. Motekaitis, *Determination and Use of Stability Constants*, VCH Publishers, New York, (1988).

12. M. Molina, C. Melios, J. O. Tognolli, L. C. Luchrari and M. Jafelicci, *J. Electroanal. Chem*., 105, 237 (1979).

13. W. H. Zachariasen, *J. Am. Chem. Soc*., 54, 3841 (1932).

14. K. Schwabe, In: H. W. Nürnberg, *Advances in Analytical chemistry and instrumentation*, John Wiley and Sons, London, Vol. 10 (1974).

CHAPTER 7

EXPERIMENTAL

7.1 Materials and Method.

7.1.1 Reagents.

Citric acid was obtained from BDH (Analar Grade). DL-pyroglutamic acid and L-glutamic acid hydrochloride were supplied by Sigma Chemical Co. DL-lactic acid, L-aspartic acid and pyridoxine hydrochloride were supplied by Fluka. The purity of these ligands, determined by alkalimetric titrations, was found > 99 % ; all were then used without further purification. HEPES, obtained from Sigma Chemical Co., was dried for 5 hours in an oven at 80°C, and stored in a desiccator over phosphorus pentoxide. NaCl and KCl, obtained from BDH (Analar Grade), were dried at 110°C. Stock solutions of $MgCl_2$ and $CaCl_2$, prepared from Analar $MgCl_2.6H_2O$ (BDH), previously dried in an oven at 80°C, and BDH volumetric 1 mol/L $CaCl_2$ standard solution, respectively, were standardized by titration with EDTA [1]. HCl, NaOH and KOH solutions were prepared from BDH convol concentrated ampoules; NaOH and KOH solutions were then standardized against HCl, using the Gran plot method [2, 3] provided with the Molspin program for end point detection. The NBS standards, KHPhthalate (0.05 mol/L) at 37 °C and KH_2PO_4 (0.08695 mol/L) + Na_2HPO_4 (0.03043 mol/l), with pH of 4.022 and 7.369 at 37 °C, respectively, were prepared from BDH samples as recommended [4]. Deionised (Milli-Q, low conductivity: R>18 MΩ.Cm) carbon dioxide-free water was used for preparing all of the solutions.

For the preparation of the membranes for the magnesium and calcium ion-selective electrodes, the following chemicals (obtained from Fluka)

were used: for the Mg electrode, 1 wt % magnesium ionophore ETH 4030, 33 wt % high molecular mass PVC, 65 wt % chloroparaffin and potassium tetra(4-chlorophenyl)borate (KTpClPB) in a molar ratio of 0.7 relative to the ligand; for the Ca electrode, 1 wt % calcium ionophore ETH 1001, 33 wt % PVC, 66 wt % 2-nitro phenyl octyl ether (o-NPOE) and KTpClPB in a molar ratio of 0.5 relative to the ligand. THF, obtained from BDH, was used for dissolving the membrane components; it was dried over CaH_2 and freshly distilled prior to use.

7.1.2 Apparatus and Instrumentation.

The components of the titration system are illustrated schematically in figure 7.1. The titration cell was a double-walled glass vessel with a capacity of about 120 ml. It was fitted with a cap made from an inert material (Teflon or polycarbonate [5]) which would not react with the titration mixure components. The cap had five (or six when the metal ISE was used) openings of different sizes designed to accommodate the glass electrode, reference electrode, metal ion-selective electrode, burette tube, temperature probe and nitrogen bubbler. The titration solution inside the cell was thermostatted at 37 °C by circulation of water from a thermostat bath through the space between the vessel walls (Thermostat/pump type Techne Tempette Junior TE-8J).The temperature inside the vessel was monitored using the temperature probe (PLATINUM Resistance Probe, Class A) which is connected to Molspin apparatus and program. The titration solution was mixed by a magnetic stirrer. To avoid the possibility of interference from atmospheric carbon dioxide, all titrations were carried out under an atmosphere of purified nitrogen (available commercially in cylinders), bubbled through the solution.

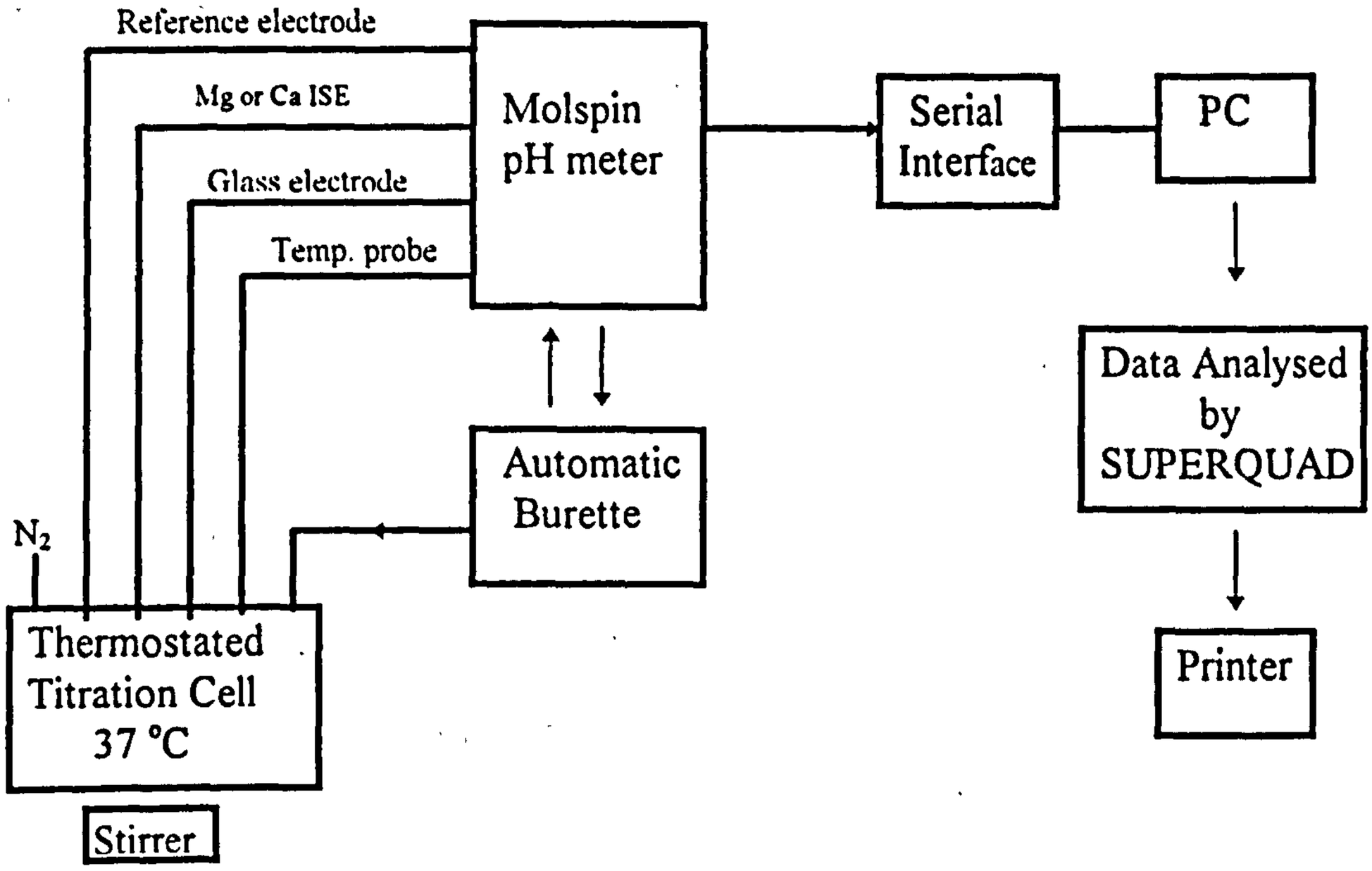

Fig. 7.1 Titration System

The potentiometric measurements were recorded using a Molspin computer linked pH meter (Molspin Ltd. TWIN Input RS232 pH Meter). This covers two voltage ranges (±300 mV and ±1000 mV) and accommodates simultaneously two independent ion selective electrode inputs with a common reference electrode. The measurements were made with a Russell SW2 glass electrode and Mg ISE based on ETH 4030, or Ca ISE based on ETH 1001, in conjunction with a Russell CRR2 Calomel reference electrode. The Mg and Ca electrodes were of a dip-type constructed as described in section 3.2. The internal reference electrodes of the Mg and Ca ISE were thermal electrolytic silver/silver chloride electrodes formed on platinum wire. The pH meter was linked to a Mol-AcS computer controlled burette employing a precision motor driven 10 ml glass syringe (10 cc syringe gas tight) with a plastic capillary feeding directly into the titration cell.

The measuring equipment was linked to an IBM-PC compatible computer and controlled by software provided by Molspin Ltd. The program allowed the titration to be performed automatically using 1 or 2 indicator electrodes with measurements in either mV or pH for each electrode. The titration was performed using the titration option in which the total volume to be delivered, increment size, time delay and required electrode stability between additions were set before starting the titration, as shown in figure 7.2. It is due to the control given by these latter two quantities (delay and drift options) that a sufficient time can be allowed for equilibration before taking the readings, especially when the equivalence point is closely approached, and thus that precise and accurate measurements can be obtained. The titration curves were displayed on the computer screen both numerically (volume-pH/mV) and graphically and

Fig. 7.2 Titration Parameters

```
Load titration from disk (N,Y)  ?  N

Choose Titration Parameters:

    Total Volume of burette (ml)          :   10.000
    Volume Increments (ml)                :    0.0500
    Total Volume to add (ml)              :   10.0000
    Max. drift (mV) in DELAY sec.         :    0.09
    DELAY time (sec.)                     :    1.00
    Number of active electrodes           :    2
    Measurements in pH or mV ?            :    mV    Elec.2 ? : mV
    Volume increments will be (ml)        :   0.05000
    Number of steps will be               :   200
    Total volume to be added will be (ml):   10.000


The titration can be stopped at any point by pressing <ESCAPE>
Pressing P will make the computer pause until P is pressed again.
Pressing S will over-ride the computer and force the next increment BUT
pH/mV value may be nonsense.

Press any key to start titration, Q to QUIT
```

the data were saved to a computer disk in a SUPERQUAD compatible format and as a text file if required. The program SUPERQUAD, a non-linear least squares fitting programs, is one of the most powerful PC-based programs for calculating acid dissociation constants and metal complex stability constants and the Molspin pH meter software is designed to work in conjunction with it.

The potentiometric data was subsequently analysed using SUPERQUAD.

7.1.3 Titration Procedure.

The titrations of known concentrations of the ligands with standard NaOH or KOH were carried out, in the absence of magnesium and calcium ions, to determine the acidity constants. When magnesium or calcium ions are present the potentiometric titrations yield the formation constants of magnesium or calcium complexes. An excess of strong acid (HCl) was added to solutions to be titrated in order to reach high degrees of protonation for the ligands. NaCl or KCl (0.15 mol/L) were used as a background electrolyte to maintain the activity coefficients of the reactants constant and to ensure isotonicity of the solutions with blood plasma ($I \approx 0.15$ mol/L in blood plasma [6]).

On the 2-Input model of the Molspin pH meter, titrations were performed using a glass electrode and a Mg or Ca ISE to obtain simultaneous measurement of pH and pMg or pCa. When determining the ligand protonation constants, the glass electrode only was employed.

The pH glass electrode was calibrated with the NBS phthalate and phosphate buffers (section 7.1.1), pre-warmed to 37 °C before each titration. The procedure for calibration is detailed in the Molspin manual [7].

The Mg and Ca electrodes were calibrated before each titration run at 37 °C using serially diluted magnesium and calcium solutions (10^{-4} - 10^{-1} mol/L at 37 °C), respectively, in the presence of 0.15 mol/L NaCl or KCl. Emf vs. log c_{Mg} or log c_{Ca} calibration curves were then constructed to calculate the slope and E°, the values of which were entered into a SUPERQUAD data file for calculation of metal complex stability constants. The calibration procedure was repeated after the titration in order to recheck the performance of the electrodes.

The calomel and metal ion-selective electrodes were dipped into the titration solution to a level exceeding their internal filling solutions in order to maintain their temperatures at as steady a state as possible, and thus obtain stable measurements. When not in use the calomel electrode was stored at 37 °C in saturated KCl solution.

Before starting the titration, the burette was calibrated. The procedure for calibration is found in the Molspin manual [7]. The burette was then filled and all air-bubbles expelled from the delivery tube. To fill the syringe, the syringe plunger was withdrawn using the manual 'Backwards' button on the control unit and then moved forwards to a starting position using the 'Forward' button. The last movement before commencing the titration was always forwards to remove any backlash in the stepper motor and delivery tube. The tip of the delivery tube was wiped gently with a tissue and dipped into the titration solution. The titrant was added in 0.015-0.05 ml increments. The titration solution was maintained at 37 °C, monitored by the temperature probe, and this temperature was used in all pH/emf calculations, and was entered automatically into the SUPERQUAD data files.

References.

1. A. I. Vogel, *Textbook of Quantitative Inorganic Analysis*, 4th ed., Longmans, London, p. 320 (1978).

2. G. Gran, *Analyst*, 77, 661 (1952).

3. D. C. Harris, *Quantitative Chemical Analysis*, W. H. Freeman and Company, New York, 4th ed., p. 292 (1994).

4. British Standard Institution, BS 1647: *pH measurement*, Part 2, (1984).

5. 'Rhiamer' Polycarbonate, M & B Plastics Ltd., London.

6. S. M. Willatts, *Lecture notes on fluid and electrolyte balance*, 2nd edition, Blackwell Scientific publications, Oxford, 1987.

7. L. D. Pettit, Molspin Software for Molspin pH Meter, Academic Software, 1992.

CHAPTER 8

CALCULATION OF STABILITY CONSTANTS.

8.1 Computer Programs for the Potentiometric Determination of Stability Constants.

Several computer programs have been developed for the evaluation of the potentiometric titration data, the most widespread being LETAGROP, ESTA, SCOGS, MINIGUAD and SUPERQUAD. These programs aim to determine a model (*i.e.* composition of the species present in solution and their respective stability constants) which gives a satisfactory fit to the experimental data. All programs utilise the non-linear least-squares method to minimise the sum of squared differences S between the observed quantities f_i^{obs} and those calculated by the model f_i^{calc}:

$$S = \sum_{i=1}^{N} w_i \left(f_i^{obs} - f_i^{calc} \right)^2 \qquad (8.1)$$

where N is the number of observations (measurements) and w_i the statistical weight of the i^{th} observation.

Despite sharing the least-squares method, the programs differ significantly in the following features [1, 2]:

(a) Definition of residuals function f and numerical procedure utilised for the minimisation of the sum of squared differences S.

(b) The statistical weighting scheme for the evaluation of w_i factors.

(c) The species selection procedure and the ability to refine some titration parameters.

Table 8.1 compares the main features of these programs [1].

Table 8.1 Comparison of potentiometric titration computer programs.

Topic	LETAGROP	ESTA	SCOGS	MINIQUAD	SUPERQUAD
Residuals minimised	T_H [a], e.m.f.	T_H [a], e.m.f.	Titrant volume	All T_i [b]	e.m.f.
Statistical weighting	–	✓	–	–	✓
Derivatives [c]	Numerical	Analytical	Numerical	Analytical	Analytical
Execution times (sec) [d]	50	26	40	6	9
Parameters refinement [e]	✓	✓	–	–	✓
Automatic model selection [f]	–	–	–	✓	✓

(a) T_H = the total analytical concentration of the hydrogen.
(b) T_i = the total analytical concentration of the reactant *i*.
(c) Analytically calculated derivatives lead to faster convergence (less iterations) and reduced program execution times [1,3].
(d) Times cited were obtained from the solution of the same problem with an IBM 370 computer; they should only be considered comparatively.
(e) *E.g.* standard potentials, slope response of electrode, analytical concentrations of reactants.
(f) If after refinement of β_j's a formation constant is found to be ill defined (i.e. β_j negative or its calculated standard deviation is more than 33 % of its value), a new model is automatically generated from which the ill-defined species is rejected.

8.2 Overview of SUPERQUAD.

SUPERQUAD [4], which was developed as an improvement of MINIQUAD, is the specific program utilised in this work. The selection was based on its good overall performance in terms of ease of usage (user-friendly input file), accurate fitting capabilities and comprehensive output information (*e.g.* statistical analysis and residual plots, species distribution curves).

During a titration, electrodes are used to measure the variation in the free concentration of one or more reactants in solution, that is realised after the gradual addition of the titrant in small volume increments.

SUPERQUAD utilises the least-squares method to determine the value of the formation (or stability) constants β_j of each species j so as to minimise the squared difference between the experimentally observed e.m.f. of the electrode (or equivalently the free electro-active ion concentration) and the respective one calculated by the model.

SUPERQUAD has been used by several workers to calculate formation constants of species in solution equilibria. For example, Kataky [5] evaluated the binding constants for a range of 'Good' buffers, including HEPES, with metal cations, Na^+, K^+, Ca^{2+}, using pH-metric titrations and analysing the data with SUPERQUAD. Bal et al. [6] used SUPERQUAD to calculate the formation constants of the Ca-squalestatin complex. The method applied was potentiometric titration with a glass electrode. Dick [7] has extended the application of SUPERQUAD to analyse data obtained by ISEs and coulometry.

According to the SC-database, SUPERQUAD has not previously been used to analyse the data obtained by using Mg or Ca ISE in potentiometric titrations. Such data, however, has been analysed by miniQUAD [8].

8.2.1 Mathematical Modelling of Titration.

Each model in essence predicts the complex species that exist in equilibrium in the solution of a number of elementary reactants *A*, *B*, *etc.* The model is specified by a set of coefficients a_j, b_j, *etc.* that describe the composition of the complex species j according to the following formation reaction:

$$a_j A + b_j B + \ldots \rightarrow A_{a_j} B_{b_j} \ldots, \quad \text{for all complex species } j \qquad (8.2)$$

For each complex species j there is a chemical constant, the formation constant β_j, that dictates the equilibrium composition, expressed as a concentration quotient:

$$\beta_j = \frac{\left[A_{a_j}\ B_{b_j}\ ....\right]}{\left[A\right]^{a_j}\left[B\right]^{b_j}...} \tag{8.3}$$

where $[A]$, $[B]$ are the concentrations of free reactants and $[A_{aj}, B_{bj},...]$ is the concentration of the complex species j. Electrical charges may be attached to any species, but they are omitted for simplicity and generality. For given total concentrations of the reactants T_A, T_B, *etc.*, there is a unique distribution of reactants among the various complex species, according to the magnitude of each formation constant β_j. If the values for the β_j are given, the free concentrations $[A]$, $[B]$, *etc.* may be obtained by solving the set of non-linear mass balance equations applicable to each reactant:

$$T_A = \left[A\right] + \sum_j \left\{a_j \left[A_{a_j}\ B_{b_j}...\right]\right\} = \left[A\right] + \sum_j \left\{a_j\, \beta_j \left[A\right]^{a_j}\left[B\right]^{b_j}...\right\}$$

$$T_B = \left[B\right] + \sum_j \left\{b_j\, \beta_j \left[A\right]^{a_j}\left[B\right]^{b_j}...\right\} \tag{8.4}$$

The summations run through all complex species $j = 1, 2, ..., N_C$.

After the free concentration of the electroactive ion (e.g. $[A]$) is determined, the corresponding electrode potential can be calculated. Assuming a pseudo-Nernstian behaviour of the electrode:

$$E = E^0 + S_L \log\left[A\right] \tag{8.5}$$

where E is the measured potential and E^o and S_L are parameters associated with the specific electrode in use, namely the standard electrode potential

and the slope, respectively. These parameters are usually obtained in a separate calibration experiment.

In the previous steps (8.3-8.5) it has been demonstrated that, given a model for the complex species present (set of coefficients a_j, b_j, ...), it is possible to calculate the electrode potential E that corresponds to a specific titration point t (fixed values of T_A, T_B, ...), once the formation constants β_j are known. These calculated values can be subsequently compared to the experimentally *observed* potentials E^{obs}; ideally the two values should be identical.

8.2.2 The Principle of Non-Linear Least Squares Fitting.

In practice, the values of the β_j are unknown. Indeed it is the main objective of the titration to calculate these formation constants values. In the experiment, the effect of adding titrant volume (independent or controlled variable) on the electrode potential (dependent or measured variable) is determined. A total of N_T of experimental points are examined, corresponding to a different volume of titrant V_t added.

It has been shown in the previous section how it is possible to calculate the free reactant concentrations and the electrode potential E at each experimental point t, by assuming the β_j values. The total concentration of at least one reactant (e.g. B, the one added with the titrant) varies as the titration progresses:

$$T_B^t = \frac{n_B + C_B V_t}{V_0 + V_t} \tag{8.6}$$

where the index t denotes the specific titration point when a volume of titrant equal to V_t has been added in the reaction vessel. The initial amount of reactant B n_B, the initial volume of the reaction mixture V_0 and the

concentration of the reactant in the burette C_B are constant parameters of the experiment.

These differences in the total concentrations at each titration point t are translated by the model as different free reactant compositions (by the solution of the mass balances in 8.4) and in turn as different electrode potentials E_t (from equation 8.5). By proper selection of the β_j values it is possible to bring all the values calculated by the model E_t close to those experimentally observed E_t^{obs} at each titration point t. This can be equivalently expressed as bringing the differences E_t^{obs} - E_t (residuals or deviations) close to zero. The objective of the non-linear least-squares method utilised by SUPERQUAD is precisely to calculate the best values of the formation constants so as to minimise the residuals at all titration points. This objective can be mathematically expressed as:

$$\min_{\beta_j} S = \sum_{t=1}^{N_T} \left\{ w_t \left(E_t^{obs} - E_t \right)^2 \right\} \tag{8.7}$$

Elaborate numerical procedures are involved in the solution of the minimisation problem in (8.7) for the values of the formation constants β_j. An iterative procedure is adopted in which the β_j values are refined during each cycle, through the differentiation of the mass balances in (8.4). Details can be found elsewhere [4].

The idea behind least squares is to fit a curve of calculated electrode potential as a function of titrant volume added, $E_t = f(V_t)$, that passes as close to the experimental points as possible. A few outliners (i.e. possible experimental errors) can adversely affect the whole fit by displacing the curve away from the "correct" points. One way to alleviate this drawback is the use of the weight factors w_t in equation (8.7). When all w_t are equal to 1, then all titration points are assumed to have comparable accuracy and

are considered to *weight* identically in the procedure for the determination for the best fit (values of the β_j). In the case, however, when some titration points are suspected to be less accurate, then a lower value of the respective weight factors ($w_t < 1$) will ensure that these points will exhibit a smaller (comparatively) effect in the determination of β_j values, thus avoiding the possible "contamination" due to inaccurate experimental measurements.

More specifically in the case of potentiometric determination of stability constants, it is well known that electrode readings in the region of an end-point are unreliable because a small titre error can have a significant effect on them. In statistical terms, the electrode potential registered in this region will have a large *variance*, therefore the respective weight factors will have to be reduced. A standard error propagation formula is used in SUPERQUAD to calculate the expected error (variance) in the measured potential at each point *t* [4]:

$$\sigma_t^2 = \sigma_E^2 + \left(\frac{\partial E}{\partial V}\right)_t^2 \sigma_V^2 \qquad (8.8)$$

where σ^2_t is the calculated variance of measurement, σ^2_E and σ^2_V are the estimated variances of the electrode and volume readings taken individually and $\partial E/\partial V$ is the slope of the titration curve. According to this expression, data near the end point, where the slope is large, are correctly associated with larger variances. The weight factors at each titration point t are automatically calculated by SUPERQUAD as the inversed variances, *i.e.* $w_t = 1/\sigma^2_t$. In this way, large variances are translated to small weight factors.

8.2.3 Usage of SUPERQUAD.

SUPERQUAD is a powerful general purpose computer program for stability constant estimation. It can handle experimental data from all known systems of potentiometric titration [4]. The data of several titrations can be also combined before equilibrium constants are calculated. A data input file has to be created containing the titration data along with various program control parameters. A brief description of the input file is presented later. A sample SUPERQUAD data file can be found in Appendix D.

8.2.3(a) Input Data File.

The experimental data regarding all aspects of titration must be inserted in the input file, including the initial solution volume and reactant concentrations in the vessel, concentration of the reactant in the burette, and electrode related parameters, such as the standard potential and the slope. The experimental titration curve is supplied as a list of titre volume increments along with the respective electrode readings (in either mV or pH).

The model under investigation has to be subsequently inserted, *i.e.* the composition of the complex species that are present in the solution, in terms of stoichiometric coefficients. The initial estimate of the log β_j of each complex species is required, to assist the numerical solution efficiency. In general, the closest these estimates are to the real values of the stability constants, the faster the convergence to the exact values.

The stability constants of all species present need not be simultaneously refined. This is especially useful for instance in the case of acid dissociation constants that are frequently known from previous titration

experiments. SUPERQUAD permits such values to be fixed and thus excluded from the refinement procedure. In that case where fewer parameters need to be refined, an improvement of the execution efficiency (*i.e.* speed) is usually observed. In a similar fashion, an option allows for some β_j values to be *ignored* initially.

The user can specify in the input file whether other titration parameters are to be refined, except for the β_j that are normally refined. These parameters are called *dangerous* in SUPERQUAD terminology, and include the standard potential and slope of the electrode, and the concentrations of some of the reactants. The refinement of the latter is especially important in case of substances that are not available in a high state of purity. Refinement of the concentration of such substances is essential, otherwise systematic errors will result in cluttered curves and hence poor model predictions. The developers of SUPERQUAD suggest [4] that the use of these dangerous parameters should be avoided whenever possible; more careful experimental procedures should be adopted instead.

The final elements of the input file are various statistically related parameters. Since the goodness of fit exhibited by a model is statistically evaluated, it is very important to provide good estimates of the expected experimental errors (variances) of the titre volume measurement SIGMAV and electrode readings SIGMAE (the variances σ^2_V and σ^2_E in equation 8.8, respectively). Realistic estimates of these errors must be evaluated by considering the accuracy of the specific experimental set-up in use.

Finally, as far as the statistical weighting scheme is concerned, SUPERQUAD offers the options of either variable weight factors (as in equation 8.8) or equal unit weights for all points ($w_t = 1$).

8.2.3(b) Program Execution.

The big advantage offered by SUPERQUAD is that many different models can be easily tested simultaneously. Since there is usually some doubt regarding the detailed composition of the true model (*i.e.* species present) a greater number of species might be originally specified in the input file, so as to cover all existence possibilities. In case that the presence of some complex species is inconsistent with experimental observations, SUPERQUAD will detect and exclude that species of the model. A species is ignores if its formation constant is *ill defined*, or in other words the β_j is either negative (physically meaningless) or its calculated standard deviation is more than 33% of its value. In this sense of automatic model selection, SUPERQUAD will refine for the remaining species β_j values just as if the excluded species was never specified.

Beginning from the initial estimates of the log β_j supplied in the input file, SUPERQUAD utilises an iterative least squares method, where during each consecutive cycle the β_j values are refined until the best possible fit is attained. Given that no formation constant is ill-defined, the model is accepted by SUPERQUAD as eligible for the explanation of the true complex species present in the solution. The best model is selected on statistical terms, as the one that exhibits the lowest sample standard deviation, defined as [4]:

$$s = \sqrt{\frac{\sum_t \left\{ w_t \left(E_t^{obs} - E_t \right)^2 \right\}}{N_T - n}} \qquad (8.9)$$

where N_T is the number of measurements and n the number of parameters refined. This statistic roughly conveys the goodness of fit offered by the model, or otherwise how close are the calculated E values to those observed.

The value of the χ^2 (chi-squared) statistic is also provided as an additional indication of the closeness of fit. The formal definition of chi-squared distribution is through the (more general) Gamma distribution, as follows [9]:

For a random variable x

$$f(x) = \frac{1}{\Gamma(\frac{\gamma}{2}).2^{\gamma/2}} . x^{(\frac{\gamma}{2}-1)} . e^{-\frac{x}{2}} \qquad (8.10)$$

where γ is a parameter of the distribution called "degrees of freedom",

$\Gamma(\ )$ is the Gamma function defined by

$$\Gamma(\alpha) = \int_0^\infty z^{\alpha-1} e^{-z} dz \qquad \alpha > 0 \qquad (8.11)$$

This $\Gamma(\ )$ can not be calculated analytically (very complex integration) and is usually tabulated.

If x_i is a normal random variable (I = 1, 2, 3, ...N), then the squared sum $(x_1^2 + x_2^2 + x_3^2 + ... + x_N^2)$ is a random variable following the chi-squared distribution with {N} degrees of freedom. The variance of a random variable x is calculated as:

$$\sigma^2 = \sum_{i=1}^{N} \frac{(x_i - \mu)^2}{N-1} = \frac{1}{N-1}\left[(x_1 - \mu)^2 + (x_2 - \mu)^2 + ... + (x_N - \mu)^2\right] \qquad (8.12)$$

where μ is the mean and N are the observation on x. If x is normal then the variance σ^2 is chi-squared distributed.

The developers of SUPERQUAD quote some limits to the values of the s and χ^2 statistics, which, when exceeded, lead to the rejection of the model on statistical grounds [4].

A plot of residuals (E_t^{obs} - E_t) for each experimental point is provided. It can be used to detect large experimental errors, where abnormally large

residuals are observed. In absence of systematic error, the distribution of the residuals in the plot should be random.

Finally, the species distribution curves are produced as program output. In these curves, the distribution of some reactant in the various complex species is presented (in terms of % of total concentration in the solution) as a function of some experimental parameter (*e.g.* pH).

References.

1. E. Casassas, R. Tauler and M. Filella, *Anal. Chim. Acta*, 191, 399 (1986).

2. L. Lomozik, M. Jaskólski and A. Gasowska, *J. Chem. Education*, 72, 27 (1995).

3. I. Nagypal and I. Paka, *Talanta*, 25, 549 (1978).

4. P. Gans, A. Sabatini and A. Vacca, *J. Chem. Soc. Dalton Trans.*, 1195 (1985).

5. R. Kataky, *Ion-Selective Sensors Applied to the Analysis of Blood Electrolytes*, PhD Thesis, University of Newcastle-upon-Tyne, 1988.

6. W. Bal, A. F. Drake, M. Jezowska-Bojczuk, H. Kozlowski, L. D. Pettit and P. J. Sadler, *J. Chem. Soc., Chem. Commun.*, 555 (1994).

7. J. Dick, *Analytical Applications of Ion-Selective Devices*, PhD Thesis, University of Newcastle-upon-Tyne, 1991.

8. A. Craggs, G. J. Moody and J. D. R. Thomas, Analyst, 104, 961 (1979).

9. J. S. Milton, J. C. Arnold, *Introduction to Probability and Statistics*, second edition, Mcgraw-Hill, (1990), p. 97.

CHAPTER 9

RESULTS AND DISCUSSION

The stability constants for complexation of magnesium with the physiologically important ligands citrate, lactate, glycinate, aspartate, glutamate, pyroglutamate, pyridoxine and HEPES have been determined using pH glass and Mg ISE titrations.

Accurate values of the protonation constants of the ligands are required for the calculation of the formation constants of the metal complexes, therefore, the protonation constants of the above ligands were also determined.

Due to possible calcium competition with magnesium in forming complexes with these ligands in biological applications, the formation constants of the calcium complexes have also been determined.

In the calculation of the stability constants, the ionic product of water was taken as log K = -13.38 [2]. The values of the formation constants of different magnesium [79, 80] or calcium [79, 81] hydroxide complexes, considered in this work were as follows:

$\log \beta_{MgOH} = -11.5$, $\log \beta_{Mg_2(OH)_2} = -21$, $\log \beta_{Mg_3(OH)_4} = -39$

$\log \beta_{CaOH} = -11.7$, $\log \beta_{Ca(OH)_2} = -24.17$.

SUPERQUAD was used to analyse each set of titration data individually.

9.1 Results and Discussion.

The acid protonation constants for citrate, lactate, glycinate, aspartate, glutamate, pyroglutamate and pyridoxine and their formation constants with magnesium and calcium ions are given in detail in tables 9.1- 9.21.

The stability constants for HEPES system will be given later (section 9.6). A summary of the results is given in table 9.22.

Analysing the data by using SUPERQUAD for statistical fitting gave a model of $\chi^2 < 12$, $\sigma < 3$ and SD of formation constant < 33 % of its value, which agree with the criteria of acceptability with the SUPERQUAD program.

Both glass electrode and Mg or Ca ISE measurements gave good agreement in the values of complex formation constants in most cases. However, agreement between the two methods was not observed in the case of magnesium pyridoxine system. This will be discussed later (section 9.4).

The evaluated ligand protonation constants show good agreement between the different experiments. This internal agreement was less satisfactory for the stability constants of metal-ligand complexes. In some cases, excessive or negative values were observed in the tables of the metal-ligand formation constants, probably due to the use of different reactant concentrations or a consequence of experimental error. In such cases the constants were removed from the model and new values were calculated for the other constants in the set of complexes.

In tables 9.23 - 9.29, the protonation constants of the ligands mentioned above obtained in this work were compared with literature values reported under comparable experimental conditions. The agreement can be regarded as satisfactory.

Tables 9.30 - 9.35 contain a comparison of values reported in the literature for the stability constants of the magnesium and calcium citrate, lactate, glycinate, aspartate and glutamate complexes, together with the values obtained in this work.

Table 9.1. Protonation Constants for Citric Acid[(a)]
(Initial concentration of KCl = 150 mmol/L, Titrant 1M KOH, Temp.= 37 °C).

C_L mmo/L	C_{HCl} mmol/L	pH range	no.of points	χ^2	σ	$\log \beta_{LH}$	$\log \beta_{LH_2}$	$\log \beta_{LH_3}$
20	0.99	2.3 - 10.5	95	8.0	0.4	5.645 ± 0.002	9.942 ± 0.003	12.810 ± 0.003
20	2.5	2.3 - 10.7	268	8.2	0.6	5.743 ± 0.003	10.120 ± 0.004	13.149 ± 0.005
20	-	2.4 - 10.7	217	5.1	0.9	5.674 ± 0.002	9.991 ± 0.002	12.905 ± 0.003
15	-	2.5 - 10.5	143	11.4	0.5	5.604 ± 0.003	9.874 ± 0.003	12.761 ± 0.005
10	0.99	2.4 - 10.8	102	10.5	0.5	5.635 ± 0.003	9.933 ± 0.004	12.794 ± 0.005
					Mean	5.660 ± 0.053	9.972 ± 0.093	12.884 ± 0.158

(a) The citrate anion was assumed to have three negative charges (i.e. number of dissociable protons of the parent acid , NDP, = 3) [11].

Table 9.2. Protonation Constants for Lactic Acid
(Initial concentration of NaCl = 150 mmol/L, Temp.= 37 °C).

C_L mmol/L	Titrant	pH range	no.of points	χ^2	σ	$\log \beta_{LH}$
4	0.1M NaOH	3.1 - 8.7	100	13.1	2.3	3.615 ± 0.006
20	0.1M NaOH	2.7 - 9.1	170	12.3	2.5	3.720 ± 0.003
100	1M NaOH	2.3 - 8.8	81	5.0	2.8	3.681 ± 0.004
					Mean	3.672 ± 0.053

Table 9.3. Protonation Constants for Glycine

(Initial concentration of NaCl = 150 mmol/L, Titrant 1M NaOH, Temp.= 37 °C).

C_L mmol/L	C_{HCl} mmol/L	pH range	no.of points	χ^2	σ	log β_{LH}	log β_{LH_2}
20	10	2.6 - 10.1	101	9.7	0.9	9.276 ± 0.002	11.665 ± 0.004
100	20	3.0 - 10.2	196	6.6	0.5	9.323 ± 0.001	11.680 ± 0.002
19.9	19.9	1.9 - 9.8	150	11.2	0.8	9.266 ± 0.003	11.677 ± 0.005
					Mean	9.288 ± 0.030	11.674 ± 0.008

Table 9.4. Protonation Constants for Aspartic Acid

(Initial concentration of NaCl or KCl = 150 mmol/L , Temp.= 37 °C).

C_L mmol/L	C_{HCl} mmol/L	Media	Titrant	pH range	no.of points	χ^2	σ	log β_{LH}	log β_{LH_2}	log β_{LH_3}
10	30	NaCl	1M NaOH	1.7 - 10.8	172	14.2	1.1	9.420 ± 0.003	13.086 ± 0.005	15.079 ± 0.007
20	30	NaCl	1M NaOH	1.8 - 11.3	142	11.0	1.0	9.401 ± 0.003	13.067 ± 0.005	15.122 ± 0.006
20	24	KCl	1M KCl	2.0 - 11.2	109	2.6	1.3	9.396 ± 0.003	13.150 ± 0.005	15.408 ± 0.007
							Mean	9.406 ± 0.013	13.101 ± 0.044	15.203 ± 0.179

Table 9.5. Protonation Constants for Glutamic Acid

(Initial concentration of NaCl = 150 mmol/L , Titrant 1M NaOH , Temp.= 37 °C).

C_L mmol/L	pH range	no.of points	χ^2	σ	log β_{LH}	log β_{LH_2}	log β_{LH_3}
10	2.3 - 10.3	108	12.2	0.8	9.266 ± 0.002	13.381 ± 0.004	15.574 ± 0.006
20	2.1 - 10.5	109	11.4	1.1	9.258 ± 0.003	13.362 ± 0.005	15.533 ± 0.006
15	2.2 - 10.3	109	12.1	1.1	9.265 ± 0.003	13.376 ± 0.005	15.547 ± 0.007
				Mean	9.263 ± 0.004	13.373 ± 0.010	15.551± 0.021

Table 9.6. Protonation Constants for Pyroglutamic acid
(Initial concentration of NaCl or KCl = 150 mmol/L , Temp. = 37 °C).

C_L mmol/L	C_{HCL} mmol/L	Media	Titrant	pH range	no.of points	χ^2	σ	log β_{LH}
20	9.9	KCl	1M KOH	2.0 - 10.1	47	3.7	0.9	3.126 ± 0.005
20	10	NaCl	1M NaOH	2.0 - 10.1	32	10.5	0.6	3.114 ± 0.002
60	1	NaCl	1M NaOH	2.2 - 10.3	64	8.8	1.4	3.089 ± 0.003
75	-	KCl	1M KOH	2.2 - 9.3	109	12.6	0.9	3.185 ± 0.002
75	-	NaCl	1M NaOH	2.2 - 9.0	109	13.3	0.6	3.124 ± 0.001
100	-	NaCl	1M NaOH	2.1 - 9.3	103	12.7	0.7	3.120 ± 0.001
100	1	NaCl	1M NaOH	2.1 - 9.4	103	5.9	0.6	3.136 ± 0.001
100	-	NaCl	1M NaOH	2.1 - 9.4	180	18.6	0.6	3.133 ± 0.001
							Mean	3.128 ± 0.027

Table 9.7. Protonation Constants for Pyridoxine
(Initial concentration of NaCl = 150 mmol/L, titrant 1M NaOH , Temp. = 37 °C).

C_L mmol/L	C_{HCL} mmol/L	pH range	no.of points	χ^2	σ	log β_{LH}	log β_{LH_2}
20	5	2.3 - 10.4	70	11.8	0.7	8.681 ± 0.003	13.482 ± 0.004
50	-	3.1 - 10.2	106	12.4	1.0	8.729 ± 0.003	13.527 ± 0.004
80	5	2.3 - 10.3	134	10.2	1.3	8.696 ± 0.003	13.462 ± 0.004
100	5	2.3 - 10.4	166	8.3	1.2	8.719 ± 0.002	13.510 ± 0.003
100	5	2.3 - 10.3	166	12.2	1.3	8.696 ± 0.003	13.483 ± 0.004
104	4	2.4 - 10.4	303	6.0	1.3	8.718 ± 0.002	13.521 ± 0.002
					Mean	8.707 ± 0.018	13.498 ± 0.026

Table 9.8. Formation Constants for Magnesium-Citrate

(Initial concentration of KCl = 150 mmol/L , Titrant = 1M KOH , Temp.= 37 °C).

C_M	C_L (mmol/L)	C_{HCl}	Method[a]	pH range	No. of points	χ^2	σ	$\log \beta_{MLH_2}$	$\log \beta_{MLH}$	$\log \beta_{ML}$	$\log \beta_{ML_2}$	$\log \beta_{ML(OH)_2}$	$\log \beta_{M_2L_2(OH)_2}$
10	20	2.5	G.E	2.3 - 11.0	284	12.2	1.1	11.026 ± 0.061	7.435 ± 0.022	3.401 ± 0.011	4.817 ± 0.027	-18.832 ± 0.047	-13.011 ± 0.051
9	10	0.98	G.E	2.4 - 10.8	99	9.1	0.8	10.649 ± 0.065	7.405 ± 0.024	3.242 ± 0.009	4.983 ± 0.020	-18.547 ± 0.035	-12.813 ± 0.047
5	20	0.98	G.E	2.3 - 11.0	102	11.4	0.6	10.820 ± 0.020	7.298 ± 0.017	3.281 ± 0.012	4.856 ± 0.016	-18.532 ± 0.064	-12.745 ± 0.098
10	20	2.5	Mg.E	3.1 - 10.3	197	4.1	0.5	11.614 ± 0.009	7.698 ± 0.010	3.026 ± 0.004	4.490 ± 0.171		
9	10	0.98	Mg.E	3.2 - 10.2	66	8.4	0.5	11.540 ± 0.014	7.732 ± 0.013	3.277 ± 0.004	4.673 ± 0.147		
5	20	0.98	Mg.E	3.2 - 10.2	67	7.3	0.4	11.408 ± 0.007	7.627 ± 0.009	3.156 ± 0.005	4.568 ± 0.121		
			G.E				Mean	10.832 ± 0.189	7.397 ± 0.072	3.308 ± 0.083	4.885 ± 0.087	-18.637 ± 0.169	-12.856 ± 0.138
			Mg.E				Mean	11.521 ± 0.104	7.686 ± 0.054	3.153 ± 0.126	4.577 ± 0.092		

(a) Abbreviations

G.E = Potentiometric titration at glass electrode.

Mg.E = Potentiometric titration at magnesium ion- selective electrode.

Table 9.9. Formation Constants for Calcium-Citrate

(Initial concentration of KCl = 150 mmol/L , Titrant = 1M KOH , Temp. = 37 °C).

C_M	C_L (mmol/L)	C_{HCl}	Method[(a)]	pH range	No. of points	χ^2	σ	$\log \beta_{MLH_2}$	$\log \beta_{MLH}$	$\log \beta_{ML}$	$\log \beta_{ML_2}$	$\log \beta_{ML(OH)}$	$\log \beta_{ML_2(OH)_2}$
9.84	20	0.99	G.E	2.2 - 11.3	113	9.5	0.7	11.129 ± 0.040	7.647± 0.015	3.402 ± 0.009	4.743 ± 0.034	-8.879 ± 0.035	-18.737 ± 0.028
10	10	1	G.E	2.4 - 11.0	107	4.5	0.5	10.768 ± 0.082	7.422 ± 0.014	3.274 ± 0.007	4.517 ± 0.029	-8.782 ± 0.016	excessive
5	20	1	G.E	2.3 - 11.2	108	6.3	0.7	10.871 ± 0.035	7.355 ± 0.026	3.314 ± 0.006	4.557 ± 0.061	-8.704 ± 0.029	-18.532 ± 0.020
9.84	20	0.99	Ca.E	3.1 - 10.1	71	1.8	0.6	11.805 ± 0.009	8.022 ± 0.013	3.517 ± 0.007	excessive		
10	20	1	Ca.E	3.1 - 10.0	69	2.4	0.4	11.498 ± 0.012	7.826 ± 0.015	3.281 ± 0.009	4.783 ± 0.166		
5	20	1	Ca.E	3.1 - 10.0	70	6.2	0.5	11.340 ± 0.016	7.347 ± 0.014	3.205 ± 0.004	4.675 ± 0.153		
			G.E				Mean	10.923 ± 0.186	7.475 ± 0.153	3.330 ± 0.066	4.606 ± 0.121	-8.788 ± 0.088	-18.635 ± 0.145
			Ca.E				Mean	11.548 ± 0.237	7.732 ± 0.347	3.334 ± 0.163	4.729 ± 0.076		

(a) Abbreviations

G.E = Potentiometric titration at glass electrode.

Ca.E = Potentiometric titration at calcium ion- selective electrode.

Table 9.10. Formation Constants for Magnesium-Lactate
(Initial concentration of NaCl = 150 mmol/L , Temp. =37°C).

C_M (mmol/L)	C_L	Titrant	Method[a]	pH range	No. of points	χ^2	σ	$\log \beta_{ML}$
10	20	1M NaOH	G.E	2.6 - 8.8	63	7.6	1.5	1.007 ± 0.043
4.98	19.9	0.5M NaOH	G.E	2.6 - 9.5	67	12.9	2.7	1.058 ± 0.049
10	100	1M NaOH	G.E	2.2 - 8.2	81	13.1	3.0	1.134 ± 0.062
10	20	1M NaOH	Mg.E	3.1 - 8.8	45	5.4	0.4	1.104 ± 0.015
4.98	19.9	0.5M NaOH	Mg.E	3.1 - 9.5	48	10.3	0.4	1.001 ± 0.011
10	100	1M NaOH	Mg.E	3.1 - 8.2	56	8.4	0.5	1.022 ± 0.009
			G.E				Mean	1.066 ± 0.064
			Mg.E				Mean	1.042 ± 0.054

(a) Abbreviations: see table 9.8.

Table 9.11. Formation Constants for Calcium-Lactate
(Initial concentration of NaCl = 150 mmol/L , Temp. =37°C).

C_M (mmol/L)	C_L	Titrant	Method[a]	pH range	No. of points	χ^2	σ	$\log \beta_{ML}$
10.15	20	1M NaOH	G.E	2.6 - 9.8	27	11.8	3.5	1.203 ± 0.045
5	20	0.5M NaOH	G.E	2.6 - 9.6	70	5.7	1.5	1.020 ± 0.027
10	100	1M NaOH	G.E	2.2 - 9.2	83	9.9	1.8	1.069 ± 0.043
10.15	20	1M NaOH	Ca.E	3.1 - 9.8	19	7.4	0.8	0.902 ± 0.008
5	20	0.5M NaOH	Ca.E	3.1 - 9.6	49	5.3	0.5	0.974 ± 0.023
10	100	1M NaOH	Ca.E	3.1 - 9.2	58	6.3	0.4	0.941 ± 0.006
			G.E				Mean	1.097 ± 0.095
			Ca.E				Mean	0.939 ± 0.036

(a) Abbreviations: see table 9.9.

Table 9.12. Formation Constants for Magnesium-Glycinate

(Initial concentration of NaCl = 150 mmol/L , Titrant 1M NaOH , Temp. =37°C).

C_M	C_L (mmol/L)	C_{HCl}	Method[a]	pH range	No. of points	χ^2	σ	log $\beta_{ML_2H_2}$	log β_{MLH}	log β_{ML}	log $\beta_{ML(OH)}$
10	20	20	G.E	2.1 - 9.8	150	5.38	0.7	20.298 ± 0.154	10.131 ± 0.058	1.535 ± 0.022	-8.910 ± 0.023
10	20	10	G.E	2.6 - 9.9	101	3.16	0.7	20.529 ± 0.085	10.049 ± 0.073	1.530 ± 0.021	-8.924 ± 0.024
10	100	20	G.E	3.0 - 10.1	192	11.4	0.6	20.014 ± 0.094	10.151 ± 0.055	1.542 ± 0.046	-9.556 ± 0.064
10	20	20	Mg.E	3.1 - 9.6	69	5.2	0.5	21.014 ± 0.018	10.082 ± 0.071	1.657 ± 0.009	
10	20	10	Mg.E	3.2 - 9.9	76	8.6	0.6	21.304 ± 0.020	10.625 ± 0.016	1.926 ± 0.010	
10	100	20	Mg.E	3.2 - 9.7	155	7.1	0.6	21.125 ± 0.015	10.112 ± 0.014	1.912 ± 0.004	
			G.E				Mean	20.280 ± 0.258	10.110 ± 0.054	1.536 ± 0.006	-9.130 ± 0.369
			Mg.E				Mean	21.148 ± 0.146	10.273 ± 0.305	1.832 ± 0.151	

(a) Abbreviations: see table 9.8

Table 9.13. Formation Constants for Calcium-Glycinate

(Initial concentration of NaCl = 150 mmol/L , Titrant 1M NaOH , Temp. =37°C).

C_M	C_L (mmol/L)	C_{HCl}	Method[a]	pH range	No. of points	χ^2	σ	log β_{MLH}	log β_{ML}	log $\beta_{ML(OH)}$
10	20	10	G.E	2.6 - 10.1	100	7.2	0.6	10.354 ± 0.031	0.957 ± 0.049	-9.493 ± 0 .035
10	100	20	G.E	3.0 - 10.2	198	11.4	0.5	10.020 ± 0.060	1.355 ± 0.029	-9.458 ± 0.031
5	20	27	G.E	1.9 - 10.2	157	10.5	0.4	10.283 ± 0.046	1.161 ± 0.022	-9.435 ± 0.034
10	20	10	Ca.E	3.1 - 9.8	69	7.8	0.5	9.869 ± 0.054	1.386 ± 0.021	
10	100	20	Ca.E	3.1 - 9.6	139	10.3	0.6	10.072 ± 0.015	1.204 ± 0.008	
5	20	27	Ca.E	3.1 - 9.5	60	5.6	0.6	10.032 ± 0.063	1.223 ± 0.034	
			G.E				Mean	10.219 ± 0.176	1.158 ± 0.199	-9.462 ± 0.029
			Ca.E				Mean	9.991 ± 0.108	1.271 ± 0.100	

(a) Abbreviations: see table 9.9.

Table 9.14. Formation Constants for Magnesium-Aspartate
(Initial concentration of NaCl = 150 mmol/L , Titrant 1M NaOH , Temp. =37°C).

C_M	C_L (mmol/L)	C_{HCl}	Method[(a)]	pH range	No. of points	χ^2	σ	$\log \beta_{MLH_2}$	$\log \beta_{MLH}$	$\log \beta_{ML}$	$\log \beta_{M_2L}$	$\log \beta_{ML(OH)}$
10	10	30	G.E	1.7 - 10.1	176	14.1	0.7	14.401 ± 0.039	11.085 ± 0.021	2.433 ± 0.019	4.277 ± 0.061	-8.388 ± 0.028
10	20	24	G.E	1.9 - 10.2	95	6.2	0.6	14.488 ± 0.063	11.209 ± 0.044	2.597 ± 0.031	4.760 ± 0.091	-8.164 ± 0.007
10	20	30	G.E	1.8 - 10.1	124	4.8	0.4	14.633 ± 0.018	11.204 ± 0.013	2.637 ± 0.008	-ve	-8.461 ± 0.017
5	20	24	G.E	1.9 - 10.1	92	9.2	0.5	14.281 ± 0.050	11.019 ± 0.024	2.572 ± 0.018	4.172 ± 0.073	-8.419 ± 0.028
10	10	30	Mg.E	3.1 - 9.8	64	3.8	0.4	excessive	10.867 ± 0.019	1.984 ± 0.03		excessive
10	20	30	Mg.E	3.1 - 10.2	72	5.1	0.6	14.580 ± 0.032	11.248 ± 0.011	2.463 ± 0.014		-8.899 ± 0.159
10	20	24	Mg.E	3.1 - 10.2	47	6.1	0.4	14.536 ± 0.080	11.063 ± 0.020	2.361 ± 0.016		-8.724 ± 0.115
			G.E				Mean	14.451 ± 0.148	11.129 ± 0.093	2.560 ± 0.089	4.403 ± 0.314	-8.358 ± 0.133
			Mg.E				Mean	14.558 ± 0.031	11.059 ± 0.191	2.269 ± 0.252		-8.812 ± 0.124

(a) Abbreviations: see table 9.8.

Table 9.15. Formation Constants for Calcium-Aspartate
(Initial concentration of NaCl or KCl = 150 mmol/L , Temp. =37°C).

C_M	C_L (mmol/L)	C_{HCl}	Medium	titrant	Method[(a)]	pH range	No. of points	χ^2	σ	$\log \beta_{MLH_2}$	$\log \beta_{MLH}$	$\log \beta_{ML}$	$\log \beta_{ML(OH)}$
10	20	30	NaCl	1M NaOH	G.E	1.8 - 10.5	125	23.2	1.1	14.542 ± 0.049	11.190 ± 0.032	2.058 ± 0.028	-9.620 ± 0.108
10	10	30	NaCl	1M NaOH	G.E	1.7 - 10.5	179	11.5	1.2	14.403 ± 0.062	10.951 ± 0.047	1.875 ± 0.032	-9.672 ± 0.040
9.84	20	24	KCl	1MKOH	G.E	2.0 - 10.4	98	4.0	1.0	13.971 ± 0.126	10.614 ± 0.056	1.648 ± 0.036	-9.774 ± 0.090
10	20	30	NaCl	1M NaOH	Ca.E	3.2 - 9.9	53	3.9	0.6	14.812 ± 0.017	11.225 ± 0.010	2.103 ± 0.020	
9.84	20	24	KCl	1MKOH	Ca.E	3.1 - 10.0	52	7.3	0.4	14.634 ± 0.016	11.035 ± 0.013	2.028 ± 0.011	
					G.E				Mean	14.305 ± 0.298	10.918 ± 0.289	1.860 ± 0.205	-9.689 ± 0.078
					Ca.E				Mean	14.723 ± 0.126	11.130 ± 0.134	2.066 ± 0.053	

(a) Abbreviations: see table 9.9.

Table 9.16. Formation Constants for Magnesium-Glutamate
(Initial concentration of NaCl = 150 mmol/L , Titrant 1M NaOH , Temp. =37°C).

C_M (mmol/L)	C_L (mmol/L)	Method[(a)]	pH range	No. of points	χ^2	σ	log β_{MLH_2}	log β_{MLH}	log β_{ML}	log $\beta_{ML_2(OH)}$
10	10	G.E	2.3 - 9.8	102	18.0	1.4	-ve	10.351 ± 0.091	1.640 ± 0.048	-6.963 ± 0.103
10	20	G.E	2.1 - 9.9	102	10.2	0.7	14.448 ± 0.057	10.581 ± 0.038	1.677 ± 0.027	-7.255 ± 0.060
5	20	G.E	2.1 - 9.8	102	12.3	0.6	14.603 ± 0.080	10.733 ± 0.051	1.758 ± 0.043	-7.181 ± 0.101
10	10	Mg.E	3.1 - 9.6	65	4.5	0.4	excessive	10.552 ± 0.034	1.540 ± 0.059	
10	20	Mg.E	3.1 - 9.7	66	4.2	0.5	15.063 ± 0.015	11.151 ± 0.009	2.058 ± 0.013	
5	20	Mg.E	3.1 - 9.7	69	2.8	0.5	14.928 ± 0.015	11.092 ± 0.008	1.984 ± 0.016	
		G.E				Mean	14.526 ± 0.110	10.555 ± 0.192	1.692 ± 0.060	-7.133 ± 0.152
		Mg.E				Mean	14.996 ± 0.096	10.932 ± 0.330	1.861 ± 0.280	

(a) Abbreviations: see table 9.8.

Table 9.17. Formation Constants for Calcium-Glutamate
(Initial concentration of NaCl = 150 mmol/L , Titrant 1M NaOH , Temp. =37°C).

C_M (mmol/L)	C_L (mmol/L)	Method[(a)]	pH range	No. of points	χ^2	σ	log β_{MLH_2}	log β_{MLH}	log β_{ML}	log $\beta_{ML(OH)}$
10	10	G.E	2.3 - 10.1	104	7.5	1.0	-ve	10.012 ± 0.051	1.023 ± 0.044	-9.851 ± 0.120
10	20	G.E	2.1 - 9.9	104	9.4	0.9	13.761 ± 0.071	9.932 ± 0.044	1.158 ± 0.040	-9.674 ± 0.035
5	20	G.E	2.1 - 9.9	104	6.1	0.9	13.879 ± 0.112	10.066 ± 0.059	1.204 ± 0.047	-9.527 ± 0.069
10	10	Ca.E	3.1 - 9.6	65	3.6	0.5	excessive	10.101 ± 0.064	1.403 ± 0.053	
10	20	Ca.E	3.1 - 9.5	63	4.4	0.4	14.147 ± 0.053	10.329 ± 0.040	1.466 ± 0.032	
5	20	Ca.E	3.1 - 9.5	63	3.1	0.4	14.215 ± 0.016	10.301 ± 0.011	1.411 ± 0.012	
		G.E				Mean	13.820 ± 0.084	10.003 ± 0.067	1.128 ± 0.094	-9.684 ± 0.162
		Ca.E				Mean	14.181 ± 0.048	10.244 ± 0.124	1.427 ± 0.034	

(a) Abbreviations: see table 9.9.

Table 9.18. Formation Constants for Magnesium-Pyroglutamate
(Initial concentration of NaCl or KCl = 150 mmol/L , Temp. =37°C).

C_M	C_L	C_{HCl} (mmol/L)	Medium	Titrant	Method[(a)]	pH range	No. of points	χ^2	σ	log β_{ML}	log $\beta_{ML(OH)}$
10	20	10	NaCl	1M NaOH	G.E	2.0 - 4.8	31			No Complex	
10	20	10	NaCl	1M NaOH	Mg.E	3.2 - 4.8	10			No Complex	
40	100	-	NaCl	1M NaOH	G.E	2.1 - 9.4	104	4.5	0.7	0.938 ± 0.008	-9.951 ± 0.022
40	100	1	NaCl	1M NaOH	G.E	2.0 - 9.6	104	12.1	0.8	0.825 ± 0.011	-9.883 ± 0.024
20	100	-	NaCl	1M NaOH	G.E	2.1 - 9.3	180	9.9	0.6	0.943 ± 0.016	-9.940 ± 0.025
40	75	-	KCl	1M KOH	G.E	2.2 - 9.2	111	13.8	0.7	0.791 ± 0.015	-9.539 ± 0.018
40	75	-	NaCl	1M NaOH	G.E	2.2 - 9.2	111	16.7	1.1	0.698 ± 0.025	-9.653 ± 0.029
40	90	1	NaCl	1M NaOH	G.E	2.0 - 9.5	95	13.6	0.8	0.863 ± 0.009	-9.794 ± 0.030
40	100	1	NaCl	1M NaOH	Mg.E	3.2 - 9.5	47	11.4	0.2	0.867 ± 0.006	
20	100	-	NaCl	1M NaOH	Mg.E	3.2 - 9.3	78	13.5	0.5	0.689 ± 0.007	
40	75	-	KCl	1M KOH	Mg.E	3.2 - 9.2	46	11.2	1.4	0.964 ± 0.015	
40	75	-	NaCl	1M NaOH	Mg.E	3.2 - 9.2	46	4.3	0.5	0.895 ± 0.007	
					G.E			Mean		0.843 ± 0.093	-9.793 ± 0.167
					Mg.E			Mean		0.854 ± 0.117	

(a) Abbreviations: see table 9.8.

Table 9.19. Formation Constants for Calcium-Pyroglutamate
(Initial concentration of NaCl = 150 mmol/L , Titrant 1M NaOH , Temp. =37°C).

C_M	C_L	C_{HCl} (mmol/L)	Method[a]	pH range	No. of points	χ^2	σ	$\log \beta_{ML}$	$\log \beta_{ML(OH)}$
40	100	-	G.E	2.1 - 9.7	103	5.0	0.6	0.790 ± 0.007	-10.511 ± 0.026
40	100	1	G.E	2.0 - 9.8	103	8.6	0.6	0.737 ± 0.008	-10.729 ± 0.020
40	80	-	G.E	2.2 - 9.5	112	5.4	0.7	0.652 ± 0.008	-10.581 ± 0.031
40	100	-	Ca.E	3.1 - 9.8	47	6.0	0.5	0.684 ± 0.007	
40	100	1	Ca.E	3.1 - 9.7	47	5.6	0.3	0.761 ± 0.006	
40	80	-	Ca.E	3.1 - 9.5	51	3.5	0.8	0.609 ± 0.021	
			G.E			Mean		0.726 ± 0.070	-10.607 ± 0.111
			Ca.E			Mean		0.685 ± 0.076	

(a) Abbreviations: see table 9.9.

Table 9.20. Formation Constants for Magnesium-Pyridoxine
(Initial concentration of NaCl = 150 mmol/L , Titrant 1M NaOH , Temp. =37°C).

C_M	C_L	C_{HCl} (mmol/L)	Method[a]	pH range	No. of points	χ^2	σ	log β_{ML}	log β_{MLH}	log $\beta_{ML_3H_3}$
10	20	5	G.E	2.4 - 9.6	66			excessive	-ve	excessive
20	20	5	G.E	2.3 - 9.6	78			excessive	excessive	excessive
20	100	5	G.E	2.3 - 9.5	156	6.7	0.6	1.658 ± 0.009	9.558 ± 0.015	-ve
20	100	5	G.E	2.3 - 9.5	156	10.9	0.7	1.546 ± 0.018	9.422 ± 0.025	-ve
30	100	5	G.E	2.3 - 9.5	157	14.4	0.7	1.419 ± 0.013	9.238 ± 0.029	-ve
40	104	4	G.E	2.4 - 9.5	287	7.8	0.6	1.144 ± 0.006	8.956 ± 0.016	-ve
20	20	5	Mg.E	3.1 - 9.5	77	9.3	0.6	1.490 ± 0.022	10.135 ± 0.013	excessive
20	50	-	Mg.E	3.1 - 9.6	95	5.0	0.7	1.561 ± 0.013	10.142 ± 0.013	excessive
20	80	5	Mg.E	3.2 - 9.5	121	4.6	0.5	1.723 ± 0.005	9.601 ± 0.042	30.601 ± 0.029
20	100	5	Mg.E	3.1 - 9.6	152	8.4	0.7	1.989 ± 0.005	9.835 ± 0.025	30.520 ± 0.021
20	100	5	Mg.E	3.1 - 9.6	150	1.8	0.6	2.260 ± 0.004	9.825 ± 0.023	30.949 ± 0.012
			G.E				Mean	1.442 ± 0.221	9.294 ± 0.260	
			Mg.E				Mean	1.805 ± 0.368	9.908 ± 0.231	30.690 ± 0.228

(a) Abbreviations: see table 9.8.

Table 9.21. Formation Constants for Calcium-Pyridoxine
(Initial concentration of NaCl = 150 mmol/L , Titrant 1M NaOH , Temp. =37°C).

C_M	C_L (mmol/L)	C_{HCl}	Method[(a)]	pH range	No. of points	χ^2	σ	$\log \beta_{ML}$
10	20	-	G.E	2.4 - 9.6	67			No complex
30	100	5	G.E	2.3 - 9.6	159	6.5	0.7	0.619 ± 0.033
40	100	5	G.E	2.3 - 9.5	158	8.9	0.6	0.510 ± 0.008
30	100	5	Ca.E	3.1 - 9.6	150	12.9	0.5	0.624 ± 0.027
20	80	5	Ca.E	3.1 - 9.6	148	7.1	0.4	0.542 ± 0.018
			G.E				Mean	0.565 ± 0.077
			Ca.E				Mean	0.583 ± 0.058

(a) Abbreviations: see table 9.9.

Table 9.22. A summary of the Formation Constants obtained in this work. The formula of the general complex is MpLqHr.

System	p	q	r	log β G.E	log β Mg or Ca.E	Mean log β (G.E + Mg or Ca.E)/2
Proton Citrate	0	1	1	5.660 ± 0.053		
	0	1	2	9.972 ± 0.093		
	0	1	3	12.884 ± 0.158		
Mg-Citrate	1	1	2	10.832 ± 0.189	11.521 ± 0.104	11.176 ± 0.487
	1	1	1	7.397 ± 0.072	7.686 ± 0.054	7.533 ± 0.217
	1	1	0	3.308 ± 0.083	3.153 ± 0.126	3.231 ± 0.110
	1	2	0	4.885 ± 0.087	4.577 ± 0.092	4.731 ± 0.218
	1	1	-2	-18.637 ± 0.169		
	2	2	-2	-12.856 ± 0.138		
Ca-Citrate	1	1	2	10.923 ± 0.186	11.548 ± 0.237	11.236 ± 0.442
	1	1	1	7.475 ± 0.153	7.732 ± 0.347	7.604 ± 0.182
	1	1	0	3.330 ± 0.066	3.334 ± 0.163	3.332 ± 0.003
	1	2	0	4.606 ± 0.121	4.729 ± 0.076	4.668 ± 0.087
	1	1	-1	-8.788 ± 0.088		
	1	2	-2	-18.635 ± 0.145		
Proton Lactate	0	1	1	3.675 ± 0.038		
Mg-Lactate	1	1	0	1.066 ± 0.064	1.042 ± 0.054	1.054 ± 0.017
Ca-Lactate	1	1	0	1.097 ± 0.095	0.939 ± 0.036	1.018 ± 0.112
Proton-Glycinate	0	1	1	9.288 ± 0.030		
	0	1	2	11.674 ± 0.008		
Mg-Glycinate	1	2	2	20.280 ± 0.258	21.148 ± 0.146	20.714 ± 0.614
	1	1	1	10.110 ± 0.054	10.273 ± 0.305	10.192 ± 0.115
	1	1	0	1.536 ± 0.006	1.832 ± 0.151	1.684 ± 0.209
	1	1	-1	-9.130 ± 0.369		
Ca-Glycinate	1	1	1	10.219 ± 0.176	9.991 ± 0.108	10.105 ± 0.161
	1	1	0	1.158 ± 0.199	1.271 ± 0.100	1.215 ± 0.080
	1	1	-1	-9.462 ± 0.029		
Proton-Aspartate	0	1	1	9.406 ± 0.013		
	0	1	2	13.101 ± 0.044		
	0	1	3	15.203 ± 0.179		
Mg-Aspartate	1	1	2	14.451 ± 0.148	14.558 ± 0.031	14.505 ± 0.076
	1	1	1	11.129 ± 0.093	11.059 ± 0.191	11.094 ± 0.050
	1	1	0	2.560 ± 0.089	2.269 ± 0.252	2.415 ± 0.206
	1	1	-1	-8.358 ± 0.133	-8.812 ± 0.124	-8.585 ± 0.321
	2	1	0	4.403 ± 0.314		
Ca-Aspartate	1	1	2	14.305 ± 0.298	14.723 ± 0.126	14.514 ± 0.296
	1	1	1	10.918 ± 0.289	11.130 ± 0.134	11.024 ± 0.150
	1	1	0	1.860 ± 0.205	2.066 ± 0.053	1.963 ± 0.146
	1	1	-1	-9.689 ± 0.078		

Table 9.22 (cont.).

System	p	q	r	log β G.E	log β Mg or Ca.E	Mean log β (G.E + Mg or Ca.E)/2
Proton-Glutamate	0	1	1	9.263 ± 0.004		
	0	1	2	13.373 ± 0.010		
	0	1	3	15.551 ± 0.021		
Mg-Glutamate	1	1	2	14.526 ± 0.110	14.996 ± 0.096	14.761 ± 0.332
	1	1	1	10.555 ± 0.192	10.932 ± 0.330	10.744 ± 0.267
	1	1	0	1.692 ± 0.060	1.861 ± 0.280	1.777 ± 0.120
	1	2	-1	-7.133 ± 0.152		
Ca-Glutamate	1	1	2	13.820 ± 0.084	14.181 ± 0.048	14.001 ± 0.255
	1	1	1	10.003 ± 0.067	10.244 ± 0.124	10.124 ± 0.170
	1	1	0	1.128 ± 0.094	1.427 ± 0.034	1.278 ± 0.211
	1	1	-1	-9.684 ± 0.162		
Proton-Pyroglutamate	0	1	1	3.128 ± 0.027		
Mg-Pyroglutamate	1	1	0	0.843 ± 0.093	0.854 ± 0.117	0.849 ± 0.008
	1	1	-1	-9.793 ± 0.167		
Ca-Pyroglutamate	1	1	0	0.726 ± 0.070	0.685 ± 0.076	0.706 ± 0.029
	1	1	-1	-10.607 ± 0.111		
Proton-Pyridoxine	0	1	1	8.707 ± 0.018		
	0	1	2	13.498 ± 0.026		
Mg-Pyridoxine	1	1	0	1.442 ± 0.221	1.805 ± 0.368	1.624 ± 0.257
	1	1	1	9.294 ± 0.260	9.908 ± 0.231	9.601 ± 0.434
	1	3	3		30.690 ± 0.228	
Ca-Pyridoxine	1	1	0	0.565 ± 0.077	0.583 ± 0.058	0.574 ± 0.013

Table 9.23. Summary of Reported Values for the Protonation Constants of Citrate.

Method[(a)]	Temp. (°C)	Medium (Conc. in mol/L)	$\log \beta_{LH}$	$\log \beta_{LH_2}$	$\log \beta_{LH_3}$	Reference	Year
Pot. (G.E)	25	0.15	5.62	9.96	12.90	1	1959
Pot. (G.E)	37	0.15 $NaClO_4$	5.539	9.775	12.644	2	1978
Pot. (G.E)	37	0.14 KNO_3	5.652	9.954	12.836	3	1980
Pot. (G.E)	25	0.16 KCl 0.16 NaCl	5.595 5.545	9.892 9.812	12.792 12.691	4	1990
Coul.	37	0.15 NaCl	5.75	10.17	13.15	5	1993
Pot. (G.E)	37	0.15 KCl	5.660	9.972	12.884	This work	

Table 9.24. Summary of Reported Values for the Protonation Constants of Lactate.

Method[(a)]	Temp. (°C)	Medium (Conc. in mol/L)	$\log \beta_{LH}$	Reference	Year
Pot. (G.E)	37	0.15 $NaClO_4$	3.666	6	1987
Coul.	37	0.15 NaCl	3.70	5	1993
Pot. (G.E)	37	0.15 NaCl	3.675	This work	

Table 9.25. Summary of Reported Values for the Protonation Constants of Glycinate.

Method[(a)]	Temp. (°C)	Medium (Conc. in mol/L)	$\log \beta_{LH}$	$\log \beta_{LH_2}$	Reference	Year
Pot. (G.E)	37	0.15 $NaClO_4$	9.239	11.654	7	1981
Pot. (G.E)	37	0.15 NaCl	9.216	11.522	8	1985
Pot. (G.E)	37	0.15 NaCl	9.210	11.524	78	1990
Pot. (G.E)	37	0.15 NaCl	9.288	11.674	This work	

Table 9.26. Summary of Reported Values for the Protonation Constants of Aspartate.

Method[(a)]	Temp. (°C)	Medium (Conc. in mol/L)	$\log \beta_{LH}$	$\log \beta_{LH_2}$	$\log \beta_{LH_3}$	Reference	Year
Pot. (G.E)	37	0.15 $NaClO_4$	9.27	12.87	14.81	9	1976
Pot. (G.E)	37	0.15 $NaClO_4$	9.305	12.973	14.997	10	1982
Pot. (G.E)	37	0.15 NaCl	9.354	12.929	14.881	78	1990
Pot. (G.E)	37	0.15 NaCl or KCl	9.406	13.101	15.203	This work	

(a) Abbreviations: see table 9.30.

Table 9.27. Summary of Reported Values for the Protonation Constants of Glutamate.

Method[a]	Temp. (°C)	Medium (Conc. in mol/L)	$\log \beta_{LH}$	$\log \beta_{LH_2}$	$\log \beta_{LH_3}$	Reference	Year
Pot. (G.E)	37	0.15 $NaClO_4$	9.176	13.256	15.440	10	1982
Pot. (G.E)	37	0.15 NaCl	9.26	13.36	15.54	8	1985
Pot. (G.E)	37	0.15 NaCl	9.263	13.373	15.551	This work	

Table 9.28. Summary of Reported Values for the Protonation Constants of Pyroglutamate.

Method[a]	Temp. (°C)	Medium (Conc. in mol/L)	$\log \beta_{LH}$	Reference	Year
Pot. (G.E)	37	0.15 $NaClO_4$	3.090	6	1987
Pot. (G.E)	37	0.15 NaCl or KCl	3.128	This work	

Table 9.29. Summary of Reported Values for the Protonation Constants of Pyridoxine.

Method[a]	Temp. (°C)	Medium (Conc. in mol/L)	$\log \beta_{LH}$	$\log \beta_{LH_2}$	Reference	Year
Pot. (G.E)	37	0.154 NaCl	8.59	13.51	12	1984
Pot. (G.E)	37	0.15 $NaClO_4$	8.653	13.463	6	1987
Pot. (G.E)	37	0.15 NaCl	8.707	13.498	This work	

(a) Abbreviations: see table 9.30.

Table 9.30. A summary of Values Reported for the Stability Constants of Magnesium-Citrate Complexes.

Method (a)	Temp. (°C)	Medium (Conc. in mol/L)	$\log \beta_{ML}$	$\log \beta_{MLH}$ $\log K_{MLH}$	$\log \beta_{MLH_2}$ $\log K_{MLH_2}$	Other Constants	Ref.	Year
Frog Heart	25 25	0.1 0.16	3.61 3.2				13	1934
Pot. (G.E)	25	0.1	3.61				14	1938
Pol.	25	0.09	3.29	1.6			1	1959
Spect.	25 25	0.098 NaCl 0.098 Corr. (b)	3.36 3.52				15	1961
IX	25	0.1 NH_4Cl	3.16				16	1963
Fluor.	25	0.1	3.63				17	1963
Pot. (G.E)	20	0.1 $NaClO_4$	3.40	1.84	0.84		18	1964
IX	25	0	3.96				19	1964
Pot. (G.E)	25	0.1 Me_4NCl	3.73	1.85			20	1965
Enzymic Method	25 25 25 25 25 37	0.1 Me_4NCl 0.1 (0.08 NaCl) (c) 0.044 (0.022 NaCl) (c) 0.07 (0.048 NaCl) (c) 0.15 (0.13 NaCl) (c) 0.1 (0.08 NaCl) (c)	3.65 3.42 3.78 3.56 3.35 3.47				21	1969
Pot. (G.E)	25	0.1 Me_4NCl	3.85	1.92			22	1970
Pot.	25	0.1 KNO_3	3.38	7.66 1.96			23	1975
Pot. (G.E)	25 25	0.1 KCl 0	3.63 4.85	1.78 2.67	0.6 1.0		24	1980

Table 9.30 (cont.)

Method (a)	Temp. (°C)	Medium (Conc. in mol/L)	$\log \beta_{ML}$	$\log \beta_{MLH}$ $\log K_{MLH}$	$\log \beta_{MLH_2}$ $\log K_{MLH_2}$	Other Constants	Ref.	Year
Pot. (G.E)	37	0.1 KNO_3	3.51	7.47 1.75			25	1982
	37	0.1 Corr. (d)	3.66	7.63 1.77				
	37	0	4.87	8.94 2.51				
	37	0.15 KNO_3	3.34	7.33				
	37	0.15 Corr. (d)	3.54	7.54				
	37	0.2 KNO_3	3.23	7.26				
	37	0.2 Corr. (d)	3.46	7.51				
	37	0.7 KNO_3	3.07	7.63				
	37	0.7 Corr. (d)	3.49	8.10				
Pot. (G.E)	37	0.1 $NaClO_4$	3.333	7.483	11.008	$\log \beta_{ML_2} = 5.126$ $\log \beta_{ML_2H} = 10.411$ $\log \beta_{M_2L_2(OH)_2} = -12.638$ $\log \beta_{ML(OH)_2} = -18.468$	6	1987
Coul.	25	0.15 NaCl	3.27				5	1993
	37	0.15 NaCl	3.24					
Pot.	37	0.15 KCl	3.231	7.533	11.176	$\log \beta_{ML_2} = 4.731$ $\log \beta_{M_2L_2(OH)_2} = -12.856$ $\log \beta_{ML(OH)_2} = -18.637$	This Work	

(a) Abbreviations

Pot. = Potentiometry.
Pot. (G.E) = Potentiometric titration at glass electrode
Pol. = Polarography
Spect. = Spectrophotometry
IX = Ion exchange
Fluor.= Fluorimetry
Coul. = Coulometry

Table 9.30 (cont.)

Pot. (Mg.E) = Potentiometric titration at magnesium selective electrode.

(b) Corrected for Na^{+}-Cit^{3-} complex formation..

(c) Ionic strength adjusted with Me_4NCl

(d) Corrected for K^{+}-Cit^{3-} complex formation.

Table 9.31. A summary of Values Reported for the Stability Constants of Calcium-Citrate Complexes.

Method (a)	Temp. (°C)	Medium (Conc. in mol/L)	$\log \beta_{ML}$	$\log \beta_{MLH}$ $\log K_{MLH}$	$\log \beta_{MLH_2}$ $\log K_{MLH_2}$	Other Constants	Ref.	Year
Sol.	25	0	4.85				26	1929
Frog Heart	37	0.154 NaCl	3.22				13	1934
Sol.	37	0.15 NaCl	3.31					
Pot. (Amalgam Electrode)	25	0.15 NaCl	3.17				27	1946
Pot. (G.E)	25	0	4.84	3.29		$\log \beta_{ML_2} = 8.02$ $\log \beta_{ML_2H_2} = 6.79$	28	1951
Sol.	25	0	4.90	3.05	1.15		29	1953
IX	25	0.16 NaCl	3.15				30	1954
Sol.	25	0	4.68	3.09	1.10		31	1955
Pot. (G.E)	28	0.15 NaCl	3.20				32	1957
Spect.	25	0.11 NaCl	2.95				15	1961
	25	0.11 Corr. (b)	3.14					
Pot. (G.E)	20	0.1 $NaClO_4$	3.55	2.10	1.05		18	1964
Pot. (Ca.E)	25	0.1$NaClO_4$	3.67				33	1969
Rad.	19.6	0.2 NH_4Cl	3.15				34	1971
	25	=	3.11					
	28.2	=	3.10					
	38	=	3.04					
	51.4	=	2.97					
	65.0	=	2.82					
	25	0.24 NH_4Cl				$\log K_{ML_2} = 1.22$		
Pot.	37	0.15 NaCl	3.274				35	1974
Pot.	25	0.1 KNO_3	3.5	8.02 2.32			23	1975
Pot. (Ca.E)	25	0.1 NaCl	3.42				36	1979

Table 9.31 (cont.).

Method (a)	Temp. (°C)	Medium (Conc. in mol/L)	$\log \beta_{ML}$	$\log \beta_{MLH}$ $\log K_{MLH}$	$\log \beta_{MLH_2}$ $\log K_{MLH_2}$	Other Constants	Ref.	Year
Pot. (G.E)	25	0.1 KCl	3.64	2.03	1.05		24	1980
	25	0	4.86	2.92	1.45			
Pot. (G.E)	37	0.1 KNO_3	3.48	7.80 2.08			25	1982
		0.1 Corr. (c)	3.63	7.97 2.11				
		0	4.87	9.38 2.93				
		0.15 KNO_3	3.29	7.61				
		0.15 Corr. (c)	3.49	7.83				
		0.2 KNO_3	3.16	7.48				
		0.2 Corr. (c)	3.40	7.74				
		0.7 KNO_3	2.81	7.27				
		0.7 Corr. (c)	3.29	7.78				
Pot. (G.E)	37	0.15 $NaClO_4$	3.364	7.614	11.005	$\log \beta_{ML_2} = 4.965$ $\log \beta_{ML(OH)} = -8.395$ $\log \beta_{ML_2(OH)_2} = -16.808$	6	1987
Sol.	37	0.15 NaCl	3.288				37	1991
Pot. (Ca.E)	37	0.154 NaCl	3.267					
	18	0.154 NaCl	3.270					
	45	0.154 NaCl	3.250					
Coul.	37	0.15 NaCl	3.28				5	1993
	25	0.15 NaCl	3.17					
Pot.	37	0.15 KCl	3.332	7.604	11.236	$\log \beta_{ML_2} = 4.668$ $\log \beta_{ML(OH)} = -8.788$ $\log \beta_{ML_2(OH)_2} = -18.635$	This Work	

(a) Abbreviations (see table 9.30)
Pot. (Ca.E) = Potentiometric titration at calcium selective electrode
Rad.= Radiochemical method

Table 9.31 (cont.).

Sol. = Solubility method

(b) Corrected for Na^+-Cit^{3-} complex formation

(c) Corrected for K^+-Cit^{3-} complex formation.

Table 9.32. Summary of Reported Values for the Stability Constants of Magnesium and Calcium-Lactate Complexes.

Method (a)	Temp. (°C)	Medium (Conc. in mol/L)	Metal	$\log \beta_{ML}$	$\log \beta_{ML_2}$	Ref.	Year
Pot. (Hyd.E)	Unstated	0.2 KCl	Ca	1.07		76	1938
IX	25	0.16	Ca	0.8		38	1952
Sol.	25	0	Mg Ca	1.367 1.42		39	1953
Pot. (G.E)	25	1	Mg Ca	0.73 0.9	1.30 1.24	40	1965
Pot. (Ca.E)	25	0.5 NaCl	Ca	0.92	1.62	77	1981
Pot. (G.E)	37	0.15 $NaClO_4$	Mg	1.235		6	1987
Coul.	25 37	0.15 NaCl	Mg Ca Mg Ca	0.61 0.48 0.64 0.61		5	1993
Pot.	37	0.15 NaCl	Mg Ca	1.054 1.018		This Work	

(a) Abbreviations (see table 9.30).
Hyd.E=Hydrogen Electrode.

Table 9.33. Summary of Values Reported for the Stability Constants of Magnesium and Calcium-Glycinate Complexes.

Method (a)	Temp. (°C)	Medium (Conc. in mol/L)	Metal	$\log \beta_{ML}$	$\log \beta_{MLH}$	Other Constants	Ref.	Year
Sol.	25	0	Ca	1.43			47	1950
Pot. (Hyd. E.)	25	3.0 $NaClO_4$	Mg Ca	1.53 0.75		$\log \beta_{ML_2} = 2.26$	41	1982
Pot. (G.E)	20	0.7 $NaClO_4$ 0.7 NaCl	Mg Ca Mg Ca	1.3 1.0 1.3 1.1			42	1982
Pot. (G.E)	10 25 37	0.25	Ca	1.08 1.05 1.03	10.21 9.85 9.70		43	1985
Spect.	25	1.0 Me_4NCl	Mg Ca	1.17 0.55			44	1987
Pot. (G.E)	37	0.15 $NaClO_4$	Mg	1.979	10.879	$\log \beta_{ML_2H_2} = 21.614$ $\log \beta_{ML(OH)} = -8.735$	6	1987
Pot. (G.E + Ca.E)	37	0.15 NaCl	Ca	1.465			78	1990
Pot.	37	0.15 NaCl	Mg Ca	1.684 1.215	10.192 10.105	$\log \beta_{ML_2H_2} = 20.714$ $\log \beta_{ML(OH)} = -9.13$ $\log \beta_{ML(OH)} = -9.462$	This Work	

(a) Abbreviations (see table 9.30)
Hyd.E = Hydrogen Electrode
Sol. = Solubility Method.

Table 9.34. Summary of Reported Values for the Stability Constants of Magnesium and Calcium-Aspartate Complexes.

Method (a)	Temp. (°C)	Medium (Conc. in mol/L)	Metal	$\log \beta_{ML}$	$\log \beta_{MLH}$	$\log \beta_{MLH_2}$	Other Constants	Ref.	Year
Pot. (G.E)	25	0.1 KCl	Mg Ca	2.43 1.6				45	1953
Pot.	25	0.7 KCl	Ca	1.53				46	1966
Pot. (G.E)	37	0.15 $NaClO_4$	Mg Ca	2.04 1.135	10.501 10.59	14.074 14.128	$\log \beta_{M_2L} = 4.426$ $\log \beta_{ML(OH)} = -8.666$ $\log \beta_{M_2L} = 3.855$ $\log \beta_{ML(OH)} = -9.241$	6	1987
Pot. (G.E + Ca.E)	37	0.15 NaCl	Ca	1.989	10.567			78	1990
Pot.	37	0.15 NaCl or KCl	Mg Ca	2.415 1.963	11.094 11.024	14.505 14.514	$\log \beta_{M_2L} = 4.403$ $\log \beta_{ML(OH)} = -8.585$ $\log \beta_{ML(OH)} = -9.689$	This Work	

(a) Abbreviations (see table 9.30)

Table 9.35. Summary of Reported Values for the Stability Constants of Magnesium and Calcium-Glutamate Complexes.

Method (a)	Temp. (°C)	Medium (Conc. in mol/L)	Metal	$\log \beta_{ML}$	$\log \beta_{MLH}$	$\log \beta_{MLH_2}$	Other Constants	Ref.	Year
Sol.	25	0	Ca	2.06	11.12			47	1950
Pot. (G.E)	25	0.1 KCl	Mg	1.9				45	1953
			Ca	1.43					
Pot.	25	0.7 KCl	Ca	1.20				46	1966
Pot. (G.E)	37	0.15 $NaClO_4$	Mg	2.196	11.081	14.876	$\log \beta_{ML_2(OH)} = -6.125$	6	1987
			Ca	1.474	10.377	14.02	$\log \beta_{ML(OH)} = -9.071$		
Pot. (G.E)	25	1.0 NaCl	Mg	1.33				48	1988
			Ca	0.60					
Pot.	37	0.15 NaCl	Mg	1.777	10.744	14.761	$\log \beta_{ML_2(OH)} = -7.133$	This Work	
			Ca	1.278	10.124	14.001	$\log \beta_{ML(OH)} = -9.684$		

(a) Abbreviations (see table 9.30).

9.1.1 Citrate Complexes.

The stability constants for the magnesium and calcium citrate systems have been determined by several workers, the most recent being those of Glab et al. [5] who employed a coulometric method at ionic strength of 0.15 mol/L and obtained log β_{MgL} = 3.24 and log β_{CaL} = 3.28, which are in good agreement with the values obtained in this work (log β_{MgL} = 3.231, log β_{CaL} = 3.332). The values of log β_{CaL} , determined by Blaquiere and Berthon [6] and Amico et al. [25] at I=0.15 mol/L and 37 °C using a potentiometric titration method with a glass electrode, are also in good agreement with the results of this work, whereas the log β_{MgL} values obtained by them and by Blair [21] are slightly higher. Blair has measured the stability constants of the magnesium complexes of both citric and isocitric acids by studying the effect of magnesium ions on the aconitase equilibrium [21]. Hastings et al. [13] measured the stability constant by inhibiting the contraction of perfused frog heart by calcium citrate in the presence of varying amounts of magnesium. Their data gave log β_{MgL} = 3.2 at ionic strength close to 0.15 mol/L, which agrees with the value obtained in this work. The formation constants of CaL obtained by the same authors using a calcium carbonate solubility method is also in good agreement. Singh et al. [37] have employed a calcium electrode in combination with silver/silver chloride reference electrode for determination of calcium citrate complexation by measuring the change in potential caused by the addition of sodium citrate to solutions containing calcium and sodium chlorides. They also used a calcium oxalate solubility method. The values of log β_{CaL} obtained by the two methods at 37 °C are log β_{CaL} = 3.288 (solubility method) and log β_{CaL} = 3.276 (Ca ISE), which are in fair agreement with the constant of this work, as is also the log β_{CaL} value of

3.274 for the calcium citrate complex determined by Mayer [35] by potentiometric titrations. The same constant was determined by Schubert [30] (ion exchange method) and by Lefebvre [32] (glass electrode). The agreement with the value obtained in this work may be regarded as satisfactory.

For the protonation complex MLH, the log β_{CaLH} values obtained in this work agree reasonably well with those of Amico et al. [25], and Blaquiere and Berthon [6], although the log β_{MgLH} of Amico et al. is slightly lower. The rest of the constants for the magnesium and calcium citrate complexes detected in this work (see tables 9.30 and 9.31) agree with those of Blaquiere and Berthon [6]. However, the existence of the MgL_2H complex demonstrated by them was not confirmed by the data of this work.

9.1.2 Lactate.

In the case of the magnesium and calcium lactate systems, the value of log β_{ML} obtained in this work for calcium lactate compared well with the value of Cannan and Kibrick [76], and that for magnesium lactate is in reasonable agreement with that of Blaquiere and Berthon [6]. The values of log β_{ML} for magnesium and calcium lactate complexes determined by Glab et al. [5] coulometrically seem to be low.

The presence of ML_2 constants for the magnesium and calcium lactate systems, suggested by others [40, 77], was not confirmed by the data of this work. However, lactate may form ML_2 complexes with magnesium and calcium when the ligand presents in much higher concentrations.

9.1.3 Glycinate, Aspartate and Glutamate.

The magnesium(II)-glycine system has been studied by Monk [49], and by Murphy and Martell [50]. They explained their experimental data by assuming the formation of MgL, alone. Greenwald [51] concluded that the formation of MgL_2 rather MgL provided a better explanation. Bottari and Porto [41] have obtained values for the formation constants of CaL, MgL and MgL_2 glycine complexes by means of emf measurements carried out with a hydrogen electrode at 25 °C in 3.00 mol/L $NaClO_4$.

The complex formation between calcium (II) and glycine was initially investigated by comparing the solubility of $Ca(IO_3)$ in the presence and absence of glycine [47, 52]. The increase in solubility in the presence of glycine was explained by assuming the formation of CaL with values of stability constant varying from log β_{CaL} = 1.35 to 1.43. Daniele et al. [43] have studied the calcium complexes of glycine, potentiometrically using a glass electrode, at different temperatures and ionic strengths. They found that glycine forms ML and MLH complexes with Ca^{2+}, and obtained log β_{CaL} = 1.03 and log β_{CaLH} = 9.7 at I = 0.25 mol/L and 37 °C. These are in fair agreement with the values of log β_{CaL} = 1.215 and log β_{CaLH} = 10.105 obtained in this work, however, they were determined under different experimental conditions. Recently, Maeda et al. [78] have investigated the complex formation of calcium with glycine and aspartic acid, at 37 °C in 0.15 mol/L NaCl, by potentiometric titration using both calcium-ion selective and glass electrodes. Their results for the glycine system fitted a model with only one species (CaL) and those for the aspartic acid system with two, CaLH and CaL. The formation constants reported by them were log β_{ML} = 1.465 for the Ca-glycine complex and log β_{ML} = 1.989 and log β_{MLH} = 10.567 for the Ca-aspartate system. These values are in good agreement when compared with the corresponding values obtained in this work (log β_{ML} = 1.215 for the Ca-glycine complex and log β_{ML} = 1.963

and log β_{MLH} = 11.024 for the Ca-aspartate complexes), apart from their log β_{MLH} value for Ca-aspartate, which was much lower.

The stability constants for the magnesium glycinate complexes (see table 9.33), as well as for magnesium and calcium aspartate (table 9.34) and glutamate (table 9.35), measured and determined in this work agree satisfactorily with those of Blaquiere and Berthon [6]. However, the ML_2 complex for calcium aspartate detected by them was not characterised in this work, as it was made negative during SUPERQUAD refinements.

9.1.4 Pyroglutamate and Pyridoxine.

In the case of the magnesium and calcium pyroglutamate and pyridoxine systems (except for magnesium pyridoxine with Mg ISE), the results show no evidence of complex formation at low concentration. This agrees with Blaquiere and Berthon's study [6]. However, when the concentrations were increased, the complexes could be detected (tables 9.18 - 9.21). In the case of Mg-pyridoxine, with an Mg ISE the complexes could be detected even at low concentrations (see section 9.4).

9.2 Species Distribution Curves.

The species distribution diagrams (vs. pH) for the metal-ligand systems are shown in figures 9.1- 9.15. They were calculated by using the SPECIES program. The average values of stability constants obtained from the glass electrode and Mg or Ca ISE studies were used in the calculations. In the case of Mg-pyridoxine, due to the fact that there is disagreement between the results obtained by the two methods, two plots of species distribution diagram have been drawn, one using the stability constant values obtained with the glass electrode (figure 9.13) and the other with Mg ISE (figure 9.14).

The species distribution diagrams are very useful for visualizing the nature of the equilibrium situation. It can be seen from the distribution diagram of, for example, the Mg-citrate system (figure 9.1) that ML (M=Mg, L=cit) is the predominate species in solution over the pH range 5.5-10, where it exists with a maximum percentage of ≈ 75 %. In natural body fluids, which have a neutral or slightly alkaline pH, ML and ML_2 species are present. In acidic biofluids, such as urine, the previous species are present, with additionally, the protonated MLH and MLH_2 complexes. The hydroxide complexes are only formed at very high alkaline pH.

9.3 Effect of pH change on ISE Response in the Metal-Ligand Solution.

Figures 9.16a - 9.28a show the response of the ISE (Mg or Ca) to pH changes in the metal-ligand solutions (in each figure, not all of the experimental points are shown, for clarity). These curves are very useful to confirm the reliability of the stability consatnt results. In the case of, for example, the magnesium-citrate system, the Mg ISE shows a great decrease in mV (≈30 mV) over pH 3~6 (figure 9.16a). This decrease in mV, i.e. decrease in free Mg^{2+} concentration, indicates that complexation between Mg^{2+} and citrate has occurred. The amount of decrease in mV of the Mg ISE in Mg-citrate solution over the whole pH change (pH 3-10) is much greater than in other systems such as Mg-lactate (≈6 mV, figure 9.18a) or Mg-pyroglutamate (≈3 mV, figure 9.26a). This indicates that Mg^{2+} forms a stronger complex with citrate than with lactate or pyroglutamate, and/or magnesium-citrate solution contains more complex species. The results of measurement of stability constants, obtained using a

pH glass electrode and a Mg ISE (see table 9.22), have shown that the value of log β_{ML} for complexation of magnesium with citrate is higher than those of lactate or pyroglutamate and also other stoichiometries of Mg-citrate complexes were formed.

The above curves (figures 9.16a - 9.28a) of ISE response to pH change in the metal-ligand solutions can be also qualitatively compared with the corresponding species distribution curves of the metal-ligand system observed in figures 9.16b - 9.28b. For the metal-citrate system, the ISE response to pH change of Mg or Ca-citrate (figure 9.16a or 9.17a) shows a large decrease in mV of Mg or Ca ISE at pH range 3~6. Above pH 6, the metal ISE response was slightly affected by pH change and the curve shows very little decrease in mV over a wide pH range (6-10). This curve is very similar to that of the free Mg or Ca percentage distribution curve (figure 9.16b or 9.17b) which shows a large decrease in the percentage of free Mg or Ca at pH range 3~6 and then a slight decrease over pH 6-10.

In the case of metal-lactate and pyroglutamate, the response of Mg or Ca ISE shows a decrease of about 5 mV and 2.5 mV, respectively, between pH 3 and 5. The corresponding species distribution curves also show a decrease in the percentage of free Mg or Ca distribution at the same pH range.

For the Ca-pyridoxine system, the Ca ISE response shows a decrease of about 2 mV at pH range 7-9.5 (figure 9.28a). This decrease agrees with the decrease in the distribution of the percentage of free calcium observed in figure 9.28b.

The curves of Mg or Ca ISE response to pH change of Mg or Ca glycinate, aspartate and glutamate generally decrease over the pH range 3~5, slightly decrease over pH 5~8, and then decrease sharply above pH

≈8. These curves compare well with their corresponding free metal distribution curves observed in figures 9.20b - 9.25b.

The above agreement obtained between the curves of ISE response to the pH change and the percentage of the free metal distribution in the corresponding metal-ligand system confirms the reliability of the results of this work.

Quantitative Comparison:

The above comparison between the free metal percentage distribution curves and ISE response to pH change in the metal-ligand solutions can also be made quantitatively. In the case of, for example, the Mg-citrate system, the decrease in mV for the Mg ISE between pH (3.2-7) is 33 mV. From Mg species distribution diagrams of Mg-citrate (see figure 9.16b), the decrease in mV (ΔE) between pH (3.2-7) can be calculated, using the following approximate form of the Nernst equation:

$$E = E^{o} + (\text{slope}) \log C_{Mg} \times \left(\frac{\%}{100}\right) \qquad \text{(see equation 2.1)} \qquad (9.1)$$

$$\Delta E = 30 \times \log (5.4/82.6) = 35.5 \text{ mV}$$

It can be seen that the calculated mV decrease (35.5 mV) is close in magnitude to the experimental value (33 mV).

For the Mg-lactate system, the calculated mV decrease, in figure 9.18b, between pH (3.2-5) was 6 mV. This mV decrease is in good agreement with that obtained experimentally using the Mg ISE which shows a decrease of about 5.7 mV over the same pH range.

The potentiometric response of the Mg or Ca ISE, as a function of pH for a metal-ligand system, can also be converted to a percentage of free metal distribution by using equation 9.1. This calculated percentage distribution curve (% Calc) was then compared with the corresponding

free metal percentage distribution curves which were calculated using the stability constant results. Figures (9.29 - 9.32) show examples of comparisons between the calculated free metal percentage distribution curves (% Calc) and those drawn by using the values of stability constants obtained in this work (% Mg or Ca.E, % G.E and % Mean). The same titration used to derive % Calc curve was analysed, using SUPERQUAD, to obtain stability constant values from fit of Mg or Ca ISE data. These values were then used to produce % Mg or Ca.E distribution curves. The % G.E distribution curve was calculated from stability constant results obtained by the glass electrode in titration with the same concentrations used to produce % Mg or Ca.E curve. The % Mean (G.E + Mg or Ca.E) distribution curve was calculated from the mean stability constants for all titrations (including different concentrations and electrodes). The concentrations used to produce the species distribution curves were the same as those used in the experiment.

The free metal percentage distribution curves (% Mg or Ca.E) drawn using the stability constant values obtained with the Mg or Ca ISE, when compared with the % Calc distribution, can be used as another indication, instead of χ^2 (see chapter 8), of the closeness of fit offered by the stability constant results. Those of the glass electrode (% G.E) give evidence about how close are the stability constant results obtained compared to those obtained by the Mg or Ca ISE. An indication about how good is the agreement between the different experiments (including different concentrations and electrodes) can also be obtained when the % Mean distribution curves are compared.

In figures 9.29 - 9.32, the distribution of free Mg or Ca as a function of pH for the metal-pyroglutamate and aspartate systems are illustrated.

For each system, it can be seen that the fit offered by the stability constant results obtained with the Mg or Ca ISE is excellent. The figures also reveal good agreement between the results obtained from the Mg or Ca ISE and glass electrode. The agreement between the different experiments is also good, however, it was less satisfactory for the Mg or Ca-aspartate (figure 9.31 or 9.32).

In the same manner, the percentage of free metal in the species distribution diagrams can be converted to mV (equation 9.1). The curve of calculated mV is then compared directly with the corresponding experimental curve obtained by using the Mg or Ca ISE in the pH titration. Figure 9.33 shows comparisons between the calculated and experimental mV responses for the Mg-pyridoxine system at different concentrations. The stability constant values obtained from the glass electrode and Mg ISE results were used to calculate the mV curves. In the case of the Mg ISE calculated mV curve, the stability constants obtained from each titration (table 9.20) were used. The concentrations (C_M and C_L shown in table 9.20) were inserted to produce the species distribution curves. For the glass electrode calculated mV curve, the stability constants used were obtained by using the glass electrode at 100 mmol/L pyridoxine and 20 mmol/L Mg. These concentrations were used, as well, to produce the species distribution curve.

The figure shows that a good fit of the stability constant results was obtained with the use of Mg ISE at each concentration. However, the fit was less satisfactory at high ligand concentrations (C_L=100 mmol/L). The glass electrode mV calculated curve shows a poor fit with the corresponding experimental mV curve (Exp100 in figure 9.33). Hence,

Fig. 9.1 Species Distribution Diagram of Mg-Citrate
(C_{Mg} = 20 mmol/L, C_{Cit} = 20 mmol/L)

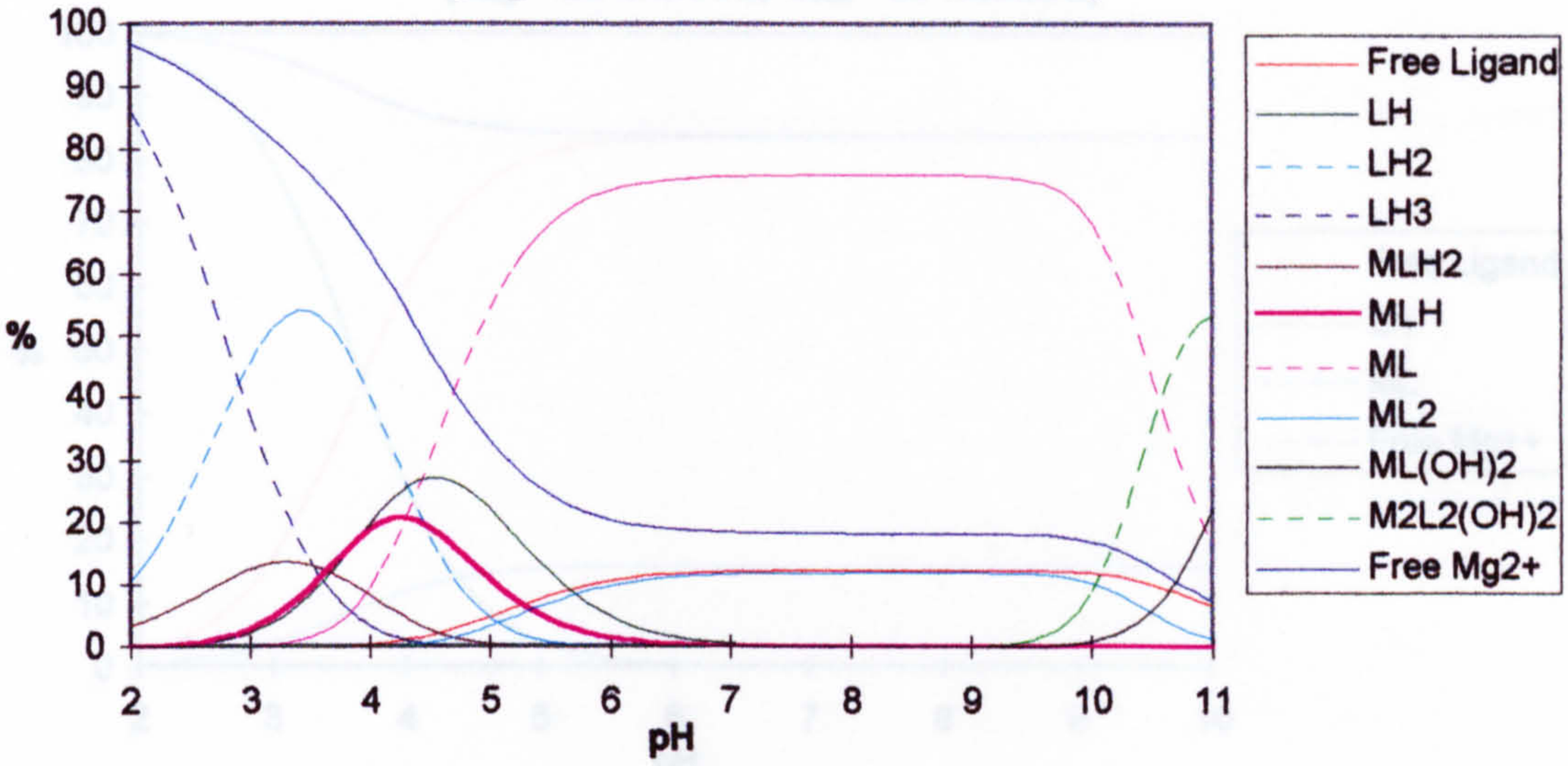

Fig. 9.2 Species Distribution Diagram of Ca-Citrate
(C_{Ca} = 20 mmol/L, C_{Cit} = 20 mmol/L)

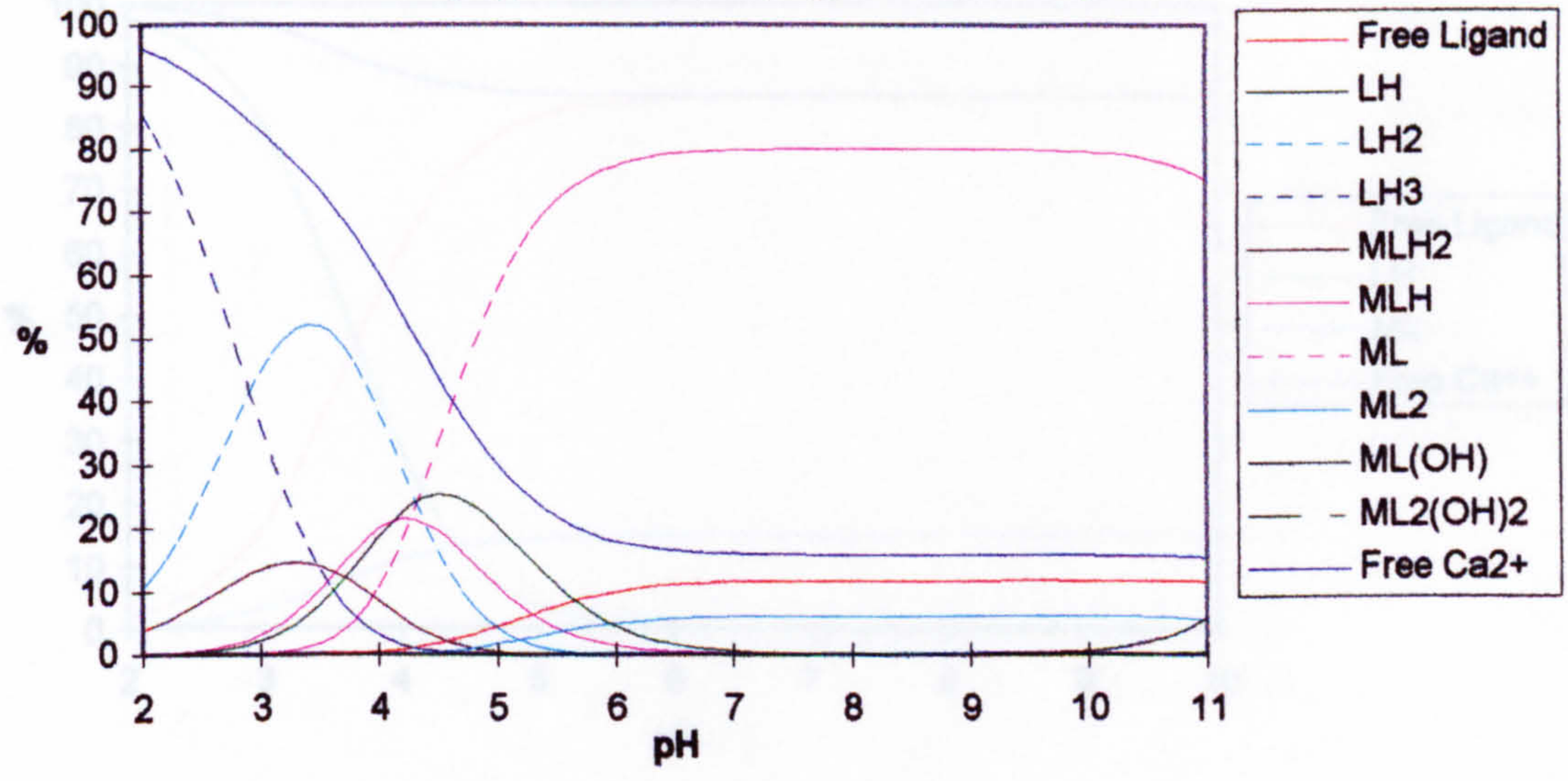

Fig. 9.3 Species Distribution Diagram of Mg-Lactate
(C_{Mg} = 20 mmol/L, C_{Lac}= 20 mmol/L)

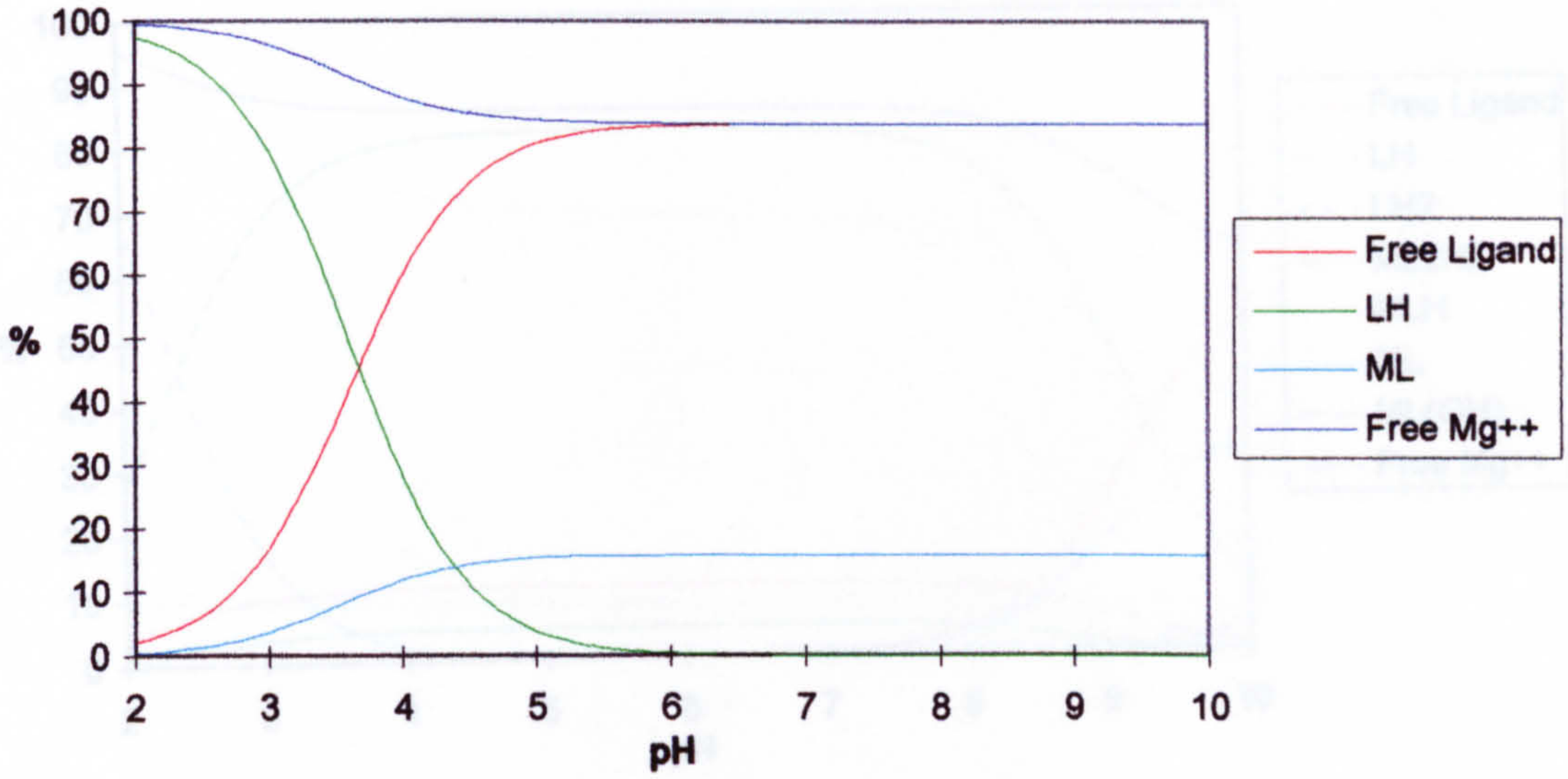

Fig. 9.4 Species Distribution Diagram of Ca-Lactate
(C_{Ca} = 20 mmol/L, C_{Lac} = 20 mmol/L)

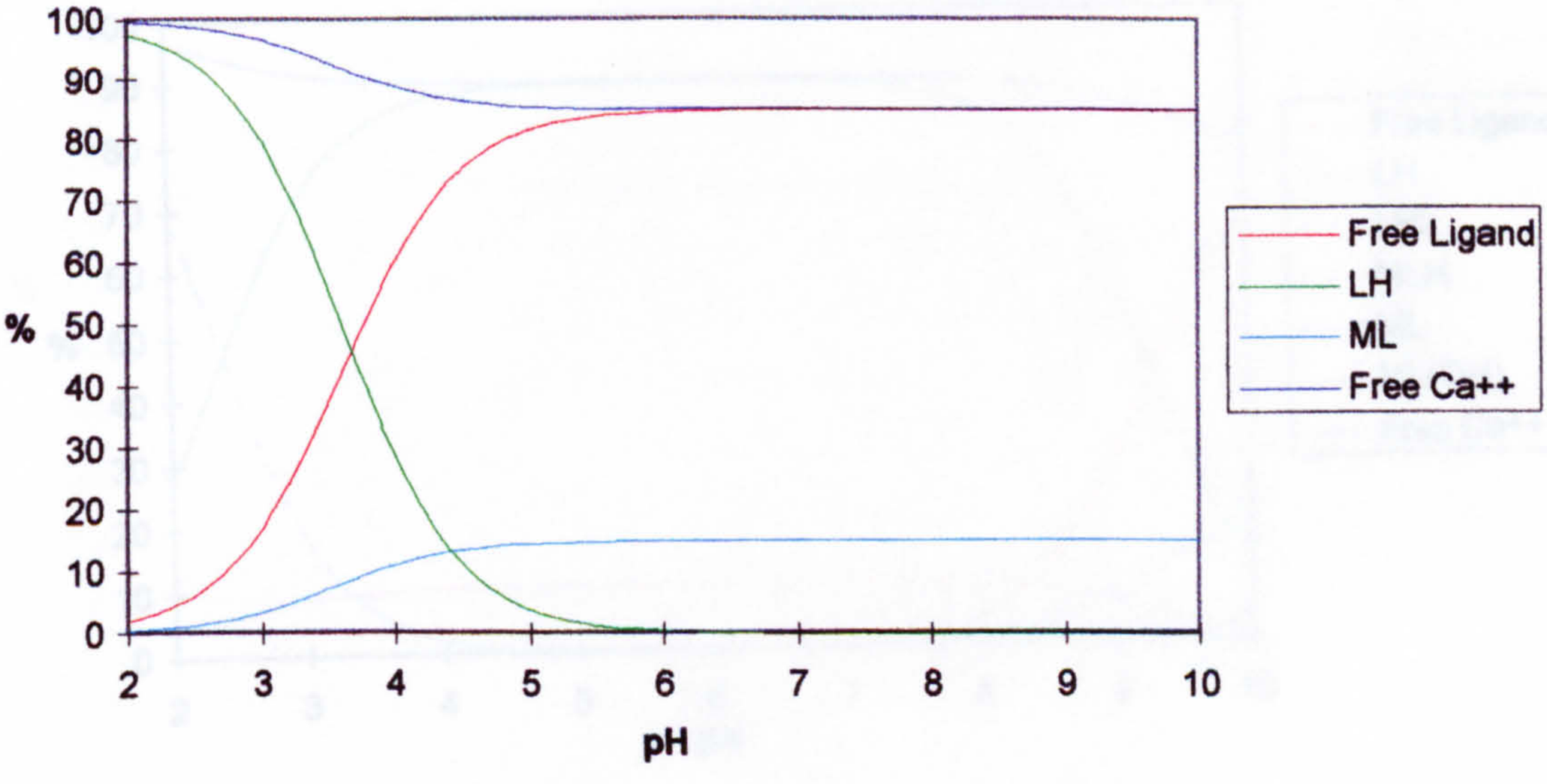

Fig. 9.5 Species Distribution Diagram of Mg-Glycinate
(C_{Mg} = 20 mmol/L, C_{Gly} = 20 mmol/L)

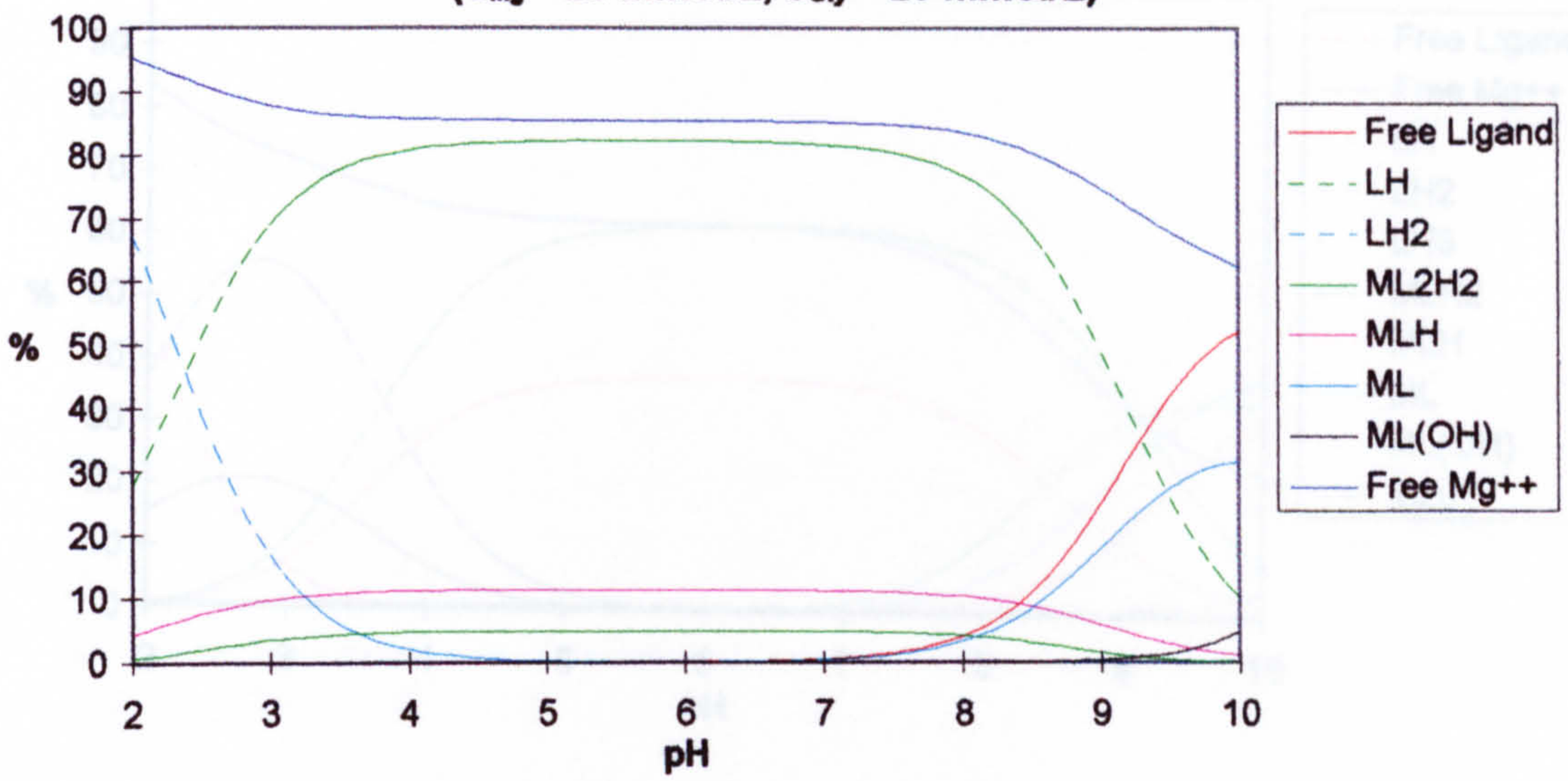

Fig. 9.6 Species Distribution Diagram of Ca-Glycinate
(C_{Ca} = 20 mmol/L, C_{Gly} = 20 mmol/L)

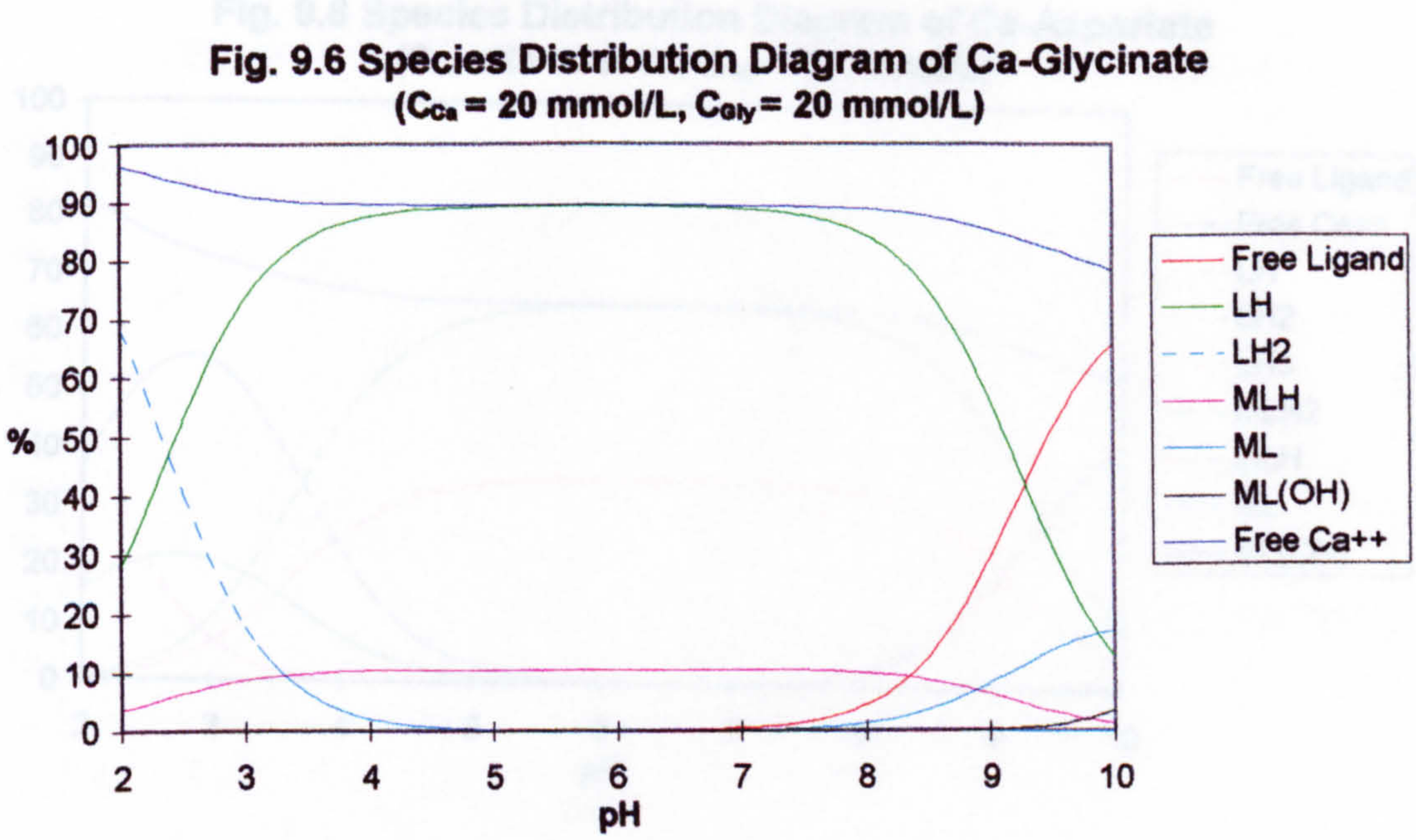

Fig. 9.7 Species Distribution Diagram of Mg-Aspartate
(C_{Mg} = 20 mmol/L, C_{Asp} = 20 mmol/L)

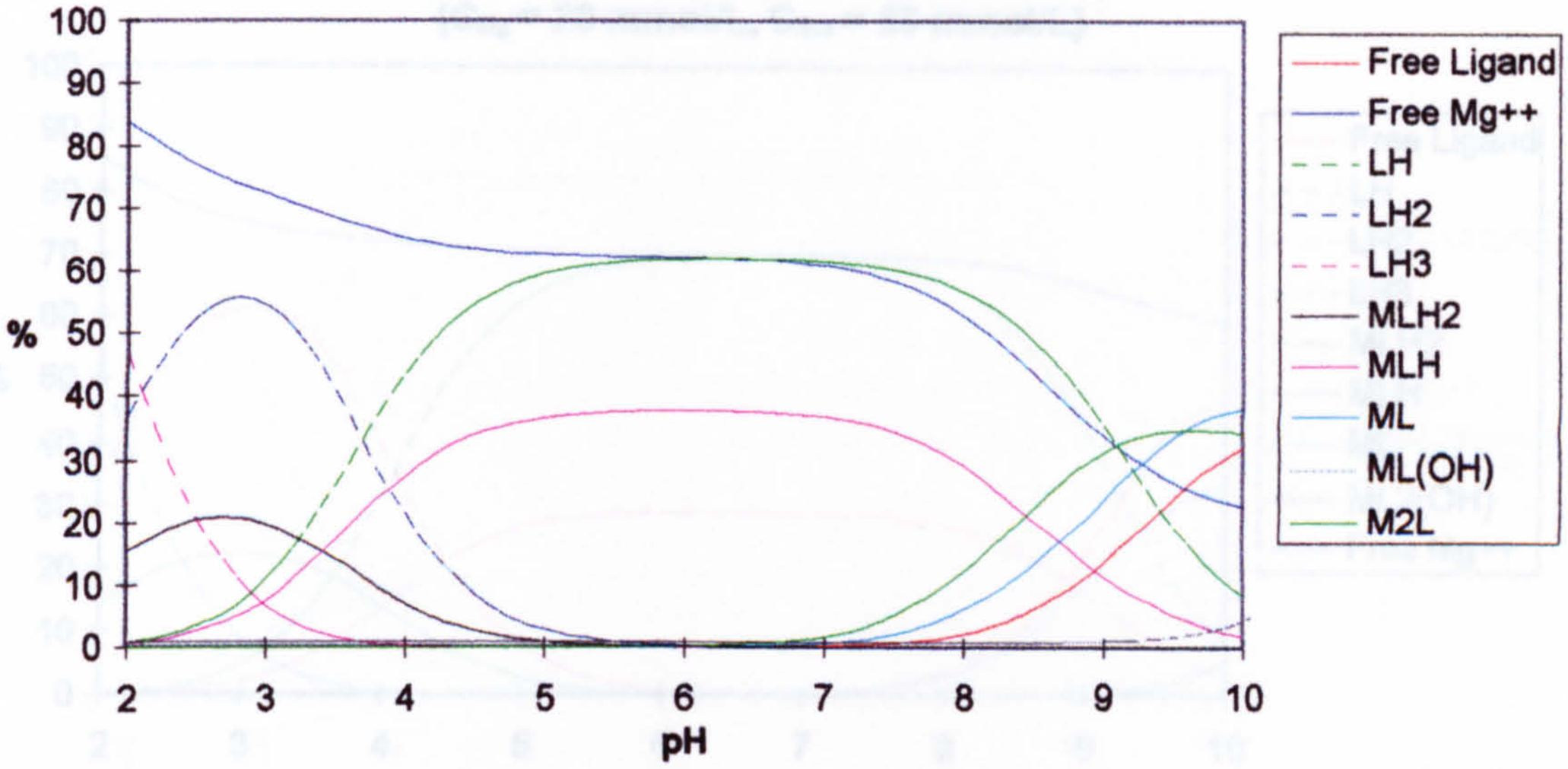

Fig. 9.8 Species Distribution Diagram of Ca-Aspartate
(C_{Ca} = 20 mmol/L, C_{Asp} = 20 mmol/L)

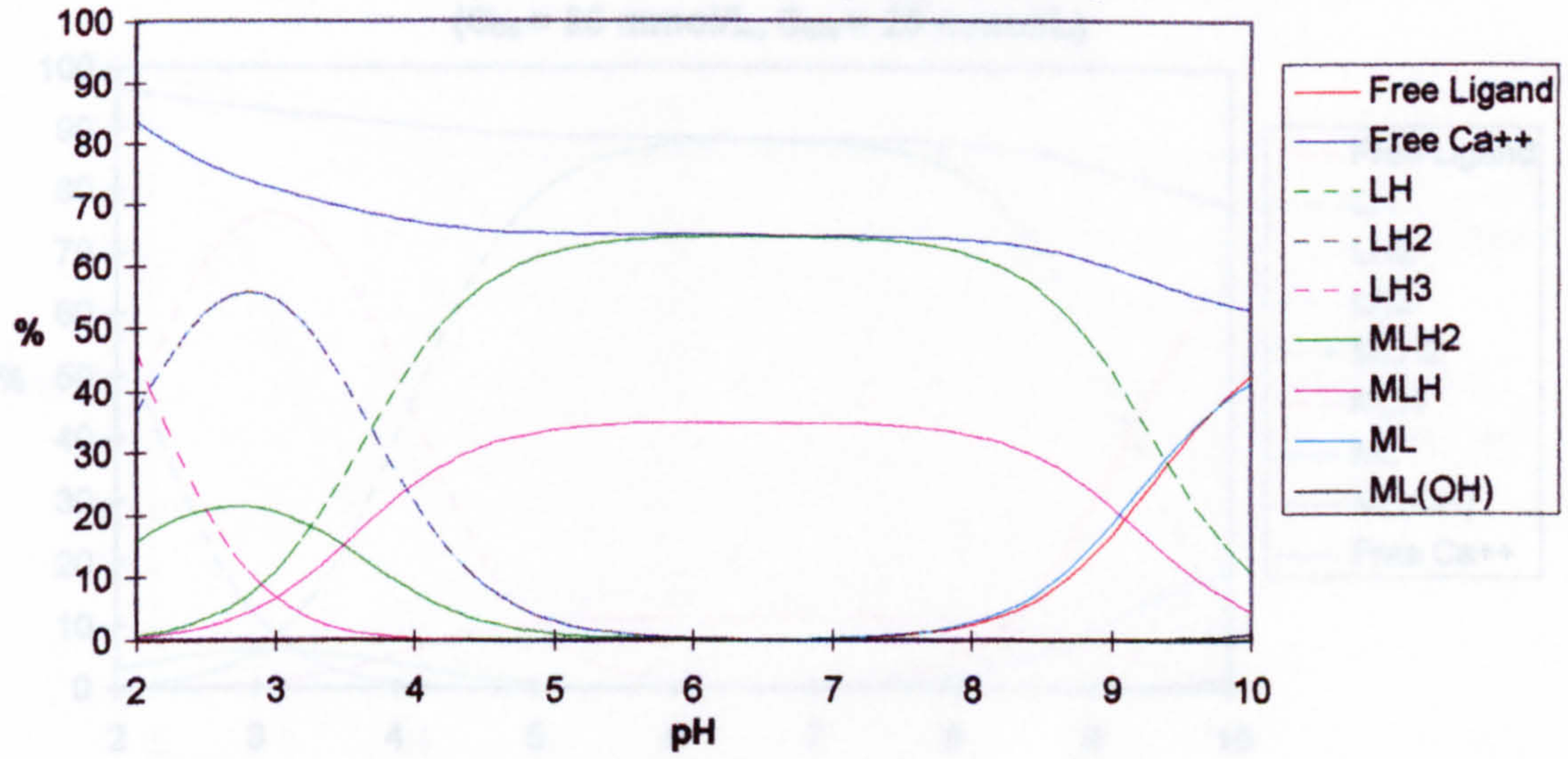

Fig. 9.9 Species Distribution Diagram of Mg-Glutamate
(C_{Mg} = 20 mmol/L, C_{Glu} = 20 mmol/L)

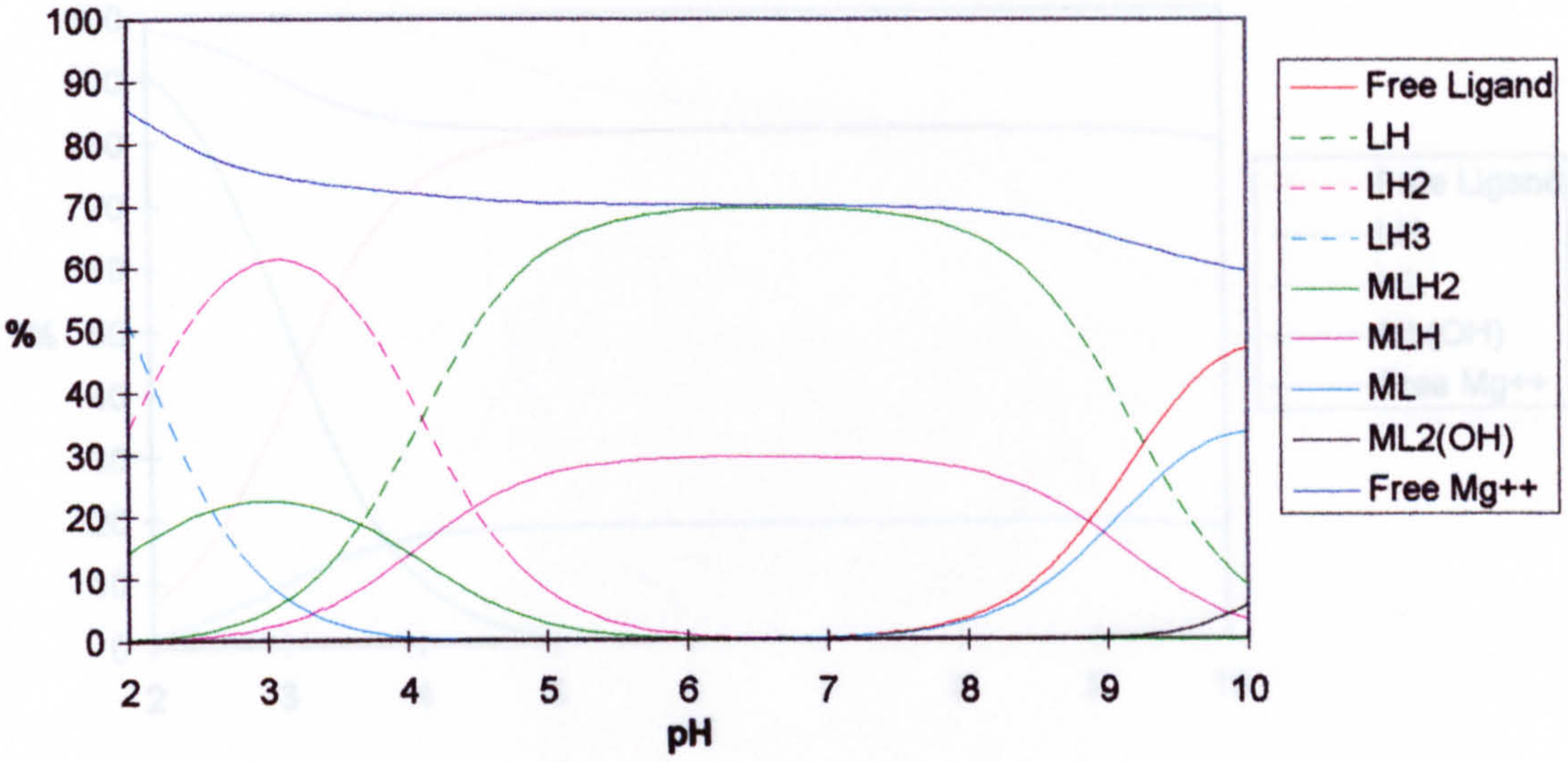

Fig. 9.10 Species Distribution Diagram of Ca-Glutamate
(C_{Ca} = 20 mmol/L, C_{Glu} = 20 mmol/L)

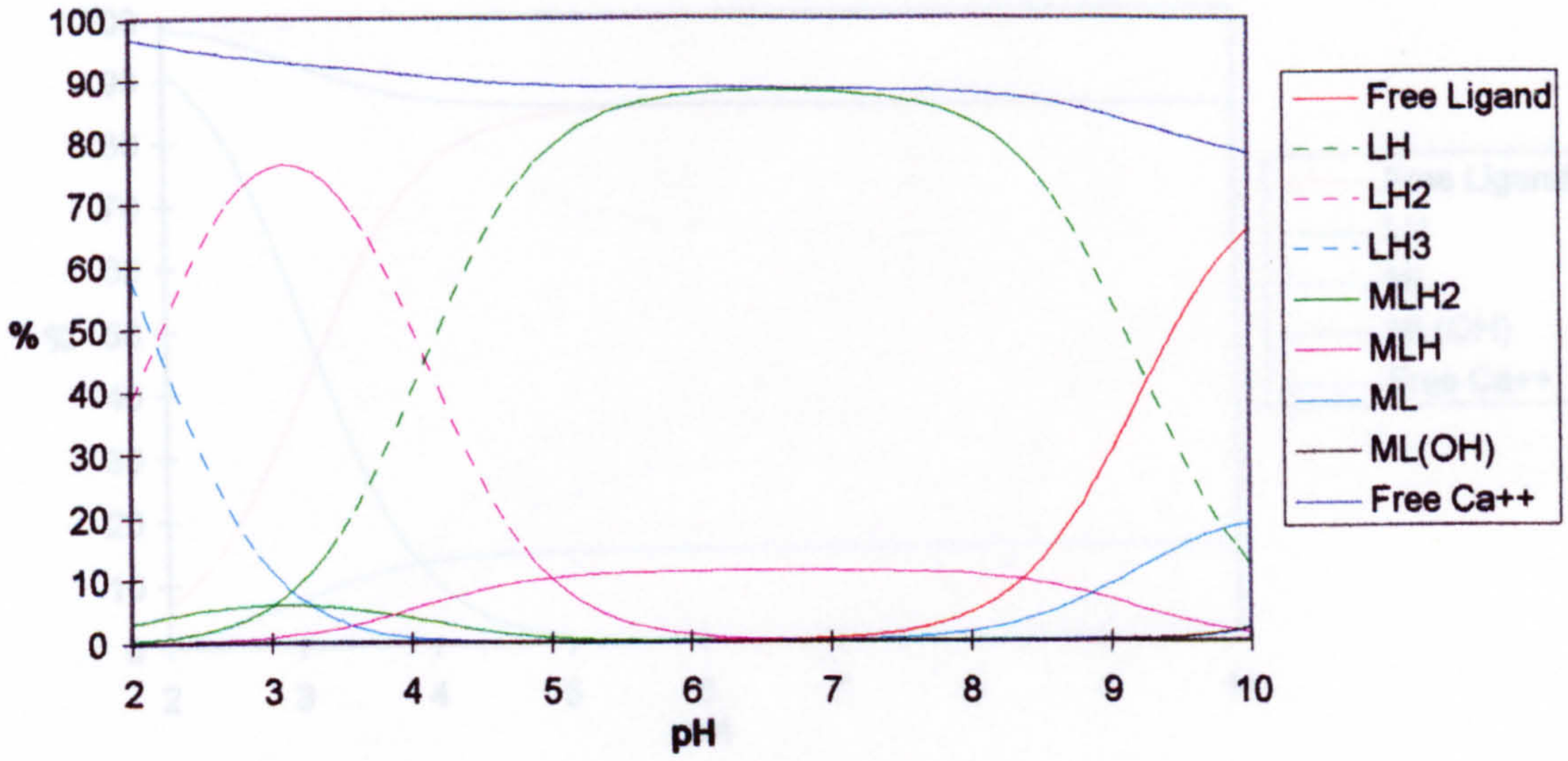

Fig. 9.11 Species Distribution Diagram of Mg-Pyroglutamate
(C_{Mg} = 40 mmol/L, C_{Pyrog} = 40 mmol/L)

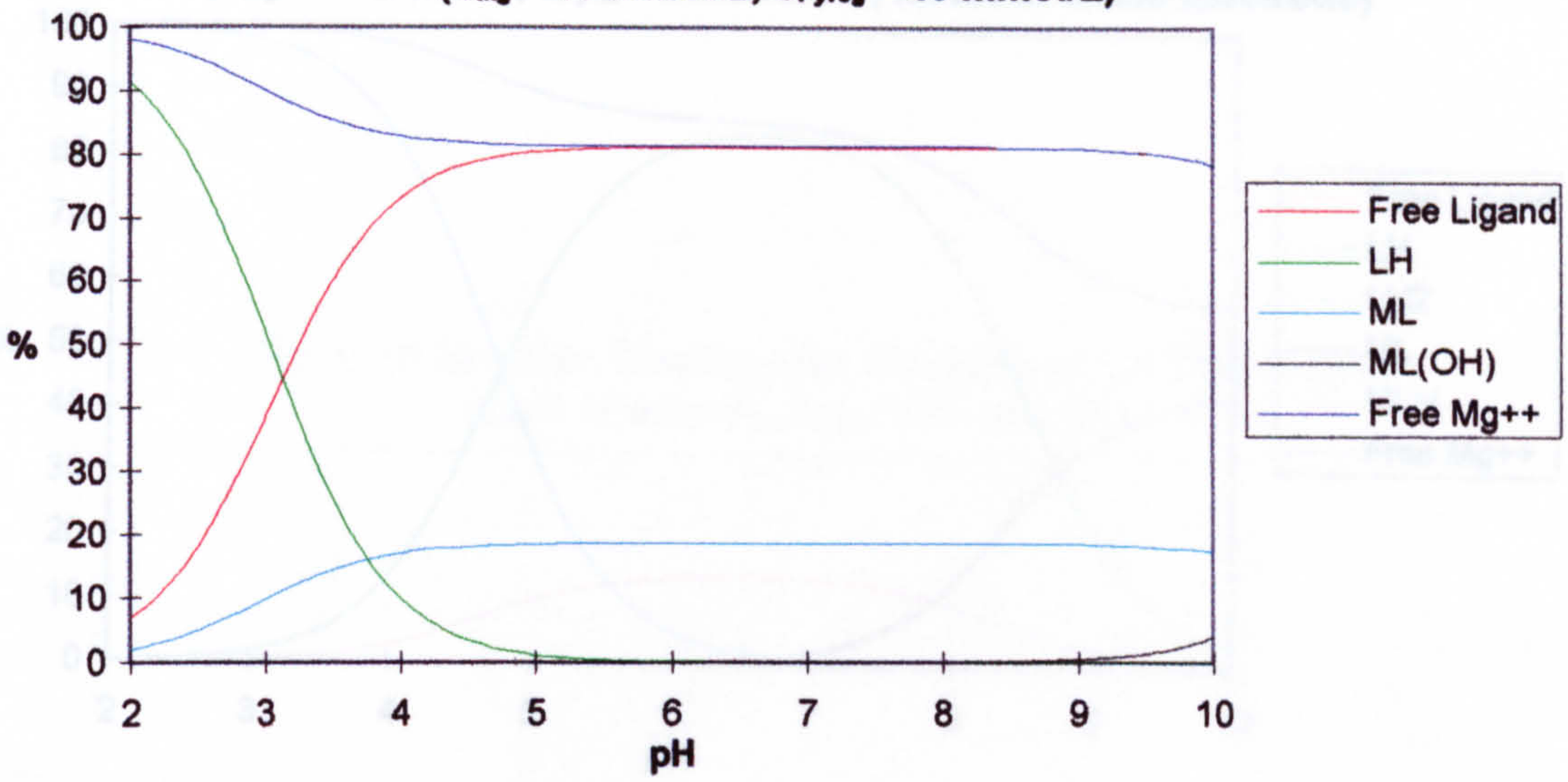

Fig. 9.12 Species Distribution Diagram of Ca-Pyroglutamate
(C_{Ca}=40 mmol/L, C_{Pyrog}=40 mmol/L)

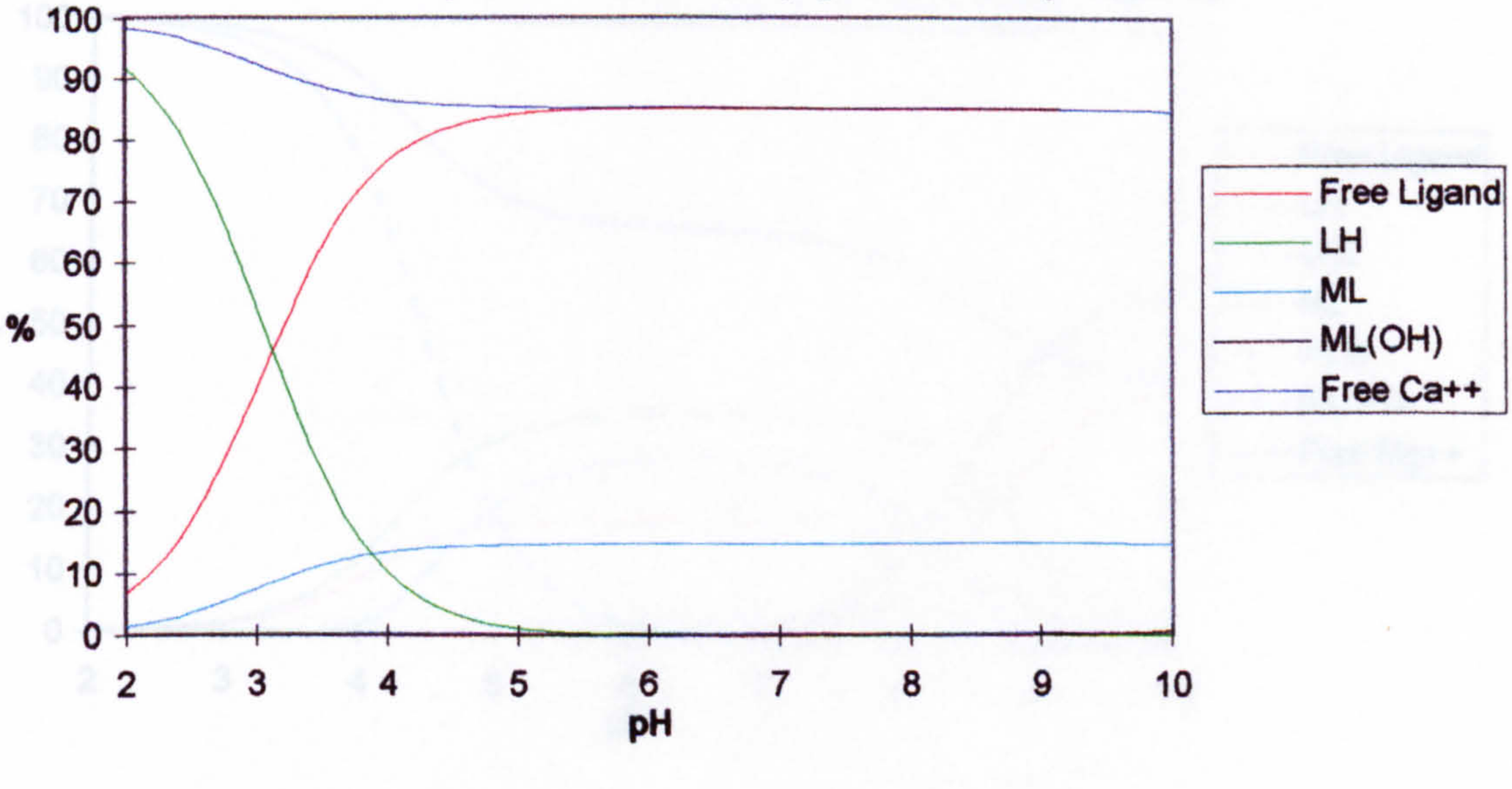

Fig. 9.13 Species Distribution Diagram of Mg-Pyridoxine
(C_{Mg} = 50 mmol/L, C_{Pyrid} = 50 mmol/L ; Method: Glass Electrode)

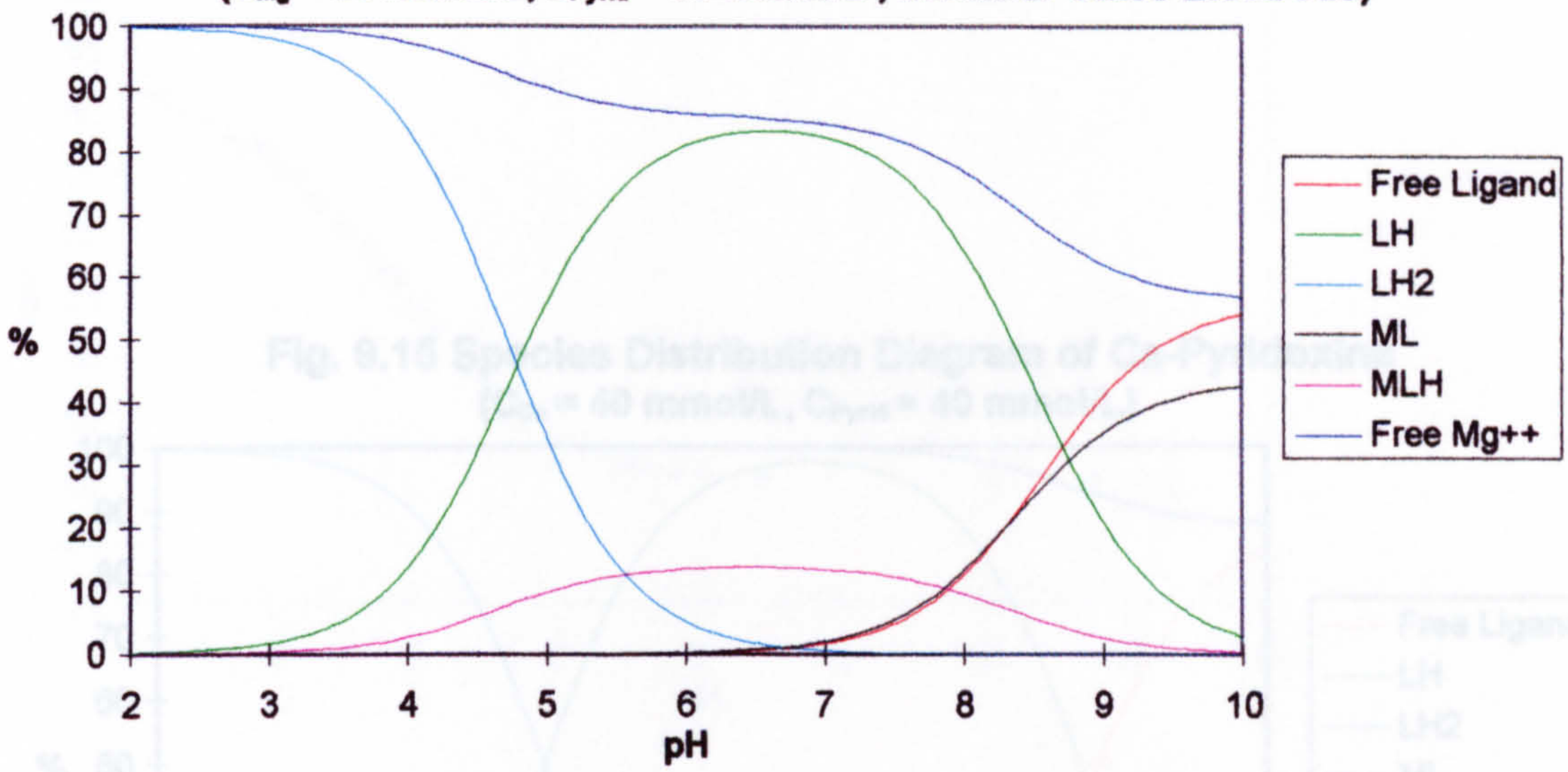

Fig. 9.14 Species Distribution Diagram of Mg-Pyridoxine
(C_{Mg} = 50 mmol/L, C_{Pyrid} = 50 mmol/L ; Method: Mg ISE)

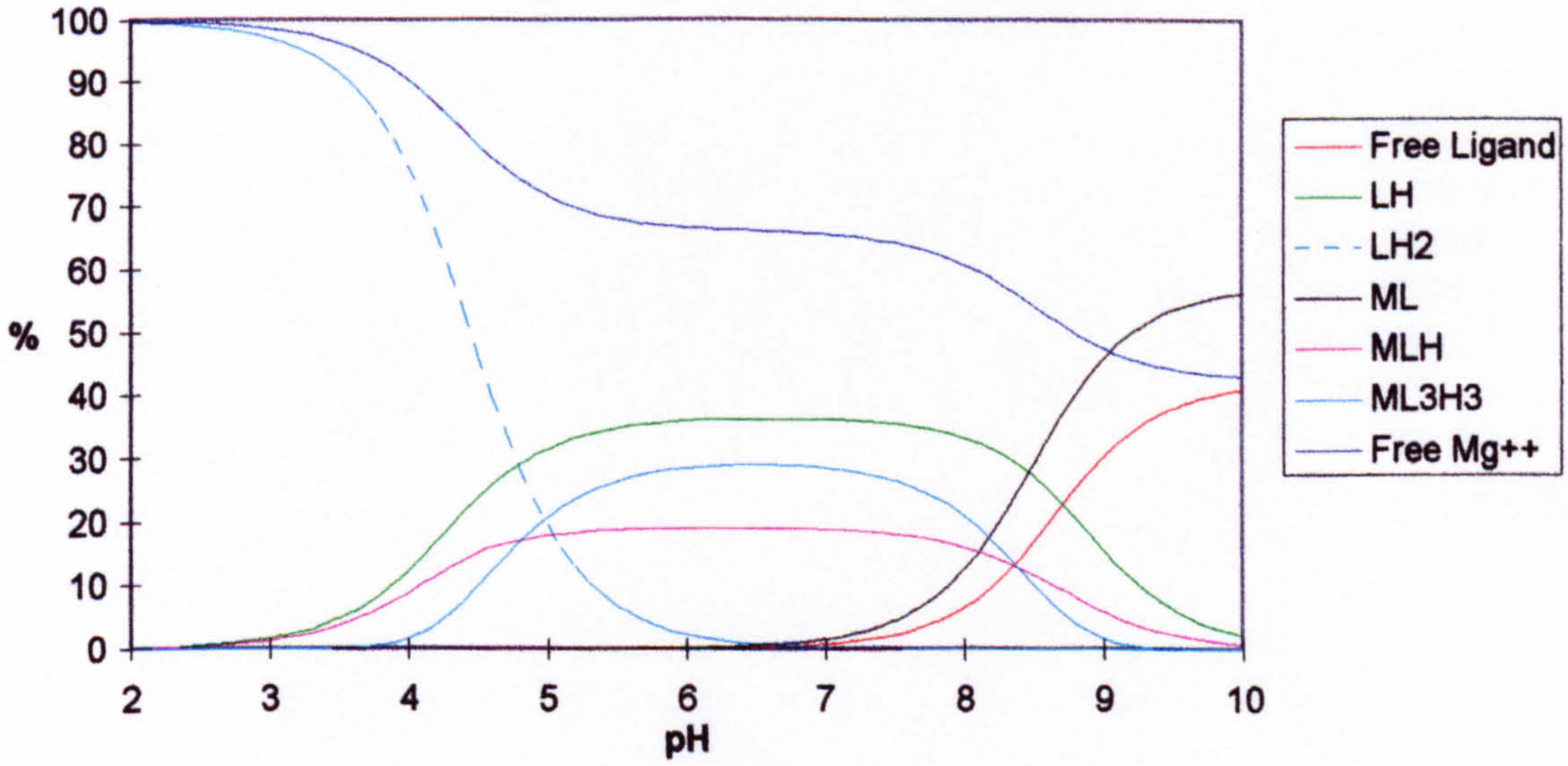

Fig. 9.15 Species Distribution Diagram of Ca-Pyridoxine
(C_{Ca} = 40 mmol/L, C_{Pyrid} = 40 mmol/L)

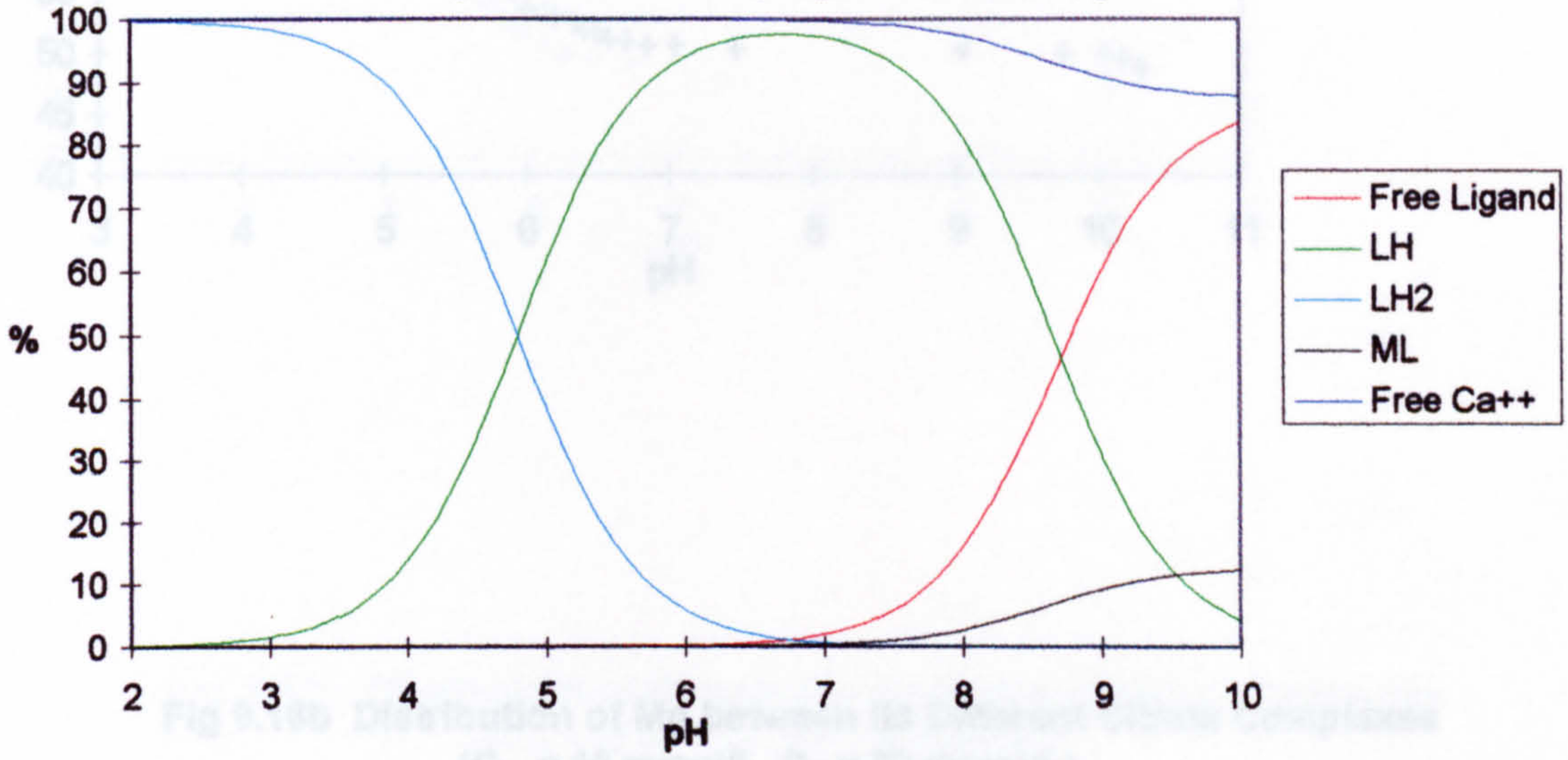

Fig. 9.16a Mg ISE Response to pH Change of Mg-Citrate
(C_{Mg} = 10 mmol/L, C_{Cit} = 20 mmol/L, C_{HCl} = 2.5 mmol/L, C_{KCl} = 150 mmol/L)

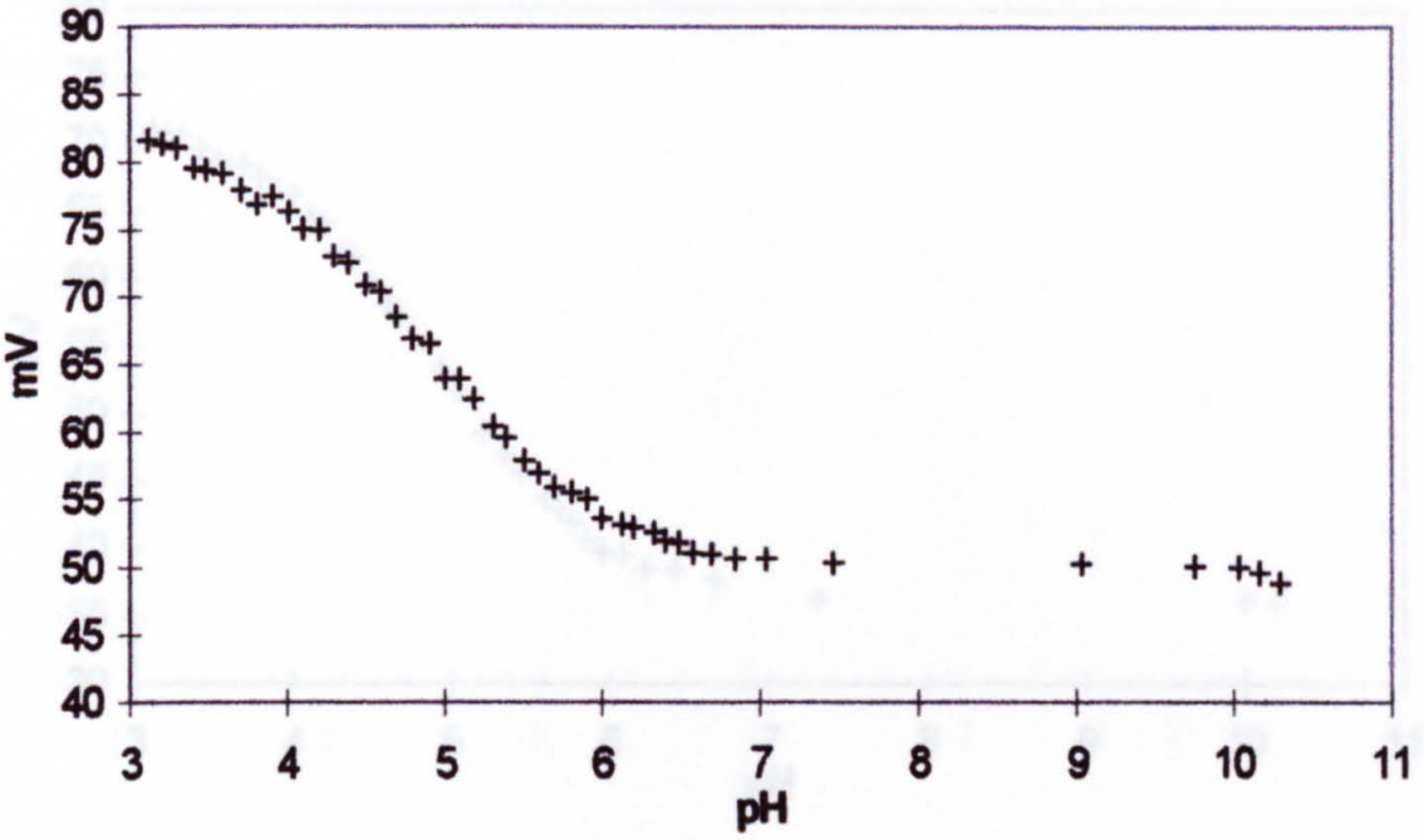

Fig 9.16b Distribution of Mg between its Different Citrate Complexes
(C_{Mg} = 10 mmol/L, C_{Cit} = 20 mmol/L)

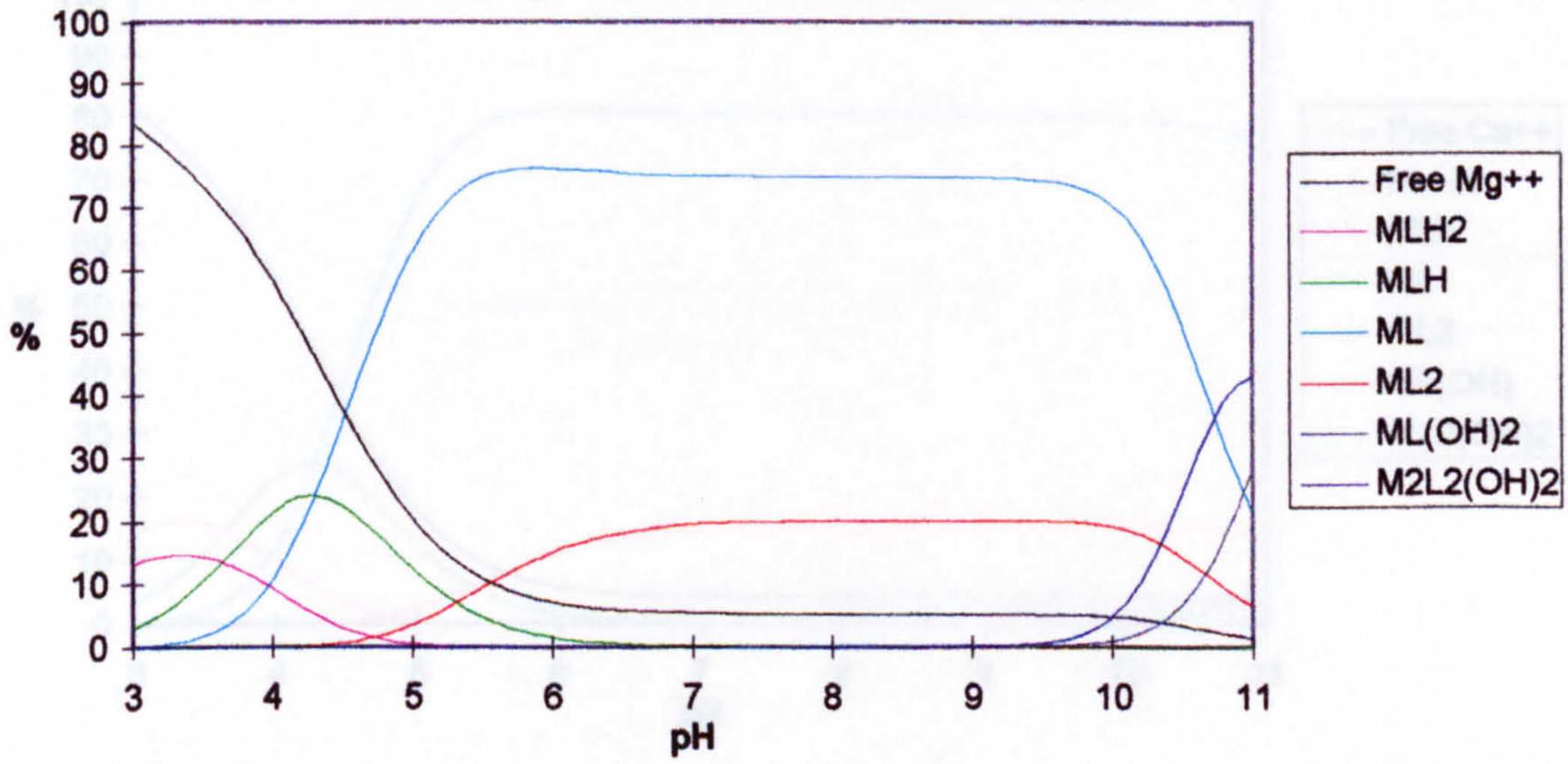

Fig. 917a Ca ISE Response to pH Change of Ca-Citrate
(C_{Ca} = 10 mmol/L, C_{Cit} = 20 mmol/L, C_{HCl} = 1 mmol/L, C_{KCl} = 150 mmol/L)

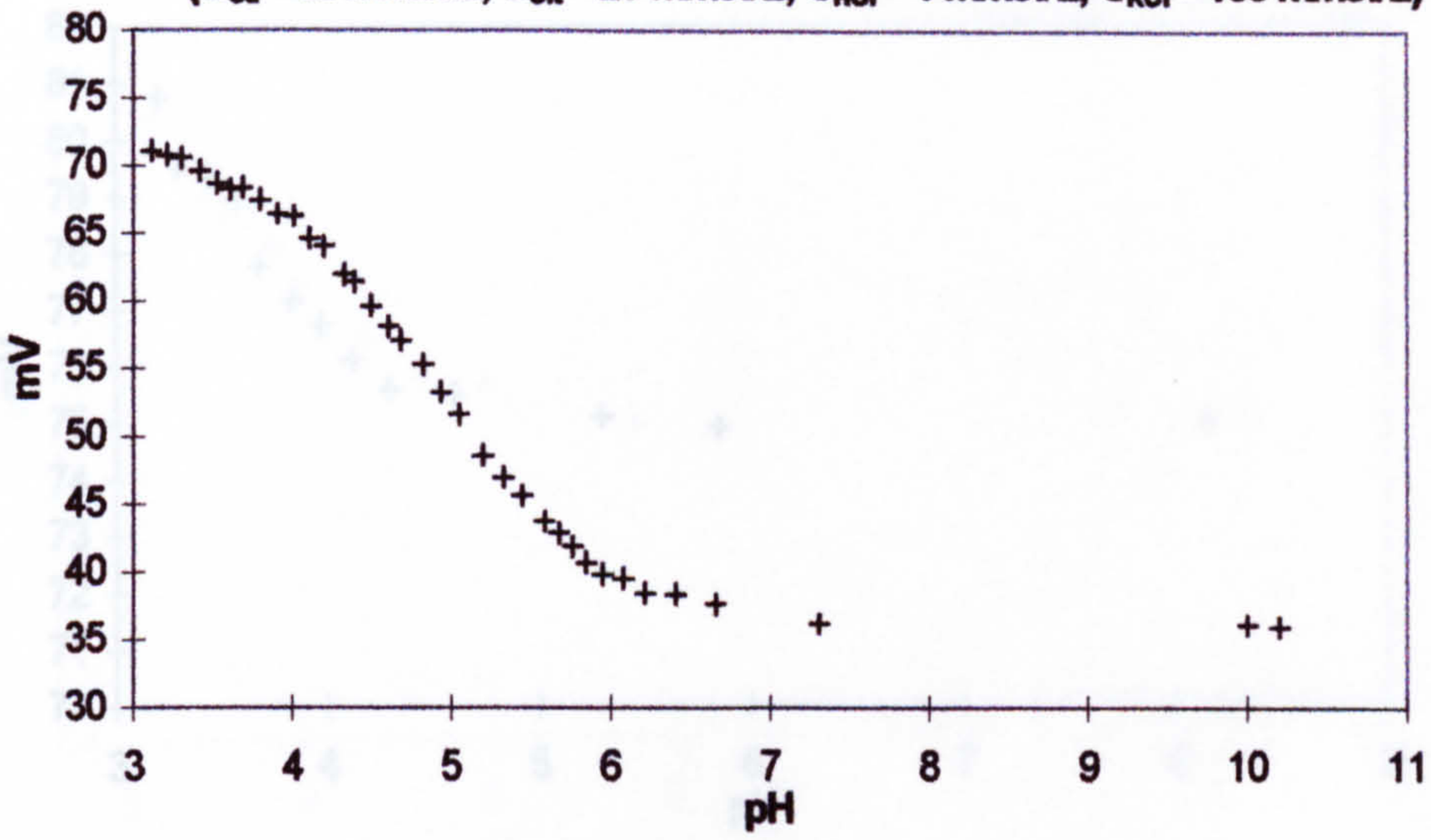

Fig. 9.17b Distribution of Ca between its Different Citrate Complexes
(C_{Ca} = 10 mmol/L, C_{Cit} = 20 mmol/L)

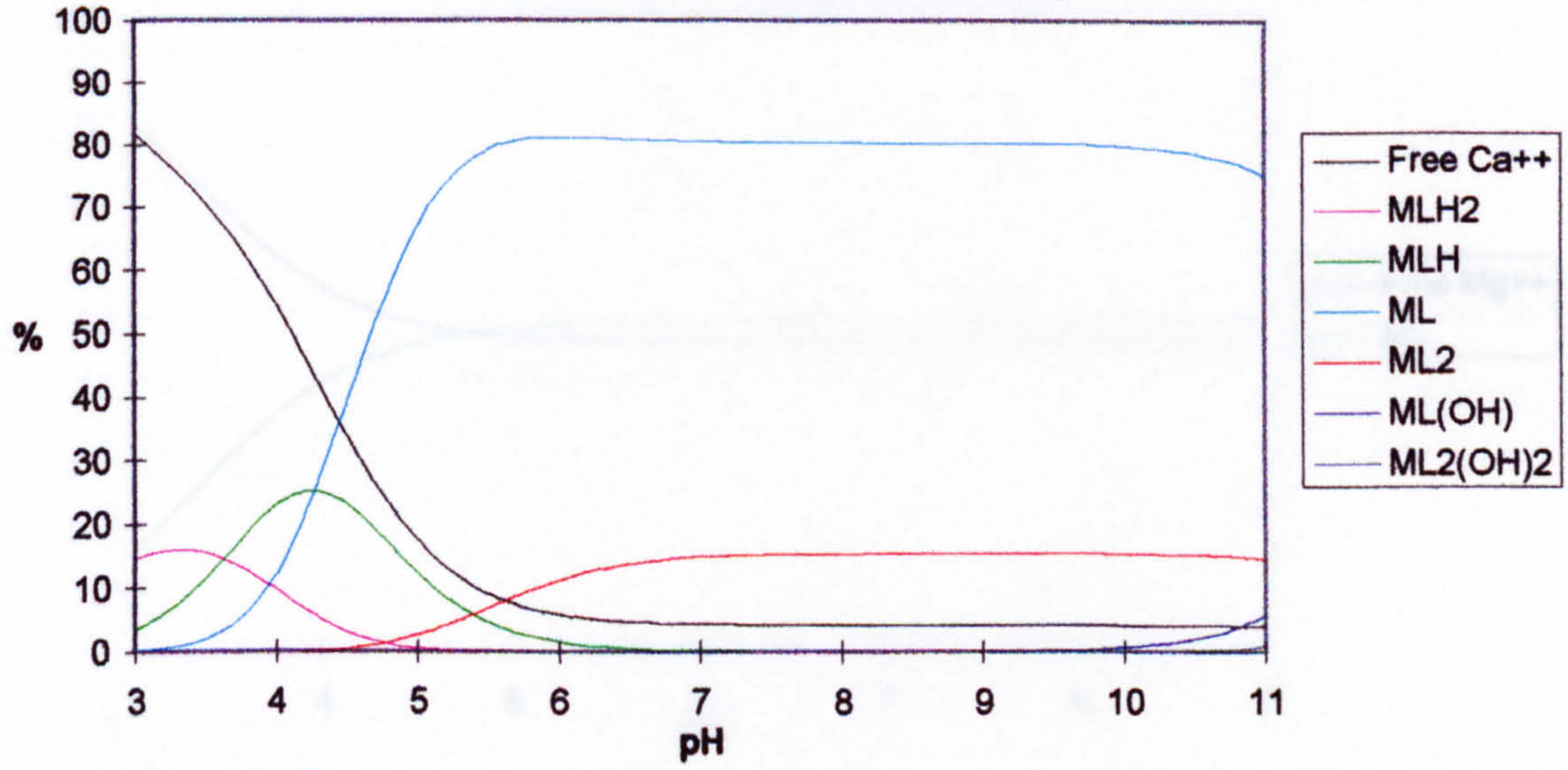

Fig. 9.18a Mg ISE Response to pH Change of Mg-Lactate
(C_{Mg} = 10 mmol/L, C_{Lac} = 100 mmol/L, C_{NaCl} = 150 mmol/L)

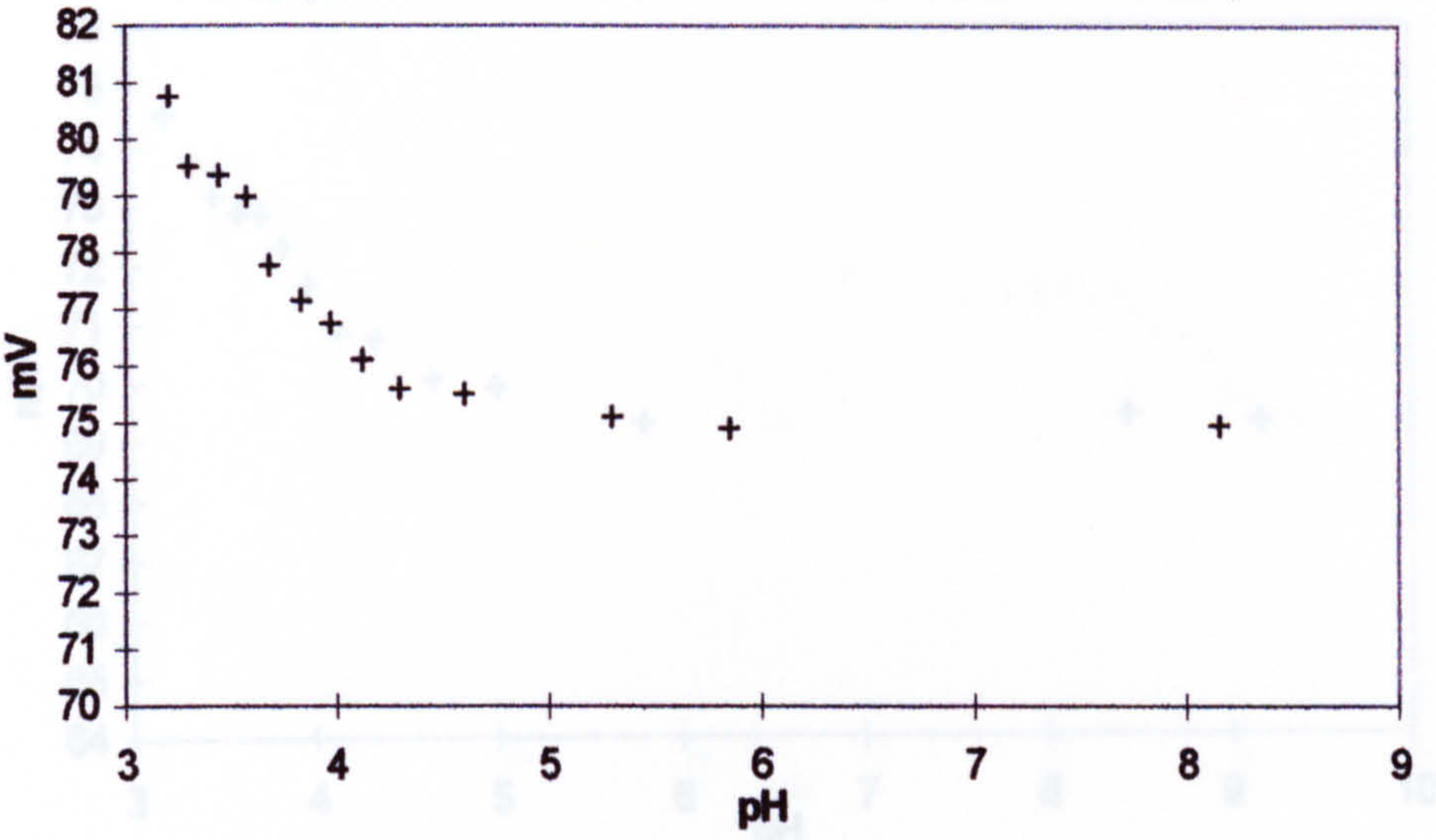

Fig. 9.18b Distribution of Mg between its Lactate Complex
(C_{Mg} = 10 mmol/L, C_{Lac} = 100 mmol/L)

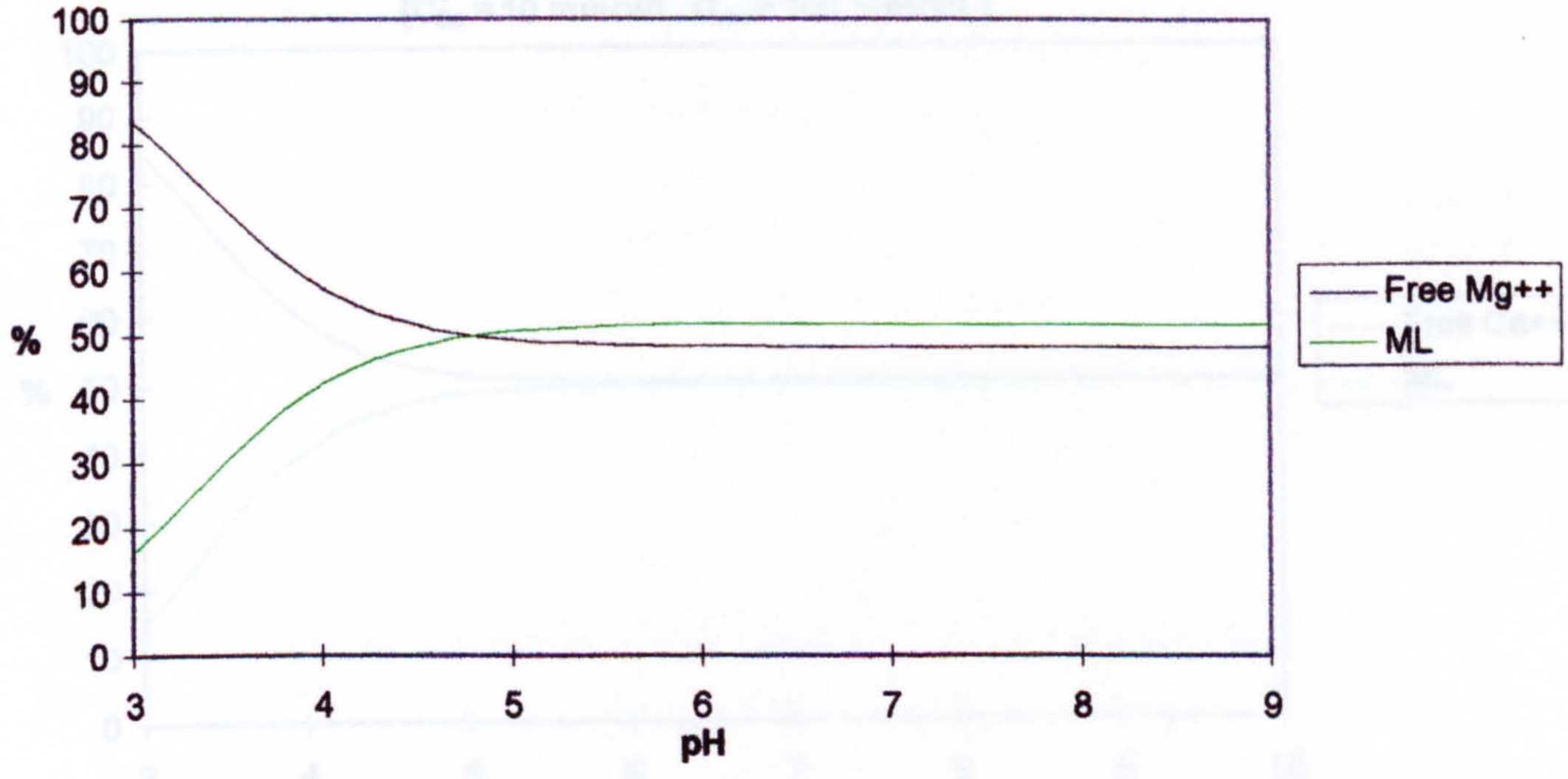

Fig. 9.19a Ca ISE Response to pH Change of Ca-Lactate
(C_{Ca} = 10 mmol/L, C_{Lac} = 100 mmol/L, C_{NaCl} = 150 mmol/L)

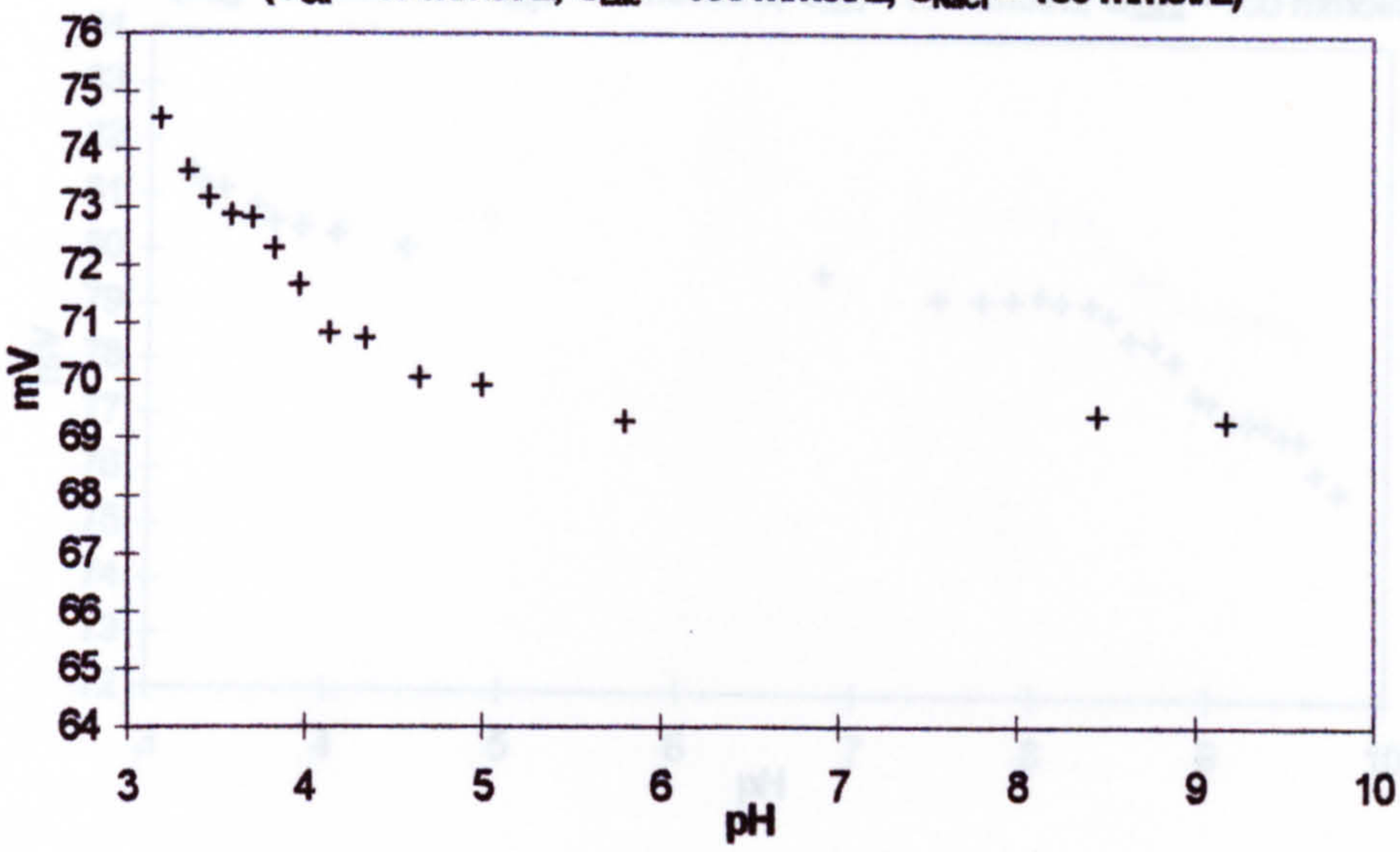

Fig. 9.19b Distribution of Ca between its Lactate Complex
(C_{Ca} = 10 mmol/L, C_{Lac} = 100 mmol/L)

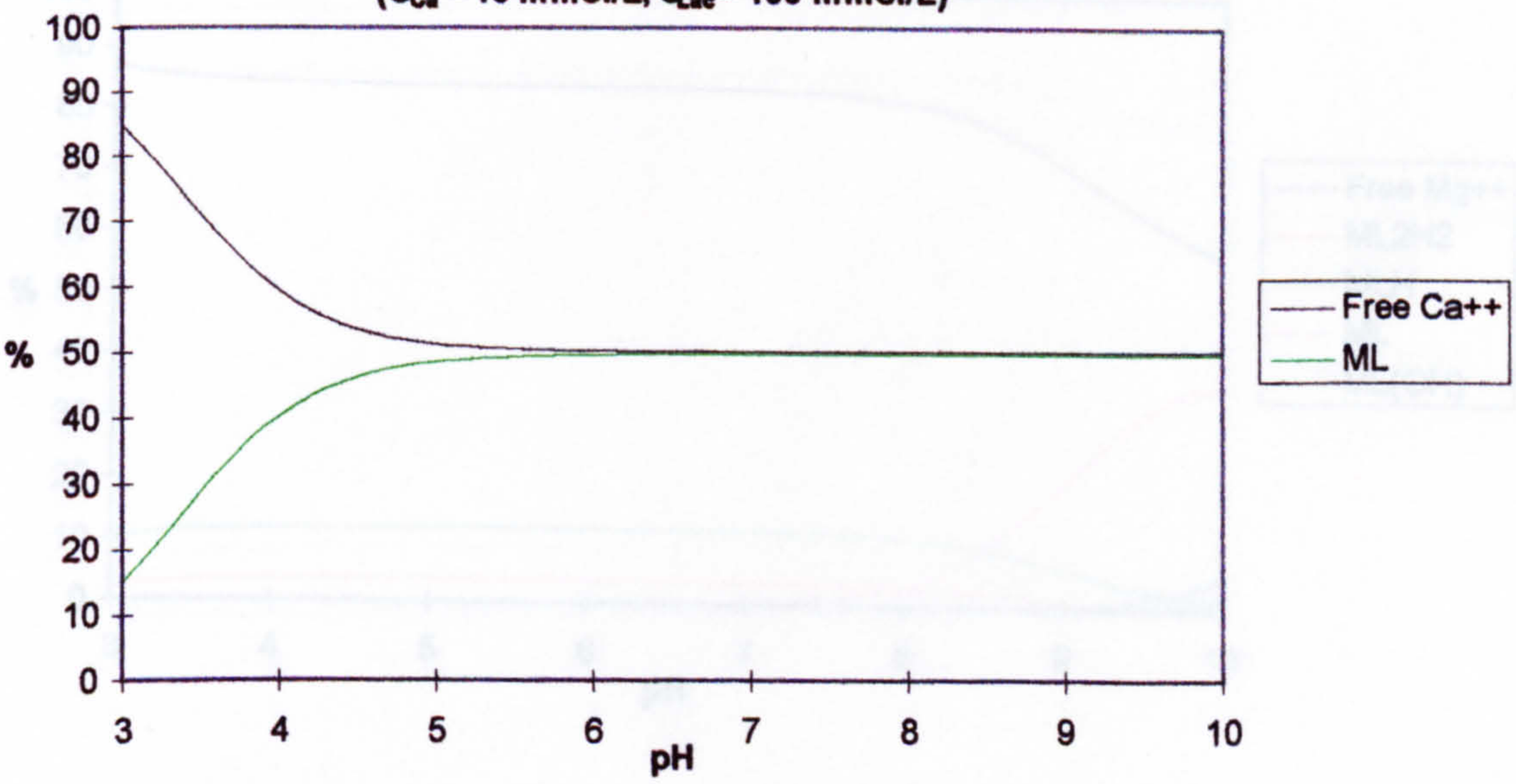

Fig. 9.20a Mg ISE Response to pH Change of Mg-Glycinate

(C_{Mg} = 10 mmol/L, C_{Gly} = 20 mmol/L, C_{HCl} = 10 mmol/L, C_{NaCl} = 150 mmol/L)

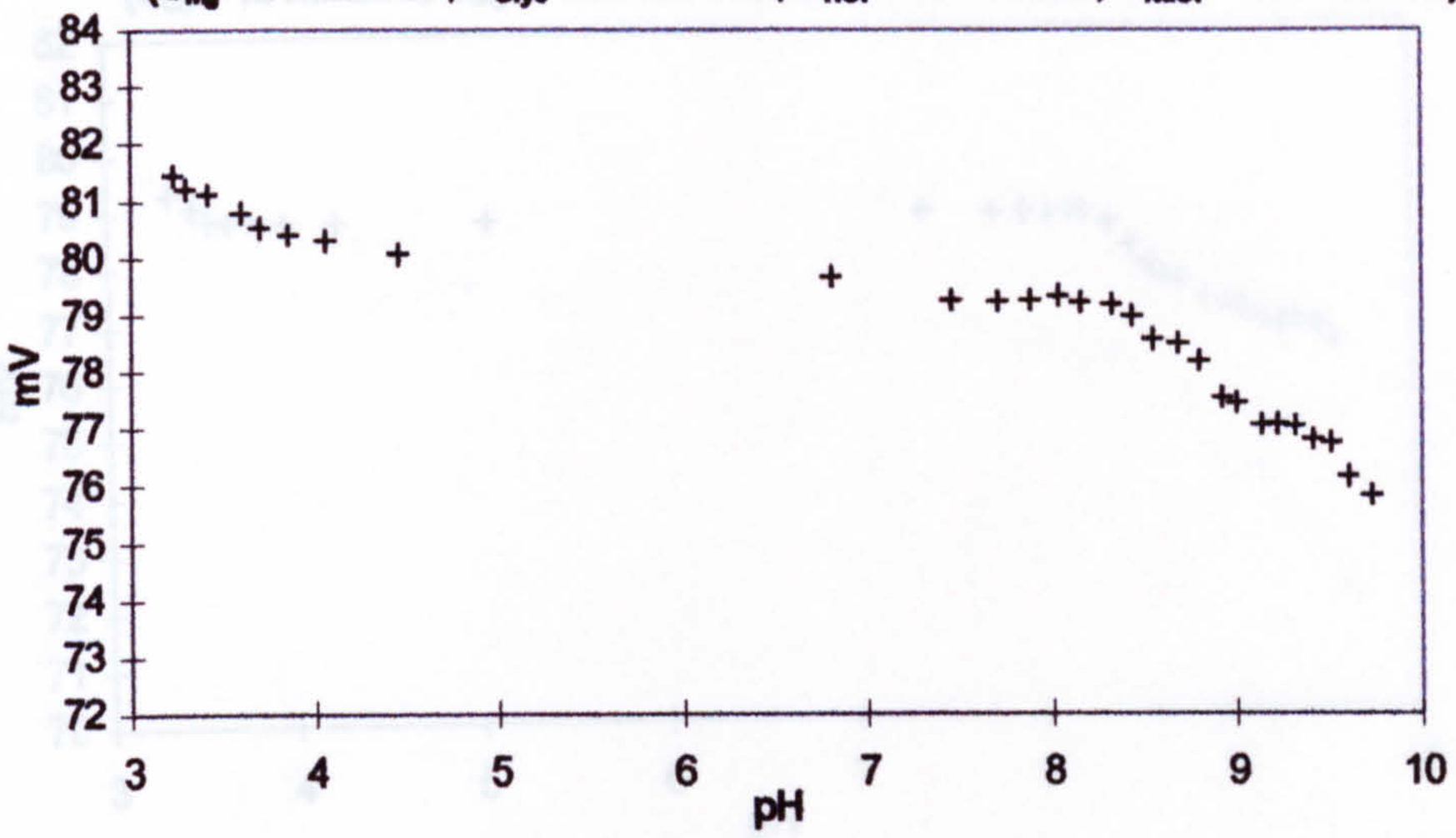

Fig. 9.20b Distribution of Mg between its Glycinate Complexes

(C_{Mg} = 10 mmol/L, C_{Gly} = 20 mmol/L)

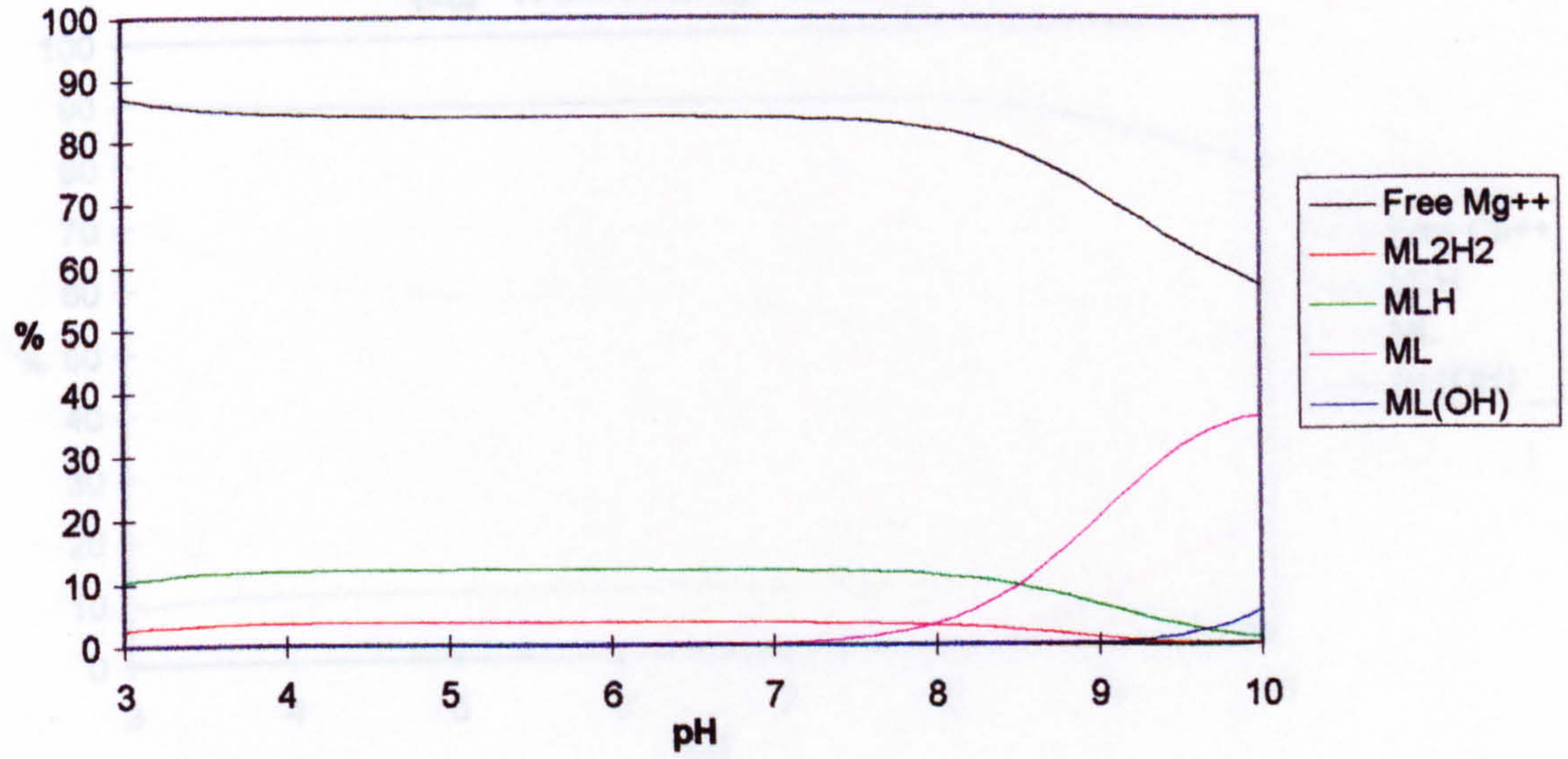

Fig. 9.21a Ca ISE Response to pH Change of Ca-Glycinate

(C_{Ca} = 10 mmol/L, C_{Gly} = 20 mmol/L, C_{HCl} = 10 mmol/L, C_{NaCl} = 150 mmol/L)

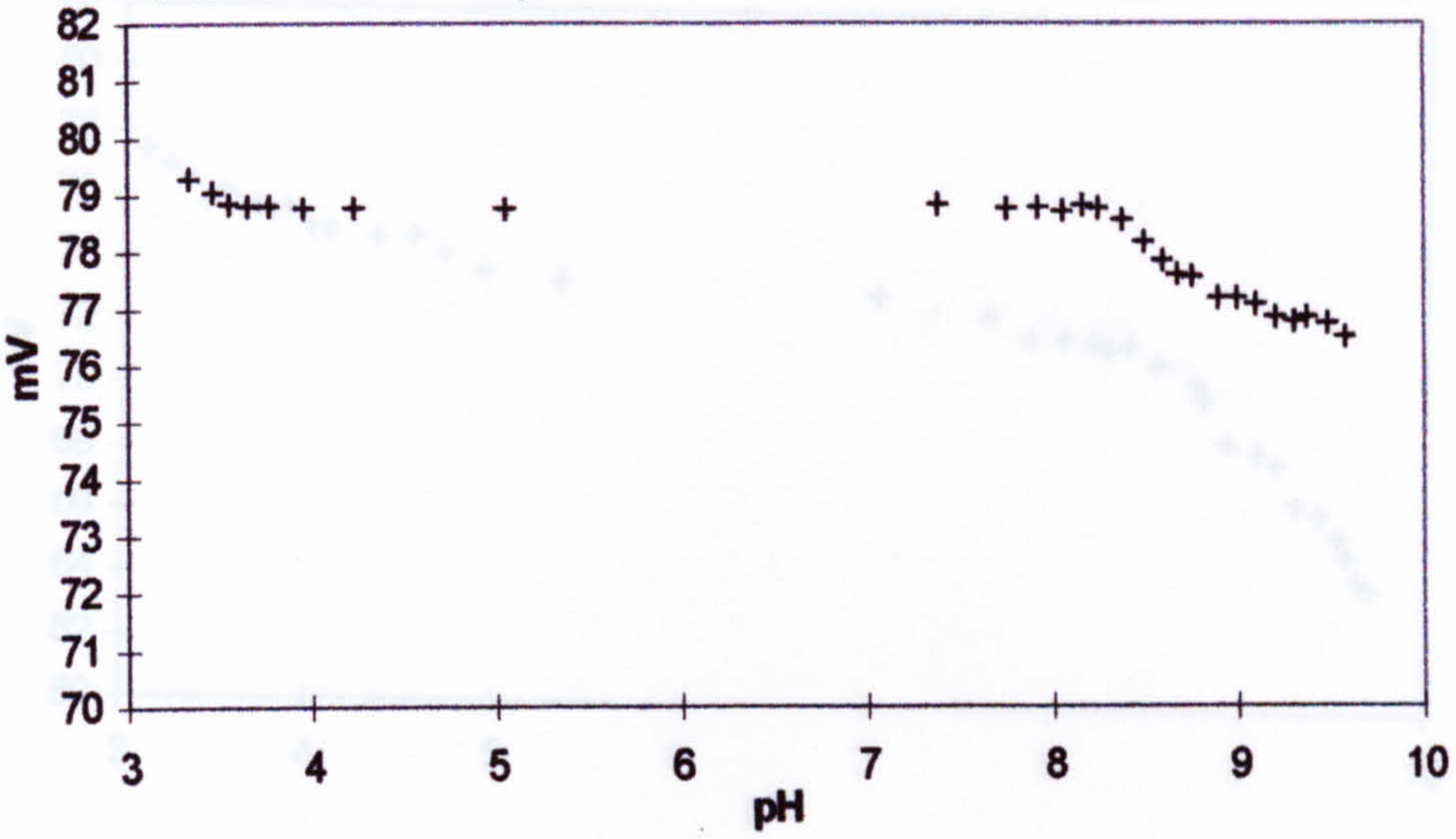

Fig. 9.21b Distribution of Ca between its Glycinate Complexes

(C_{Ca} = 10 mmol/L, C_{Gly} = 20 mmol/L)

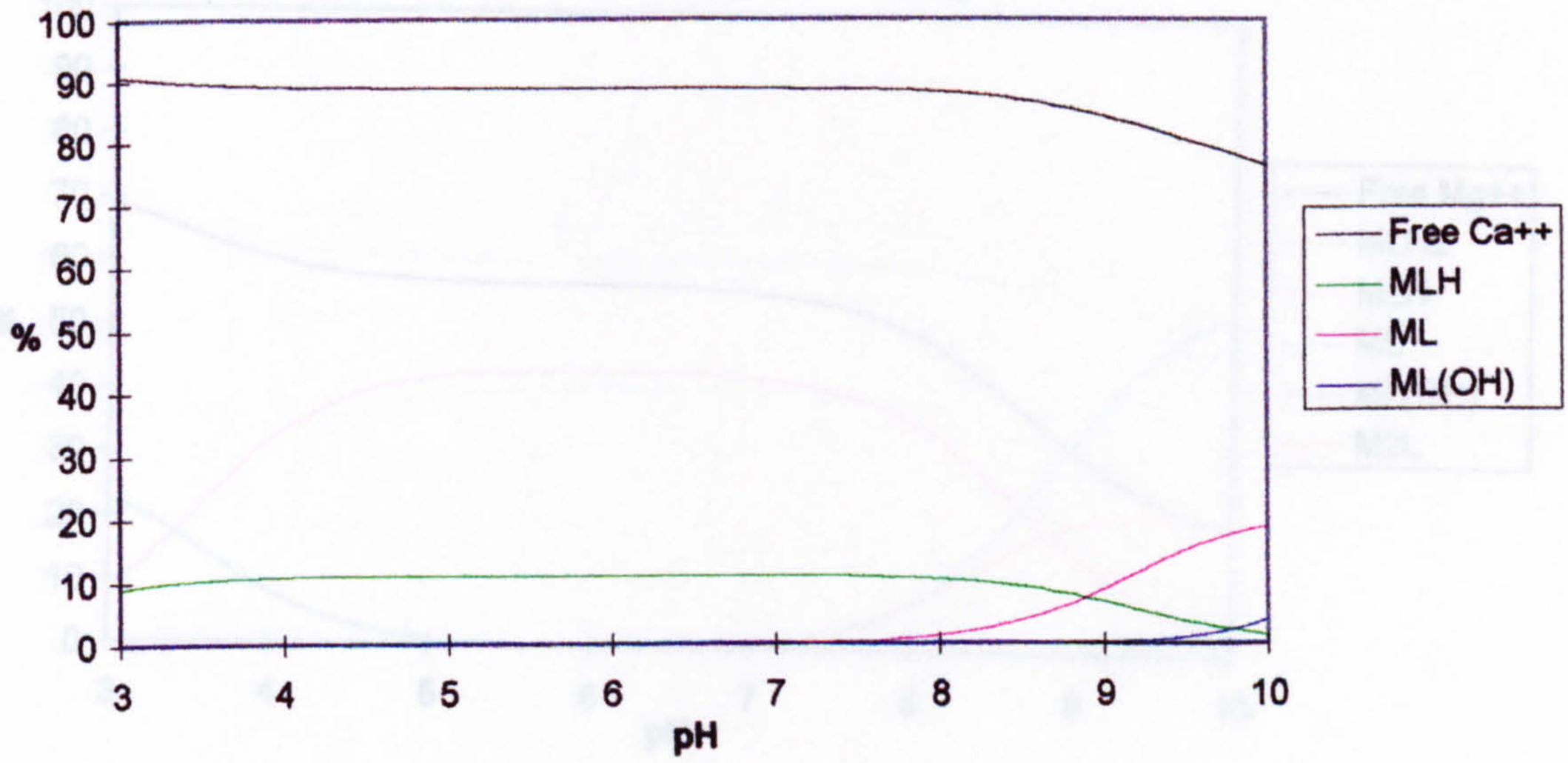

Fig 9.22a Mg ISE Response to pH Change of Mg-Aspartate

(C_{Mg} = 10 mmol/L, C_{Asp} = 20 mmol/L, C_{HCl} = 30 mmol/L, C_{NaCl} = 150 mmol/L)

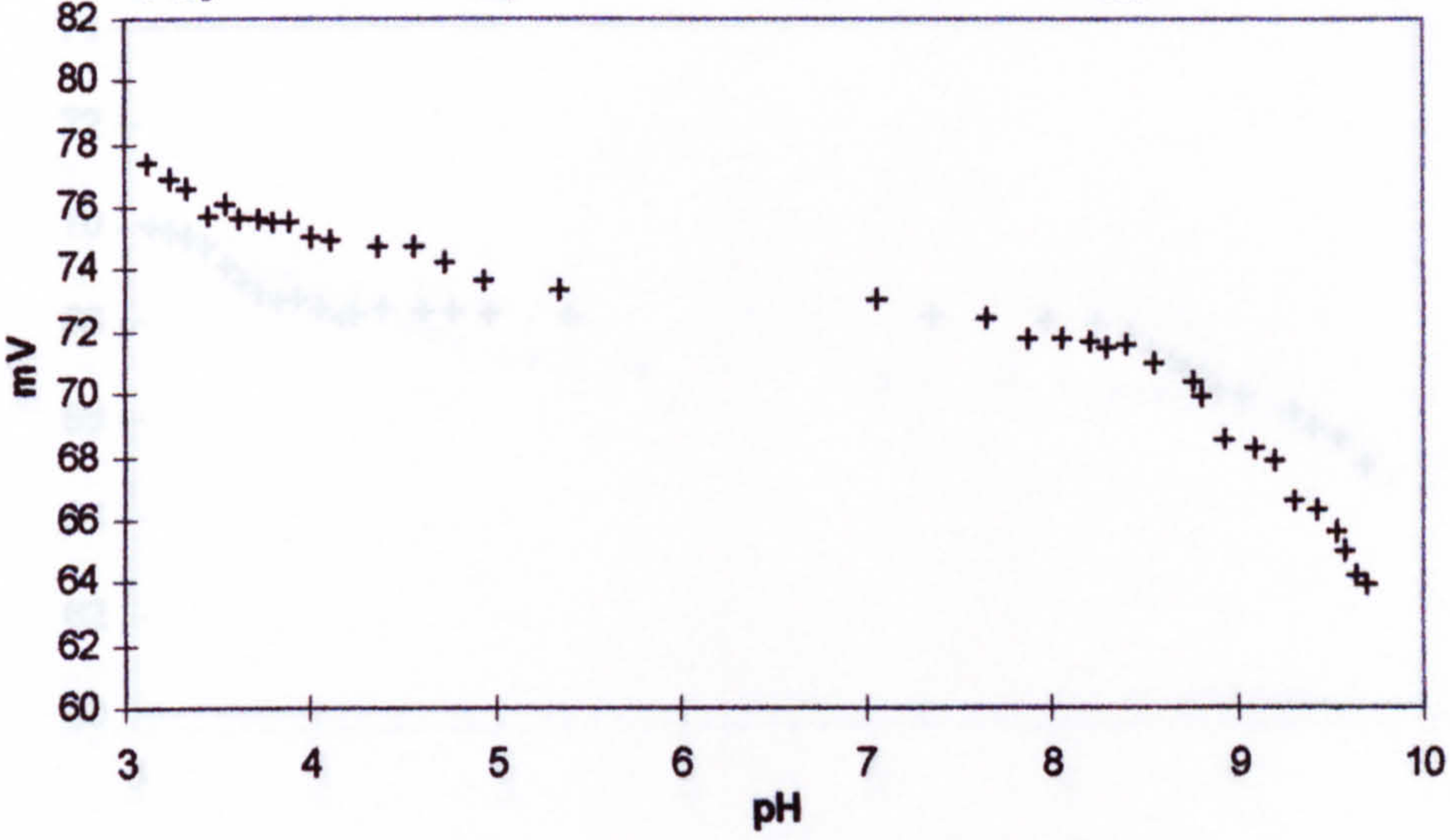

Fig. 9.22b Distribution of Mg between its Aspartate Complexes

(C_{Mg} = 10 mmol/L, C_{Asp} = 20 mmol/L)

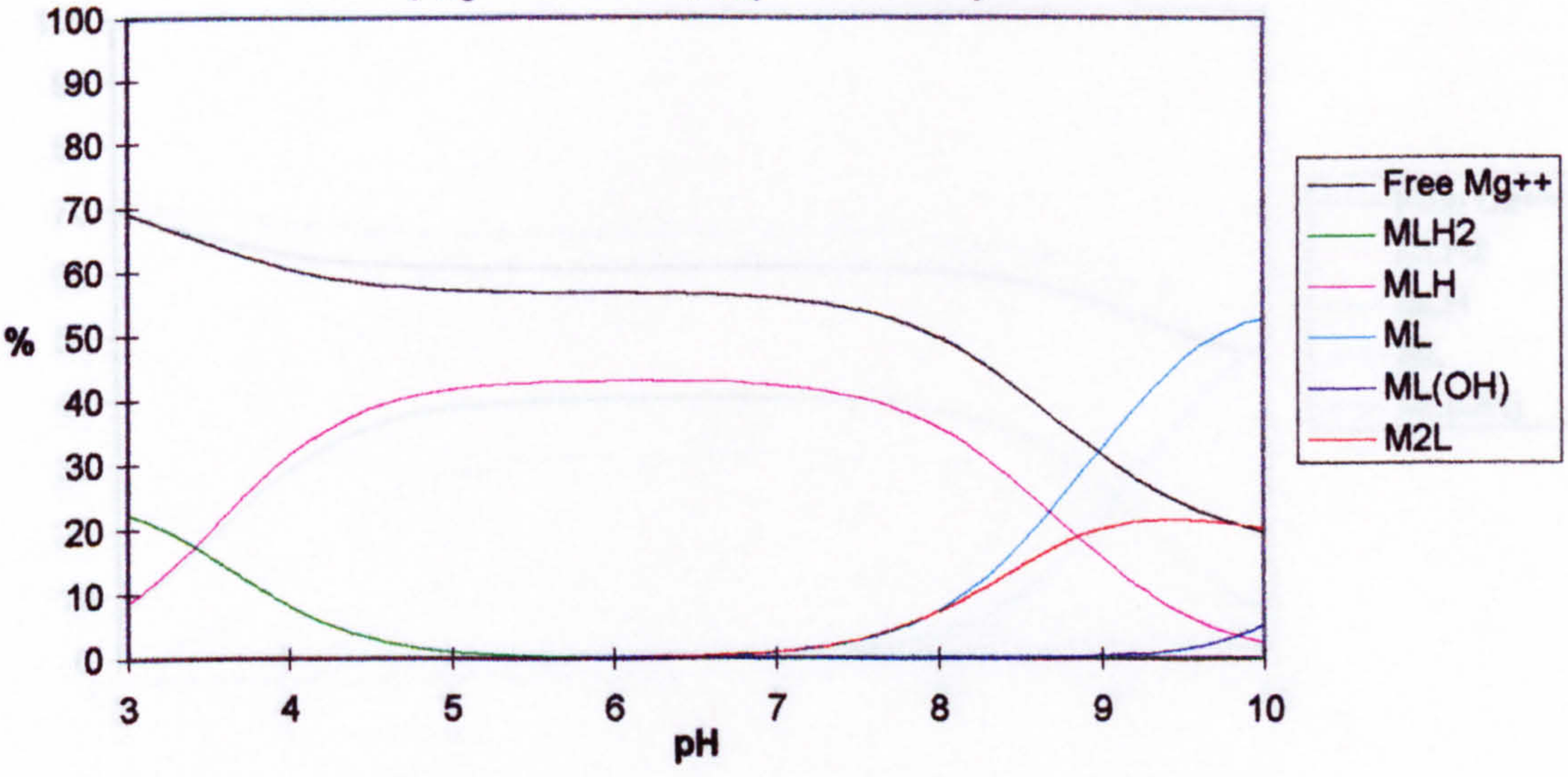

Fig 9.23a Ca ISE Response to pH Change of Ca-Aspartate

(C_{Ca} = 10 mmol/L, C_{Asp} = 20 mmol/L, C_{HCl} = 30 mmol/L, C_{NaCl} = 150 mmol/L)

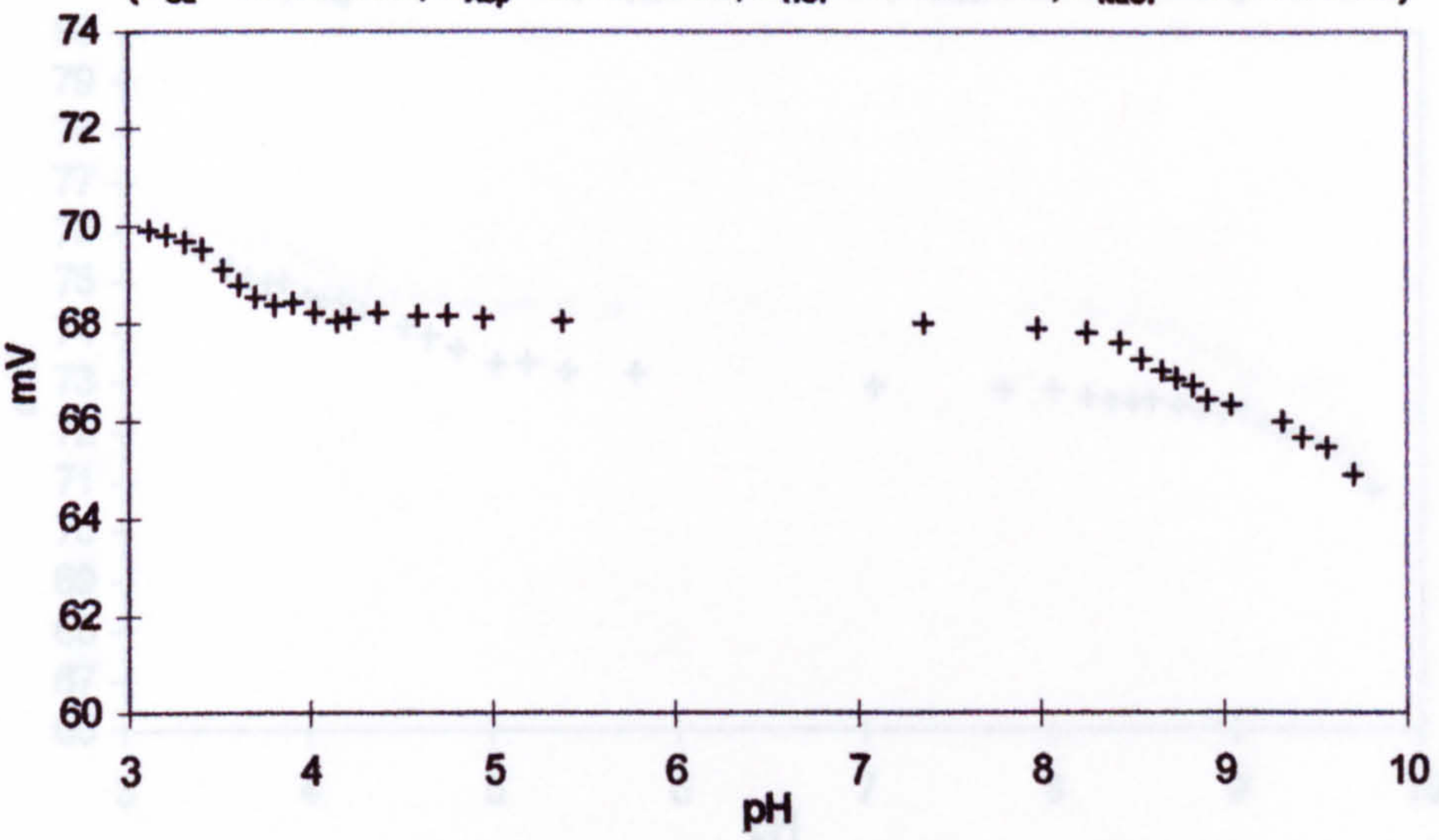

Fig. 9.23b Distribution of Ca between its Aspartate Complexes

(C_{Ca} = 10 mmol/L, C_{Asp} = 20 mmol/L)

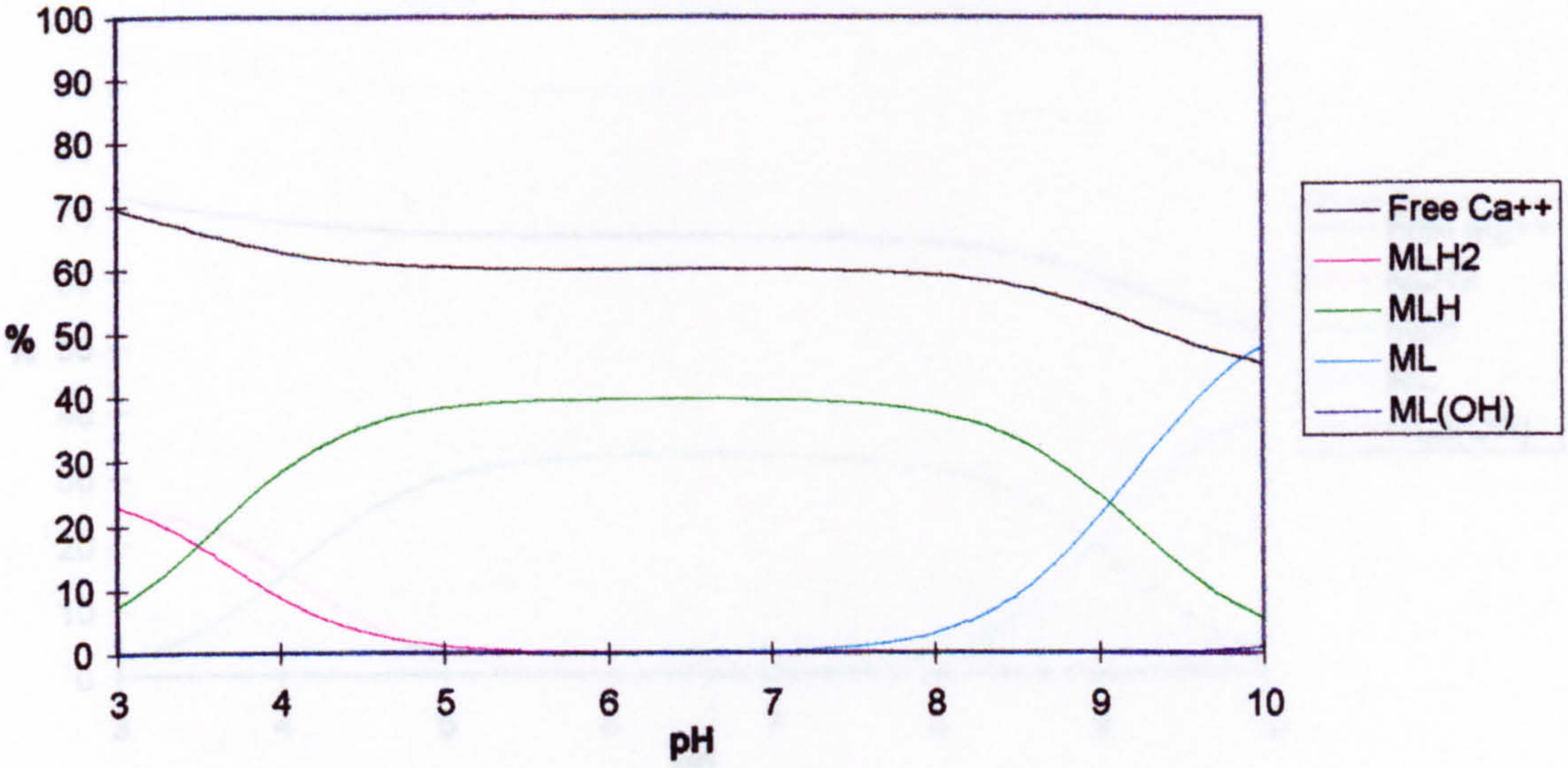

Fig 9.24a Mg ISE Response to pH Change of Mg-Glutamate
(C_{Mg} = 10 mmol/L, C_{Glu} = 20 mmol/L, C_{NaCl} = 150 mmol/L)

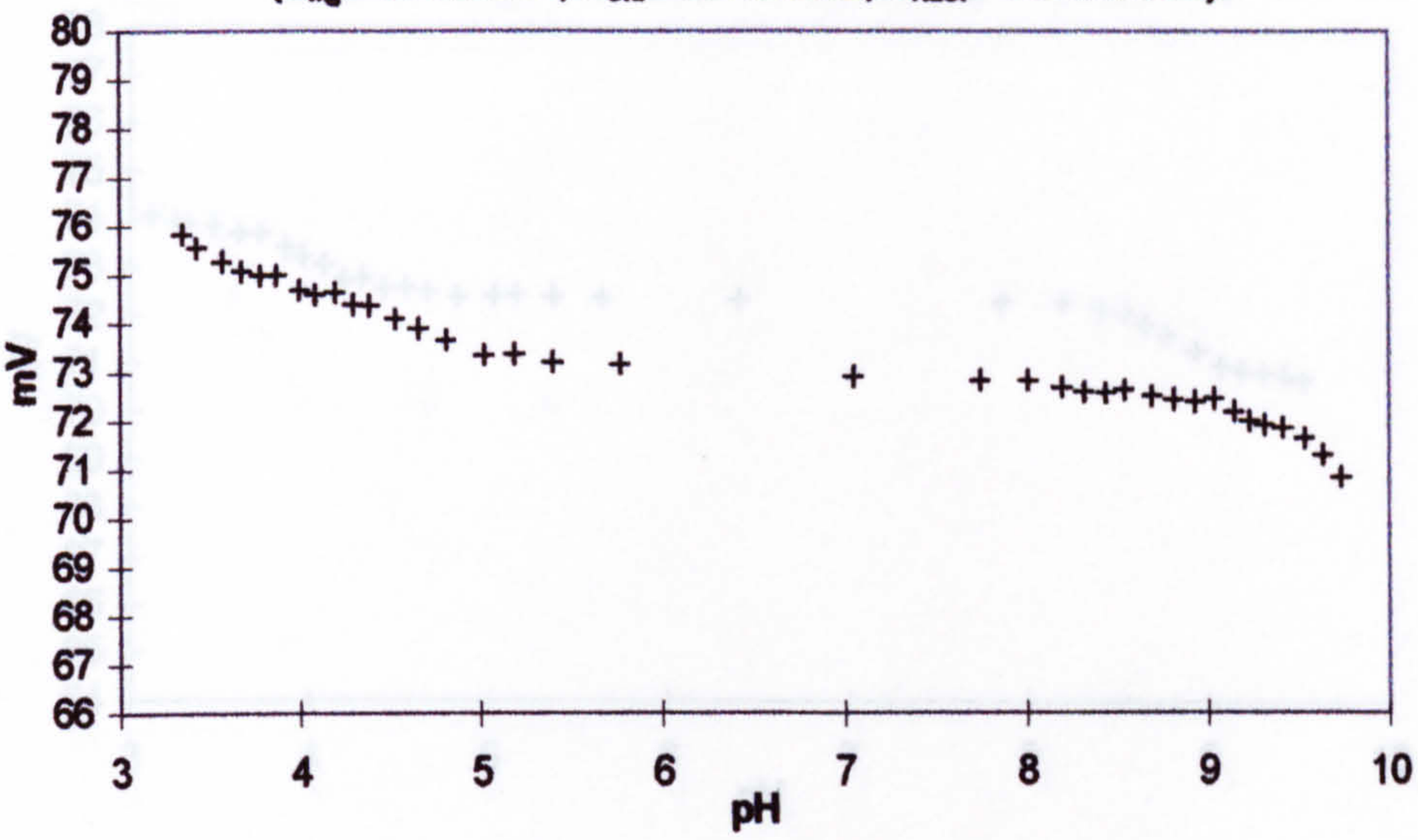

Fig. 9.24b Distribution of Mg between its Glutamate Complexes
(C_{Mg} = 10 mmol/L, C_{Glu} = 20 mmol/L)

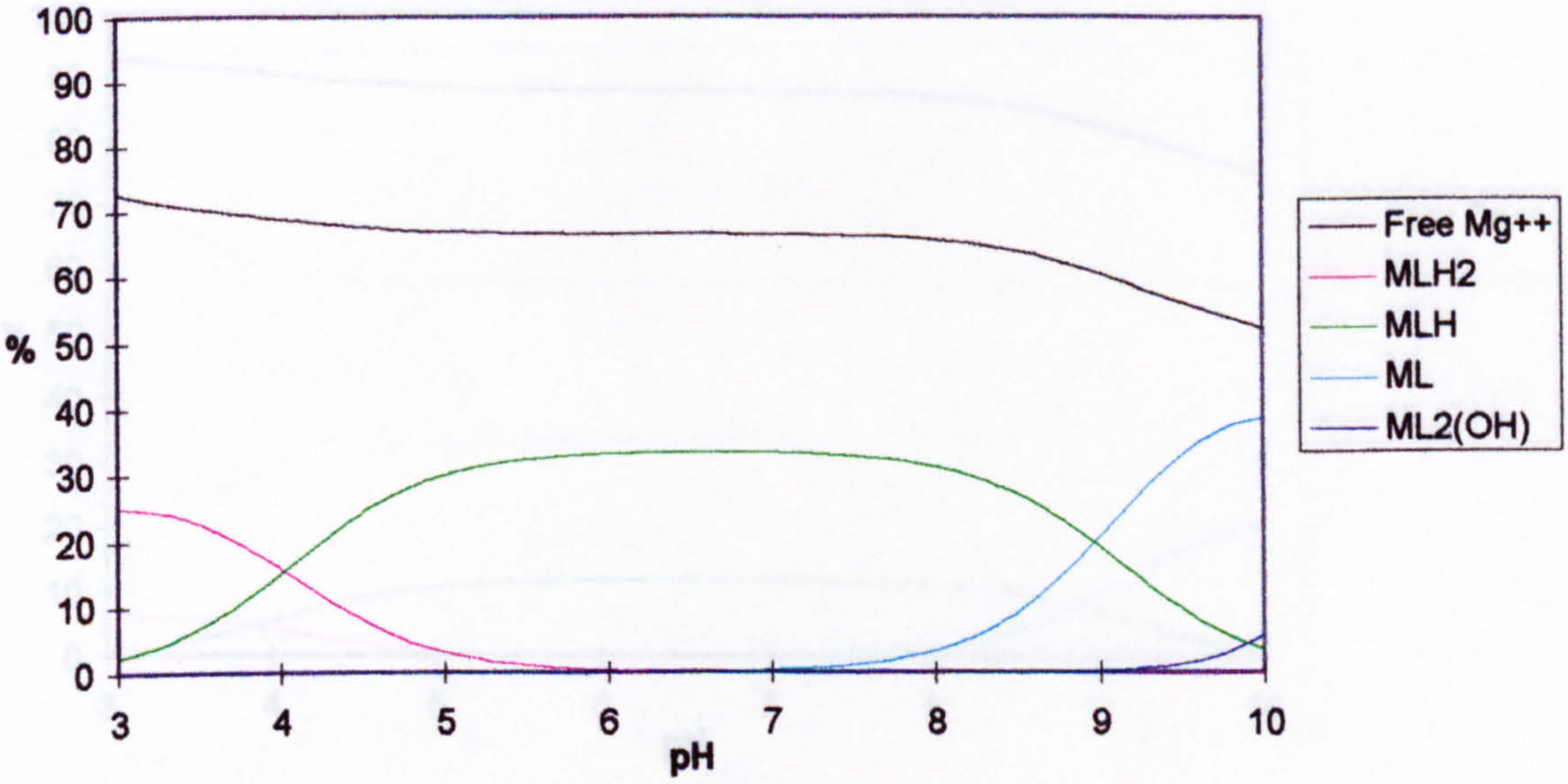

Fig 9.25a Ca ISE Response to pH Change of Ca-Glutamate
(C_{Ca} = 10 mmol/L, C_{Glu} = 20 mmol/L, C_{NaCl} = 150 mmol/L)

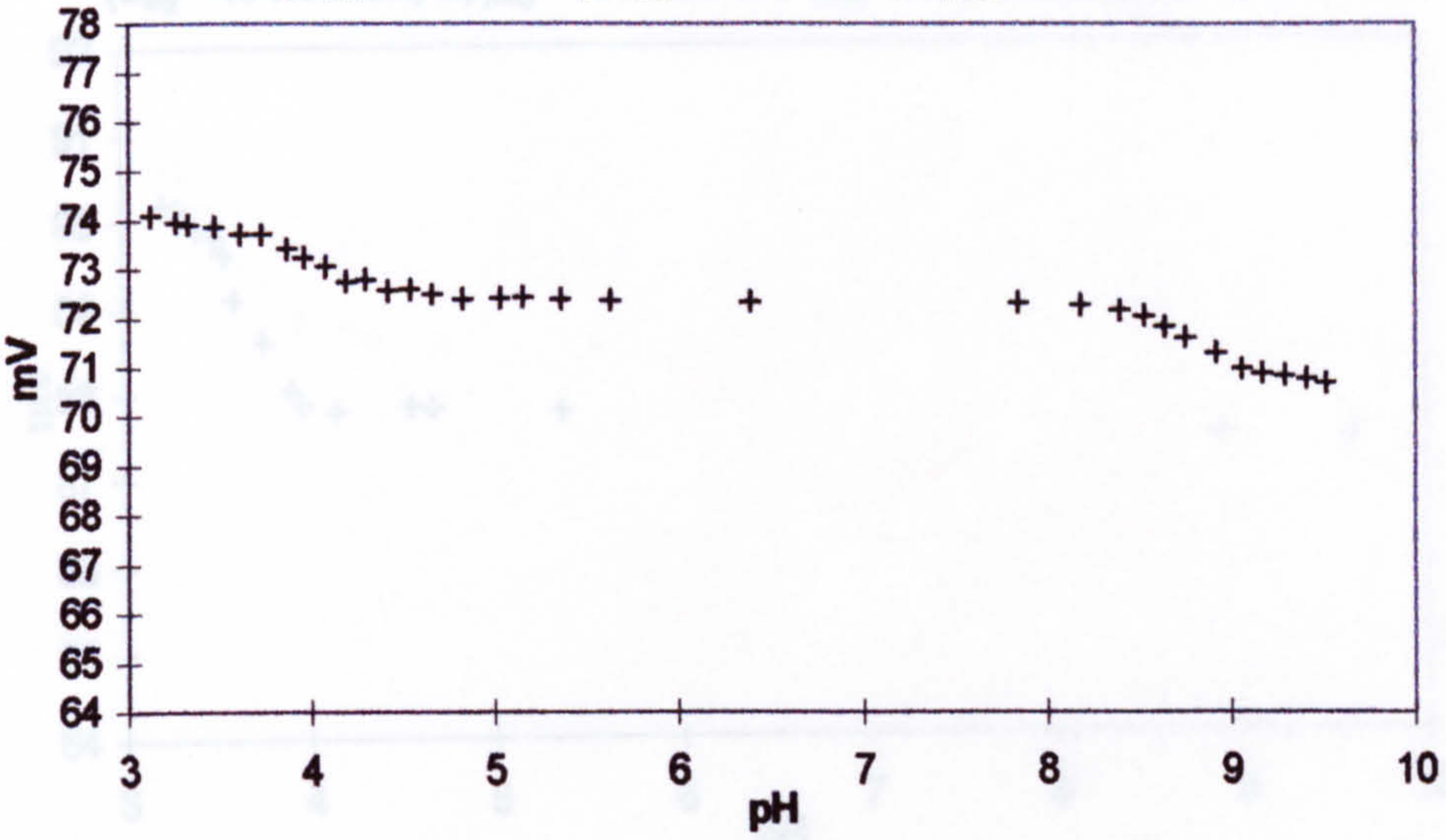

Fig. 9.25b Distribution of Ca between its Glutamate Complexes
(C_{Ca} = 10 mmol/L, C_{Glu} = 20 mmol/L)

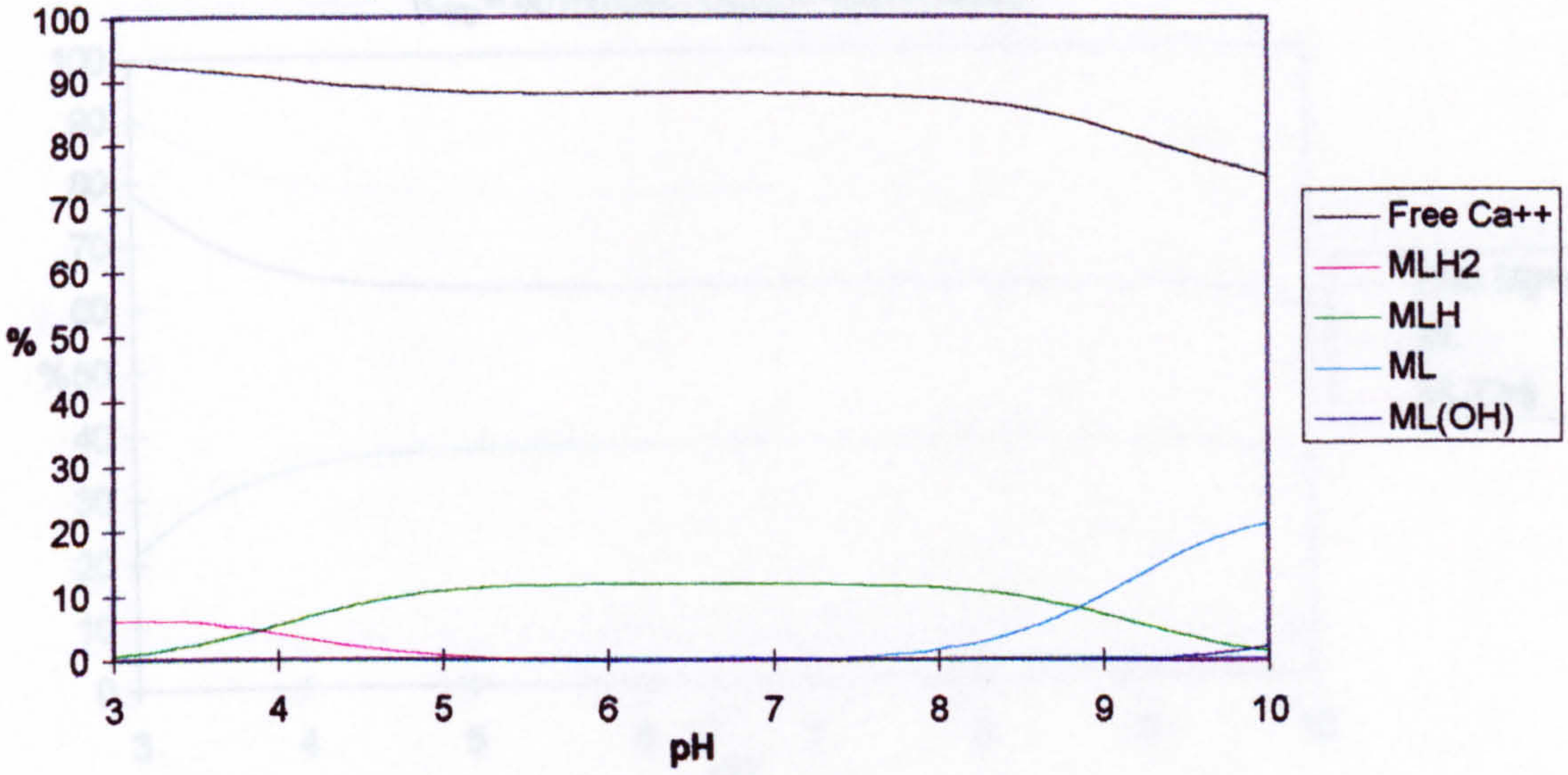

Fig. 9.26a Mg ISE Response to pH Change of Mg-Pyroglutamate
(C_{Mg} = 40 mmol/L, C_{Pyrog} = 100 mmol/L, C_{HCl} = 1 mmol/L, C_{NaCl} = 150 mmol/L)

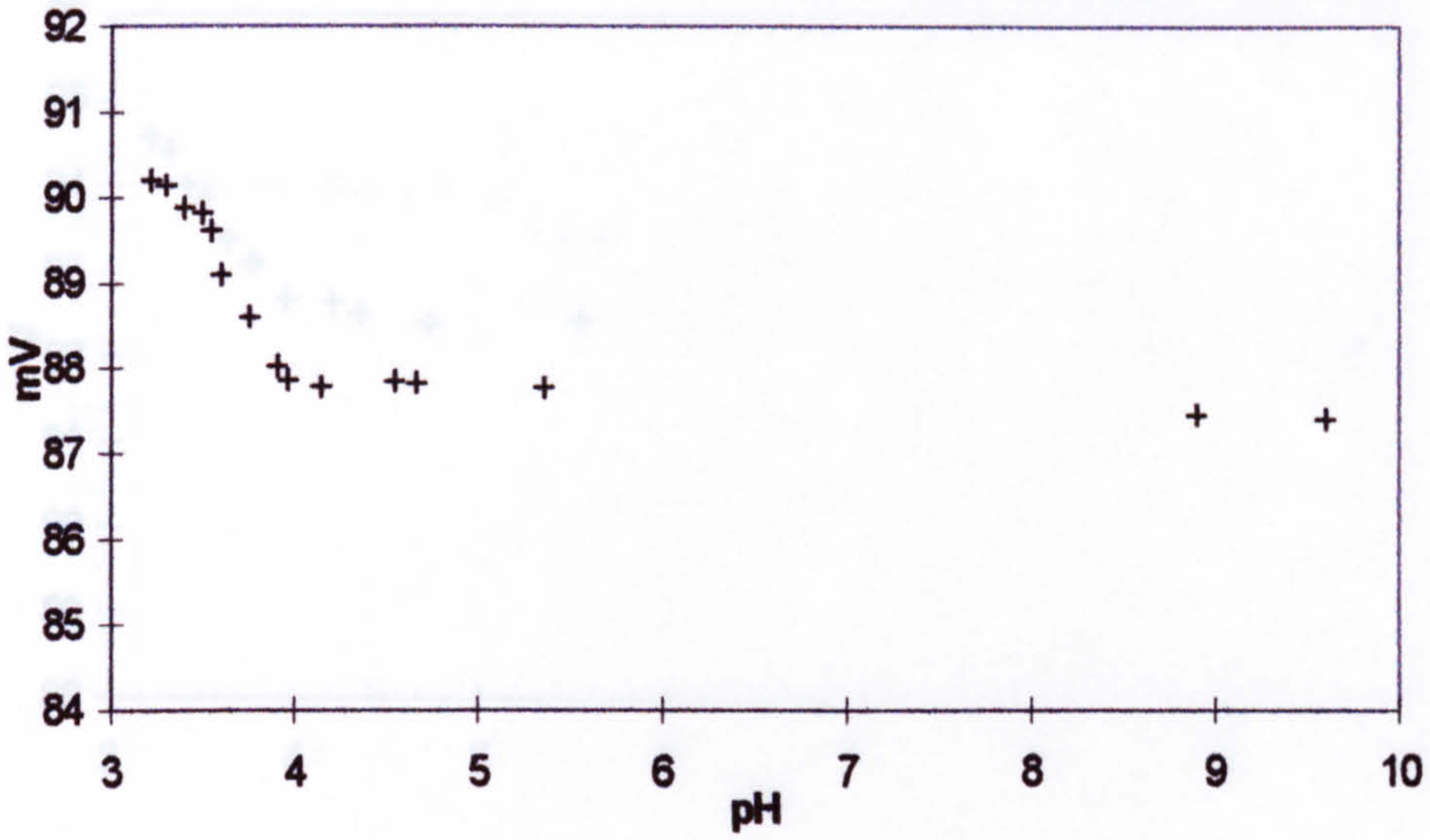

Fig. 9.26b Distribution of Mg between its Pyroglutamate Complexes
(C_{Mg} = 40 mmol/L, C_{Pyrog} = 100 mmol/L)

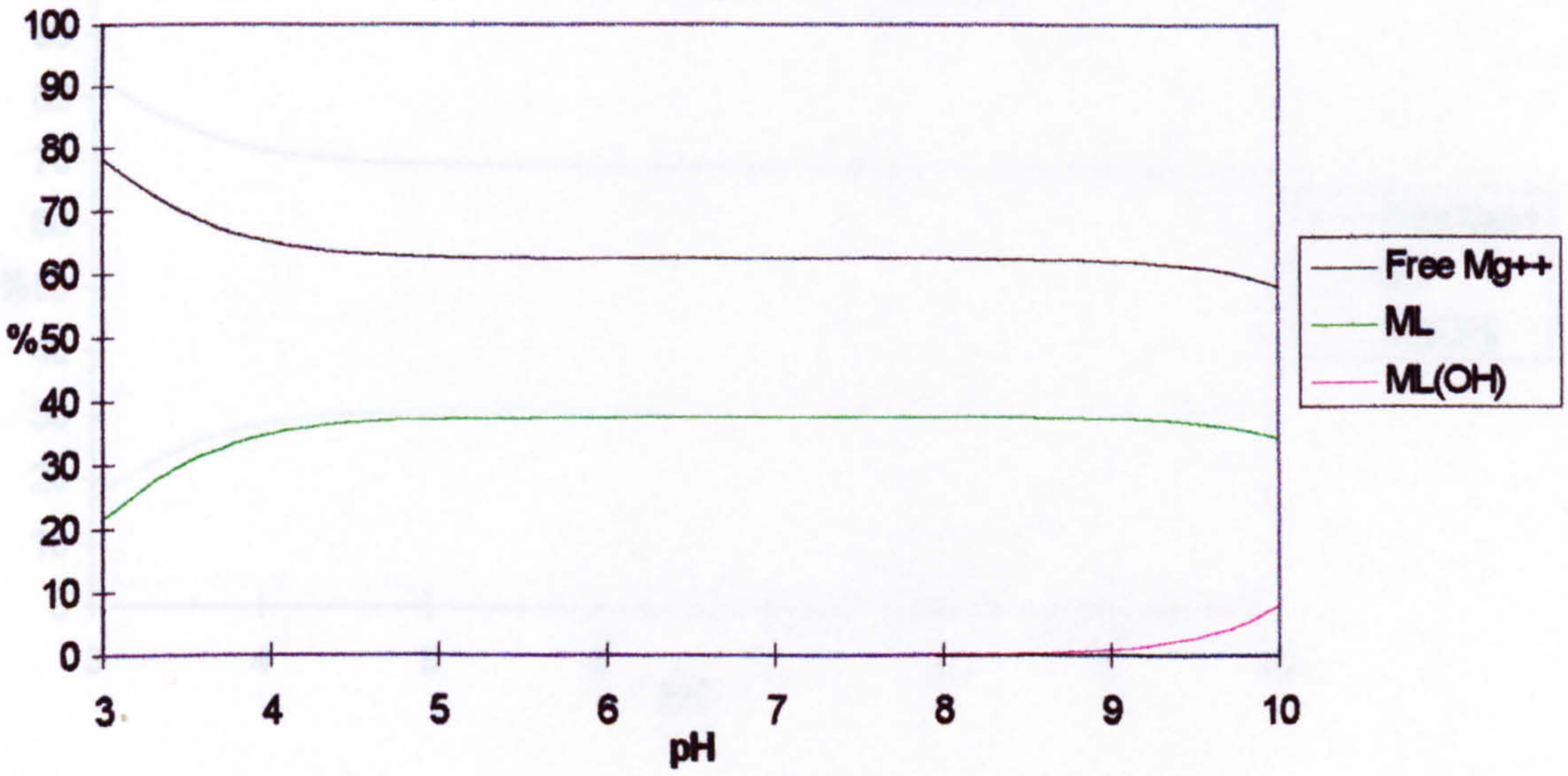

Fig. 9.27a Ca ISE Response to pH Change of Ca-Pyroglutamate
(C_{Ca} = 40 mmol/L, C_{Pyrog} = 100 mmol/L, C_{HCl} = 1 mmol/L, C_{NaCl} = 150 mmol/L)

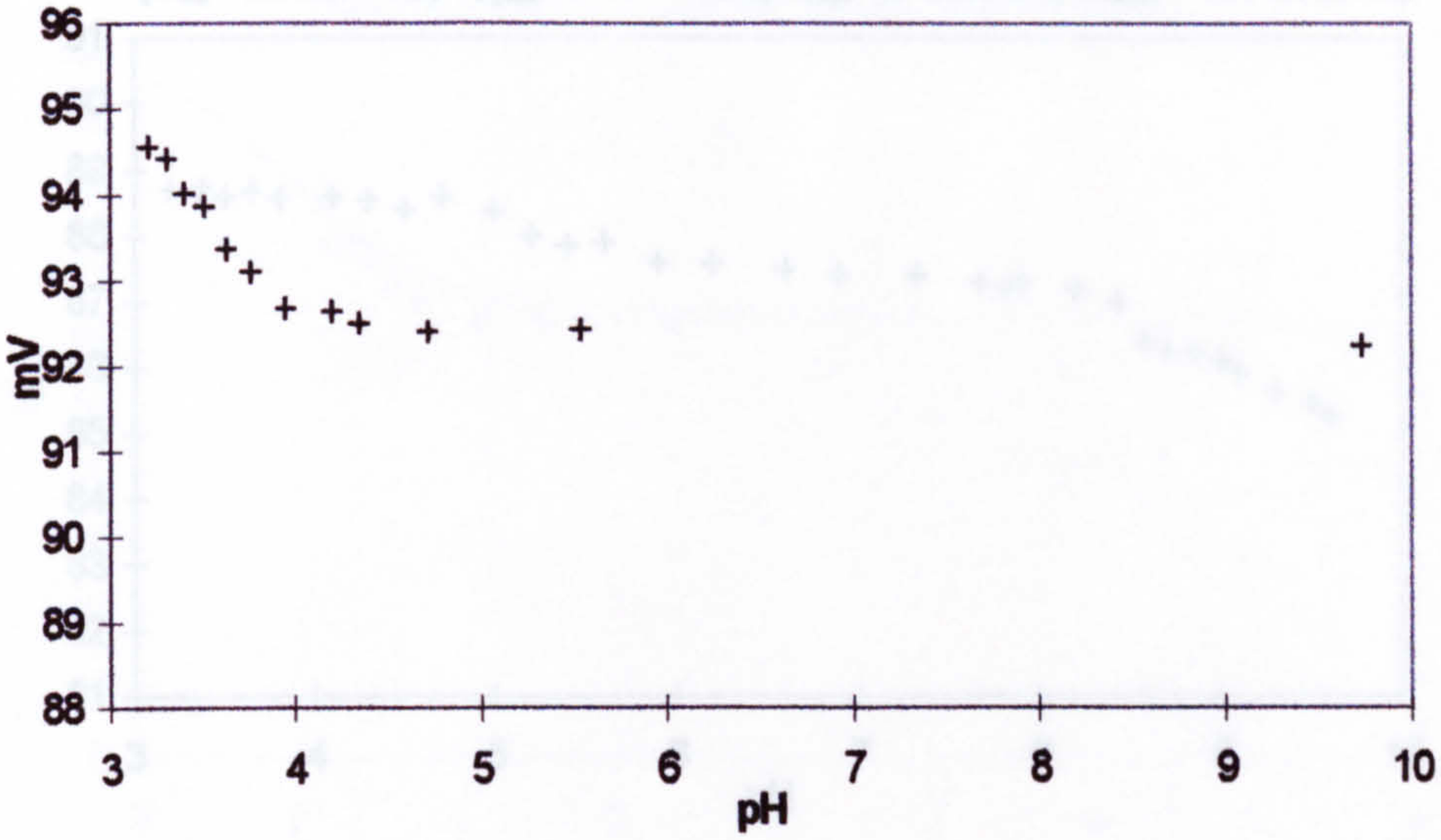

Fig. 9.27b Distribution of Ca between its Pyroglutamate Complexes
(C_{Ca} = 40 mmol/L, C_{Pyrog} = 100 mmol/L)

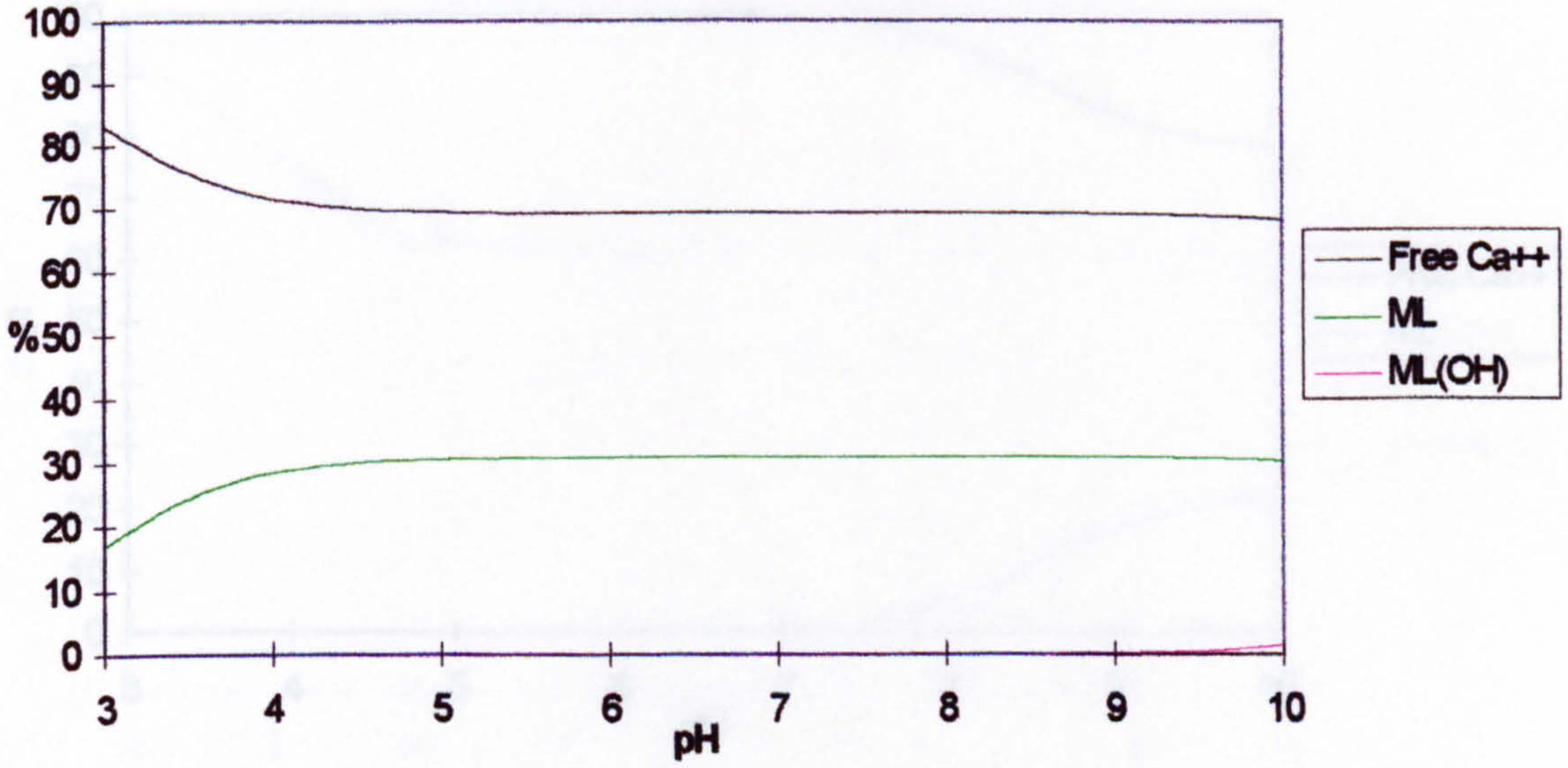

Fig. 9.28a Ca ISE Response to pH Change of Ca-Pyridoxine
(C_{Ca} = 20 mmol/L, C_{Pyrid} = 80 mmol/L, C_{HCl} = 5 mmol/L, C_{NaCl} = 150 mmol/L)

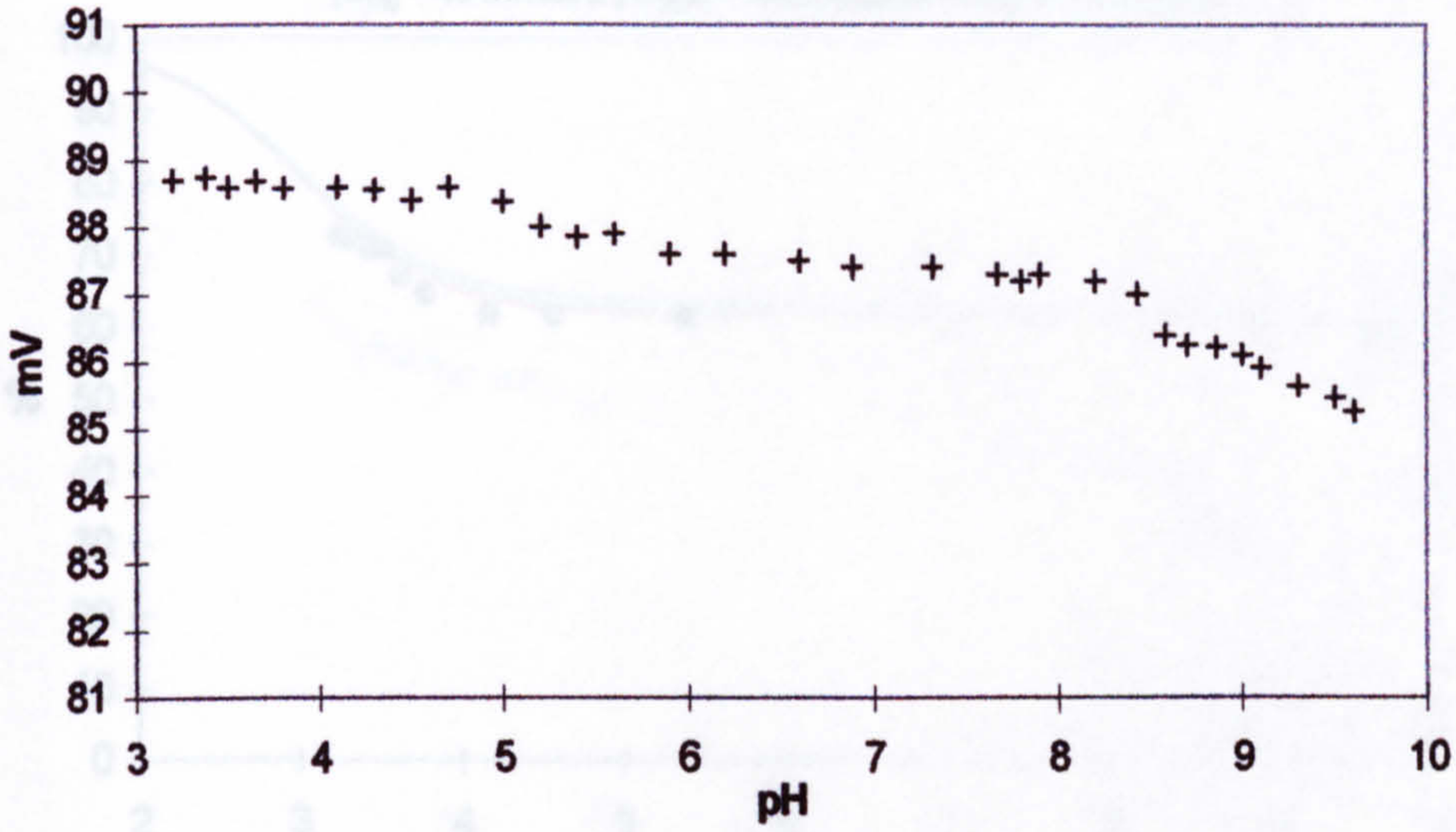

Fig. 9.28b Distribution of Ca between its Pyridoxine Complex
(C_{Ca} = 20 mmol/L, C_{Pyrid} = 80 mmol/L)

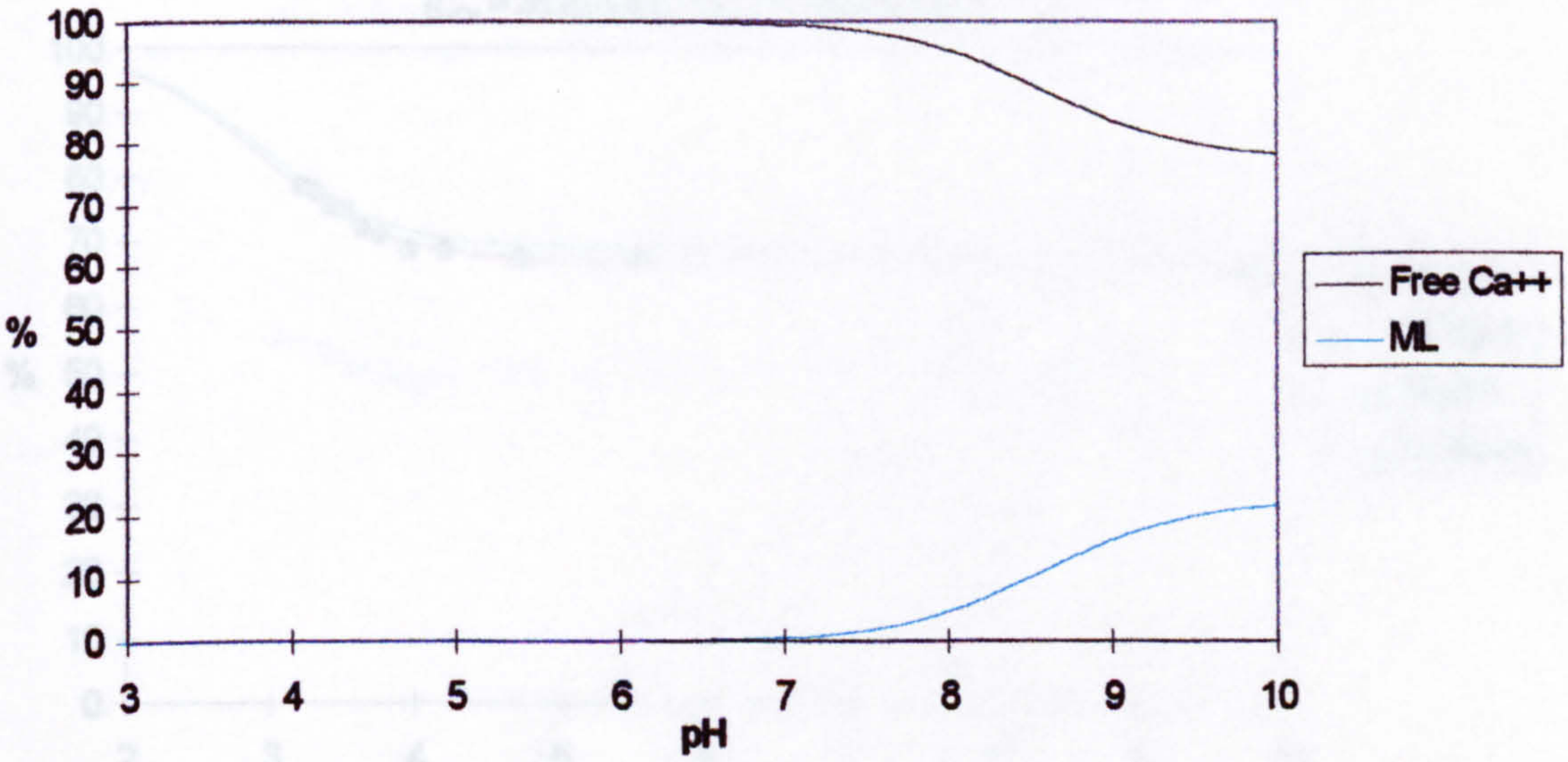

Fig. 9.29 Distribution of free Mg as a function of pH for Mg-pyroglutamate
(C_{Mg} = 40 mmol/L , C_{pyro} = 100 mmol/L , C_{HCl} = 1 mmol/L)

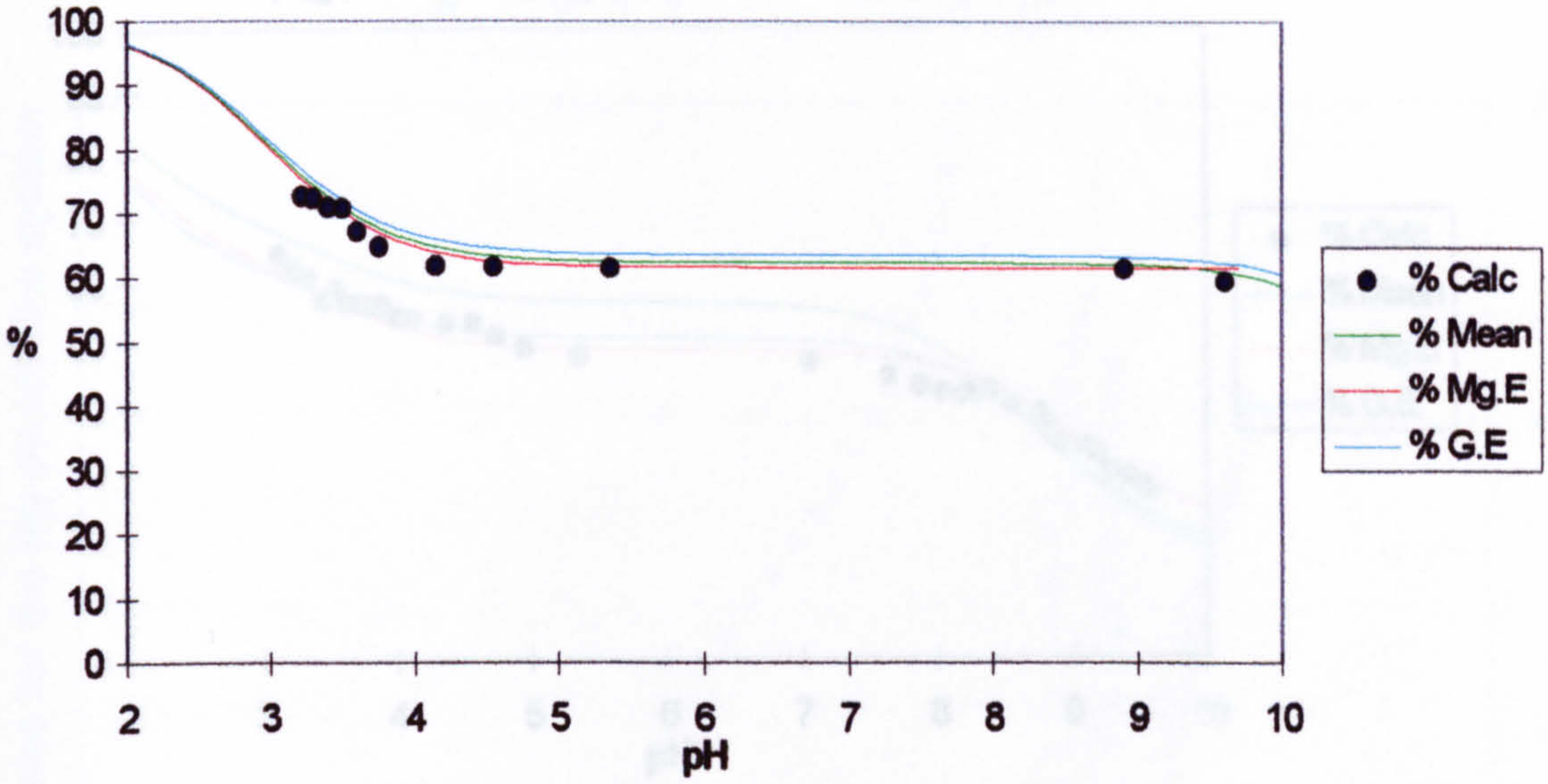

Fig. 9.30 Distribution of free Ca as a function of pH for Ca-pyroglutamate
(C_{Ca} = 40 mmol/L , C_{pyro} = 100 mmol/L)

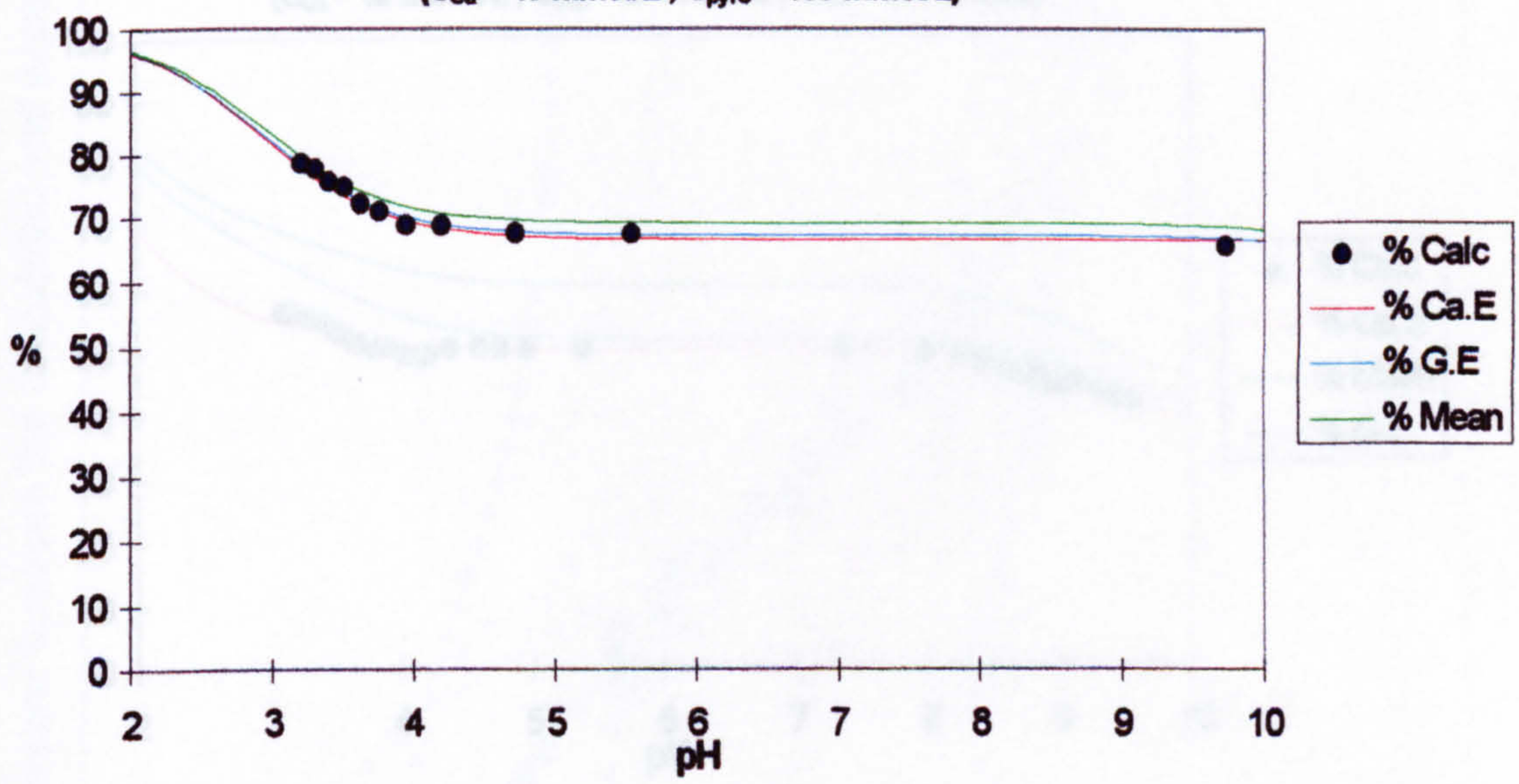

Fig. 9.31 Distribution of free Mg as a function of pH for Mg-aspartate
(C_{Mg} = 10 mmol/L , C_{asp} = 20 mmol/L , C_{HCl} = 30 mmol/L)

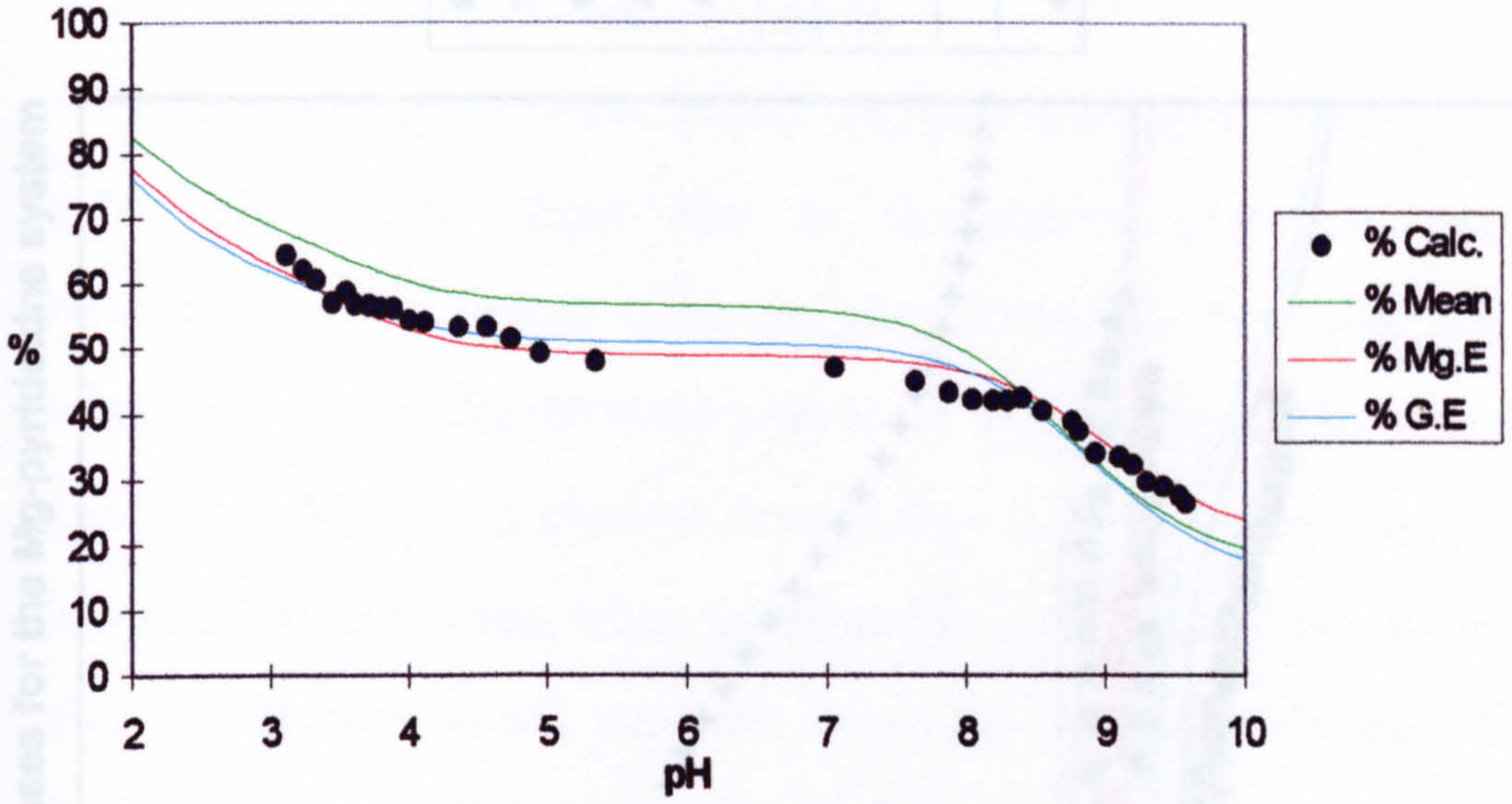

Fig. 9.32 Distribution of free Ca as a function of pH for Ca-aspartate
(C_{Ca} = 10 mmol/L , C_{asp} = 20 mmol/L , C_{HCl} = 30 mmol/L)

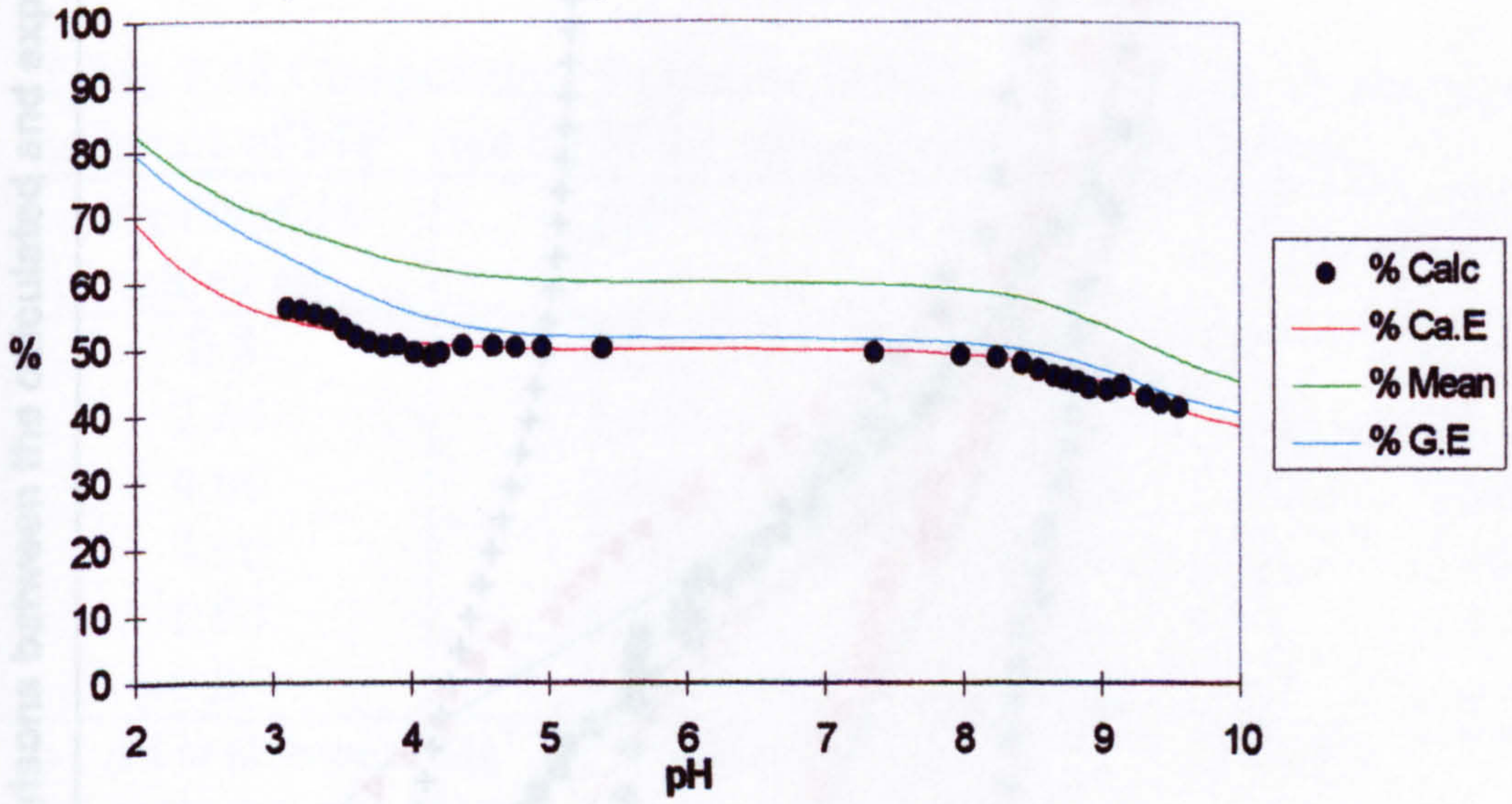

Fig. 9.33 Comparisons between the calculated and experimental mV responses for the Mg-pyridoxine system

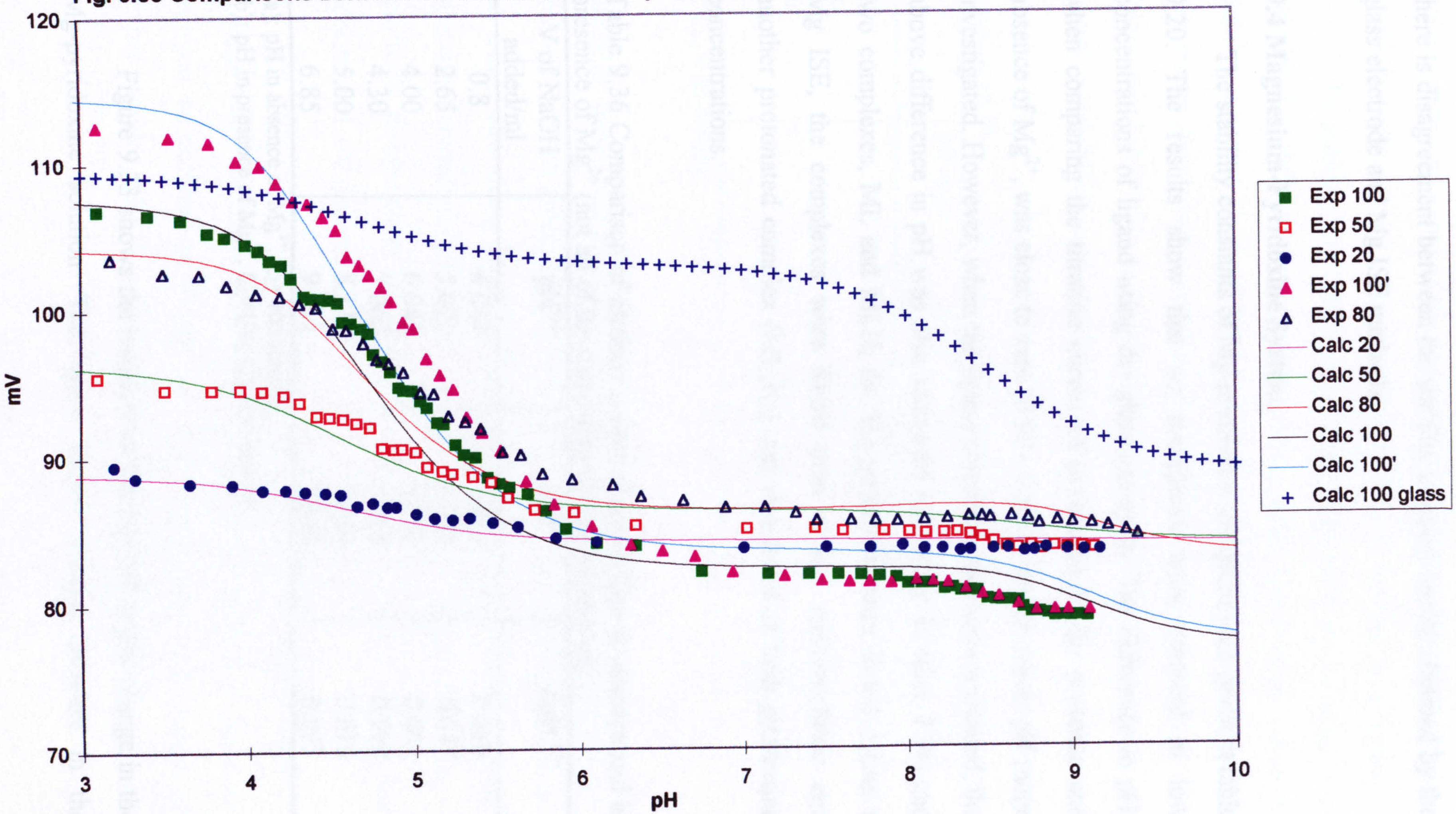

there is disagreement between the stability constant results obtained by the glass electrode and Mg ISE methods.

9.4 Magnesium-Pyridoxine System.

The stability constants of Mg-pyridoxine complexes are given in table 9.20. The results show that no complexes were detected at low concentrations of ligand using the glass electrode. The difference in pH, when comparing the titration curves of pyridoxine in the presence and absence of Mg^{2+}, was close to zero (0.00 ~ 0.03) over the whole pH range investigated. However, when the ligand concentrations were increased, the above difference in pH was also increased (as shown in table 9.36) and two complexes, ML and MLH, for Mg-pyridoxine were found. Using a Mg ISE, the complexes were found even at low concentrations and another protonated complex (ML_3H_3) was also found at high pyridoxine concentrations.

Table 9.36 Comparison of titration curves of pyridoxine in absence and in presence of Mg^{2+} (not all of the experimental data are shown).

V of NaOH added/ml	$pH^{(a)}$	$pH^{(b)}$	ΔpH^{a-b}
0.8	4.042	4.023	0.019
2.65	5.022	4.985	0.037
4.00	6.042	5.999	0.043
4.30	7.062	6.964	0.098
5.00	8.110	8.034	0.076
6.85	9.061	8.988	0.073

(a): pH in absence of Mg^{2+}, C_L=100 mmol/L
(b): pH in presence of Mg^{2+}, C_L=100, C_{Mg}=20 mmol/L

Figure 9.33 shows the response of the Mg ISE to pH change in the Mg-pyridoxine solution. The figure shows a large decrease in the

potentiometric response of the Mg ISE in the pH region 3-6. The decrease in mV becomes greater when the concentration of the ligand is increased.

The species distribution diagrams for Mg-pyridoxine system were calculated at different ligand concentrations using the average values of stability constant obtained from the glass electrode. From the free Mg percentage distribution curves, the decrease in mV of the Mg ISE was calculated. Table 9.37 contains a comparison between the calculated and experimental mV decrease (ΔE).

Table 9.37.(*)

C_L (mmol/L)	pH range: 3.2-6		3.2-9	
	$\Delta E_{calc.}$	$\Delta E_{exp.}$	$\Delta E_{calc.}$	$\Delta E_{exp.}$
20	0.84	4.6	3.4	5.2
50	2	8.5	7.6	11.6
80	3.1	16	11	18.5
100	3.8	22.2	13	26.3

(*) C_{Mg} = 20 mmol/L.

The table shows that for each ligand concentration, the experimental mV decrease is much greater than that calculated, and the difference between the ΔE_{calc} and ΔE_{exp} becomes greater at high ligand concentrations, especially between pH 3.2 and 6. At C_L=100 mmol/L, figure 9.33 shows a significant disagreement between the calculated (Calc 100 glass) and experimental mV decreases.

The large decrease in mV of the Mg ISE results in a higher value of log β_{MLH} being obtained with the Mg ISE than that obtained with the glass electrode, as occurred at 20 and 50 mmol/L pyridoxine, or formation of another complex, ML_3H_3, which was found only in the case of high ligand

concentrations. The value of log β_{ML} at high concentrations was also higher.

Protonation and deprotonation reactions for pyridoxine are [69]:

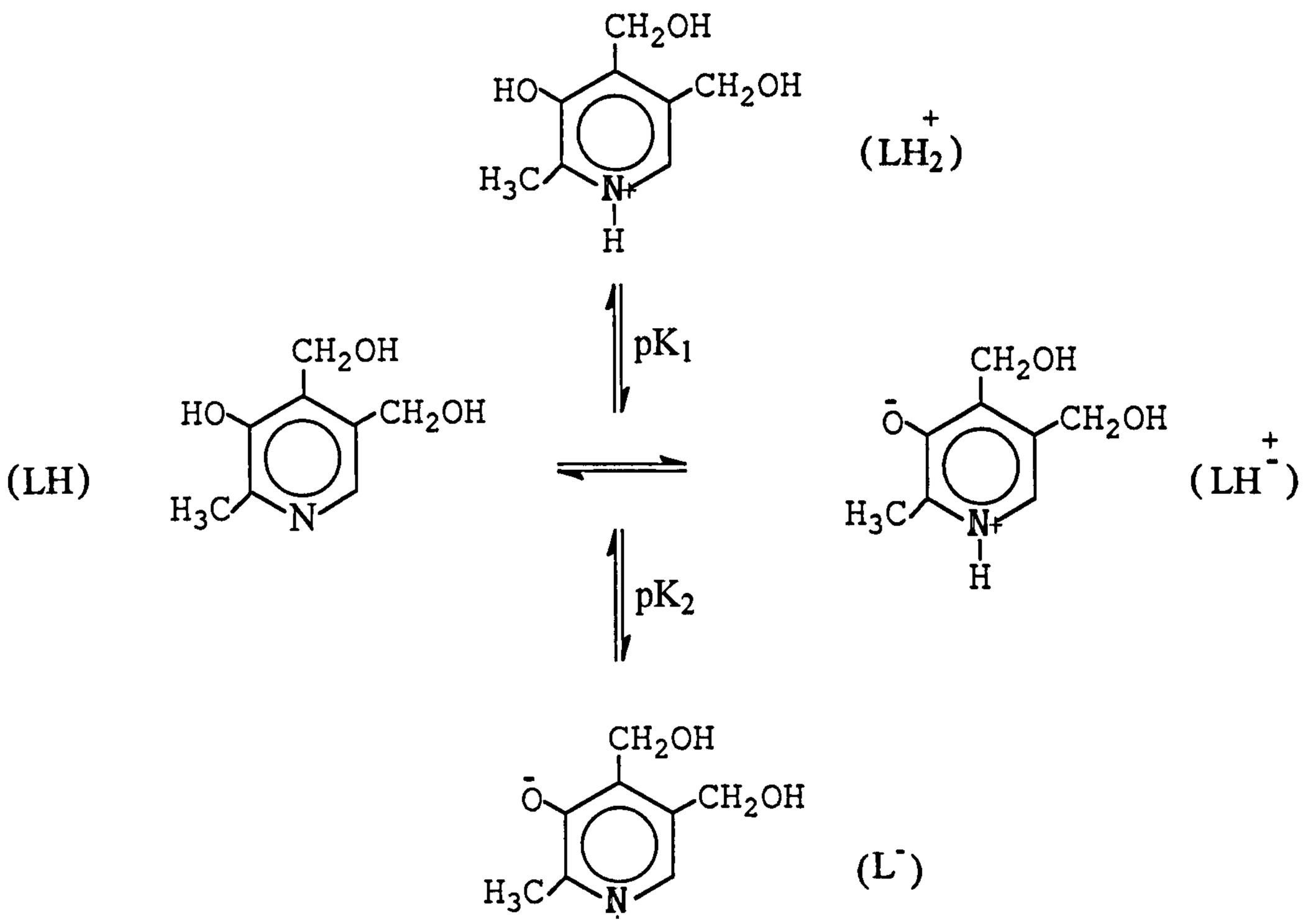

At neutral pH, the zwitterionic form ($LH^{\pm}$) predominates over the non-dipolar form (LH).

Possible explanations of the disagreement in the values of stability constants obtained with pH and Mg electrodes at high pyridoxine concentration are that the large decrease in the potentiometric response of the Mg ISE might occur due to:

-the LH_2^+ ion acting as an interferent ion on the response of the Mg ISE to Mg^{2+}. As the pH is increased, the concentration of LH_2^+ decreases (see figure 9.13) so if the membrane responds to LH_2^+, the emf will decrease with increasing pH.

-an effect on the Mg^{2+} activity and liquid junction potential (omitted from equation 9.1) due to the changing composition of the solution as pH is increased. The electrostatic interaction forces between Mg^{2+} and other ions present in the solution become greater at high ligand concentrations and vary more with changes in the composition of the solution. The background electrolyte concentration (0.15 mol/L) is too small at C_L=100 mmol/L to keep activity and liquid junction potential constant. The existence of the MLH complex in the Mg-pyridoxine system may play a major role in this as in the case of the Ca-pyridoxine system the MLH complex was not formed and the Ca ISE did not show the large emf decrease.

Thus the apparent existence of an ML_3H_3 complex for Mg-pyridoxine may be spurious.

9.5 The Nature of the Metal-Ligand Coordination.

In order to determine the nature of the metal ligand coordination, the stability constants of the complexes of the metal ions with amino acids and hydroxy acids obtained in this work were compared with the metal-ligand complexation constants for corresponding acids found previously. Table 9.38 gives the formula of these acids and their formation constants with magnesium and calcium ions.

An X-ray diffraction study of crystals of magnesium citrate decahydrate [57] has shown that the hydroxy group of the citrate is involved in the chelation of magnesium ions and that citrate acts as a tridentate ligand with one five-membered and one six-membered ring respectively, the hydroxyl being common to both rings. The values obtained for the stability constants of metal citrate complexes were found to be higher than those of

Table 9.38. Stability Constant of Magnesium and Calcium Complexes.

Ligand	Formula (acid form)	Metal	log K_{ML}	log K_{MLH}	log K_{MLH_2}	Temp. (°C)	Medium (Conc. in mol/L)	Ref.
Tricarballylic-acid	$HOOCCH(CH_2COOH)_2$	Mg Ca	2.06 2.17	1.20 1.46	0.77 0.88	20	0.1 $NaClO_4$	18
Acetic Acid	CH_3COOH	Mg Ca Ca	0.55 0.57 0.59			25 25	0.16 $R_4N.X$ 0.15 KNO_3	53 54
Succinic acid	$HOOCCH_2CH_2COOH$	Mg Ca	1.0 0.95	0.58		25 25	0.07 0.15 KNO_3	55 54
Pyridine	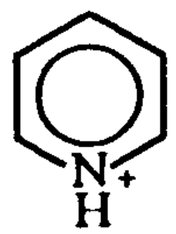	Mg Ca	-0.42 -0.45			25	1.0 KCl	56

tricarballylic acid ($HOOCCH(CH_2COOH)_2$). The chelate structure mentioned above may be responsible for this.

Davies [58] found that lactate and glycine have a stronger tendency to associate with the calcium ion in aqueous solution than does acetic acid. He therefore suggested a chelate structure (I) for lactate and (II) for glycinate

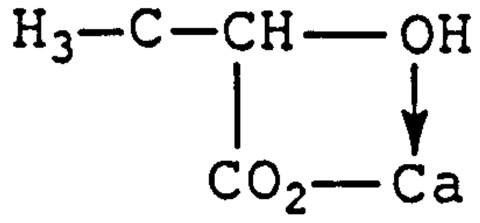

I

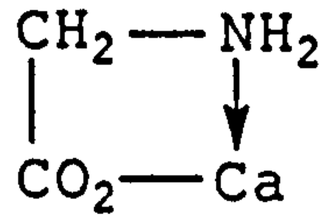

II

The values of log β_{ML} for calcium lactate and glycinate in this work agree with Davies's findings in that they were found to be higher than log β_{ML} for calcium acetate. The crystal structures of calcium salts of α-hydroxy acids [59] and α-amino acids [60] confirm Davies's prediction that α-hydroxy acids use the oxygen atom of the α-hydroxy group, α-amino acids use the nitrogen atom of the α-amino group, and one oxygen atom from the carboxyl group to chelate calcium ions. Nitrogen-14 and ^{17}O n.m.r spectral measurements [78] also suggested that both the amino and carboxylate groups co-ordinate to Ca^{2+} within the complexes in the glycine system.

In the case of aspartate and glutamate, the results in the present work agree with those of Lumb and Martell [45] that the formation constants (log K_{ML}) of magnesium and calcium aspartates and glutamates are higher than those of succinate, and similar in magnitude to those for glycine. For this reason, these authors suggested the binding is only through the glycine-like part of the aspartate or glutamate ligand. The greater value of log β_{ML} (log K_{ML}) for aspartate may be due to the inductive effect of the negative carboxylate group in the β position (structure III) that increases

the basicity of the donor groups toward the metal ion and accordingly increases the stability of the aspartate chelate.

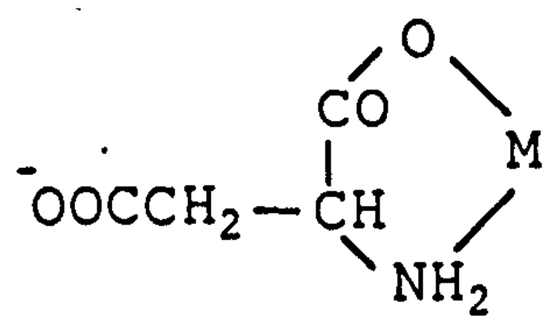

III Aspartate chelate

The crystal structure of Caglu.$3H_2O$ [60] supports the view of binding mentioned above, although possibly either amino acid could act as a tridentate ligand because the crystal structures of calcium proteins, many of which have very high ratios of aspartyl and glutamyl residues, show metal binding by the sidechain carboxylates of these amino acids [61].

For protonated complexes, Davies and Waind [47] found the formation constant of $CagluH^+$ corresponds better to a glutaric acid-like structure than a glycine-like one, a structure suggested by Schubert [30] even for the depronated complexes. The sequence of proton dissociation in the α-amino acids can give evidence about the type of coordination. The carboxylic groups undergo dissociation first, and only at pH values above 7 (see, for example, figure 9.7) does the proton from the amino group dissociate. Therefore, the formation of MLH corresponds to the protonation of the aminic group, i.e. the formation constants of MLH for glutamate and aspartate correspond to glutaric acid and succinic acid-like structures, respectively.

Regarding pyroglutamate, a common mode of coordination in the complexes of such amino-acids with heavy metal ions is through the amino and the carboxyl groups of the ligands, forming a stable five-membered chelate ring [62, 63]. However, Hung et al. [64] have suggested that the

carboxylate group in such ligands is the primary complexing group for magnesium and calcium. The type of the magnesium and calcium coordination to pyroglutamate might be indicated by comparing the values of the stability constant log β_{ML} for pyroglutamate complexes of magnesium and calcium with those of cyclopentyl carboxylate. If the values for log β_{ML} are significantly higher for pyroglutamate, this would suggest chelation involving the amino and carboxyl groups jointly.

In the case of mononuclear pyridoxine complexes, pyridoxine may act either as unidentate ligand and bind the metal ion through the pyridine nitrogen [65, 66], or as a bidentate ligand and chelate the metal ion through the phenolate oxygen and the adjacent hydroxy methyl group [67, 68] (structure IV). The values of the stability constant (log β_{ML}) of magnesium and calcium pyridoxine complexes obtained in this work were found to be much higher than those of pyridine, which suggests the same mode of chelation . A ^{13}C nmr study of metal ion binding to pyridoxine [69] has shown that the coordination of magnesium by pyridoxine is through the C-3 and C-4′ oxygens in aqueous solution. The coordination is shifted to nitrogen on addition of dimethylsulfoxide (DMSO).

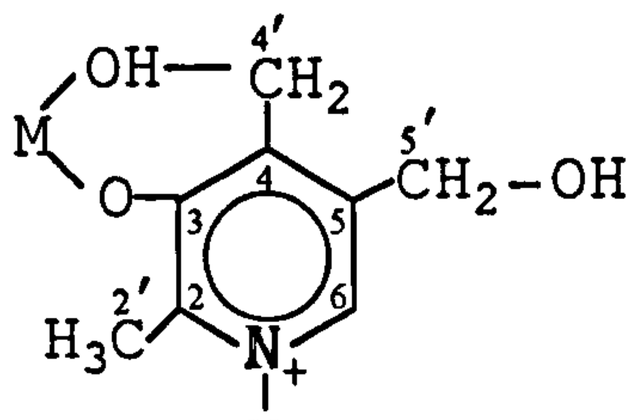

IV

9.6 Determination of the formation constants of magnesium and calcium HEPES.

9.6.1 Introduction.

In chapter 4 of part (I) of this work, the secondary calibration solutions for blood electrolyte measurements, used for determination of the concentrations of free magnesium ions with Mg ISEs, contain HEPES, [N-(2-hydroxyethyl)piperazine-N-ethanesulfonic acid] as a buffer. However, aminosulphonic acid compounds may complex with the free magnesium ions present in the calibration standards. This would mean that the concentration of free magnesium ions would no longer known accurately. For this reason, the formation constants of magnesium HEPES complexes have been evaluated. These values can then be used to correct measurements to account for the complexation of the magnesium ions with the buffer. The complexation constants of HEPES with calcium have also been determined for comparson with literature values.

The complex formation between magnesium and calcium and HEPES was investigated by Good et al. [70] using a pH titration method. They assumed that metals form a coordination bond with the amino nitrogen of the buffer and in so doing compete with protons. However, their results did not show any significant binding between magnesium or calcium and HEPES.

In later studies, the binding between calcium and HEPES was quantified by Bowers et al. [71, 72]. They employed a calcium electrode, referenced to a sodium electrode to eliminate the liquid junction potential, for determination of the association (binding) constant of Ca-HEPES by measuring the difference in potential between solutions containing calcium alone and solutions containing calcium and HEPES. The solutions, each

containing the same quantity of sodium and having the same ionic strength, were given a total ionic strength of 303 mmol/L instead of the 160 mmol/L applicable to measurements in blood. This was necessary to obtain measurable emf differences above the inherent noise of the system. Thus the results may be affected by activity coefficient differences. Their results are shown in table 9.39.

Table 9.39.

$[Ca^{2+}] = 1$ mmol/L , T = 37 °C , pH = 7.4

Solution	[HEPES] mmol/L	% Ca^{2+} bound	K(1:1) mmol/L
A	0	0	-
B	137	7.7 ± 1.1	0.61 ± 0.09
C	274	15.6 ± 1.6	0.68 ± 0.08
D	548	31.1 ± 1.3	0.82 ± 0.05

The percentage binding was found to give a linear relationship with the total concentration of HEPES buffer as follows:

$$\% \text{ binding} = 0.057 \text{ (total HEPES / mmol } L^{-1}) - 0.050$$

The complexation of HEPES by calcium ions has also been determined by Covington and Kataky [73, 74] using a glass electrode pH titration (see table 9.43).

9.6.2 Results and Discussion.

The protonation constants for HEPES and the formation constants of its magnesium and calcium complexes are given in detail in tables 9.40-9.42. A summary of the results, together with other published values, is given in table 9.43.

For Ca-HEPES solutions, the results agree with those of Kataky [73] in which two Ca-HEPES complexes were found. These were the 1:1 calcium HEPES zwitterion complex ($MLH^{\pm}$) and 1:1 calcium protonated HEPES complex (MLH_2^{+}) .

In the case of Mg-HEPES solutions (pH glass titration), there is no evidence for a 1:1 magnesium HEPES zwitterion complex, but only the 1:1 magnesium protonated HEPES complex was formed, which is not important in the physiological range as it is only present at low pH. Figure 9.34 shows the species distribution curve of Mg-HEPES.

Using the Mg ISE method, the value of $MgLH_2^{+}$ constant was excessive by SUPERQUAD due to elimination of data points at low pH values ($pH \leq 3$). Use of the Mg ISE is restricted to pH more than 3 as explained in section 6.4.

The results for Ca-HEPES show good agreement between values of the complex formation constants obtained from pH glass and Ca ISE titrations.

Figure 9.36a shows the response of an Ca ISE to a pH change in the Ca-HEPES solution. The figure shows the trend in mV of the Ca ISE agrees with the change in the distribution of the percentage of free calcium observed in figure 9.36b. Figure 9.35 shows the species distribution curve of Ca-HEPES.

The percentage of metal ion bound to the buffer shown in table 9.44 was calculated, using the constant for the CaLH complex which is the only complex of interest in the physiological pH range, according to the following equation [75]

$$\% \text{ binding} = \{1 - (1 + K_{CaLH}\,[LH])^{-1}\} \,.\, 100$$

The concentrations of free zwitterionic buffer, [LH], were assumed to be equal to their total concentrations, as the amount bound is very small.

Table 9.40. Protonation Constants of HEPES
(Initial concentration of NaCl or KCl = 150 mmol/L , Temp. = 37 °C).

C_{HEPES} (mmol/L)	C_{HCl}	Medium	Titrant	pH range	No. of points	χ^2	σ	log β_{LH}	log β_{LH_2}
20	20	NaCl	1M NaOH	2.4 - 8.1	134	10.9	0.6	7.284 ± 0.002	10.252 ± 0.003
20	20	KCl	1M KOH	2.4 - 8.2	39	11.3	2.4	7.331 ± 0.006	10.333 ± 0.008
10	20	KCl	1M KOH	2.2 - 8.1	76	10.8	2.1	7.277 ± 0.003	10.259 ± 0.005
							Mean	7.297 ± 0.029	10.281 ± 0.045

Table 9.41. Formation Constants for Magnesium-HEPES
(Initial concentration of NaCl or KCl = 150 mmol/L , Temp. = 37 °C , Method : glass electrode).

C_M	C_{HEPES} (mmol/L)	C_{HCl}	Medium	Titrant	pH range	No. of points	χ^2	σ	log β_{MLH_2}	log K_{MLH_2}
20	20	20	NaCl	1M NaOH	2.4 - 8.1	133	8.9	1.1	10.591 ± 0.101	0.339
20	20	20	KCl	1M KOH	2.4 - 8.0	40	11.2	1.2	10.880 ± 0.073	0.547
9.85	10	20	KCl	1M KOH	2.1 - 8.0	72	12.6	1.9	10.663 ± 0.087	0..382
								Mean	10.711 ± 0.150	0.423 ± 0.110

Table 9.42. Formation Constants for Calcium-HEPES
(Initial concentration of NaCl or KCl = 150 mmol/L , Temp. = 37 °C).

C_M	C_{HEPES} (mmol/L)	C_{HCl}	Medium	Titrant	Method[a]	pH range	No.of points	χ^2	σ	log β_{MLH_2}	log K_{MLH_2}	log β_{MLH}	log K_{MLH}
20	20	20	NaCl	1M NaOH	G.E	2.4 - 8.1	133	12.6	1.3	10.834 ± 0.080	0.582	7.331 ± 0.042	0.047
20	20	20	KCl	1M KOH	G.E	2.4 - 8.1	42	10.1	1.8	11.247 ± 0.093	0.914	7.403 ± 0.065	0.072
10	10	20	KCl	1M KOH	G.E	2.1 - 8.0	74	10.3	1.5	11.180 ± 0.128	0.921	7.321 ± 0.091	0.044
20	20	20	NaCl	1M NaOH	Ca.E	3.1 - 8.1	96	6.2	0.3	10.898 ± 0.145	0.646	7.409 ± 0.063	0.125
20	20	20	KCl	1M KOH	Ca.E	3.1 - 8.0	28	7.3	0.4	11.096 ± 0.053	0.763	7.402 ± 0.031	0.071
10	10	20	KCl	1M KOH	Ca.E	3.1 - 8.0	56	4.8	0.4	11.204 ± 0.101	0.945	7.371 ± 0.056	0.094
					G.E			Mean		11.087 ± 0.222	0.806 ± 0.194	7.352 ± 0.045	0.054 ± 0.015
					Ca.E			Mean		11.066 ± 0.155	0.785 ± 0.151	7.394 ± 0.020	0.097 ± 0.027

(a) Abbreviations: see table 9.9.

Table 9.43 Summary of the protonation constants of HEPES and the formation constants of Mg- and Ca-HEPES
(Conc. of the background electrolyte = 0.15 mol/L , T = 37 °C).

$\log K_{LH_2}$ (pK_{a_1})	$\log K_{LH}$ (pK_{a_2})	$\log K_{CaLH_2}$	$\log K_{CaLH}$	$\log K_{MgLH_2}$	Reference
2.90	7.42	1.2	0.09	-	Covington and Kataky [74]
2.984	7.297	0.796	0.076	0.423	This work

Table 9.44 Calcium binding of HEPES calculated for various concentrations of zwitterionic HEPES acid.

[HEPES] mmol/L	% Ca^{2+} bound (Kataky)	% Ca^{2+} bound (This work)
1	0.120	0.119
4.06	0.497	0.481
10	1.215	1.177
100	10.955	10.643

Fig. 9.34 Species Distribution Diagram of Mg-HEPES
(C_{Mg} = 20 mmol/L, C_{HEPES} = 20 mmol/L)

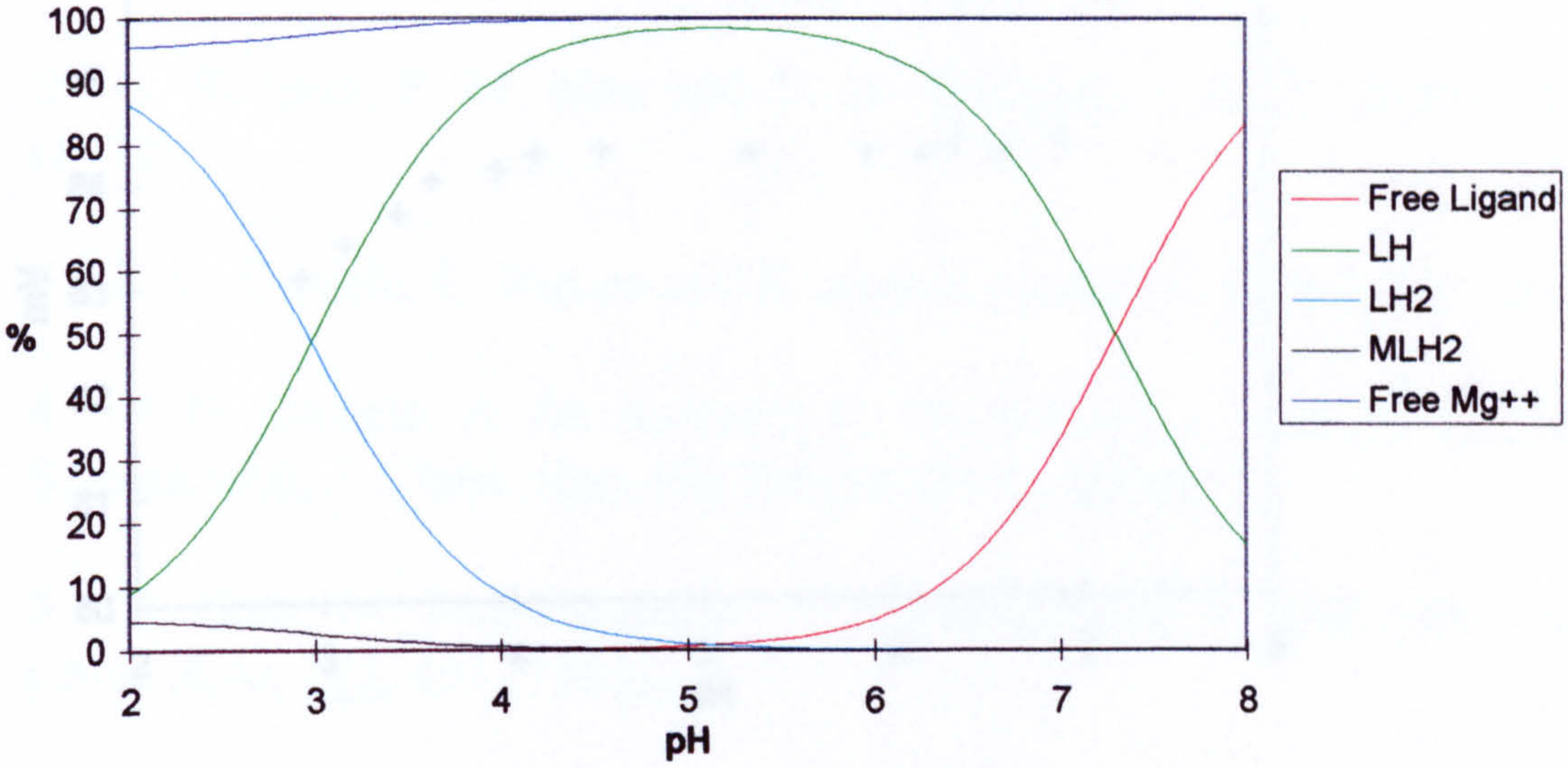

Fig. 9.35 Species Distribution Diagram of Ca-HEPES
(C_{Ca} = 20 mmol/L, C_{HEPES} = 20 mmol/L)

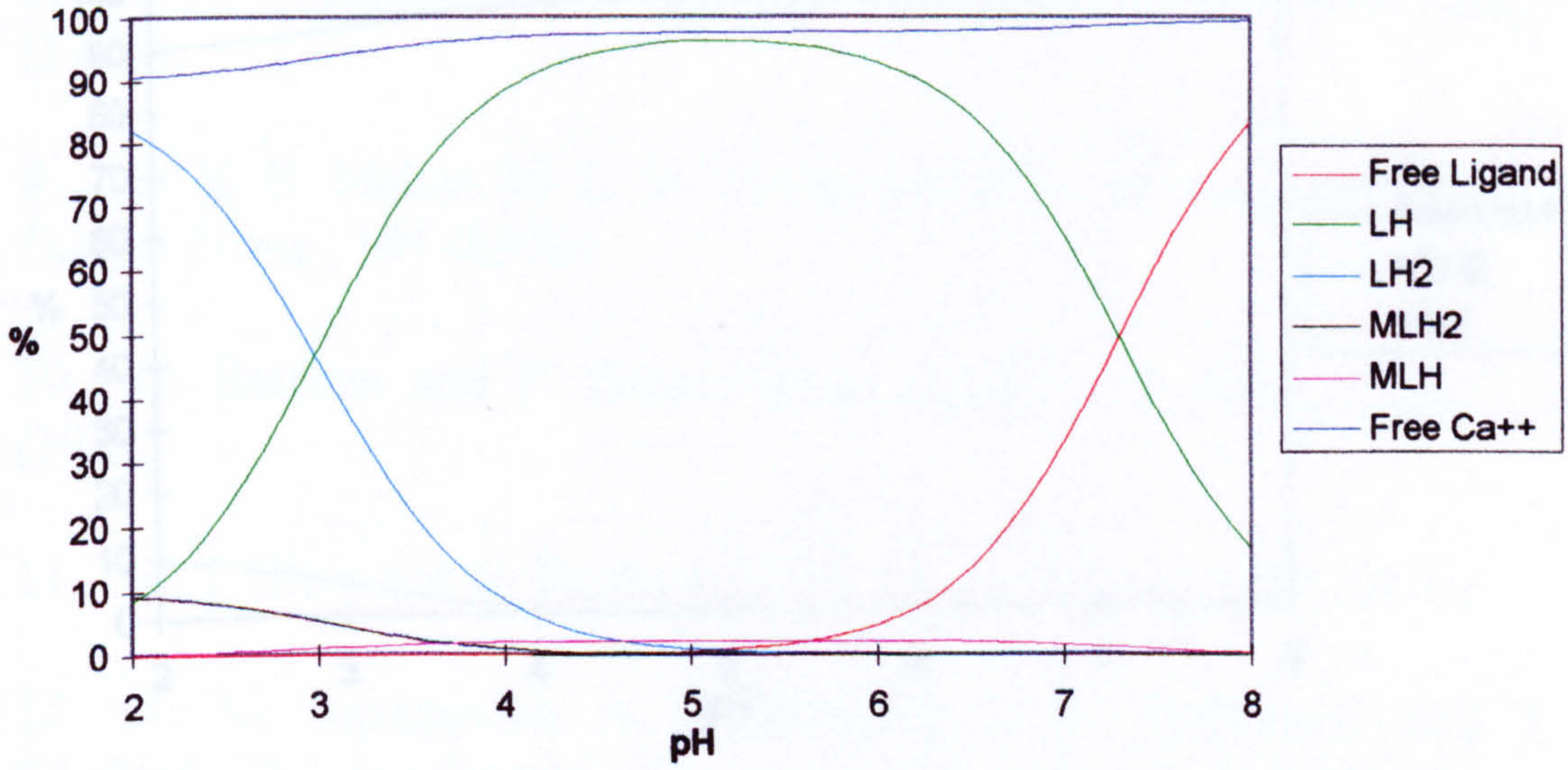

Fig. 9.36a Ca ISE Response to pH Change of Ca-HEPES
(C_{Ca} = 20 mmol/L, C_{HEPES} = 20 mmol/L, C_{HCl} = 20 mmol/L, C_{KCl} = 150 mmol/L)

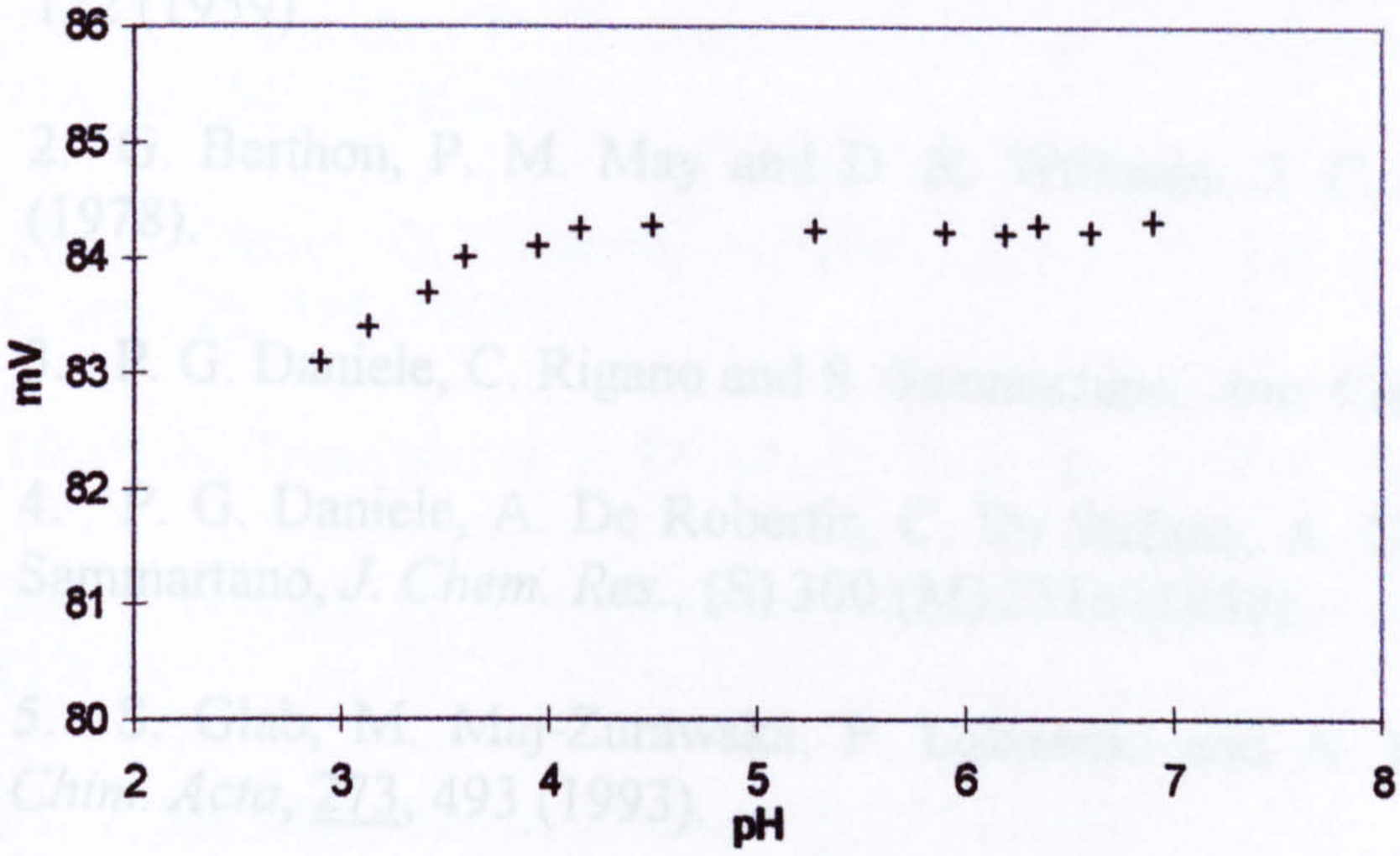

Fig. 9.36b Distribution of Ca between its HEPES Complexes
(C_{Ca} = 20 mmol/L, C_{HEPES} = 20 mmol/L)

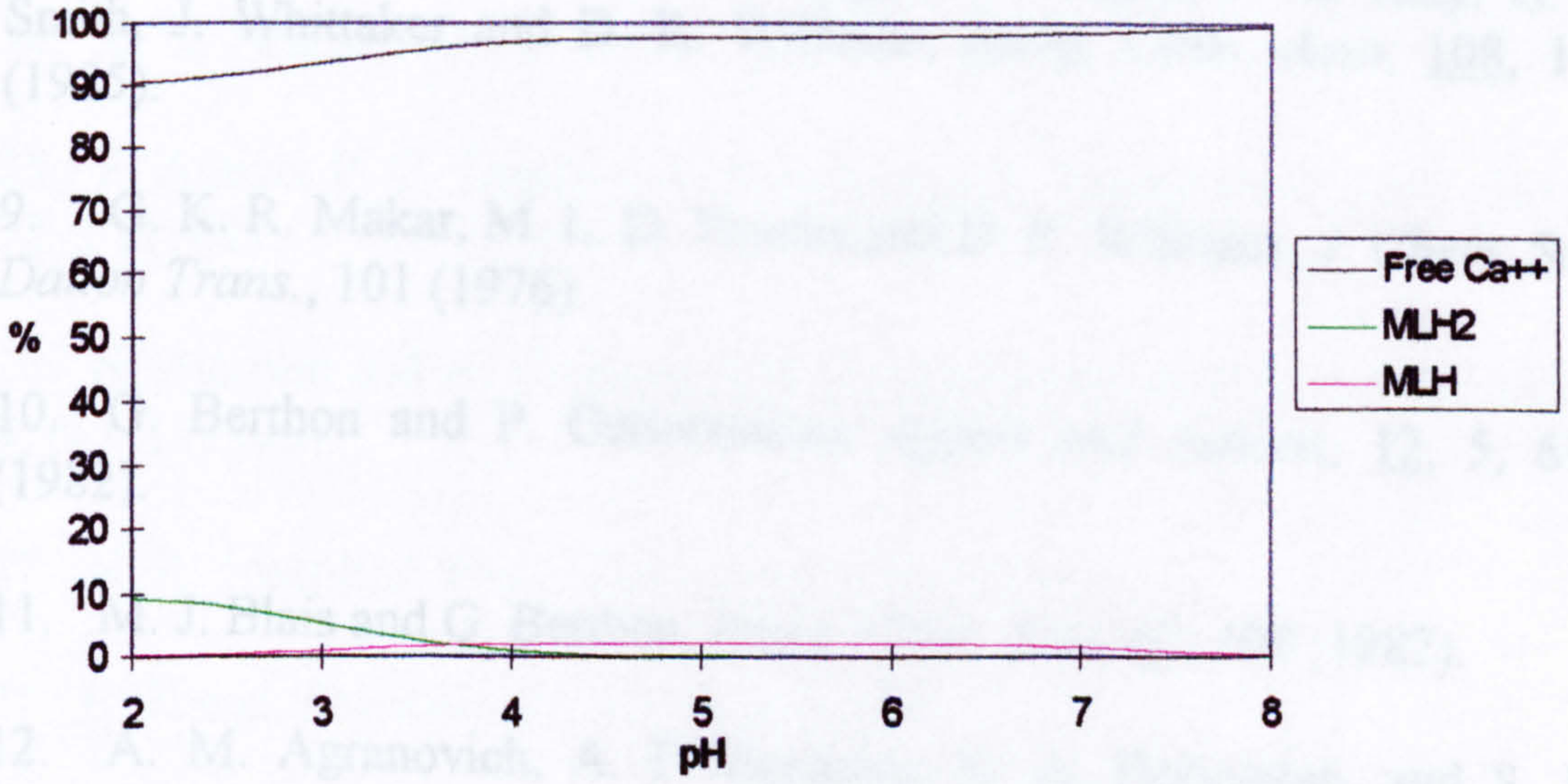

References.

1. N. C. Li, A. Lindenbaum and J. M. White, *J. Inorg. Nucl. Chem.*, 12, 122 (1959).

2. G. Berthon, P. M. May and D. R. Williams, *J. C. S. Dalton*, 1433 (1978).

3. P. G. Daniele, C. Rigano and S. Sammartano, *Ann. Chim.*, 119 (1980).

4. P. G. Daniele, A. De Robertis, C. De Stefano, A. Gianguzza and S. Sammartano, *J. Chem. Res.*, (S) 300 (M) 2316 (1990).

5. S. Glab, M. Maj-Zurawska, P. Lukomski and A. Hulanicki, *Anal. Chim. Acta*, 273, 493 (1993).

6. C. Blaquiere and G. Berthon, *Inorg. Chim. Acta*, 135, 179 (1987).

7. T. Alemdaroglu and G. Berthon, *Bioelectrochemistry and Bioenergetics*, 8, 49 (1981).

8. A. Cole, C. Furnival, Z-X. Huang, D. C. Jones, P. M. May, G. L. Smith, J. Whittaker and D. R. Williams, *Inorg. Chim. Acta*, 108, 165 (1985).

9. G. K. R. Makar, M. L. D. Touche and D. R. Williams, *J. Chem. Soc. Dalton Trans.*, 101 (1976).

10. G. Berthon and P. Germonneau, *Agents and Actions*, 12, 5, 619 (1982).

11. M. J. Blais and G. Berthon, *Inorg. Chim. Acta*, 67, 109 (1982).

12. A. M. Agranovich, A. P. Borisova, N. A. Dobrynina, and S. P. Gladkikh, *Russian Journal of Inorganic Chemistry*, 29, 7, 1012 (1984).

13. A. B. Hastings, F. C. Mclean, L. Eichelberger, J. L. Hall and E. Da Costa, *J. Biol. Chem.*, 107, 351 (1934).

14. R. Nordbö, *Skand. Arch. Physiol.*, 80, 341 (1938).

15. M. Walser, *J. Phys. Chem.*, 65, 159 (1961).

16. S. K. Tobia and N. E. Milad, *J. Chem. Soc.*, 734 (1963).

17. S. Watanabe, T. Trosper, M. Lynn and L. Evenson, *J. Biochem.* (*Tokyo*), 54, 17 (1963).

18. E. Campi, G. Ostacolt, M. Meirone and G. Saini, *J. Inorg. Nucl. Chem.*, 26, 553 (1964).

19. S. K. Tobia and N. E. Milad, *J. Chem. Soc.*, 1915 (1964).

20. S. S. Tate, A. K. Grzybowski and S. P. Datta, *J. Chem. Soc.*, 3905 (1965).

21. J. Mc Blair, *Eur. J. Biochem*, 8, 287 (1969).

22. A. K. Grzybowski, S. S. Tate and S. P. Datta, *J. Chem. Soc.* (A), 241 (1970).

23. T. B. Field, J. Coburn, J. L. Mc Court and W. A. E. Mc Bryde, *Anal. Chim. Acta*, 74, 101 (1975).

24. K. N. Pearce, *Aust. J. Chem.*, 33, 1511 (1980).

25. P. Amico, P. G. Daniele, C. Rigano and S. Sammartano, *Ann. Chim.*, 72, 1 (1982).

26. N. Bjerrum and A. Unmack, *Kgl. Danske Videnscab*, Mat-Fys Medd., 9, No. 1 (1929).

27. N. R. Joseph, *J. Biol. Chem.*, 164, 529 (1946).

28. E. Heinz, *Biochem. Z.*, *321*, 314 (1951).

29. C. W. Davies, B. E. Hoyle, *J. Chem. Soc.*, 4134 (1953).

30. J. Schubert, *J. Am. Chem. Soc.*, 76, 3442 (1954).

31. C. W. Davies, B. E. Hoyle, *J. Chem. Soc.*, 1038 (1955).

32. J. Lefebvre, *J. Chim. Phys.*, 54, 567 (1957).

33. G. A. Rechnitz and T. M. Hseu, *Anal. Chem.*, 41, 111 (1969).

34. N. A. Rumbaut, *Bull. Soc. Chim. Belges*, 80, 63 (1971).

35. J. L. Meyer, *Anal. Biochem.*, 62, 295 (1974).

36. A. Craggs, G. J. Moody and J. D. R. Thomas, *Analyst*, 104, 961 (1979).

37. R. P. Singh, Y. D. Yeboah, E. R. Pambid and P. Debayle, *J. Chem. Eng. Data*, 36, 52 (1991).

38. J. Schubert and A. Lindenbaum, *J. Am. Chem. Soc.*, 74, 3529 (1952).

39. P. B. Davies and C. B. Monk, *Trans. Faraday Soc.*, 50, 132 (1953).

40. F. Verbeek and H. Thun, *Anal. Chim. Acta*, 378 (1965).

41. E. Bottari and R. Porto, *Monat. Chem.*, 113, 1245 (1982).

42. M. L. S. Simões Gonçalves and P. Valenta, *J. Electroanal. Chem.*, 132, 357 (1982).

43. P. G. Daniele, A. D. Robertis, C. D. Stefano, S. Sammartano and C. Rigano, *J. Chem. Soc. Dalton Trans.*, 2353 (1985).

44. L. Harju, *Talanta*, 34, No. 9, 817 (1987).

45. R. F. Lumb and A. E. Martell, *J. Phys. Chem.*, 57, 690 (1953).

46. M. Hardel, *Hoppe-Seyler's Z. Physiol. Chem.*, 346, 224 (1966).

47. C. W. Davies and G. M. Waind, *J. Chem. Soc.*, 301 (1950).

48. K. Burger, P. Sipos, M. Véber, I. Horváth, B. Noszál and M. Löw, *Inorg. Chim. Acta*, 152, 233 (1988).

49. C. B. Monk, *Trans. Faraday Soc.*, 47, 297 (1951).

50. C. B. Murphy and A. E. Martell., *J. Biol. Chem.*, 226, 37 (1957).

51. I. Greenwald, *J. Phys. Chem.*, 43, 379 (1939).

52. C. A. Colman-Porter and C. B. Monk, *J. Chem. Soc.*, 4363 (1952).

53. A. D. Robertis, C. D. Steffano, C. Rigano, S. Sammartano and R. Scarcella, *J. Chem. Res.*, 42 (1985).

54. P. G. Daniele, A. De Robertis, C. De Stefano, C. Rigano and S. Sammartano, *Ann. Chim.*, 73, 619 (1983).

55. H. Simms, *J. Phys. Chem.*, 32, 1121 (1928).

56. S. Capone, A. Casale, A. Curro and A. Robertis, *Ann. Chim.*, 76, 441 (1986).

57. J. P. Glusker, D. V. der Helm, W. E. Love, M. L. Dornberg, J. A. Minkin, C. K. Johnson and A. L. Patterson, *Acta Cryst.*, 19, 561 (1965).

58. C. W. Davies, *J. Chem. Soc.*, 277 (1938).

59. W. J. Cook and C. E. Bugg, *Acta Cryst.*, B 29, 215 (1973).

60. H. Einspahr and C. E. Bugg, *Acta Cryst.*, B 30, 1037 (1974).

61. F. L. Siegel, Calcium-binding proteins, *Structure and bonding*, 17, 221 (1973).

62. A. Albert, Biochem. J., 47, 531 (1950).

63. M. C. Lim, *J. Chem. Soc. Dalton*, 726 (1978).

64. Z. X. Huang, P. M. May, D. R. Williams and M. Gosálvez, *Inorg. Chim. Acta*, 56, 41 (1981).

65. J. H. K. A. Acquaye and M. F. Richardson, *Inorg. Chim. Acta*, 201, 101 (1992).

66. M. A. Makhyoun, N. A. Al-Salem and M. S. El-Ezaby, *Inorg. Chim. Acta*, 123, 117 (1986).

67. T. A. Franklin and M. F. Richardson, *Inorg. Chim. Acta*, 46, 191 (1980).

68. S. P. S. Rao, K. A. Varughese and H. Manohar, *Inorg. Chem.*, 25, 734 (1986).

69. J. S. Hartman and E. Kelusky, *Can. J. Chem.*, 57, 2118 (1979).

70. N. E. Good, G. D. Winget, W. Winter, T. N. Connolly, S. Izawa and R. M. M. Singh, *Biochemistry*, 5, 467 (1966).

71. G. N. Bowers, Jr. , R. W. Burnett, S.F. Sena and T. F. Christiansen, In: A. H. J. Maas, F. B. T. J. Boink, N. E. L. Saris, R. Sprokholt and P. D. Wimberley, *Methodology and clinical applications of ion-selective electrodes*, IFCC, 7, 49 (1986).

72. S. F. Sena, R. W. Burnett and G. N. Bowers. Jr; Private comm. Cited in reference 73.

73. R. Kataky, *Ion-selective sensors applied to the analysis of blood electrolytes*, PhD Thesis, University of Newcastle-upon-Tyne, 1988.

74. A. K. Covington and R. Kataky, In: A. H. J. Mass, B. Buckley, H. Marsoner, N. E. L. Saries and R. Sprokholt, *Methodology and clinical applications of ion-selective electrodes*, IFCC, 8, 35 (1987).

75. Reference 73, p. 180.

76. K. Cannan and A. Kibrick, *J. Am. Chem. Soc.*, 60, 2314 (1938)

77. M. Masone and M. Vicedomini, *Ann. Chim.*, 71, 517 (1981).

78. M. Maeda, K. Okada, Y. Tsukamoto, K. Wakabayashi and K. Ito, *J. Chem. Soc. Dalton Trans.*, 2337 (1990).

79. C. Childs, *Inorg. Chem.*, 9, 2465 (1970).

80. H. Einaga, *J. Inorg. Nucl. Chem.*, 43, 229 (1981).

81. Reference 73, p. 215.

CHAPTER 10

SOURCES OF ERROR IN THE DETERMINATION OF ACIDITY AND STABILITY CONSTANTS.

Two types of error may arise in experimental measurements, systematic and random. Systematic error is a consistent error that may be detected and corrected while random error cannot be corrected and is always present in experimental measurements. The uncertainty introduced by random error may be minimised by taking the mean value of repeated measurements. An estimate of its magnitude is given by the standard deviation (sd) of the measurements from the mean.

10.1 Sources of Errors.

There are many possible sources of errors in the determination and computation of stability constants from pH glass and Mg ISE titrations. Some of these may arise from:

(i) Error in preparing the material for the titration such as:

- Error in sample weighings and dilutions.
- Using impure ligands or contaminated water.
- Error in standardising acid, base and/or metal salt solutions.
- Error in the quantity of the supporting electrolyte added and therefore in ionic strength.
- Error in the total volume of the solution in the titration cell.
- Incorrect calibration of the pH meter-electrode system.
- Error in the calibration of the micrometer syringe burette.

(ii) Error due to limitations of the apparatus or experimental technique used such as:

- Liquid junction potential variation.
- Noisy electrode response caused by stirring of solution.
- Non-Nernstian indicator electrode response.
- Drifting measurements.
- Error in titre readings and pH at a titration point.
- Error in determining the end point titre.
- Error in calculating pH from the measured potential difference.
- Temperature variations during the titration.
- Variation of ionic strength during the titration if not completely controlled by the supporting electrolyte.

(iii) Incorrect data analysis due to:

- Using incorrect values for the acidity (protonation) constants to calculate stability constants.
- Using an inappropriate value for the ionisation constant of water.
- Misuse of SUPERQUAD program.

(iv) Inaccurate data may also result due to the occurrence of unwanted or unpredicted reactions such as:

- Interaction between the supporting electrolyte and the acid anion.
- Interaction of the complex cation with the supporting electrolyte anion.
- Formation of complexes between the acid and the metal ion of a type not taken into account in the data analysis.

Methods for the elimination or minimization of some of these errors are detailed in reference [1], some of which will be discussed in this chapter.

10.2 Pseudo-Systematic Errors.

From the results of the formation constants obtained in this work (see tables 9.1-9.21, in chapter 9), it can be seen that each individual calculated standard deviation of the constants computed from a single titration is smaller than the standard deviation of the constants from the mean calculated for a serious of titrations. Due to the fact that each titration involves its own single measurements of such properties as the end point titre and the total volume of solution, these measurements are subject to random errors over a series of titrations. However, these properties are constants for a particular titration and therefore they contribute to the systematic error of stability constants calculated from the titration data.

For each titration, the precision of the calculated constants, decreases in the order

$\mathrm{sd}\left(\log\beta_{\mathrm{LH}}\right) < \mathrm{sd}\left(\log\beta_{\mathrm{LH_2}}\right) < \mathrm{sd}\left(\log\beta_{\mathrm{LH_3}}\right)$ for the protonation constants

and

$\mathrm{sd}\left(\log\beta_{\mathrm{ML}}\right) < \mathrm{sd}\left(\log\beta_{\mathrm{MLH}}\right) < \mathrm{sd}\left(\log\beta_{\mathrm{MLH_2}}\right)$ for the complex formation constants,

as the additional errors in the protonation constants, $\log K_{\mathrm{LH}}$, then $\log K_{\mathrm{LH_2}}$, are included in the overall error of $\log\beta_{\mathrm{LH_2}}$ and $\log\beta_{\mathrm{MLH}}$, and $\log\beta_{\mathrm{LH_3}}$ and $\log\beta_{\mathrm{MLH_2}}$ respectively. The values of the metal-ligand formation constants show lower precision than those of the corresponding protonation constants $\left(\text{e.g: sd of } \log\beta_{\mathrm{LH}} < \text{ sd of } \log\beta_{\mathrm{MLH}}\right)$ as the uncertainty associated with the corresponding protonation constant is included in their calculation.

10.3 Interaction between the Supporting Electrolyte and the Acids.

The large amount of Na^+ or K^+ present in the solution as a background salt may compete with divalent cations in the formation of complexes. The citrate anion was found to form complexes with Na^+ and K^+. Table 10.1 contains values for their formation constants reported in the literature at I = 0.15 mol/L and 37 °C.

Table 10.1

Metal	Log K_{ML}	Log K_{MLH}	Reference
Na^+	0.68	0.1	2
K^+	0.56	-0.3	3

Walser [4] has applied a correction for the complex $NaCit^{2-}$ to the values of dissociation constants of $MgCit^-$ and $CaCit^-$ complexes.

The dissociation constant for $NaCit^{2-}$ is

$$K_{NaCit}^{2-} = [Na^+]\,[Cit^{3-}] / [NaCit^{2-}] \qquad (10.1)$$

As the sodium ion is present in large excess as a background salt, $[Na^+]$ can be taken as equal to total [Na]. Therefore

$$K_{NaCit}^{2-} = [Na]\,[Cit^{3-}] / [NaCit^{2-}] \qquad (10.2)$$

$$[NaCit^{2-}] = [Na]\,[Cit^{3-}] / K_{NaCit}^{2-} \qquad (10.3)$$

The dissociation constant for the complex $CaCit^-$ or $MgCit^-$, K_{MCit}^-, is

$$K_{MCit}^- = [M^{2+}]\,[Cit^{3-}] / [MCit^-] \qquad (10.4)$$

But the dissociation constant for the complex $CaCit^-$ or $MgCit^-$, reported without considering the formation of the $NaCit^{2-}$ complex, is

$$K`_{MCit}^- = ([M^{2+}] / [Mcit^-]) \times ([Cit^{3-}] + [NaCit^{2-}]) \qquad (10.5)$$

Substitution of (10.3) in (10.5) gives

$$K`_{MCit}^- = ([M^{2+}]\,[Cit^{3-}] / [Mcit^-]) \times (1 + [Na] / K_{NaCit}^{2-})$$

The corrected value, K_{MCit}^{-}, is therefore obtained as

$$K_{Mcit}^{-} = K`_{MCit}^{-} / (1+ [Na] / K_{NaCit}^{2-}) \qquad (10.6)$$

or in terms of the formation constants

$$K_{Mcit}^{-} = K`_{MCit}^{-} (1+ K_{NaCit}^{2-} [Na])$$

$$\text{or} \qquad \beta_{Mcit}^{-} = \beta`_{MCit}^{-} (1+ K_{NaCit}^{2-} [Na]) \qquad (10.7)$$

The general form of equation (10.7) is

$$\beta_{pqr} = \beta`_{pqr} (1+ K_{pqr\,M^+} [M^+]) \qquad (10.8)$$

where K_{M^+} is the formation constant for alkali-metal citrate complexes and $[M^+]$ is the concentration of alkali metal ion.

In order to obtain a correction, for complexation of the citrate ion by K^+ or Na^+ ions, to the values of the stability constants of calcium and magnesium citrate complexes, two methods may be used :

(i) Correction of the β_{pqr} values ($\beta`_{pqr}$), calculated without taking into account the weak interaction between alkali-metal ion and citrate, according to the expression

$$\beta_{pqr} = \beta`_{pqr} (1+ K_{pqr\,M^+} [M^+]) \qquad \text{(see above)}$$

(ii) By introducing into the computer program, used to calculate the stability constants, another mass balance equation that refers to the concentration of the alkali metal ion, and using the values of protonation constants calculated considering the alkali metal citrate complexes.

Pearce [5, 6] has applied a correction to the values of pK_3 ($\log K_{LH}$) of citric acid for complexation of citrate ion by potassium or sodium ion and he found [6] the application of this correction improved the agreement between the results of the magnesium and calcium stability constants reported by different workers. The correction for K^+-Cit^{3-} complex formation employed by Amico et al. [7] to the values of the stability constants of Mg^{2+}-Cit^{3-} and Ca^{2+}-Cit^{3-} at I= 0.15 mol/L, T=37 °C produced

a difference (+ve shift) of ≈ 0.2 in the log K_{ML} value and ≈ 0.02 for log K_{MLH}. A shift of 0.3 in log K_{ML} resulted when the correction was applied for $NaCit^{2-}$.

When the correction for $KCit^{2-}$ and $NaCit^{2-}$ complexes was calculated using equation 10.8, the following shifts in the values of the stability constants of Mg^{2+}-Cit^{3-} and Ca^{2+}-Cit^{3-} in this work were obtained

Correction for	$\log K_{ML}$	$\log K_{MLH}$
K^+-Cit^{3-}	0.189	0.032
Na^+-Cit^{3-}	0.235	0.075

It seems that the use of potassium salt as a supporting electrolyte in citrate solutions is somewhat preferable to the use of sodium, as K^+ forms less stable complexes with citrate. Some workers use a tetramethyl ammonium salt as the supporting electrolyte in order to minimise complex formation [8].

The other acids used in this work may also form complexes with the alkali metal cations. These alkali metal complexes are expected to be weak and unimportant as the anions of these acids form weaker complexes than the citrate anion.

A second possible interaction is that between the complex cation and the supporting electrolyte anion. Grzybowski et al. [8] have applied a correction to the values of the stability constants of the magnesium citrate complexes for $MgCl^+$ complex formation. They employed a value of $K_{MgCl^+} = 3.4$ at I = 0.1 and 25 °C ($\log K_{MgCl^+} = 0.53$). However, such a correction is expected to have negligible effect as values for the formation constant of the ion pair ($Mg^{2+}Cl^-$) reported in the literature [9, 10] (e.g. log

K_{MgCl^+} = -0.98, medium: ~ 3M $NaClO_4$, T = 25 °C [9]) are much smaller than that of Grzybowski et al.

10.4 Liquid Junction Potential.

Liquid junction potentials arise when two electrolyte solutions of different composition and/or concentration are brought into contact. In the operational pH cell

$$Hg \mid Hg_2Cl_2 \mid KCl \parallel \text{standard solution, s} \mid \text{glass electrode} \quad \text{(I)}$$

and

$$Hg \mid Hg_2Cl_2 \mid KCl \parallel \text{test solution, x} \mid \text{glass electrode} \quad \text{(II)}$$

The liquid junction potentials E_{Js} and E_{Jx} arise between the standard and test solutions, and the bridge solution KCl, respectively. The pH of the test solution, $pH_{(x)}$, is then given by

$$pH_{(x)} = pH_{(s)} - \frac{1}{(RT/F)\ln 10}\left[(E_x - E_s) + (E_{JX} - E_{JS})\right] \qquad (10.9)$$

where pH(s) is the pH of the standard buffer solution, E_s and E_x are the e.m.f values of cell (I) and (II), respectively. The difference (E_{Jx} - E_{Js}) between the standard and test solutions is called the residual liquid junction potential, ΔE_J. The residual liquid junction potential inherent in the use of the pH meter, produces an error $\Delta pH \left(= \text{residual } E_j \times \frac{1}{(RT/F)\ln 10}\right)$ in the determination of the practical pH, the magnitude of which may not always be calculable. The error can be minimised by using background concentrations of equal concentrations of the same inert salt for calibration and measurement.

10.5 Effect of H^+ and OH^- on E_J.

Under conditions of constant ionic strength, maintained by an inert supporting electrolyte, the potential difference of the cell (I) or (II) mentioned above varies linearly with the log (hydrogen ion concentration) as well as with the log (hydrogen ion activity). In the pH range 3-11, the liquid junction potentials remain almost constant as the supporting electrolyte is the dominant ionic conductor. Below pH 3 and above pH 11 [11], hydrogen ions and hydroxide ions, because of their large ionic mobilities, begin to be responsible for appreciable fractions of conductance [11], so that the liquid junction potential will change, causing errors in the pH measurements. Therefore, accurate measurements of hydrogen ion concentration (or activity) with a glass electrode-reference electrode systems are restricted to the pH range 3-11.

10.6 pH_X to $p[H]_X$ Correction.

In order to obtain exact determinations of the acidity constants (concentration constants) of the ligands and the corresponding metal-ligand stability constants (concentration stability constants), a determination of the concentration of the hydrogen ion in the test solution is required (see section 6.2.2). Therefore, it is necessary to correct the measured pH values of the test solution in the following manner [13]:

$$p[H]_X = pH_X - A \qquad (10.10)$$

$$\text{with} \quad A = \text{Log } f - \Delta E_J \qquad (10.11)$$

where [H] is the concentration of hydrogen ions

f is the activity coefficient of hydrogen ions

ΔE_J is the residual liquid junction potential

A is termed the 'conversion factor'

SUPERQUAD, the computer program used in this work to calculate stability constants, does not provide any means of correction for liquid junction effects. Gans [12] suggested that such corrections are negligible in the pH range 3-11.

10.7 The Conversion Factor *A*.

The conversion factor *A* allows a measured pH, based on a calibration with NBS standard buffers, to be converted into the corresponding pH defined in terms of concentration (eq. 10.10). It may be determined by measuring the pH of a solution of a strong acid of known hydrogen ion concentration, in the same matrix (background electrolyte) as used in the titration. The pH is measured by calibration with NBS buffer solutions and the difference between the measured pH and the concentration scale pH ($-\log[H^+]$) is equal to the conversion factor, *A* :

$$A = pH_{meas} - p[H^+] \qquad (10.12)$$

Several workers have determined the conversion term *A* [13-17]. The most recent work is that of Sigel et al. [17] who employed glass electrodes to investigate solutions in the presence of $NaNO_3$ (I = 0.1 mol/L) and KNO_3 (I = 0.1 and 0.5 mol/L) against a concentrated (KCl) calomel electrode. They found the *A* value to be very similar in each instance. They considered that the *A* value is independent of the ionic strength at I = 0.1-0.5 and of the inert salt used. The type and origin of the glass electrodes and the buffers used for calibration (provided they are based on the NBS scale), and of the type of equipment and methods of measurement employed were also considered to have very little effect on the *A* value. A conversion value of *A* = 0.03 was generally recommended for I = 0.1- 0.5 mol/L at 25 °C. The same value was also recommended for the range I =

1- 2 mol/L. Sigel et al. concluded that, in order to convert the acidity constants, pK_a , calculated from direct pH meter readings (practical constants) into concentration constants, 0.03 in pK should be subtracted from the pK_a value.

Irving et al. [13] have found the calibration of a pH meter (a) with buffers or (b) with a strong acid or base of known concentration, so as to read directly -log $[H^+]$, leads to superimposable titration curves. Superimposable curves would show that *A* did not vary over the range of pH used in the titration, so a constant adjustment could be used, p[H] = pH - *A* and $pK_{a\ (conc)} = pK_{a\ (activities)} - A$, the parallel displacement gives the value of *A*. The values obtained are given in table 10.2. If the curves were not superimposable, a more complicated adjustment would be necessary and the equation p[H] = pH - *A*, would not hold.

Table 10.2.

Cell	Cell (1)		Cell (2)	
Buffer	0.05 phth	0.05 phth/0.05 KCl	0.05 phth	0.05 phth/0.05 KCl
A	0.08±0.01	0.10±0.01	0.00±0.01	0.06±0.01

Cell (1): Hg_2Cl_2/Hg/sat.KCl // titration solution in 0.1M KCl / glass electrode.

Cell (2): Hg_2Cl_2/Hg/sat.KCl // 0.1M KCl bridge // titration solution in 0.1M KCl / glass electrode

Sigel et al. [17] state that *A* does not affect metal-ligand stability constants if the pK_a (activity scale) values are determined without the metal present and these values are used in analysing data from titrations with the metal present, i.e. *A* cancels out. So, *A* would only affect the pK_a values and should not be applied to pK_a's used in analysing the metal-ligand titration data. Therefore, applying the conversion factor would have very little effect on the pK_a values and it should not be used in calculation

of the stability constants of metal ion complexes determined by potentiometric pH titrations, which therefore can be defined as concentration constants.

References.

1. A. E. Martell and R. J. Motekaitis, *Determination and use of stability constants*, VCH Publishers, New York, 33 (1988).

2. G. Arena, R. Cali, M. Grasso, S. Musumeci, S. Sammartano and C. Rigano, *Thermochim. Acta*, 36, 329 (1980).

3. P. G. Daniele, C. Rigano and S. Sammartano, *Ann. Chim.*, 70, 119 (1980).

4. M. Walser, *J. Phys. Chem.*, 65, 159 (1961).

5. K. N. Pearce, Ph.D. Thesis, Massey University, (1972).

6. K. N. Pearce, *Aust. J. Chem.* , 33, 1511 (1980).

7. P. Amico, P. G. Daniele, C. Rigano and S. Sammartano, *Ann. Chim.*, 72, 1 (1982).

8. A. K. Grzybowski, S. S. Tate and S. P. Datta, *J. Chem. Soc.* , A, 241 (1970).

9. J. Havel and E. Hogfeldt, *Acta Chem. Scand.*, 27, 3323 (1973).

10. R. H. Byrne, C. H. van der Weijden, D. R. Kester and R. W. Zuehlke, *J. Solution Chem.*, 12, 581 (1983).

11. G. G. Manov, N. J. DeLollis and S. F. Acree, *J. Res. Nat. Bur. Stand.*, 34, 115 (1945).

12. P. Gans, A. Sabatini and A. Vacca, *J. Chem. Soc. Dalton Trans.*, 1195 (1985)

13. H. M. Irving, M.G. Miles and L. D. Pettit, *Anal. Chim. Acta*, 38, 475 (1967).

14. O. Yamauchi, Y. Hirano, Y. Nakao and A. Nakahara, *Can. J. Chem.*, 47, 3441 (1969).

15. O. Yamauchi, H. Seki and T. Shoda, *Bull. Chem. Soc. Jpn.*, 56, 3258 (1983).

16. O. Yamauchi, K. Tsujide and A. Odani, *J. Am. Chem. Soc.*, 107, 659 (1985).

17. H. Sigel, A. D. Zuberbühler and O. Yamauchi, *Anal. Chim. Acta*, 255, 63 (1991).

CHAPTER 11
CONCLUSIONS

This work was concerned with a reference cell method for ionized magnesium and the determination of magnesium binding constants for substances of physiological interest.

In the course of the work, magnesium ionophores were tested for applicability in the reference cell method and in study of complexes. A prototype reference cell proposed for the reference method for ionized calcium was tested to determine its suitability for measuring magnesium ion concentration. For various ligands, the protonation constants and stability constants of magnesium (and calcium) complexes were determined, the latter using a new method employing simultaneously a pH glass and a Mg (or Ca) electrode.

11.1 Calibration and Selectivity Measurements.

Calibration and selectivity measurements have been applied to magnesium ion-selective electrodes based on the ionophores ETH 1117, 4030 and 7025 in order to judge their suitability in a reference cell method for the measurement of ionized magnesium in blood and in alkalimetric titrations for determination of stability constants of metal complexes.

None of the three ionophores studied showed sufficient selectivity for magnesium over calcium and sodium, so for the reference method it would be necessary to run calcium, and maybe sodium, alongside magnesium for serum samples. ETH 7025, however, showed the best selectivity to magnesium over calcium and ETH 4030 to magnesium over sodium.

The effect of pH on the response of the electrodes showed that the Mg ISE based on the ETH 7025 was influenced by pH changes mostly in the pH range 5-8, and the ETH 1117 membrane showed stronger hydrogen interference. The Mg ISE based on the ETH 4030 was found to show high selectivity to magnesium over pH, as well as sodium and potassium, and was chosen for use in alkalimetric titrations, carried out in the presence of high concentrations of sodium or potassium ion as a background electrolyte, to determine the stability constants of magnesium complexes.

The Ca ISE based on the ETH 1001 has also been tested and was found to show high selectivity for calcium over sodium, potassium and pH, and was used to determine the stability constants of calcium complexes.

11.2 The Reference Cell.

The performance of the reference cell proposed for calcium measurements in blood was tested when applied to the determination of magnesium ion concentration, which has a lower concentration than calcium in blood. The appraisal tests detailed in the IFCC draft ionized calcium document [1] have been carried out. The magnesium membrane used was based on the ionophore ETH 7025, which is currently used in some commercial Mg ISE analysers. Two sets of calibration solutions, similar to the IFCC calibration solutions proposed for ionized calcium measurements in blood (but adapted for use with magnesium), have been used in these studies.

The reference cell showed excellent results for ionized magnesium concentration when used with the primary or secondary reference solutions and the performance with the ETH 7025 magnesium membranes was found to be better than for ETH 1001 calcium ionophore in the

corresponding solutions. The reference cell results, however, showed a deviation from the IFCC specifications in some calibrations due to a drift in emf of the cell.

The effect of protein on the ETH 7025 based magnesium membrane was determined. The result showed that the electrode was affected by protein contamination, evidenced by the difference in emf obtained from this electrode in aqueous standards, before and after exposure to protein-containing solution. The protein-induced potential shift was similar in magnitude to that for the ETH 1001-based PVC calcium membrane obtained by D'Orazio et al. [2], who found the replacement of PVC in the calcium membrane with polyurethane eliminated this effect. Therefore, the contamination of the magnesium membrane by protein was attributed to the PVC in the magnesium membrane and not to the ETH 7025 ionophore.

11.3 Determination of Stability Constants.

Potentiometric (alkalimetric) titrations, using a glass electrode in conjunction with a Mg ISE for simultaneous pH and pMg measurements, were used to redetermine the stability constants for magnesium complexes of citrate, lactate, glycinate, aspartate and glutamate. The complexation constants of magnesium pyroglutamate and pyridoxine were determined for the first time. The calibration solutions, used in this work for standardisation of magnesium measurement, contained HEPES buffer. Magnesium binding to this buffer has also been evaluated. The complexation constants of calcium with the above ligands were determined for comparison. The ligand proton formation constants, necessary for the calculation of the metal complex formation constants, were also

determined. A non-linear least squares data fitting program, SUPERQUAD, was used to calculate the constants from the titration data.

In general, the glass electrode and Mg or Ca ISE methods gave good agreement in the values of complex formation constants. However, agreement between the two methods was not observed in the case of the magnesium pyridoxine system. The Mg ISE, in contrast to the glass electrode, was found to give values for stability constants of Mg-pyridoxine complexes at low concentrations and another protonated complex, ML_3H_3, was also found at high pyridoxine concentrations. The response of the Mg ISE to pH change in Mg-pyridoxine solution showed a large decrease in the pH region 3-6, and that decrease in mV became greater when the concentration of the ligand was increased. This large decrease in the potentiometric response of the Mg ISE, which caused the disagreement in the values of stability constants obtained with the two methods could be due to the interference of the LH_2^+ ion on the response of the Mg ISE to Mg^{2+}. The concentration of the LH_2^+ ion decreases as the pH increases from 3 to 6, therefore, if it interfered, the emf of the Mg ISE would decrease over this pH range. Another possibility for the large emf decrease is the effect on the Mg^{2+} activity and liquid junction potential due to the changing composition of the solution as pH is increased. The electrostatic interaction forces between Mg^{2+} and other ions present in the solution become greater at higher ligand concentrations and vary more with changes in the composition of the solution. The existence of the MLH complex in the Mg-pyridoxine system would be expected to play a major role in this as in the case of the Ca-pyridoxine system the MLH complex was not formed and the Ca ISE did not show the large emf decrease. Thus the apparent existence of an ML_3H_3 complex for Mg-pyridoxine, which

was found only in the case of using the Mg ISE at high ligand concentrations, is considered to be spurious.

A summary of the formation constants obtained in this work is shown in table 11.1. The protonation constants of the ligands were found to agree well with literature values. The results for magnesium and calcium-citrate, lactate, glycinate, aspartate and glutamate complexation constants compare well with recently published data [3]. In the case of the pyroglutamate and pyridoxine systems, the complexation of the ligands to magnesium and calcium was found to occur at high concentrations. At low concentrations (except for magnesium pyridoxine with a Mg ISE), the results agree with Blaquiere and Berthon [3] who found no evidence for complex formation.

The Good buffer, HEPES, would be a suitable buffer for use in multi-ion magnesium calibration solutions as it was found not to complex magnesium at physiological pH. The results of complexation constants for calcium-HEPES agree with those of Covington and Kataky [4].

The response of ISEs (Mg or Ca) to pH changes in the metal-ligand solutions were compared to the percentage of free metal distribution curves. It was found that for each system (except for Mg-pyridoxine), the change in mV of the ISE, qualitatively and, in most cases, quantitatively, agrees with the change in the percentage of the free metal distribution, which indicates the reliability of the results obtained on this work.

Thus, the employment of both a Mg (or Ca) ISE and a glass electrode simultaneously in potentiometric pH titrations is undoubtedly useful for the study of ionic equilibria, giving greater confidence in the accuracy of the stability constant results obtained. However, it should be pointed out that the response of ion-selective electrodes must be carefully checked and

Table 11.1 A summary of the Formation Constants obtained in this work. The formula of the general complex is $M_pL_qH_r$.

System	p	q	r	log β
Proton Citrate	0	1	1	5.660
	0	1	2	9.972
	0	1	3	12.884
Mg-Citrate	1	1	2	11.176
	1	1	1	7.533
	1	1	0	3.231
	1	2	0	4.731
	1	1	-1	-18.637
	2	2	-2	-12.856
Ca-Citrate	1	1	2	11.236
	1	1	1	7.604
	1	1	0	3.332
	1	2	0	4.668
	1	1	-1	-8.788
	1	2	-2	-18.635
Proton Lactate	0	1	1	3.675
Mg-Lactate	1	1	0	1.054
Ca-Lactate	1	1	0	1.018
Proton-Glycinate	0	1	1	9.288
	0	1	2	11.674
Mg-Glycinate	1	2	2	20.714
	1	1	1	10.192
	1	1	0	1.684
	1	1	-1	-9.130
Ca-Glycinate	1	1	1	10.105
	1	1	0	1.215
	1	1	-1	-9.462

Table 11.1 (cont.)

System	p	q	r	log β
proton-Aspartate	0	1	1	9.406
	0	1	2	13.101
	0	1	3	15.203
Mg-Aspartate	1	1	2	14.505
	1	1	1	11.094
	1	1	0	2.415
	1	1	-1	-8.585
	2	1	0	4.403
Ca-Aspartate	1	1	2	14.514
	1	1	1	11.024
	1	1	0	1.963
	1	1	-1	-9.689
Proton-Glutamate	0	1	1	9.263
	0	1	2	13.373
	0	1	3	15.551
Mg-Glutamate	1	1	2	14.761
	1	1	1	10.744
	1	1	0	1.777
	1	2	-1	-7.133
Ca-Glutamate	1	1	2	14.001
	1	1	1	10.124
	1	1	0	1.278
	1	1	-1	-9.684
Proton-Pyroglutamate	0	1	1	3.128
Mg-Pyroglutamate	1	1	0	0.849
	1	1	-1	-9.793
Ca-Pyroglutamate	1	1	0	0.706
	1	1	-1	-10.607

Table 11.1 (cont.)

System	p	q	r	log β
Proton-Pyridoxine	0	1	1	8.707
	0	1	2	13.498
Mg-Pyridoxine (G.E)	1	1	0	1.442
	1	1	1	9.294
(Mg.E)	1	1	0	1.805
	1	1	1	9.908
	1	3	3	30.690
Ca-Pyridoxine	1	1	0	0.574
Proton-HEPES	0	1	1	7.297
	0	1	2	10.281
Mg-HEPES	1	1	2	10.711
Ca-HEPES	1	1	2	11.077
	1	1	1	7.373

account has to be taken of their limitations under the selected experimental conditions.

11.4 Future Work.

There is scope for future work in the following areas:

a- Reference Cell.

In order to increase the precision of the measurements, the following improvements are required:

1)-Magnesium membranes:

-development of a magnesium ionophore with a higher selectivity for magnesium over sodium and calcium.

-investigation of different membrane compositions to obtain a membrane unaffected by protein, while maintaining a high selectivity for magnesium.

2)-Cell design:

In order to overcome the drift in emf for the cell, some improvements in the cell design are required, such as [5]:

-use of a better seal of the internal electrode into the electrode body to prevent solution evaporation.

-use of an inverted V shaped sample path to improve solution contact at the membrane.

-use of a flow configuration junction type such as T-shaped liquid junction. This shape of T-junction has been used for sea-water measurements [6, 7]. The liquid junction is renewable for each solution to prevent contamination or dilution at the liquid junction.

3)-Measurement Protocol:

The measurement protocol in the draft IFCC proposal for ionized calcium was found to be very time consuming. It should be altered to reduce the

time to replicate measurements, while still containing checks for carry-over, drift and protein effect on the membrane [5].

b- Determination of complex stability constants.

1)-Magnesium and calcium membranes:

-The application of the ETH 4030 Mg and ETH 1001 Ca ISEs in alkalimetric titrations to determine the stability constants of metal complexes was restricted to pH greater than 3, due to interference by hydrogen ions in the strong acidic medium of pH $\leq$ 3. Therefore, it would be necessary to investigate other magnesium and calcium ionophores to overcome the hydrogen ion interference in order to extend the use of both the Mg and Ca ISEs to a very low pH.

2)-Magnesium complexes:

-For the magnesium pyridoxine system, further work needs to be performed to find out the reason for the great decrease in the potentiometric response of the Mg ISE in pH region 3-6. This might be achieved by:

(i) testing the response of the Mg ISE to pH change in pyridoxine solutions in the absence of Mg^{2+}. If a decrease in the emf of the Mg ISE is also observed in this case, this would mean that the LH_2^+ ion was acting as interferent ion on the response of the Mg ISE to Mg^{2+} in Mg-pyridoxine solutions.

(ii) increasing the concentration of the background electrolyte in Mg-pyridoxine pH titrations as less effect on the Mg^{2+} activity and liquid junction potential would then be expected from the composition changes during the titration.

-In order to obtain more confidence in the accuracy of the stability constant results, other methods should be used to study the speciation of magnesium with ligands, where possible.

3)-SUPERQUAD:

Although the SUPERQUAD software is designed to work in conjunction with the Molspin pH meter with two simultaneous independent ISE inputs, SUPERQUAD can only analyse the potentiometric data obtained by the first electrode input. The data file required rewriting for SUPERQUAD input of the titration data from the second electrode. This procedure is, of course, time consuming. So, if SUPERQUAD is to be used routinely for analysis of potentiometric data obtained by glass and a metal ion-responsive ISE, the program requires slight modification to its data file input.

References.

1. A. B. T. J. Boink, B. M. Buckley, T. F. Christiansen, A. K. Covington, A. H. J. Mass, O. Mueller-Plathe, C. Sachs and O. Siggaard-Andersen, In: A. H. J. Mass, B. Buckley, H. Marsoner, N. E. L. Saris and R. Sprokholt (editors), *Methodology and Clinical Applications of Ion-selective Electrodes*, IFCC, 8, 39 (1987).

2. P. D'Orazio, I. Laios and G. N. Bowers, In: P. D'Orazio, M. F. Burritt and S. F. Sena, *Electrolyte, Blood Gases and other Critical Analytes: the Patient, the Measurement and the Government*, IFCC, 14, 21 (1992).

3. C. Blaquiere and G. Berthon, *Inorg. Chim. Acta*, 135, 179 (1987).

4. A. K. Covington and R. Kataky, In: A. H. J. Mass, B. Buckley, H. Marsoner, N. E. L. Saris and R. Sprokholt (editors), *Methodology and Clinical Applications of Ion-selective Electrodes*, IFCC, 8, 35 (1987).

5. P. M. Kelly, *Proposed Reference Method for the Measurement of Ionized Calcium in Blood*, PhD Thesis, University of Newcastle-upon-Tyne, (1993).

6. C. H. Culberson, in: M. Whitfield and D. Jagner (editors), *Marine Electrochemistry*, Wiley, New York, (1981), p. 187.

7. P. D. Whalley, *Factors Affecting the Precision of pH measurements in Freshwater*, PhD Thesis, University of Newcastle-upon-Tyne, (1982), chapter 6.

APPENDIX A

Equations for Conversion between Molarity and Molality

In terms of units:

$$C_i\,(\text{mol L}^{-1}) = \frac{m_i\,(\text{mol kg}^{-1})\,\rho\,(\text{g ml}^{-1})\,1000\,(\text{ml L}^{-1})}{1000\,(\text{g kg}^{-1}) + \sum_j m_j(\text{mol kg}^{-1})\,M_j(\text{g mol}^{-1})}$$

where i = the solute for which the conversion is being carried out

j = all solutes in the solution, including I

ρ = the density of the solution (g ml^{-1})

C = molarity (mol L^{-1})

m = molality (mol kg^{-1})

M_j= molecular mass of the solute j (g mol^{-1})

In summary:

$$C_i = \frac{1000\,\rho\,m_i}{1000 + \sum_j m_j\,M_j}$$

and

$$m_i = \frac{1000\,C_i}{1000\,\rho - \sum_j C_j M_j}$$

APPENDIX B

Detailed Results of Ionized Magnesium Analysis

1- Primary calibration solutions

Sample x = Solution 2

Sol. no.	n_1	n_2	n_3	n_4	n_5
1	38.10	38.55	40.23	40.52	40.82
2	30.41	30.84	32.60	32.86	33.01
1	38.39	38.78	40.35	40.60	40.88
3	43.19	43.60	45.20	45.38	45.51
1	38.62	39.01	40.50	40.69	41.06
2	30.94	31.10	32.64	32.80	33.15
1	38.87	39.18	40.73	40.68	41.02
3	43.60	43.80	45.46	45.43	45.73
1	38.97	39.38	40.86	40.76	41.07
X	31.32	31.50	32.60	32.83	33.21
1	39.10	39.23	40.64	40.80	41.00
X	31.08	31.58	32.63	32.96	33.30
1	39.26	39.33	40.59	40.82	41.16
Δ Ex	7.908	7.753	8.068	7.900	7.803
Δ Es	7.820	7.910	7.833	7.793	7.865
S_2	0.912	0.922	0.913	0.909	0.917
S_3	0.904	0.890	0.911	0.911	0.890
Cx	0.298	0.304	0.294	0.297	0.302

Sample x = Solution 1

Sol. no.	n_1	n_2	n_3	n_4	n_5
1	23.32	23.83	24.14	14.72	14.18
2	16.18	16.72	17.02	7.52	6.93
1	23.54	23.89	24.20	14.61	14.12
3	28.39	28.85	29.14	18.94	18.45
1	23.62	24.15	24.27	14.51	14.09
2	16.38	16.84	17.00	7.23	6.84
1	23.67	24.18	24.30	14.47	13.98
3	28.67	29.04	29.20	18.80	18.46
1	23.80	24.11	24.32	14.41	14.11
X	23.88	24.17	24.37	14.38	14.04
1	23.86	23.99	24.38	14.35	14.00
X	23.86	23.98	24.46	14.32	13.98
1	23.89	23.98	24.40	14.38	13.98
Δ Ex	-0.018	-0.043	-0.045	0.023	0.013
Δ Es	-4.873	-4.863	-4.898	7.203	7.208
S_2	0.846	0.843	0.841	0.840	0.840
S_3	0.940	0.938	0.945	0.843	0.845
Cx	0.571	0.573	0.572	0.569	0.569

Sample x = Solution 3

Sol. no.	n_1	n_2	n_3	n_4	n_5
1	14.08	13.82	13.66	13.68	12.73
2	6.80	6.52	6.48	6.52	5.56
1	14.08	13.69	13.61	13.67	12.64
3	18.20	17.98	17.87	17.84	16.88
1	13.89	13.63	13.57	13.62	12.61
2	6.70	6.52	6.23	6.42	5.48
1	13.79	13.63	13.47	13.54	12.54
3	18.17	17.91	17.80	17.85	16.80
1	13.79	13.63	13.48	13.56	12.55
X	17.99	17.88	17.72	17.79	16.80
1	13.57	13.65	13.41	13.48	12.48
X	18.12	17.95	17.70	17.74	16.62
1	13.84	13.65	13.36	13.52	12.37
Δ Ex	-4.363	-4.270	-4.295	-4.255	-4.240
Δ Es	-4.298	-4.300	-4.303	-4.248	-4.255
S_2	0.841	0.836	0.842	0.834	0.829
S_3	0.829	0.830	0.830	0.820	0.821
Cx	0.845	0.838	0.839	0.841	0.839

2- Secondary Calibration Solutions.

Sample x = Solution 2

Sol. no.	n_1	n_2	n_3	n_4	n_5
1	15.95	15.30	15.50	15.52	15.66
2	8.47	7.90	8.08	8.05	8.21
1	15.76	15.24	15.50	15.49	15.63
3	20.38	19.94	20.14	20.13	20.28
1	15.69	15.24	15.43	15.37	15.69
2	8.20	7.82	8.14	7.98	8.26
1	15.50	15.24	15.37	15.40	15.49
3	20.12	19.98	20.14	20.11	20.24
1	15.43	15.30	15.37	15.43	15.62
X	7.94	7.88	8.04	7.91	8.09
1	15.37	15.24	15.37	15.36	15.52
X	7.94	7.84	8.02	7.95	8.03
1	15.30	15.24	15.37	15.23	15.49
Δ Ex	7.428	7.395	7.340	7.415	7.478
Δ Es	7.390	7.395	7.340	7.430	7.383
S_2	0.862	0.862	0.856	0.866	0.861
S_3	0.898	0.908	0.911	0.907	0.898
Cx	0.299	0.300	0.300	0.300	0.298

Sample x = Solution 1

Sol. no.	n_1	n_2	n_3	n_4	n_5
1	16.85	16.92	18.66	18.79	18.98
2	9.43	9.49	11.44	11.49	11.57
1	16.62	16.66	18.59	18.79	18.85
3	21.27	21.30	23.30	23.49	23.54
1	16.60	16.53	18.50	18.60	18.85
2	9.23	9.17	11.25	11.43	11.48
1	16.43	16.45	18.39	18.66	18.86
3	21.09	21.04	22.92	23.30	23.60
1	16.45	16.47	18.46	18.65	18.79
X	16.47	16.47	18.43	18.55	18.83
1	16.43	16.40	18.40	18.53	18.83
X	16.53	16.47	18.41	18.50	18.79
1	16.49	16.47	18.49	18.53	18.79
Δ Ex	-0.050	-0.035	0.018	0.035	0.000
Δ Es	-4.655	-4.643	7.190	7.250	-4.733
S_2	0.851	0.852	0.838	0.845	0.858
S_3	0.898	0.896	0.893	0.911	0.913
Cx	0.572	0.572	0.569	0.568	0.570

Sample x = Solution 3

Sol. no.	n_1	n_2	n_3	n_4	n_5
1	19.72	19.60	19.54	19.76	19.98
2	12.40	12.23	12.12	12.55	12.41
1	19.61	19.53	19.45	19.95	19.79
3	24.21	24.20	24.18	24.53	24.36
1	19.62	19.50	19.39	19.89	19.60
2	12.18	12.10	12.08	12.47	12.35
1	19.48	19.40	19.30	19.80	19.66
3	24.18	24.06	24.11	24.54	24.24
1	19.59	19.46	19.45	19.85	19.60
X	24.20	24.01	24.18	24.41	24.18
1	19.54	19.40	19.52	19.77	19.53
X	24.04	23.95	24.11	24.42	24.12
1	19.55	19.34	19.39	19.75	19.53
Δ Ex	-4.565	-4.580	-4.675	-4.630	-4.603
Δ Es	-4.620	-4.658	-4.748	-4.663	-4.638
S_2	0.853	0.856	0.853	0.856	0.860
S_3	0.892	0.899	0.916	0.900	0.895
Cx	0.836	0.835	0.835	0.838	0.838

APPENDIX C

Stability Constants Database.

1

****

START of profile PRINTED on Mon 13 February 1995 @ 08:56

Stability Constants Database SCQUERY (C) 1993 IUPAC and Academic Software
SCQUERY Version 1.32 : Prof.A.Covington, U. of Newcastle

User Identifier : Prof.A.Covington, U. of Newcastle

15 expts:Profile for Citric acid/3 metals (H+/Ca++ etc))
8 refs (87BBe to 69BMb) / No experimental details specified

C6H8O7 (95) Citric acid CAS 77-92-9
2-Hydroxypropane-1,2,3-tricarboxylic acid HOOCCH2.CH(OH)(COOH).CH2COOH H3L

Metal	Mtd	Temp	Conc	Medm	Clb	Flags	Log equilibrium const	Ref	ExptNo
H+	gl	37C	0.00	oth/un			K1=6.45 B2=11.21 K3=3.10	82ADa	881
H+	gl	25C	0.10M	oth/un			K1=5.82 B2=10.17 K3=2.85	70GTa	37297
Ca++	gl	37C	0.15M	NaClO4	C		K1=3.364 B2=4.965 B(CaH2L)=11.005 B(CaHL)=7.614 B(CaH-1L)=-8.395 B(CaH-2L2)=-16.808	87BBe	25287
Ca++	gl	37C	0.10M	KNO3		I	K1=3.485 B(CaHL)=7.81 Ionic strength range: 0.03-0.3.	82ADa	5515
Ca++	gl	25C	0.00	oth/un		H	K1=4.91 K(Ca+HL)=2.81 DH1=-6.44 kJ mol-1, DS1=71.9 J mol-1 K-1.	82ADa	5517
Ca++	gl	25C	0.10M	KCl	A	I	K1=3.63 K(Ca+HL)=2.03 K(Ca+H2L)=1.04 Extrapolated to I=0.0 M: K1=4.87; K(CaHL)=3.03.	80PEa	14557
Ca++	ISE	25C	0.10M	NaCl			K1=3.42	79CMb	18468
Ca++	dis	25C	0.50M	R4N.X			K(Ca+HL)=2.52	76MKa	6926
Ca++	gl	25C	0.10M	NaClO4		M	K1=3.54 B(CaL(Cys))=5.58 K(Ca+L+HPO4)=10.72	75RMa	6850
Ca++	EMF	?	?	oth/un			K1=3.24	69BMb	37310
Mg++	gl	37C	0.15M	NaClO4	C		K1=3.333 B2=5.126 B(MgH2L)=11.008 B(MgHL)=7.483 B(MgHL2)=10.411 B(Mg2H-2L2)=-12.638 B(MgH-2L)= -18.468	87BBe	25286

Mg++	gl	37C 0.10M KNO3		I	K1=3.451		82ADa	5516
					B(MgHL)=7.23			
					Ionic strength range: 0.03-0.3.			
Mg++	gl	25C 0.00	oth/un	H	K1=4.71		82ADa	5518
					K(Mg+HL)=2.42			
					DH1=-22.00 kJ mol-1, DS1=164 J mol-1 K-1.			
Mg++	gl	25C 0.10M KCl	A	I	K1=3.63		80PEa	14558
					K(Mg+HL)=1.76			
					K(Mg+H2L)=0.54			
		Extrapolated to I=0.0 M: K1=4.85; K(MgHL)=2.67; K(MgH2L)=1.0.						
Mg++	gl	25C 0.10M R4N.X			K1=1.92	B2=3.85	70GTa	37360

87BBe C Blaquiere,G Berthon, Inorg.Chim.Acta,135,179
82ADa P Amico,P G Daniele,C Rigano et al, Ann.Chim.(Rome),72,1
80PEa K N Pearce, Australian J.Chem.,33,1511
79CMb A Craggs,G J Moody,J D R Thomas, Analyst,104,961
76MKa W J McDowell,O L Keller et al, J.Inorg.Nucl.Chem.,38,1207
75RMa S Ramamoorthy,P G Manning, J.Inorg.Nucl.Chem.,37,363
70GTa A Grzybowski,S Tate,S Datta, J.Chem.Soc.(A),241
69BMb F Boschreig,F Marti, Inform.Quim.Anal.,23,5

EXPLANATORY NOTES

DATA Flags are :-

I Data with various BACKGROUNDS
H Data for THERMOCHEMICAL quantities
M Data for TERNARY Complexes

****

START of profile PRINTED on Mon 13 February 1995 @ 09:01

Stability Constants Database SCQUERY (C) 1993 IUPAC and Academic Software
SCQUERY Version 1.32 : Prof.A.Covington, U. of Newcastle

User Identifier : Prof.A.Covington, U. of Newcastle

1 expts:Profile for Glycine/3 metals (H+/Ca++ etc))
8 refs (87BBe to 69BMb) / No experimental details specified

C2H5NO2 (85) Glycine CAS 56-40-6
2-Aminoethanoic acid H2N.CH2.COOH HL

Metal	Mtd	Temp	Conc	Medm	Clb	Flags	Log equilibrium const	Ref	ExptNo
Mg++	gl	37C	0.15M	NaClO4	C		K1=1.979 B(MgHL)=10.879 B(MgH2L2)=21.614 B(MgH-1L)=-8.735	87BBe	25284

87BBe C Blaquiere,G Berthon, Inorg.Chim.Acta,135,179

****

START of profile PRINTED on Mon 13 February 1995 @ 09:04

Stability Constants Database SCQUERY (C) 1993 IUPAC and Academic Software
SCQUERY Version 1.32 : Prof.A.Covington, U. of Newcastle

User Identifier : Prof.A.Covington, U. of Newcastle

2 expts:Profile for Aspartic ac/3 metals (H+/Ca++ etc))
8 refs (87BBe to 69BMb) / No experimental details specified

C4H7NO4 (21) Aspartic acid CAS 56-84-8
Aminobutanedioic acid H2N.CH(CH2.COOH).COOH H2L

Metal	Mtd	Temp	Conc	Medm	Clb	Flags	Log equilibrium const	Ref	ExptNo
Ca++	gl	37C	0.15M	NaClO4	C		K1=1.135 B2=3.855 B(CaH2L)=14.128 B(CaHL)=10.590 B(CaH-1L)=-9.241	87BBe	25283
Mg++	gl	37C	0.15M	NaClO4	C		K1=2.040 B2=4.426 B(MgH2L)=14.074 B(MgHL)=10.501 B(MgH-1L)=-8.666	87BBe	25282

87BBe C Blaquiere,G Berthon, Inorg.Chim.Acta,135,179

****

START of profile PRINTED on Mon 13 February 1995 @ 09:07

Stability Constants Database SCQUERY (C) 1993 IUPAC and Academic Software
SCQUERY Version 1.32 : Prof.A.Covington, U. of Newcastle

User Identifier : Prof.A.Covington, U. of Newcastle

2 expts:Profile for 2 ligands (Glutamic ac etc)/3 metals (H+/Ca++ etc))
8 refs (87BBe to 69BMb) / No experimental details specified

C5H9NO4 (22) Glutamic acid CAS 56-86-0
2-Aminopentanedioic acid H2N.CH(CH2.CH2.COOH)COOH H2L

Metal	Mtd	Temp	Conc	Medm	Clb	Flags	Log equilibrium const	Ref	ExptNo
Ca++	gl	37C	0.15M	NaClO4	C		K1=1.474 B(CaH2L)=14.020 B(CaHL)=10.377 B(CaH-1L)=-9.071	87BBe	25281
Mg++	gl	37C	0.15M	NaClO4	C		K1=2.196 B(MgH2L)=14.876 B(MgHL)=11.081 B(MgH-1L2)=-6.125	87BBe	25280

87BBe C Blaquiere,G Berthon, Inorg.Chim.Acta,135,179

****

START of profile PRINTED on Mon 13 February 1995 @ 10:19

Stability Constants Database SCQUERY (C) 1993 IUPAC and Academic Software
SCQUERY Version 1.32 : Prof.A.Covington, U. of Newcastle

User Identifier : Prof.A.Covington, U. of Newcastle

1 expts:Profile for 5-Oxoprolin/3 metals (H+/Ca++ etc))
8 refs (87BBe to 69BMb) / No experimental details specified

C5H7NO3 (2110) 5-Oxoproline CAS 149-87-1
2-Pyrrolidone-5-carboxylic acid, Pyroglutamic acid HL

Metal	Mtd	Temp	Conc	Medm	Clb	Flags	Log equilibrium const	Ref	ExptNo
H+	gl	37C	0.15M	NaClO4	C		K1=3.090	87BBe	22668

87BBe C Blaquiere,G Berthon, Inorg.Chim.Acta,135,179

****

START of profile PRINTED on Mon 13 February 1995 @ 10:11

Stability Constants Database SCQUERY (C) 1993 IUPAC and Academic Software
SCQUERY Version 1.32 : Prof.A.Covington, U. of Newcastle

User Identifier : Prof.A.Covington, U. of Newcastle

1 expts:Profile for Vitamin B6/3 metals (H+/Ca++ etc))
8 refs (87BBe to 69BMb) / No experimental details specified

C8H11NO3 (254) Vitamin B6
Pyridoxine, Vitamin B6 HL

Metal	Mtd	Temp	Conc	Medm	Clb	Flags	Log equilibrium const		Ref	ExptNo
H+	gl	37C	0.15M	NaClO4	C		K1=8.653	B2=13.46	87BBe	22669

87BBe C Blaquiere,G Berthon, Inorg.Chim.Acta,135,179

APPENDIX D

Input File for SUPERQUAD

```
                                    DATA EDITOR
Locate item to edit using cursor keys and select with <ENTER>
Enter new value in box and accept with <ENTER>. All editing keys can be used
Use <PgUp> or <PgDn> to move to other items.      Exit editing with <ESC>

Title                    mg.glu
Max.Iterations (e.g.20)                                  10
Total number of Reactants (1,2,3 or 4)                    3
Weights (0=Calc. individually, 1=All the same)  1  (2/3 for 0/1+recal. wts)
Temperature (deg. C)                                 37.000

                              Reactant    1      magnesium
                              Reactant    2      glutamic
                              Reactant    3      Hydrogen
```

```
When editing "Refine?" Keys, identify with <ENTER>, press any other key to
cycle alternatives and select with <ENTER>. Use PgUp/PgDn or EXIT with <ESC>

   Log Betas    magnesium     glutamic      Hydrogen                    Refine?
1    9.263          0             1             1                      Constant
2   13.373          0             1             2                      Constant
3   15.551          0             1             3                      Constant
4  -13.380          0             0            -1                      Constant
5   14.876          1             1             2                      Refine
6   11.081          1             1             1                      Refine
7    2.196          1             1             0                      Refine
8   -6.125          1             2            -1                      Refine
9  -11.500          1             0            -1                      Constant
10 -21.000          2             0            -2                      Constant
11 -39.000          3             0            -4                      Constant
```

```
Ctrl/D to Delete Beta, Ctrl/A to Add Beta after Cursor. All Edit keys apply
Use PgUp, PgDn, <ESC> etc. as before.                                Curve   1
With text items use ENTER to select and any other key to cycle.Accept with ENTER

 Number of Reactants in THIS titn.   3
 Number of Electrodes in THIS titn.  1
    PrCtl = Print Control (usually 1 for Metal, 0 for others)
    Tot.Quant. = Total quantity in vessel, in milliMoles
    Add.Conc. = Conc. in burette in Moles/Litre
 Reagent     PrCtl Tot.Quant.  Refine T?      Added Conc.   Refine A?
 magnesium      1   0.250000   Constant          0.000000   Constant
 glutamic       1   1.000000   Constant          0.000000   Constant
 Hydrogen       0   3.000000   Constant         -0.990000   Constant

 Coulomb. Titn?   Initial Vol.   Error in Vol increments
      No             50.00000          0.00003

 Elec.=No. electrons transferred
 SigmaE=Error in Ezero,   Slope=Nernstian Slope Factor, 1 for pH
Mv/pH Elec.  Reactant      Ezero     SigmaE    Refine E?  Slope    Refine S?
 EMF    1   Hydrogen     432.3400    0.1000   Constant    0.9976   Constant
```